Identifying New Drug Targets to Treat Breast Cancer Brain Metastasis

AUTHOR(S)

Siobhan Purcell

CITATION

Purcell, Siobhan (2019): Identifying New Drug Targets to Treat Breast Cancer Brain Metastasis. Royal College of Surgeons in Ireland. Thesis. https://doi.org/10.25419/rcsi.10764266.v1

DOI

10.25419/rcsi.10764266.v1

Identifying New Drug Targets to Treat Breast Cancer Brain Metastasis

RCSI

Siobhan Purcell BA (Hons)

Thesis presented to Royal College of Surgeons in Ireland

Submitted for Masters of Science

Endocrine Oncology Research Group

Royal College of Surgeons

St. Stephen's Green, Dublin 2

Supervisor: Professor Leonie Young

Co-supervisor: Dr. Damir Vareslija

Head of department: Professor Arnold Hill

August 2018

I declare that this thesis, which I submit to RCSI for examination in consideration of the award of a higher degree, Master of Science (MSc), is my own personal effort. Where any of the content presented is the result of input or data from a related collaborative research programme this is duly acknowledged in the text such that it is possible to ascertain how much of the work is my own. I have not already obtained a degree in RCSI or elsewhere on the basis of this work. Furthermore, I took reasonable care to ensure that the work is original, and, to the best of my knowledge, does not breach copyright law, and has not been taken from other sources except where such work has been cited and acknowledged within the text.

Signed _____

Student Number _____

Date _____

Acknowledgements

I wish to extend my heart-felt thanks to Professor Leonie Young, firstly for giving me the opportunity to take part in the important research of her lab as Research Assistant, and then encouraging and supporting me to extend my work into this research masters.

I would also like to give my sincerest gratitude to Dr. Damir Vareslija, for all of his help and mentorship during this project; I have learned an incredible amount from him.

I am also indebted to the all of the patients who donated to this research study. They form the focal point of this work and the driving force to all of the research we do.

A huge special thanks to my other fellow lab colleagues for their support and for making my work an enjoyable experience: Sinead (the mouse whisperer), for all that she has taught me both in the lab and with animals; Fiona, for keeping the lab glued together and for occasionally providing us with doughnuts; Sara, for her knowledge in all things related to science and baked goods; Brendan, for always helping me understand extremely complex analyses (being successful at most times…); Ben, for his excellent horror movie recommendations; Nicola, for our shared appreciation of cheeses; and Karen, for always keeping it very real with me.

Many thanks to the McIlroy team: Marie, Rachel and Laura, for their inspiring passion in research and positive attitudes in all aspects in life.

I would also like thank Ailis, Alacoque, Elspeth, and Azzie who were all also fantastic researchers and made great company.

Finally, I truly appreciate all of the support and encouragement that I have received from friends and family. Particularly, a special thanks to my sisters for proof-reading a lot of this thesis, regardless of how over their heads it was.

Table of Contents

Abbreviations

ASCO/CAP	American Society of Clinical Oncology/College of American Pathologists
BC	Breast cancer
bp	Base pair
BSA	Bovine serum albumin
BBB	Blood Brain Barrier
BrM	Breast cancer brain metastasis
BTB	Blood tumour barrier
CDX	Cell-derived xenograft
CNS	Central nervous system
DMEM	Dulbecco's Modified Eagle Medium
DCIS	Ductal carcinoma in situ
DFS	Disease free survival
DNA	Deoxyribonucleic acid
DTC	Disseminated tumour cell
E_2	17 β-estradiol
EGF	Epidermal growth factor
EGFR	Epidermal growth factor receptor
ER	Estrogen receptor
ESR1	Estrogen receptor 1
FCS	Foetal calf serum
FDA	Food and drug administration
FFPE	Formalin-fixed paraffin-embedded

FasL	Fas ligand
GABA	Gamma-aminobutryic acid
GDNF	Glial cell-derived neurotrophic factor
HER	Human epidermal growth factor receptor
IHC	IHC
IMS	Industrial methylated spirits
IDC	invasive ductal carcinoma
ILC	Invasive lobular carcinoma
IL	Interleukin
KPS	Karnofsky performance status
MAPK	Mitogen activated protein kinase
MBC	Metastatic breast cancer
MEM	Minimum essential medium
METABRIC	Molecular Taxonomy of Breast Cancer International Consortium
MDC	Mucinous ductal carcinoma
mL	Millilitre
MMP	Metalloproteinases
mRNA	Messenger RNA
MTC	Medullary thyroid cancer
mTOR	Mammalian target of rapamycin
n	Experimental number
NA	Not available
NSCLC	Non-small cell lung caner

OS	Overall survival
ORR	Objective response rates
p	p-value
PA	Plasminogen activator
PDX	Patient derived xenograft
PBS	Phosphate buffered saline
PCR	Polymerase chain reaction
PI3K	Phosphoinositide 3-kinase
PKA	Protein kinase A
PR	Progesterone receptor
PRF	Phenol red free
PS	Penicillin-streptomycin
qPCR	Quantitative PCR
RET	Rearranged during transfection
RTK	Receptor tyrosine kinase
RNA	Ribonucleic acid
RR	Response rate
Seq	Sequencing
SEM	Standard error of the mean
SRS	Stereotactic surgery
TBS	Tris buffered sulphate
TNBC	Triple negative breast cancer
TNF	Tumour necrosis factor
TNM	Tumour, Node, Metastasis

TV	Tumour volume
VEGF	Vascular endothelial growth factor
VEGFR	Vascular endothelial growth factor receptor
WBRT	Whole brain radiation therapy
WES	Whole exome sequencing
µL	Microlitre
µM	Micrometer
v/v	Volume by volume
w/v	Weight by volume
%	Percent

List of Figures

Table of Tables

Abstract

Breast cancer brain metastasis (BrM) is indicative of poor prognosis, with a short median survival time and limited disease management strategies. Current treatment options are restricted to surgical resection, radiation therapy and limited targeted therapies. Therefore, there is an urgent need to uncover alterations responsible for BrM and to define novel effective therapeutic targets.

RNA-sequencing (RNA-Seq) was performed to analyse gene expression differences between patient-matched breast tumours and their associated resected BrM. Importantly, common transcriptional differences in breast cancer specific genes were observed, particularly BrM–acquired aberrant enrichment in multiple receptor tyrosine kinase (RTK) driven signalling pathways. The most notable recurrent alterations were expression gains in RET and HER2. Hence, given the observed enriched kinase landscape these alterations were investigated as clinically actionable therapeutic targets in BrM.

To evaluate the effect of RET and HER2 inhibition in a preclinical setting, the efficacy of two FDA-approved agents were examined; a RET inhibitor, cabozantinib, and a pan-HER inhibitor, afatinib. Being small molecule tyrosine kinase inhibitors (TKIs), both drugs have the potential of crossing the blood brain barrier (BBB). *In vitro*, both agents demonstrated a significant effect on the cellular viability and migratory capacity of brain-metastasising cell lines and primary cells derived from a patient brain metastasis tumour. Significant anti-tumour activity was also shown for anti-HER2 and anti-RET therapies in unique patient derived *ex vivo* and patient-derived xenograft (PDX) models developed from patients undergoing BrM resection.

This study demonstrates profound and recurrent transcriptional remodelling events in BrM, which is critical to understanding the pathobiology of BrM. Furthermore, this work supports comprehensive profiling of metastasis as a compelling and underutilised tool to inform clinical care and reveal novel targeted treatment paradigms. Given the remarkably high recurrence rates of specific targetable

alterations, further clinical investigations of recurrent aberrations are in demand, especially considering some are readily druggable.

1. General Introduction

1.1. Breast cancer

Worldwide, breast cancer (BC) is the second most prevalent cancer, and the first amongst women. After lung cancer, it is the principle cause of mortality for women in the developed world (Ferlay et al., 2015). A recent report that was released by the National Cancer Registry of Ireland (NCRI) showed that from 2014-2017 approximately 2,919 women were diagnosed with breast cancer annually in Ireland, equivalent to 30% of all cancers. While there has been a continuous decline in mortality during the last 20 years, breast cancer was still the second leading cause of cancer death in Ireland during this period, accounting for 17% of all female cancer deaths (NCRI, 2016).

There are multiple factors that will increase a woman's susceptibility to developing BC, with increasing age and estrogen exposure being the central determinants (Boyd et al., 2010). A number of lifestyle factors can also contribute to elevated disease risk including smoking, obesity, poor physical activity diet and high alcohol consumption (McTiernan et al., 2003; Ligibel, 2011). Familial history is another risk factor, with the likelihood of a woman developing BC being higher if she has a close relative who was previously diagnosed with the disease. Furthermore, it has been estimated that women who harbour Breast Cancer 1 (BRCA1) gene mutations may have up to 80% chance of developing the disease, while carriers of Breast Cancer 2 (BRCA2) mutations have a 45% risk (Antoniou and Easton, 2006).

1.2. Categorising breast cancer

Although BC is generally referred to as a single disease, a massive degree of heterogeneity is observed both within and between tumours from a clinical, histological, and molecular perspective. Instead, it represents a broad “umbrella term” for a larger number of diseases. Therefore, in order to provide a better prognosis and understand the differential treatment responses of BC patients, several classification schemes have been devised to sub-divide breast tumours into more discrete entities. With recent advances in cancer research, these organisation schemes have evolved

over the years and are continuously updated as our molecular knowledge of this disease improves.

1.2.1. Traditional classification systems of breast cancer

From a broad morphological perspective, BC can be categorised into two predominant histological subtypes: in situ carcinoma and invasive carcinoma. As the disease typically descends from sites of either ductal or lobular origin, each division group is further sub-classified accordingly (Malhotra et al., 2010). The most common tumour group is invasive ductal carcinoma (IDC), accounting for up to 70-80% of all BCs (Li et al., 2005). Patients of this subtype are stratified into more clinically informative risk groups based on histological grade, which assesses mitotic rate, tubule formation, and nuclear grade in order to score the degree of tumour differentiation (Lester et al., 2009).

Staging is another key prognostic and treatment determinant of BC. The most conventional and universally accepted staging scheme is the Tumour, Node, Metastasis (TNM) system. This assigns BC into prognostic stage groups using a combined score from tumour size, lymph node stage and extent of metastatic spread (M) (Edge and Compton, 2010).

Clinical subtype division is also conducted according to the differential expression status of the hormonal receptors for estrogen and progesterone (ER and PR) as well as human epidermal growth factor receptor 2 (HER2/ERBB2), which are all known mediators of growth signalling. These classic biomarkers are routinely assessed in pathology laboratories via immunohistochemistry (IHC) in order to determine the most appropriate treatment choice for patients. For example, given that approximately 70% of invasive breast carcinomas are ER expressing BCs, the prevalence of this protein biomarker is a major predictor of their response to endocrine therapy (Dai et al., 2016).

IHC biomarkers and clinicopathological variables have proven to be quite effective in the most part for predicting patient prognosis and deciding initial treatment strategies. However, these parameters alone are still insufficient in defining

the complex underlying molecular biology of BC development. Therefore, they have limitations with respect to guiding personalised treatment therapies.

1.2.2. Molecular subclassification of breast cancer

The recent advent of sophisticated gene expression profiling techniques have introduced a paradigm shift in stratifying and treating patients by refining the classification schema for tumours beyond conventional clinicopathological criteria. This wealth of molecular knowledge has generated an entirely new outlook on the magnitude of BC heterogeneity, revealing a diverse spectrum of many biological subtypes with unique gene signatures and distinct clinical outcomes.

According to this molecular taxonomy system, five “intrinsic” molecular subtypes of BC have been distinguished, expanding upon the simple biomarker classification system. These include luminal A, luminal B, HER2-amplified, basal-like and normal like (Perou et al., 2000; Sorlie et al., 2001; Sorlie et al., 2003).

The majority of luminal A tumours are mostly ER-positive, histologically low-grade and have low expression of proliferation genes. Luminal B tumours tend to have lower expression of ER-related genes and present higher proliferation rates and histological grades (Hu et al., 2006). Luminal A tumours have the best prognosis of all the five subtypes, whereas luminal B have shown significantly worse disease-free survival in comparison as well as higher risk of local recurrence (Feeley et al., 2014; Voduc et al., 2010).

HER2-amplified and basal-like cancer lack ER signalling. The HER2-enriched subtype exhibits amplification and high expression of the ERRB2 gene as well as other proliferation genes. The basal-like subtype typically correspond to ER-negative, PR-negative and HER2-negative tumours, and hence are commonly referred to as “triple negative” BC (TNBC). These tumours are typically characterised by advanced histological grade and show increased expression levels of proliferation related genes as well as basal myoepithelial markers such as cytokeratins 5/17 and epidermal growth factor receptor (EGFR) (Sorlie et al., 2001; Weigelt et al., 2010). Both HER2-positive and TNBC patients have a much poorer prognosis than luminal-like cases (Yersal and Barutca, 2014).

In an integrative genomic and transcriptomic large-scale study of almost 2000 breast tumour samples by METABRIC (Molecular Taxonomy of Breast Cancer International Consortium), the vast extent of this intertumour heterogeneity has been further unveiled. Since then, another dimension of complexity has been introduced into the classification system; expanding it into 10 additional different subtypes with more refined features and distinctive molecular profiles. (Curtis et al., 2012). Whilst these landmark findings have provided a glimpse into the heterogeneity of BC, more extensive molecular profiling will be required to fully appreciate the entire magnitude and complexity of this disease.

1.3. Metastatic breast cancer

The most lethal aspect of cancer progression is the ability of tumour cells to detach from the primary site and colonise distant organs; a process that is called metastasis. Such invading tumour cells are highly heterogeneous, owing to their rampant genomic instability (Chiang and Massague, 2008). Despite significant advancements in treating the primary tumour, relapses do occur and metastatic breast cancer (MBC) remains the ultimate cause of death among most patients that succumb to the disease. A small minority of cases may present with distant metastases at first diagnosis. The majority of other patients are initially diagnosed with early-stage disease, 25-30% of whom will resist therapy and eventually recur with metastases in other sites, months or years later (Redig and McAllister, 2013). A combination of several factors influence the risk of developing metastasis including tumour size, patient age, grade, lymph node involvement, HER2 overexpression as well as the ER and PR status of the patient (Kennecke et al., 2010).

Metastasis is a complex orchestration of events, which can be conceptualised through a simplified sequence of stages. Firstly, the cascade initiates during the early stages of BC, as cancer cells escape from the primary tumour and invade into the local surrounding tissue. This is then followed by intravasation into the bloodstream where circulating tumour cells (CTCs) become exposed to substantial levels of stress. The final most

difficult task is to then extravasate into the parenchyma of the target host tissue and colonise its microenvironment (Massague and Obenauf, 2016). Altogether, only a small number of metastasising cells have the ability to withstand and survive against such shear selective pressures, demonstrating the inefficiency of this multi-step process. The establishment of each metastatic event is driven by: (1) the bestowal of adaptive metastatic traits to invading tumour cells by the surrounding host microenvironment (2) both the intrinsic properties of BC cells and their acquisition of new genetic and/or epigenetic alterations during metastatic progression (Valastyan and Weinberg, 2011).

1.3.1. Organotropism of breast cancer metastasis

Studies reveal that the pattern of metastatic spread is far from random chance. Instead, particular tumours tend to preferentially colonise certain organs. This phenomenon can be explained by Stephan Paget's "Seed and Soil" hypothesis, which proposes that metastatic establishment is dependent on the cross talk between invading cancer cells (the "seed") and the specific microenvironment properties of the host tissue (the "soil") (Paget, 1989). Regarding MBC, tumour cells predominantly demonstrate a proclivity to spread to the bones, lungs, brain and liver (Patanaphan et al., 1988).

Different BC subtypes show distinct preferential patterns of organ specific metastasis with noteworthy differences in survival after relapse. Within recent years, several studies have investigated the expression profiles of primary BC and their patterns of distant metastatic spread. Luminal subtypes are significantly associated with breast tumours that relapse to the bone (Kennecke et al., 2010). Patients with HER2-positive and TNBC/basal-like BC bear the most risk of succumbing to BrM with several studies reporting higher incidence rates among these subtypes relative to luminal BCs (Smid et al., 2008; Soni et al., 2015) as summarised by a recent literature review in Table 1.1 below (Witzel et al., 2016).

Table 1.1: Incidence of organ-specific metastatic spread among different breast cancer subtypes

Site of Relapse	Brain (%)	Bone (%)	Lung (%)	Liver (%)
All Subtypes[a]	12–17	48–62	23–32	15–27
Luminal A	8–15	65–67	6–7	12–29
Luminal B	11	58–71	24–30	4–32
TNBC/basal	25–27	17–39	40–43	13–21
HER2-positive	11–20	61–62	15–42	22–44

a Table adapted from (Witzel et al., 2016). Data summarised from studies by ((Smid et al., 2008; Soni et al., 2015; Kennecke et al., 2010)

1.4. Breast cancer brain metastasis

Following lung cancer, BC represents the second most common cause of BrM with relapses occurring in approximately 10-30% of patients with advanced disease (Tabouret et al., 2012). Such brain malignancies are indicative of extremely poor clinical outcome as reflected by the short median survival time with reports ranging anywhere between 2 to 25.3 months depending on treatment and primary tumour subtype (Leone and Leone, 2015). Patient prognosis for overall survival (OS) is also determined by factors such as age and the burden of disease as represented by the number of BrM and systemic tumour activity (Hung et al., 2014; Lee et al., 2008). Moreover, the patients' overall functional health and activity levels after initial diagnosis with BrM, is another chief survival determinant. The most common tool used to assess this is the Karnofsky Performance Status (KPS), of which patients scoring ≥70 tending to fare poorly (Yates et al., 1980).

BrM contribute to a significant degree of morbidity, associated with neurologic deficits, which can severely affect quality of life for many patients. The most common

presenting clinical complications include headaches, seizures, vomiting, altered mental behavior as well as impaired motor and cognitive function. Symptom manifestations can vary between patients, depending on tumour location (Saha et al., 2013).

1.5. Pathophysiology of breast cancer brain metastasis

Over the years the incidence of brain metastasis has escalated. This is most likely due to longer survival of MBC patients as a result of more effective treatments and control of systemic disease coupled with earlier diagnoses from improved neuroimaging technology (Eichler and Loeffler, 2007). The alarming prevalence of BrM and its significant impact on BC patient prognosis has led to extensive research into the molecular pathophysiology of this complex disease. Many of these studies have also provided provocative insights into brain-specific drug resistance mechanisms as detailed further below.

1.5.1. The unique brain microenvironment niche

Consistent with the seed-and-soil theory, several studies have demonstrated that specific organ microenvironments can provide hospitable and supportive metastatic niches for the growth and survival of certain types of disseminated tumour cells (DTCs). As the structure and vascular wall composition of each organ are vastly different from one another, the host tissue exerts distinct selection pressures on these cells for metastatic growth. Under these specific conditions, unique malignant cells acquire the necessary adaptive traits to survive and even thrive from these harsh surroundings, ultimately giving rise to the ‘speciation’ of a new metastatic cell population (Nguyen et al., 2009).

1.5.1.1. The blood-brain barrier

In order to colonise the brain parenchyma, invading cancer cells must have the capacity to penetrate the BBB, an intricate structure comprised of tight junctions between a layer of non-fenestrated endothelial cells. This highly selective barrier

strictly regulates the passage of substances between the circulation and central nervous system (Figure 1.1A).

However, the organisational integrity and functional permeability of this fundamental feature becomes significantly compromised in most cases of BrM, albeit to varying degrees, resulting in a 'leaky' dysfunctional structure termed as the blood tumour barrier (BTB) (Figure 1.1B) (Groothuis, 2000). Thus, there has traditionally been wide belief that the BBB plays essential role in mediating acquired resistance to chemotherapy in BrM. Under this assumption, the BBB is breached, enabling metastatic cells to traverse into cerebral compartment and exploit the barrier's restrictive properties as a protective 'sanctuary' from immune cells as well as therapeutic agents (Steeg et al., 2011). However, this mechanism of chemoresistance is still under debate as the impact of BBB breakdown and efficient drug delivery remains obscure. Although the BBB prevents the trespass of larger molecules such as monoclonal antibodies like trastuzumab, the transformed BTB can still permit the delivery of drugs, particularly at well-advanced disease stages. Both clinical and preclinical studies show supporting evidence of this claim, with the accumulation of anti-HER2 drugs in BrM. As to whether they have reached sufficient levels of clinical efficacy, however, is uncertain (Tamura et al., 2013; Askoxylakis et al., 2016).

The integrity of the BBB has been shown to be less intact in cases of larger metastases, due to the higher release of vascular endothelial growth factor (VEGF) which increases vascular permeability (Fidler et al., 2002). Despite this leakage of blood vessels however, studies have argued that in some cases of BC BrM and glioblastomas (GBM), the BTB is still sufficient to impede the drug delivery of most conventional therapeutic agents (Lockman et al., 2010; Zhou et al., 2017). Interestingly, BTB permeability also appears characteristic of certain breast tumour subtypes as IHC analyses of resected BrM from basal-type/TNBC from reveal barrier disruption, whereas HER2-positive BC tend to preserve it (Yonemori et al., 2010).

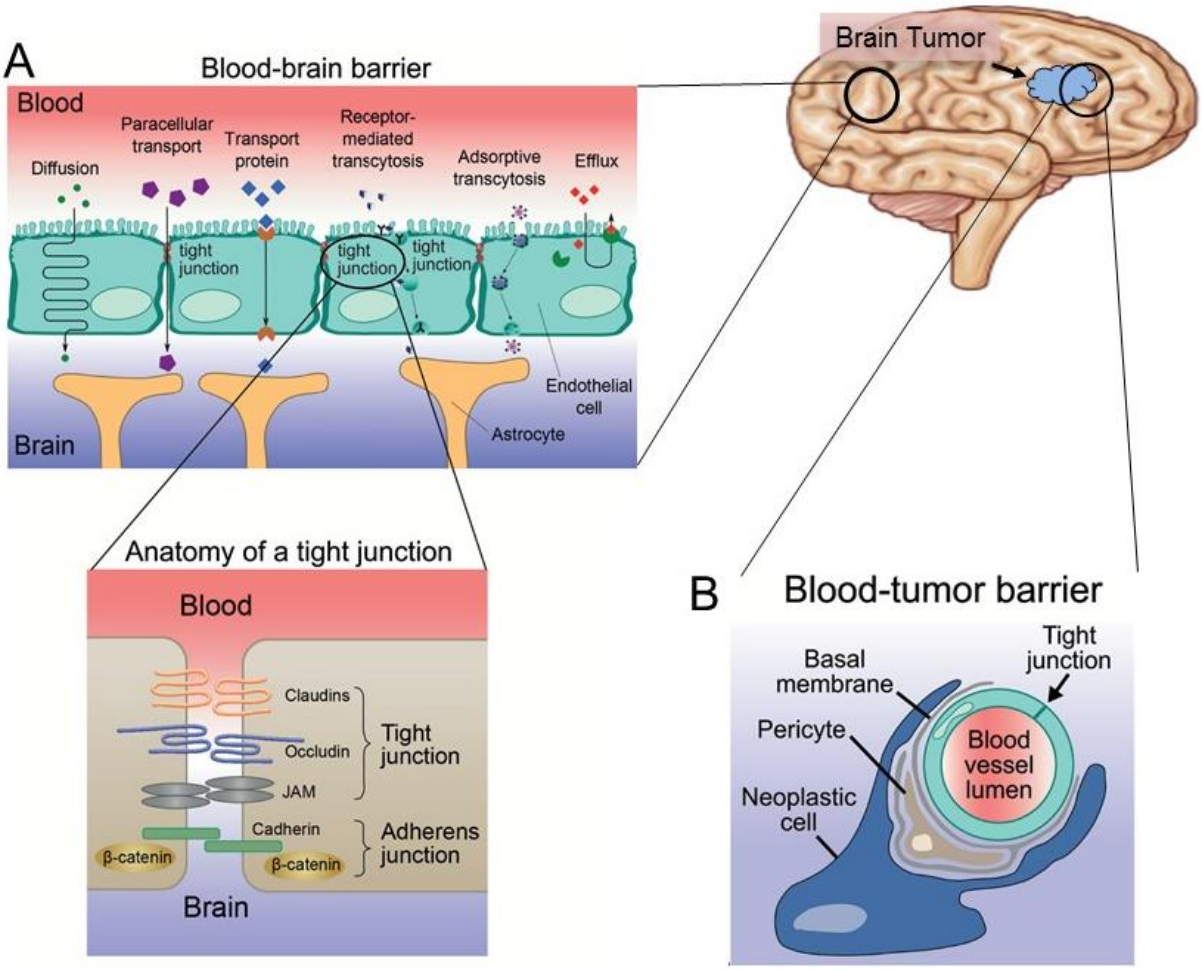

Figure 1.1: The brain-tumour microenvironment.

(A) Illustration shows the specialised structural feature of the BBB as well as some of the unique resident cells dwelling in the brain microenvironment. The barrier consists of a continuous layer of non-fenestrated endothelial cells, connected together by tight junctions and surrounded by pericytes and astrocytic perivascular end-feet. This supportive structure constitutes the protective semi-permeable membrane at the front between the brain and circulating blood. (B) When metastatic cells colonise the brain, the BBB is transformed into the BTB, which demonstrates variable degrees of vascular permeability among different brain metastases. Figure adapted from (Chamberlain et al., 2017).

1.5.1.2. The brain cellular milieu

A myriad of unique stromal cell types exists within the brain parenchyma, playing pivotal roles in both the cerebral tropism of MBC cells and their acquired resistance to targeted therapies. During brain colonisation, tumour cells have the ability to transform the microenvironment into a more permissive neural niche through active cross-talk with resident cerebral cells, the most common including endothelial, microglia, astrocytes, pericytes and neurons (Zhang and Yu, 2011).

Astrocytes are the most abundant population of glial cells in the brain and perform a number of house-keeping functions, in order to maintain homeostatic regulation within the brain microenvironment (Abbott et al., 2006). Traumatic stress can induce the activation of both astrocytes and microglia, leading to glial scar formation or gliosis. This reactive response has also been shown to be triggered by brain metastases, once the BBB has been breached (Fitzgerald et al., 2008). Typically, metastatic tumour cells are found intertwined with these activated glial cells, a histological characteristic observed from resected human BrM (Zhang and Olsson, 1995). In an attempt to eliminate such foreign invasions, astrocytes activate neuroinflammatory responses through the secretion of growth factors, cytokines, chemokines, Interleukin (IL) 1 beta, IL-6 and tumour necrosis factor (TNF). Many of these factors have been described in the literature to inadvertently enable tumour cells with oncogenic signals that facilitate tumourigenesis (O'Brien et al., 2013).

Furthermore, studies have also reported that astrocytes can potentially exert a chemoprotective effect on tumour cells against cytotoxic drugs. *In vitro* co-culture work had initially reported this adaptive mechanism to occur through the establishment of tumour-astrocyte gap junctions. In the case of melanoma-to-brain metastasis, astrocytes are able to sequester cytoplasmic calcium from tumour cells via this communication channel and mediate their chemoresistance (Lin et al., 2010). Expanding this work, a recent study demonstrated that BC cells employ these junctional features to transfer secondary messenger cGAMP to astrocytes, and exploit their neuroprotective effect by triggering pro-inflammatory secretions (Chen et al., 2016). Additionally, when BrM patient derived cells are co-cultured with astrocytes, a number of pro-survival genes such as GSTA5, BCL2L1 and TWIST1

have been shown to become upregulated, which contributes to their resistance to chemotherapy (Kim et al., 2011).

Although not as well defined, studies have demonstrated additional brain-specific adaptations that metastases acquire which facilitate exploitation of the readily available resources from unique neural milieu. Neuronal mimicry is one such modification, whereby BrM undergo major transcriptional reprogramming in order to mimic neurons and thrive within the brain microenvironment. One study found that BrM acquired increased expression of GABAergic features relative to patient-matched primary breast tumours which were necessary for metabolising neurotransmitter γ-aminobutyric acid (GABA) (Neman et al., 2013). Thus, BrM are capable of “hijacking” normal cellular processes and altering key anatomical features to support tumour outgrowth upon brain colonisation. Altogether, these extrinsic factors play major roles in the clonal evolution of BrM.

1.5.2. Genetic mediators of breast cancer brain metastasis

The unique intrinsic features of breast DTCs also play a major role in succeeding colonisation of the brain. This metastatic stage is the most critical step of the cascade and perhaps the most rate-limiting, given the extensive demands imposed by the brain tissue microenvironment on infiltrating cancer cells. Indeed, the difficulty of this task can be reflected in the long disease latency period that typically elapses between the initial diagnosis of early-stage BC and the final manifestations of BrM (Tham et al., 2006)**.** Supposedly, during this delay, a small minority of DTCs initially lack the full competence for outgrowth to distant organs, but progressively undergo genetic and/or epigenetic alterations to acquire the necessary adaptive traits for metastatic fitness. This clonal cell evolution is predominantly driven by their exposure to the selective pressures of the unique brain milieu and such chain of events result in the speciation of a brain-specific metastatic population of highly evolved cells.

Over the years, major advancements have allowed us to shed some light on the genetic basis of BrM. As of yet, only a small number of studies have reported on

genes that may contribute to BC BrM through the investigation of brain-seeking derivatives of human BC carcinoma cell lines as well as retrospective patient tissues. Such findings have uncovered the functional significance of several genes that facilitate metastatic colonisation of brain after extravasation into the parenchyma, in particular those involved with bridging their pathway across the BBB as well as their adaptation and survival against the defences of the reactive brain stroma.

Expression of the cell adhesion molecule, L1CAM, by disseminated BC cells has been shown to be necessary for vascular co-option by enabling their diffusion and adherence through the basement membrane of brain capillaries. To further aid with this process, brain metastatic tumour cells also express a high level of plasminogen activator (PA) inhibitory serpins which prevents the generation of plasmin, an enzyme that is essential for the brains defence against metastatic invasion. In doing so, the inactivation L1CAM is prevented as well as the PA-induced release of pro-apoptotic cytokine Fas ligand (FasL) from reactive astrocytes, which normally evokes death signalling in infiltrated cancer cells (Valiente et al., 2014).

In another landmark study, Bos et al. identified a set of brain-specific genes whose expression grants cancer cells with the highly specialised functions that they require for transmigrating across the paracellular membrane of the BBB including: cyclooxygenase (COX2), heparin-binding EGF-like growth factor (HBEGF), and α2,6-sialytranferase (ST6GALNAC5). Interestingly, a number of genes associated with brain relapse such as COX2, collagenase-2 (MMP1), angiopoietin-like 4 (ANGPTL4); fascin-1 (FSCN1) were found to overlap with lung metastasis gene signature which may offer an insight to the underlying association between lung and brain metastases in BC (Bos et al., 2009a). An additional study found protease cathepsin S to be another brain-specific molecular mediator of this process in breast cancer metastasis through proteolytic processing of tight junction proteins such as JAM-B that regulate BBB integrity (Sevenich et al., 2014).

1.5.3. Receptor tyrosine kinases signalling in breast cancer brain metastasis

Receptor tyrosine kinases (RTKs) are a large superfamily of receptors that are key regulators of fundamental cellular processes including apoptosis, cell proliferation, differentiation, metabolism, and survival. Upon extracellular binding with various growth factors and hormones, these kinases become rapidly activated through receptor dimerization and tyrosine autophosphorylation which subsequently activate downstream intracellular signalling pathways including the PI3K/AKT/mTOR and Ras/Raf/MEK/ERK pathway (Figure 1.2) (Lemmon and Schlessinger, 2010).

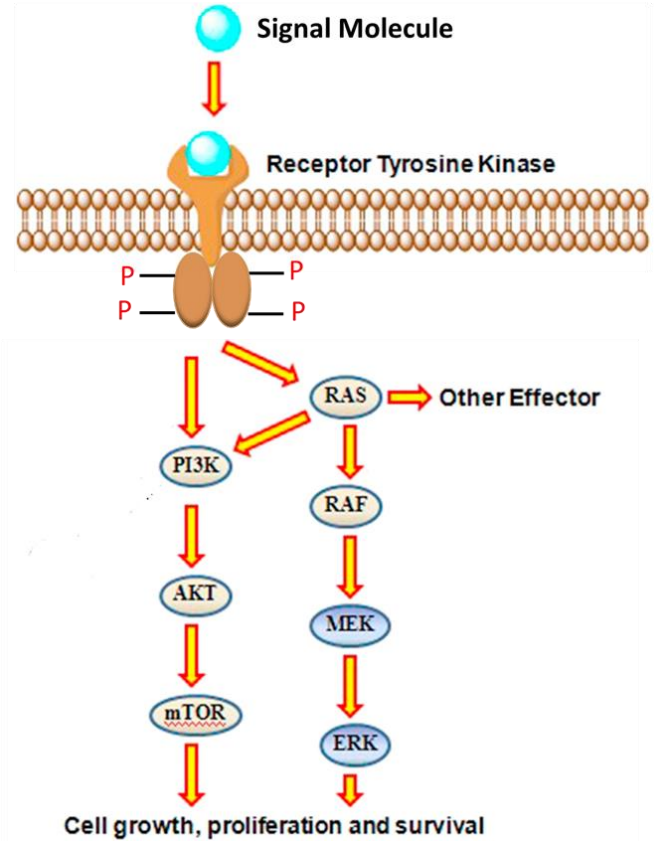

Figure 1.2: Overview of receptor tyrosine kinase dimerization and kinase activation.

Upon growth factor or hormone binding, RTKs can dimerise together leading to activation of major downstream signalling pathways such the PI3K/AKT, RAS/RAF/MEK/ERK which can promote cell growth, proliferation and survival. Figure adapted from (Asati et al., 2016).

Dysregulated signalling of RTKs has been well-established in the pathophysiology of cancer in recent years and can occur as result of aberrant activating mutations, gene amplifications or ligand and/or receptor overexpression. Only a few tyrosine kinase-activating mutations have been identified in BCs (Kan et al., 2010a). By contrast, many BCs are characterised by amplification or overexpression of receptor tyrosine kinases (Musgrove and Sutherland, 2009). Of the 20 classes of RTKs, this review will focus on discussing the signalling activity of RET and the HER family and the roles they may play in mediating BrM.

1.5.3.1. HER receptor family

There is an indisputable consensus among researchers that the HER family of transmembrane receptors play a key role in mediating BC progression and metastasis. These protein kinases are one of the most investigated cell signalling families and comprise of four members: EGFR (ERBB1), HER2 (ERBB2), HER3 (ERBB3) and HER4 (ERBB4). Extracellular ligand binding to EGFR/HER3/HER4 induces a large conformational change which consequently stimulates homodimerization or combinatorial heterodimeric interactions between HER family members (Schlessinger, 2002). As a result, this induces autophosphorylation of the intracellular tyrosine kinase domain and activation of several downstream signalling networks, including the phosphatidylinositol 3-kinase(PI3K)/AKT pathway, the Ras/Raf/MEK/ERK1/2 pathway, and the phospholipase C PLC-γ pathway (Hynes and MacDonald, 2009). HER2 is an orphan receptor as it does not bind to any known growth factor. Despite this, it can still become activated by forming heterodimers with ligand activated EGFR or ERBB3 or else via homodimerization when it becomes overexpressed in some instances such as cancer (Ghosh et al., 2011).

Of all the HER family, HER2 and EGFR are the most frequently overexpressed receptors in several cancer types including a significant subset of BC patients. Elevated levels of EGFR expression is most predominant in TNBC, and is

associated with poor clinical outcome (Abd El-Rehim et al., 2004; Viale et al., 2009). Both this and the HER2 enriched subtype display a higher prevalence of BrM, which strongly insinuates their active participation in facilitating brain-specific metastatic spread (Shao et al., 2011). Furthermore, several studies support that HER2 can enhance EGFR signalling and vice versa (Worthylake et al., 1999; Graus-Porta et al., 1997). In a more recent study, the formation of heterodimers between EGFR and HER2 was demonstrated to increase the metastatic potential of BC cell lines (Masuda et al., 2012). Taken together, these studies suggest the possibility that dual inhibition of both receptors may have an additive or synergistic anti-tumour activity (Tebbutt et al., 2013).

Several studies have investigated the clinical and functional roles of EGFR in BrM. However, the exact contribution that it makes to its progression is still unclear. As mentioned earlier, the ligand for EGFR, HBEGF, was one of the BrM signature genes identified by Bos et al and is responsible for promoting cell migration and adhesion. Both *in vitro* and *in vivo* studies have shown that EGFR may contribute to the metastatic and invasive behaviour of brain metastatic tumours but has little influence on their proliferative characteristics (Nie et al., 2012). These findings are consistent with the disappointing results from the clinical trial evaluation of EGFR inhibitors in EGFR-overexpressing BCs, all of which exhibited poor efficacy in decreasing tumour growth (O'Donovan and Crown, 2007; Saxena and Dwivedi, 2012).

Additionally, a comparative analysis of chromosomal aberrations between primary BC and brain metastatic tumours revealed a significantly higher frequency of EGFR expression gains in BrM, further indicating the association of this pathway to the disease (Wikman et al., 2012). Along similar lines, several retrospective studies have also demonstrated higher levels of EGFR expression in patients with BrM relative to patients with primary BC (Hicks et al., 2006; Tham et al., 2006). Interestingly, aberrant EGFR signalling is strongly correlated with the incidence of other brain-associated diseases. For example, mutations of EGFR are recognised as key drivers for aggressive GBM as well as non-small cell lung cancer (NSCLC), the latter of which also tends to metastasise to the brain. Such observable correlations

would suggest that these gene aberrations must supply the necessary growth signals compulsory for tumour cell survival in the brain microenvironment (Smith et al., 2001; Hsu et al., 2016). Hence, these studies further indicate that the EGFR pathway must play an important role in BrM.

HER2 is overexpressed in 20-30% of human BCs often due to amplification of the gene locus and is has become an essential biomarker and target of therapy over the years (Slamon et al., 1989). Significantly, 25-40% of HER2 positive MBC patients suffer from relapse to the brain (Sirkisoon et al., 2016). Indeed, there is certainly much evidence supporting the strong correlation between these tumour subtypes and the development of BrM (Fuchs et al., 2002; Gabos et al., 2006).

Cases of HER2 mutations have also been reported, albeit at low frequencies in BC. Most of these are missense mutations in the tyrosine kinase and extracellular domain or else duplications/insertions within its exon and have been identified in the absence of HER2 gene amplification (Slamon et al., 1989). Although activated HER2 induces similar signalling cascades with EGFR, *in vivo* studies indicate that aberrant levels of HER2 activity is instead responsible for the metastatic outgrowth of BC cells in the brain (Palmieri et al., 2007).

Being catalytically impaired, the transactivation of HER3 upon ligand binding (neuregulins, NRG1 or NRG2) is mediated by forming heterodimers with EGFR or HER2 and is dependent on their kinase activity to phosphorylate its tyrosine domain. HER3 is a critical contributor to HER2 signalling as observed by their frequent co-expression in BC cell lines and primary tumours (Bieche et al., 2003; deFazio et al., 2000). Of all the HER receptor paired combinations, the HER3/HER2 signalling complex is the most potent activator of the PI3/AKT pathway. This is principally due to the presence several phosphotyrosine residues in HER3 that serve as docking sites for the regulatory subunit (p85) of PI3K which leads to activation of this downstream module (Roskoski, 2014a). Moreover, contrary to EGFR, HER3 is preferentially phosphorylated in HER2-overexpressing BCs (Lee-Hoeflich et al.,

2008). Functional studies have demonstrated that knocking down HER3 or inhibiting HER3/HER2 dimers can significantly reduce tumour growth in HER2-amplified human BC xenografts (Lee-Hoeflich et al., 2008; Garrett et al., 2013). Given their intimate relationship, studies have also implicated HER3 signalling in mediating acquired resistance to HER2 inhibitory TKIs and monoclonal antibodies in BC (Sergina et al., 2007; Baselga and Swain, 2009).

Additionally, significant HER3 overexpression has been reported in both mouse models and human BC BrM (Da Silva et al., 2010; Kodack et al., 2017a). This is consistent with the fact that NRG1 is highly expressed in the brain and has been shown to induce the transendothelial migration of HER2/HER3-positive BC cell lines across a tight barrier of primary brain microvascular endothelia (Menard et al., 2002).

There is also evidence to suggest that HER3 activation plays a role in mediating drug resistance in BrM. Using an orthoptopic BC cell-line derived (CDX) mouse model of HER2-amplified BrM, Kodach et al. recently demonstrated HER3 upregulation within the microenvironment of BrM is responsible for the poor responses to PI3K inhibitors. However, drug sensitivity was restored upon blockade of HER3 activity. This targeted treatment strategy also circumvented resistance to HER2-targeted therapies leading to improved mouse survival. (Kodack et al., 2017a). There is therefore substantial evidence for the role of HER3 in mediating HER2 oncogenic activity in BrM.

1.5.3.2. The receptor tyrosine kinase RET

The rearranged during infection (RET) proto-oncogene encodes a transmembrane glycoprotein RTK whose activation becomes stimulated by the glial-cell derived neurotrophic factor (GDNF) family of ligands. RET signalling transduction plays an integral role in the normal development of the kidneys as well as the sympathetic, sensory and enteric nervous system. Unlike other RTKs, RET is induced to homodimerise upon indirect binding to these peptides via the GDNF receptor-α (GFR-α) family that act as Ret co ғreceptors which subsequently results in the trans-autophosphorylation of its intracellular tyrosine domains (de Groot et al., 2006).

Oncogenic activation of RET can lead to stimulation of several intracellular signalling transduction pathway involved in cellular proliferation, differentiation and migration like MAPK, PI3K, JAK-STAT, PKA and PKC pathways (Morandi et al., 2011). Activating chromosomal rearrangements and mutations are the two main mechanisms of RET-mediated oncogenesis in a number of different human cancers particularly in medullary and papillary thyroid cancers as well as lung adenocarcinomas (Sariola and Saarma, 2003; Kohno et al., 2012; Takeuchi et al., 2012a).

With regards to BC, only few activating RET kinase alterations have been reported (Kan et al., 2010b; Unger et al., 2010). However, within recent years, a large body of evidence has shown that a subset of BCs exhibit abnormally high levels of RET, especially ER-positive subtypes (Esseghir et al., 2007). The RET gene has also been shown to be a direct transcriptional target of ER and its expression is enhanced in response to estrogen treatment, suggesting a role for RET in the biology these BC subtypes (Boulay et al., 2008). Furthermore, RET may also be a potential driver of endocrine resistance. Gatelli et al. previously observed high levels of RET expression in a subset ER-positive tumours which correlated with decreased metastasis-free survival. Upon further investigation, targeting RET in an *in vivo* MBC model was shown to decrease tumour outgrowth and metastatic potential (Gattelli et al., 2013). *In vitro* studies have also demonstrated that combining RET inhibition to anti-estrogens such as letrozole and tamoxifen can restore sensitivity to endocrine therapy and improve treatment efficacy (Plaza-Menacho et al., 2010a; Andreucci et al., 2016).

1.6. The molecular evolution of breast cancer brain metastasis

Upon their newfound occupation within the brain microenvironment, metastatic tumour cells proceed to evolve, acquiring distinct mutations that may be essential for sustained outgrowth. Comparative genomic profiling between clinically matched or patient-matched pairs of primary breast tumours and their associated BrM is essential to identify these unique metastasis-associated alterations. Within recent years, a number of independent high throughput molecular characterisation studies

have been performed on both clinical and experimental samples to chart the changing (epi) genetic molecular landscape and history of BrM. Undoubtedly, such revolutionary findings have extended the depth and breadth of our understanding of this disease. Many have uncovered differentially expressed genes and mutations that are unique to BrM, which could potentially illuminate the biology underlying disease progression (Saunus et al., 2017). While several genomic studies have revealed that the overall genetic profile of BrM is shared with the breast tumour of origin, the acquisition of these BrM-specific alterations still indicate an evolutionary divergence between both disease sites. Such modifications could be critical for the formation of BrM and development of treatment resistance to targeted therapeutics as discussed below.

Via whole-exome sequencing (WES), Brastianos and colleagues reported more than half of patient-resected BrM harboured clinically actionable alterations that were absent from their corresponding primary tumour biopsies. Notably, these mutations emerged most frequently in the PI3K/AKT/mTOR, CDK, and HER2/EGFR oncogenic pathways, all of which have readily available targeted therapies. In contrast, despite this evident branching evolution, the genetic homogeneity between anatomically and temporally different patient-matched metastatic brain tumours were somehow still preserved; intracranial metastases shared nearly all potentially clinically actionable driver alterations in comparison to extracranial metastases. These landmark findings reveal that basing individualised treatment decisions for patients with BrM from their divergent primary tumour biopsies is inadequate. Instead, even determining the molecular profile from just one of multiple brain lesions would offer much more clinical information for personalised targeted therapies (Brastianos et al., 2015).

Similarly, several independent studies on smaller patient cohorts have demonstrated a significant genetic divergence between BrM and primary breast tumour tissue. Sahlia et al. performed deep genomic and epigenomic profiling on a group of unmatched BrM, and identified multiple chromosomal gains and deletions, enriched cell cycle pathways and defects in cell migration, adhesion and permeability (Salhia

et al., 2014). Targeted mutational analyses of patient-matched primary BC and BrM tumour samples have demonstrated that BrM harboured mutations in multiple oncogenic genes, namely, PIK3CA and TP53. The frequency of these aberrations were particularly higher among basal-like and HER2 enriched subtypes suggesting a correlation between the two (Lee et al., 2015b). A myriad of other 'omic studies have also reported BrM-acquired alterations in cancer-causing genes including, copy number gains of PI3KCA, overexpression of HER family members, and loss tumour suppressor PTEN expression (Bollig-Fischer et al., 2015; Priedigkeit et al., 2017a; Zhang et al., 2013; Wikman et al., 2012; Saunus et al., 2015). A few of these aberrations were also observed in BC, albeit at a lower frequency. These observations suggest that genes alterations necessary for initially breaching the BBB is hard-wired into the genome of some BC cells in order to enforce further metastatic establishment. In an IHC and array-based gene expression study, Da Silva et al showed that HER3 and its adaptor protein GRB7 were more significantly overexpressed in BrM relative to matched primary tumour from both matched and unmatched pairs (Da Silva et al., 2010). HER3 expression gains in BrM have since been confirmed, as shown by another cohort study using matched/unmatched pairs BrM and non-breast BrM originating from other primary cancer types. This suggests that HER3 elevation is a brain-specific tumour adaption, acquired by metastases to exploit the neuregulin-rich microenvironment (Saunus et al., 2015).

In addition to mutations and copy number alterations (CNAs), comparative transcriptomic profiling have also shed light on the metastatic process by revealing differential gene expression changes between resected BrM and matching primary tumours. From a targeted gene sequencing approach, one study notably identified expression gains in SOX2, which is key regulatory transcription factor of stem cell pluripotency (Lee et al., 2016). A more global view of these alterations was observed from a recent genome-wide transcriptome analysis, revealing expression changes in genes associated with migration and invasion networks which are strongly suggested to promote extravasation of BrM (Varešlija et al., 2016) .

1.7. Current clinical management of breast cancer brain metastasis

To date, there are no curative treatment options available for BrM. Instead, current management strategies are centred on providing patients with palliative care, which include the following: surgery, whole-brain radiation therapy (WBRT), stereotactic radiosurgery (SRS), chemotherapy and targeted therapies. Selecting the most appropriate method is dependent on careful assessment of a patient's KPS, their primary breast tumour subtype and systemic disease status as well as the mass, number and location of brain metastatic tumours. Therefore, a multidisciplinary and individualised treatment plan is tailored for each patient (Eichler and Loeffler, 2007).

1.7.1. Local therapies of brain metastases

Surgical resection can provide immediate significant relief of symptoms, and is an ideal treatment choice for patients with single brain lesions, or else in some cases up to 3 metastases within close proximity (Kalkanis et al., 2010). SRS is an alternative therapy for patients that are not suitable candidates for surgical removal of tumours and involves targeting a very high dose of radiation towards a small precise location in the brain, minimising the exposure to healthy surrounding tissue (Kalkanis et al., 2010).

The mainstay of local treatment for BrM is WBRT, and is important in the scenario of multiple brain lesions, which may not be detected by magnetic resonance imaging (MRI). Unlike other approaches, the goal of this method is to eliminate both macroscopic and microscopic metastases in the brain. In the post-operative setting of single brain lesions, WBRT has proven to be quite effective in the control of intracranial disease and local recurrence. Despite these remedial benefits, it has also been disapproved due to the adverse long-term neurocognitive side effects associated with brain radiation (Khuntia et al., 2006).

1.7.2. Systemic treatment modalities

Cytotoxic chemotherapy is the primary form of systemic treatment for BrM and was historically the only method available. Sadly, the chemosensitivity of most BrM is quite poor, most likely due to the inability of most cytotoxic agents to penetrate the BBB. Thus, the efficacy of this treatment route is limited to extracranial cases. However, given the recent advancements made in understanding the BBB over recent years, new treatment choices for targeted therapies have emerged such as TKIs and monoclonal antibodies. While some of these systemic agents have indeed shown promise against brain lesions, the efficacy data is still quite limited in this disease setting. This is primarily due to the frequent exclusion of this patient population from clinical trial studies of new investigational drugs (Venur and Ahluwalia, 2016). Therefore, there is still an urgent need for more preclinical and clinical studies to further evaluate the impact of these compounds on patient survival and intracranial tumour response.

1.7.2.1. Anti-HER2 agents

Following the recent advent of anti-HER2 therapies, disease management of HER2-positive BC patients with advanced disease has been revolutionised. A number of developed targeting agents have been tested for clinical application, with the monoclonal antibody, trastuzumab (Herceptin), being most widely prescribed in both the adjuvant and metastatic setting. However, despite its tremendous success over the years in treating systemic disease and improving patient survival, recent studies have disputed its efficacy in BrM. Its major limitation is highlighted by the significantly increased risk of developing BrM in HER2-positive patients after receiving adjuvant trastuzumab treatment (Olson et al., 2013) . A potential reason for this this could be due to inadequate penetration across the BBB, a common drawback shared by monoclonal antibodies that can hinder their efficacy against intracranial BrM. Therefore, this poor drug delivery system makes the brain a hospitable environment for BBB-breached metastatic cells, providing them with sanctum from cytotoxic agents (Stemmler et al., 2007; Bendell et al., 2003). An alternative hypothesis for this rising incidence of BrM could also be due to improved systemic control of both primary tumour and extracranial metastases leading to

prolonged OS (Bartsch et al., 2007). As a result, more patients that are predisposed to BrM could be exposed before succumbing to earlier disease complications.

Contrary to trastuzamab, small molecule TKIs of HER2 have demonstrated superior penetration across the BBB. Several clinical trial studies have evaluated the anti-metastatic efficacy of lapatinib, a dual reversible TKI of EGFR and HER2, in HER2-positive BC patient with progressive BrM. Disappointingly, according to the Response Evaluation Criteria In Solid Tumours (RECIST), only modest central nervous system (CNS) objective response rates (RR) of 6% were reported with single agent administrations in a phase II study (Lin et al., 2009b). However, as an amendment to this study, the addition of capecitabine to lapatinib in a separate cohort of pre-treated patients, led a significant improvement to intracranial ORR of up to 38% (Lin et al., 2009b). The most promising results of this combination therapy for BrM patients was reported in the LANDSCAPE trial. This major landmark study evaluated the administration of both agents in newly diagnosed HER2-positive BC patients with BrM administered prior to receiving WBRT, revealing a sizeable CNS ORR of 67% at the end of treatments (Bachelot et al.). The outcome these studies has encouraged further testing of lapatinib in combination with several other cytotoxic chemotherapies in BrM patients (Lim and Lin, 2014).

Furthermore, prospective clinical trials are also currently investigating the efficacy of second generation of HER2 targeting TKIs in these patients such as irreversible pan-HER inhibitors, neratinib (HKI-272) and afatinib (Gilotrif) (Kodack et al., 2015). Neratinib has shown clinical promise in treating HER2-positive BC with progressive BrM. Similar to the previous lapatinib trials, although the CNS ORR is only modest when neratinib is delivered alone (8%), a significant improvement is achieved in combination with chemotherapy, generating a CNS ORR of 49% (Freedman et al., 2016; Freedman et al., 2017). Highly selective HER2 TKI, tucatinib, also shared a similar response profile in separate pre-clinical trial studies. Again, the feasibility of this TKI was questionable as a single-agent in treating BrM with a modest CNS ORR of 7% (Metzger-Filho et al., 2014). However, recent phase Ib trials observed that a combination of tucatinib, capecitabine plus trastuzumab

demonstrated promising clinical activity in heavily pre-treated HER2-positive BC with BrM. 42% of patients had brain-specific objective response and an acceptable tolerability to treatments (Murthy et al., 2018). Taken together, these clinical trial studies highly suggest that BrM-specific resistance to anti-HER2 therapies may be circumvented in combination with chemotherapy.

Additional innovative therapeutic strategies have been designed for delivering effective HER2-targeted therapies such as novel antibody-drug conjugate ado-trastuzumab emtansine (T-DM1). This second-line agent had originally gained FDA-approval based on the phase III clinical trial EMILIA which was conducted on HER2-positive BC patients who had progressed after trastuzumab. The same study also revealed higher progression free survival (PFS) in patients receiving chemotherapy with T-DM1 instead of with lapatinib (9.6 versus 6.4 month) (Verma et al., 2012). In the setting of BrM, a recent retrospective study reported that T-DM1 yielded clinical relevant results in 10 patients with asymptomatic or progressive BrM, with an intracranial response rate of 20% (Bartsch et al., 2015). A summary of the discussed HER2-targeted therapies and their mechanism of action can be viewed in Figure 1.3 below.

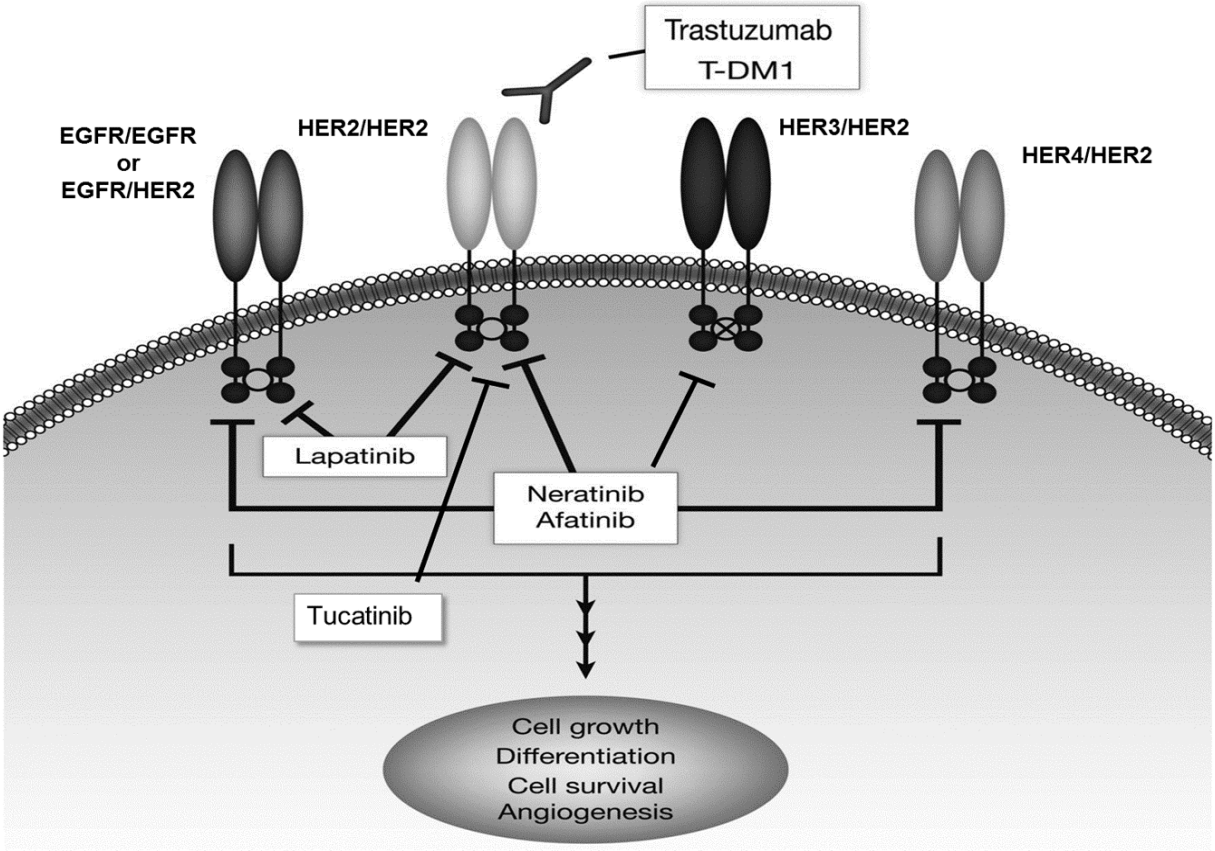

Figure 1.3: HER2-targeted therapies brain metastases in breast cancer.

Illustration summarises the FDA-approved anti-HER2 agents that have been evaluated in HER2-positive BrM patients as well as their mechanism of action. Monoclonal antibodies (trastuzumab and T-DM1) target the extracellular domain of the HER2 receptors, while TKIs (e.g. neratinib, afatinib, lapatinib and tucatinib) target the intracellular tyrosine kinase domain of their respective HER family member targets. Figure adapted from (Gradishar, 2013)

However, recent studies have shown that the HER2 expression status alone is not sufficient as a predictor for response to HER2 targeted therapies due to a number of reasons. Firstly, studies have reported alterations in HER2 status from negative in primary breast tumours to positive in brain metastases. Such findings have critical clinical implications as such patients receiving treatment according to the HER2 diagnostic profile of their primary tumour could very well benefit from anti-HER2 targeted therapies (Priedigkeit et al., 2017a). Secondly, there is an emerging

suggestion that patients with HER2-low scores may still derive benefit from anti-HER2 therapies, which was initially prompted by the response data to trastuzumab from earlier trials (Romond et al., 2005; Perez et al., 2011). However, a recent large-scale phase III study demonstrated that no improved outcomes had been observed in early non-HER2 amplified tumours post treatment with chemotherapy plus trastuzamab (Fehrenbacher et al., 2012). However, trials evaluating pan-HER inhibitors, such as SUMMT have reported significant clinical responses in HER2 or HER3 mutant cancers without HER2 gene amplification, indicating a possibility that these patients may benefit from such therapeutic approaches (Hyman et al., 2018).

1.7.2.2. Downstream HER2 signalling inhibitors

As previously mentioned, activation of HER2 results in the phosphorylation of multiple downstream molecules, which triggers a variety of signalling cascades including the RAS/RAF/MEK/ERK and PI3K/AKT/mTOR pathways. By activating different pathways, HER2 alters the gene expression levels for many proteins some of which enhance cell growth, survival and metastasis (Arteaga and Engelman, 2014). Given the high rate of acquired resistance to anti-HER2 therapy in HER2-positive BC, these downstream effectors have been explored as alternative potential targets in BrM to overcome this.

A number of clinical trials are investigating the role of targeting the mTOR pathway in managing BrM. Currently, a phase II study is being conducted to evaluate mTOR inhibitor, everolimus, in combination with trastuzumab and vinorelbine for treating HER2-positive BC patients with BrM (NCT01305941). Additionally, another ongoing clinical trial study aims to treat 47 BrM patients with a combination of lapatinib, everolimus, and capecitabine, after progressing on trastuzumab (NCT01783756).

There is also a research focus on pan- and alpha-specific PI3K inhibitors as alternative treatment strategies for BrM. Activating PIK3CA mutations represent one of the most frequent genetic aberrations in BC, with studies reporting gene enrichment in 28%–47% of hormone receptor-positive tumours and over a third of

HER2-positive tumours (Lee et al., 2015a). Notably, anecdotal evidence of CNS activity has been documented for a HER2-positive BrM patient case receiving combined treatment with trastuzumab and BEZ235, a dual PI3K and mTOR inhibitor (Krop et al., 2012). Preclinical orthotopic PDX models of HER2-positive BrM have also exhibited durable tumour regressions in response combined inhibition of PIK3 and mTOR (Ni et al., 2016). Some clinical signs of intracranial tumour shrinkage was observed from a recent a Phase Ib study in patients with progressive BrM after treatment PIK3 inhibitor, buparlisib (BKM120) in combination with trastuzumab and capecitabine. However, tumour growth in the brain was still uncontrolled and the majority of these patients had further progressed during the study. The frequency of these PIK3CA alterations is lower in TNBC cases, with reports of only 7-13% harbouring somatic variants (2012; Millis et al., 2015). Despite this, a phase II study is currently in progress to examine the effectiveness of buparlisib in combination with capecitabine for TNBC patients with BrM (NCT02000882).

1.7.2.3. Targeting the VEGF pathway

A number of studies have reported that some BrM manifest a high degree of angiogenesis as revealed by their abnormal intracranial vascular network and morphology (Bullitt et al., 2007). Experimental tumour models have shown that the vasculature system of BrM is far more enriched than their primary tumour counterpart, which strongly suggests their dependency on a well-established blood network (Monsky et al., 2002). This particular microenvironment may be essential for metastatic growth and progression by providing oxygen and nutrients via an adequate blood supply (Bergers and Benjamin, 2003). The formation of new blood vessels is stimulated by a key pro-angiogenic protein known as the vascular endothelial growth factor (VEGF). In preclinical models, targeting the receptor of this pathway with anti-angiogenic agents has shown to inhibit brain metastatic growth, re-affirming the necessity of angiogenesis for effective colonisation of the brain by BC cells (Kim et al., 2004). Thus, the clinical prospects of VEGFR inhibitors such as

bevacizumab in treating patients with MBC have been highly anticipated, especially for those with HER2-negative tumours.

Yet, multiple phase III trials have revealed poor OS in MBC patients with the addition of bevacizumab to their treatment regimens (Miller et al., 2007; Miles et al., 2013). Given the biologic nature of the drug, the majority of these studies did not include patients with BrM due to initial concerns of inducing potential intracranial brain haemorrhage. However, the safety and tolerability of bevacizumab has been proven in the management of primary brain tumours such as GBM (Chamberlain, 2011; Vredenburgh et al., 2007). Since then, the efficacy of bevacizumab plus chemotherapy for the treatment of BrM has been carried out in a number of clinical trials. One study executed a phase II clinical trial of carboplatin and bevacizumab in a cohort of BrM patients, the majority of which were HER2-positive and had been pre-treated for both intracranial and extracranial disease. A clinically promising CNS response rate of 45% in 38 patients was reported (Lin et al., 2013). In a second phase II study, progressive BrM patients that had progressed from WBRT, were pre-administered with bevacizumab 1 day before receiving etoposide and cisplatin. A significant intracranial response rate of 79% was observed in 39 recruited patients (Lu et al., 2015). The results of this treatment regime has prompted a further extension to this trial study, which is currently ongoing and actively recruiting (NCT02185352). However, while the intracranial response rates to this therapeutic strategy have been favourable, the interpretation of these results should be taken with caution. Given the anti-oedema effects of bevacizumab, accurate visualization of brain lesions can be challenging, resulting in a potential underestimation of tumour burden (Lin, 2013).

1.8. Hypothesis

BrM presents a major cause of neurologic morbidity and severely impacts on patient quality of life. Despite intensive research efforts in understanding the molecular etiology of this disease, current management strategies for BrM still remain a major clinical challenge. This deficiency was the stimulus for the work contained within this thesis.

Several genomic studies have compared the molecular profile of primary breast tumours and BrM with the hopes of discovering potential vulnerabilities exclusive to BrM. From these findings, a considerable amount of genetic divergence was reported between both neoplastic sites, implying complex evolutionary adaptations to the unique brain microenvironment. However, the possibility of exploiting these alterations as clinical targets to improve BrM treatment has been poorly investigated. To address this, our group previously conducted genome-wide RNA-Seq on a diverse clinical cohort of 21 patient-matched breast tumours and their associated resected BrM.

Following this comprehensive transcriptome analysis, recurrent BrM-acquired enrichments were identified in multiple RTKs, many of which are clinically significant. Therefore, these findings constitute the hypothesis for this thesis, being that such aberrations could offer effective therapeutic targets for the treatment of BrM tumours, with potential applicability to all BC subtypes.

1.9. Aims

The aims of this research investigation will be as follows:

1. Select the most promising actionable target RTKs and validate their observed transcriptomic changes at a protein level by performing IHC analysis on all available FFPE samples of the 21 patient-matched cases.

2. Determine the functional efficacy of inhibiting target RTKs to treat BrM using small molecule TKIs. The anti-tumour efficacy of targeted treatments will be assessed by using:
   (i) Specialised *in vitro* brain-metastasising cell lines and primary cells derived from a patient BC BrM tumour.
   (ii) An *in vivo* PDX tumour model of BC BrM
   (iii) Fresh *ex vivo* explant tissues from patients undergoing BrM resection

2. Material and Methods

2.1. Patient Sample Collection

The patient inclusion criteria consisted of BC cases that had paired formalin-fixed paraffin-embedded (FFPE) tissue from matched primary and resected BrM. A total of 21 patient-matched tumour cases were eligible and investigated for this study following informed patient consent and ethical approval from two participating institutions (University of Pittsburgh IRB#PRO15050502, RCSI IRB#13/09/ICORG09/07). A Unique Identifier Number (UIN) was applied to each patient to maintain anonymity and confidentiality. Patient databases were stored securely in an encrypted Microsoft Excel file. Detailed information about each patient can be found in Appendix I, Table 8.2.

2.1.1. Tissue processing

Sectioned FFPE blocks were H&E stained and then reviewed by a pathologist to ensure histology and tumour cell content. Eligible cases with sufficient tumour cells from both the breast and brain neoplastic tissues were subjected DNA/RNA extraction using Qiagen's AllPrep kit according to manufacturer's instructions.

2.1.2. RNA-sequencing.

Library preparation was performed using 100 ng of RNA and Illumina's TruSeq RNA Access Library Preparation protocol. Indexed, pooled libraries were then sequenced on a High Output flow cell with an Illumina NextSeq 500 (paired-end reads, 2 X 75 bp). A target of 25-50 million reads per sample was used to plan indexing and sequencing runs. Additionally, 12 samples (RCS cohort) were also processed using Illumina's TruSeq DSN library preparation protocol. Indexed, pooled libraries were then sequenced with an Illumina HiSeq 2000 (paired-end reads, 2 X 90 bp). A target of 30-50 million reads per sample was used to plan indexing and sequencing runs.

2.1.3. RNA-Seq quantification and normalization

All RNA sequencing expression quantification, normalization, data quality assessment and analysis was conducted by two bioinformaticians; Dr Ailis Fagan (EORG, RCSI) and Dr Nolan Priedigkeit (University of Pittsburgh). FASTQ files were quantified using k-mer based lightweight-alignment (*Salmon* v0.7.2, quasi-mapping mode, 31-kmer index established from GRCh38 Ensembl v82 transcript annotations, seqBias and gcBias corrections)(Patro et al., 2017). Read counts and percentage alignment were calculated. Transcript abundance estimates were collapsed to gene-level values using R package, tximport (Soneson et al., 2015). RNA-Seq data were aligned using Salmon and were uploaded into R using tximport. The imported genes were filtered to only include protein coding genes, this reduced the gene set down to 19,808 genes. A pseudocount of 1 was added to each of the count values before the counts were converted to log2 values. To exclude non- or lowly expressed genes, only genes with a TPM value greater than 0.5 in at least 10% of samples were considered for gene set enrichment and clinically actionable kinase evaluation. Log2 transformed TMM-normalised CPM (log2normCPM) values were implemented for subsequent analyses (Robinson et al., 2010; Robinson and Oshlack, 2010).

2.1.4. Gains and losses in clinically actionable kinases.

All enriched kinase genes were then prioritised according to the degree of clinical targetability. Clinically actionable and kinase gene sets were obtained from the Drug Gene Interaction Database (DGIdB 2.0) and the overlap between the two sets were used to define and prioritise clinically actionable kinases (n =105) (Wagner et al., 2016). Continuous expression fold-changes calculated from log2normCPM values with genes being considered to be up or down regulated if they exhibited a log2 fold change greater than ± 1.5 and an adjusted p-value of <0.05. These values were transformed to discrete, stringent expression gains by defining an “expression gain” as a log2FoldChange greater than the 95th percentile (log2FoldChange = 1.198) of all gene and case fold-changes. After assigning discrete expression gains, data for recurrent gains (n>1 pair) was visualised using the *oncoprint* function in

ComplexHeatmap (Gu et al., 2016). To plot and statistically assess HER2 and RET expression differences, ladder plots and paired Wilcoxon signed-rank tests (primary vs. metastasis) were implemented on normalised log2 expression values.

2.2. Whole-exome sequencing

All brain metastatic tumours from *ex vivo* and PDX work were subjected to DNA extraction following standard protocols of the Qiagen GeneRead DNA FFPE kit. Extracted genomic DNA was assessed for quantity and quality using Thermo Scientific NanoDrop spectrophotometer. Downstream bioinformatics analysis of WES data was performed by Dr. Damir Vareslija. Prior to WES library preparation, genomic DNA with acceptable purity yields were mechanically sheared by Covaris technology into fragment sizes ranging approximately between 100bp -150bp. To end repair fragmented DNA extracts, an “A” base was supplemented to the 3′-end of each strand. Adapter oligos were ligated to dA-tailed fragments before amplification and sequencing. Adapter ligated DNA fragments were amplified using ligation-mediated PCR (LM- PCR) and were then purified and hybridised to the exome array for enrichment. Non-hybridised fragments were washed out. Captured products were then circularised. The rolling circle amplification (RCA) was performed to produce DNA Nanoballs (DNBs). The resulting fragment library construction was then sequenced on BGISEQ-500 sequencing platforms (BGI Genomics, Hong Kong). All raw sequencing data for each study sample was stored in FASTQ format which was filtered to generate clean data and mapped to the human reference genome. Burrows-Wheeler Aligner (BWA) (Li and Durbin, 2009) software was used to do the alignment. Accurate variant calling was ensured by following the recommended Best Practices for variant analysis with the Genome Analysis Toolkit (GATK, https://www.broadinstitute.org/gatk/guide/best-practices). GATK (DePristo et al., 2011), was used to recalibrate base quality scores and generate local realignments around InDels. Picard tools were utilised to remove duplicate reads. The sequencing depth and coverage for each study sample was calculated from the alignments. A number of data filtering steps was performed in order to minimise any potential

background noise in the sequencing data which included (1) Removing reads that contained sequencing adapters; (2) Removing reads whose low-quality base ratio (base quality less than or equal to 5) was more than 50%; (3) Removing reads whose unknown base ('N' base) ratio was more than 10%. All genomic variations, including SNPs and InDels were identified using HaplotypeCaller of GATK (v3.6). Subsequently, a more stringent filtering approach was used to make high-confident variant calls using the SnpEff tool (http://snpeff.sourceforge.net/SnpEff_manual.html). The final variants and annotation results were used in the downstream advanced analysis. The SnpEff tool was used to annotate all SNPs or InDels that resulted in protein-coding alterations and to identify the amino acids that are affected. Several filter-based annotations were also applied to identify specific mutations, including those reported in dbSNP v141, variants with a MAF<1% in the 1000 Genomes Project, non-coding synonymous SNPs with a SIFT score of <0.05 and intergenic variants with a GERP++ score >2. All identified mutations were then cross-referenced and filtered utilising ExAC, dbSNP and ClinVar databases.

2.3. Quantitative analysis of ERBB2 amplification

Nanostring nCounter CNV assay was employed to evaluate the ERRB2 copy number alterations in 13/21 primary and metastatic paired BC samples from the Pittsburgh cohort of patients (PITT) where sufficient DNA was already available. A copy number cut-off value of ≥5 was selected for HER2 amplification. FISH testing was used to evaluate the selected matched cases from the RCSI cohort (RCS) that were borderline HER-positive (2+) in the primary BC but had changed to positive in BrM. This method employs fluorescently labelled probes which specifically hybridise to and quantifies target nucleic acid sequences. The FISH probe used was the Abbott LSI HER-2/SE17 dual-colour probe on the Leica Bond III automated platform (Cat# TA9217). All quantifications were performed by trained pathologists at the Pathology Department, Beaumont Hospital, Dublin 9, in accordance with ASCO/CAP HER-2 testing guidelines (Wolff et al., 2013).

2.4. Nucleic Acid Biochemistry

2.4.1. RNA extraction from FFPE samples

FFPE sections underwent RNA extraction using RNeasy FFPE RNA kit (Qiagen, #73504) designed specifically for effective purification of RNA from FFPE tissue sections. Using a microtome, 3-4 20 µm thick sections were freshly cut from each FFPE block. All paraffin was removed by treating sections with deparaffiniztion solution (Qiagen, #19093) and incubated at 56°C for 3 min, then allowed to cool at room temperature. If the sample became solid or waxy after cooling, an additional amount of deparaffinization solution was added and the incubation step was repeated. Buffer PKD was then added followed by a 1 minute centrifugation step at 10,000 rpm. Next, proteinase K was added to release RNA from the sections and mixed into the clear lower phase before incubating samples at 56°C for 15 minutes, then at 80°C for 15 minutes. The second incubation step reverses formalin crosslinking of the released nucleic acids, improving RNA yields and quality. After incubations, the lower phase was transferred into a new tube before incubating it for a further 3 minutes on ice, followed by a 15 minute centrifugation step at 13,500 rpm. The supernatant was transferred into a new tube taking care not to disturb the pellet. DNase Booster Buffer, equivalent to a tenth of the total sample volume was added next, along with 10 µL DNase I stock solution before mixing tube contents and incubating at RT for 15 minutes. The purpose of this step is to eliminate all genomic DNA. The lysate was then homogenised with Buffer RBC and 100% ethanol to adjust binding conditions for RNA. The sample was then transferred to an RNeasy MinElute spin column and centrifuged at ≥10,000 rpm for 15 seconds. The flow-through was discarded and the column was wash twice with 500 µL Buffer RPE. The flow-through was discarded and the column was centrifuged once more to ensure no remaining residue. Finally, the column was placed into a clean eppendorf tube and the RNA was then eluted in 20 µL of RNase-free water. RNA concentration and quality was quantified by measuring on a NanoDrop spectrophotometer. RNA was stored at -80°C for future use.

2.4.2. Reverse transcription PCR

Superscript III First Strand Synthesis System for RT-PCR (18080400, Invitrogen) was used to transcribe mRNA into complementary DNA (cDNA). 500ng of RNA was primed with 1 µL of random hexamers and 1 µL 10 mM DNTP's to a final volume of 10 µL with nuclease-free water. The sample was heated to 65°C for 5 minutes and placed on ice immediately after to cool. 10 µL of cDNA synthesis mix (Table 2.1) was added to each sample. The RNA/synthesis mix was then heated to 25°C for 10 minutes, followed by 50°C for 50 minutes. A control sample, without superscript enzyme (–RT) was also included. cDNA was stored at -20°C until ready for use.

Table 2.1: Conditions and reagents used for RT-qPCR

PCR Master Mix	Volume (µl) per sample
10x RT Buffer	2
25mM MgCl2	4
0.1M DTT	2
RNase Out	1
Superscript III	0.5
Nuclease free H2O	0.5
Total Volume	10

2.4.3. Polymerase chain reaction PCR

The polymerase chain reaction (PCR) is a frequently utilised research tool for amplifying specific target regions of DNA. The process relies on DNA polymerase and nucleotides as well DNA primers which binds specifically to the DNA region of interest on the DNA template. The reaction is repeatedly subjected to a sequence of temperature changing cycles which facilitates the synthesis of many copies of target DNA. Semi quantitative real time PCR, or qPCR was used to detect and quantify

relative levels of HER2 and RET mRNA in one of the matched tumour cases used for the *ex vivo* study (T638). Unlike conventional PCR, this technique determines the amount of amplified targeted DNA during the reaction rather than at the end. This was performed through pre-designed Taqman assays (Thermo Fisher Scientific) and analysed on the StepOnePlus Real Time System (Applied Biosystems). Master mix components and thermocycling conditions were used as per manufacturer's instructions. The amplicons are detected by fluorescent dye labelled taqman probes which emit a fluorescent signal upon hybridization with the complementary target DNA sequence. Therefore, an increase in fluorescence intensity is proportional to the amount of synthesised PCR product. Relative expression levels of target genes were calculated using the comparative $2^{-\Delta\Delta C_t}$ relative to human B-actin that was used as the control sample. Probes that were used are RET (Hs01120030_m1), ERBB2 (Hs01001580_m1) and Human ACTB was used as the control (#4333762F, Thermo Fisher Scientific).

2.5. Immunohistochemistry

IHC is a technique used to selectively evaluate the presence and cellular location of proteins in tissues. In short, this method allows a particular protein of interest to be visualised by using antibodies that binds specifically to their target antigen.

IHC was performed using the Dako EnVisionTM Kit on formalin-fixed paraffin-embedded tissue in the form of full face tumour specimens. A microtome was used to cut paraffin sections at a thickness of 5 µM which were mounted on Superfrost Plus slides. Slides were baked at 65°C for 6 hours to fix the tissue onto the slides. Sections were de-paraffinised in xylene in two separate baths for 3 minutes each. Sections were rehydrated gradually through decreasing concentrations of industrial methylated spirits (IMS, 100% twice, 70% once). The slides were then rinsed in PBS for 5 minutes. Heat-mediated antigen retrieval was performed by placing slides in a closed plastic vessel containing pre-heated 10mM sodium citrate buffer (pH 6.0) (Appendix I). Slides were then heated at high power in a domestic microwave for 8 minutes before cooling for at least 20 minutes at room temperature. Afterwards, slides were then washed twice in TBS containing 0.1% Tween (TBS-T) for 5 minutes

before drawing a hydrophobic barrier around each tissue specimen section using a water repellent marker. Endogenous peroxidase activity was blocked by incubating slides in peroxidase blocking solution (H2O2) (DAKO) for 5 minutes followed by another 5 minute wash in dH2O. Slides were then incubated with primary antibody of choice for 1 hour at 25˚C or else overnight at 4 ˚C for all phosphorylation IHC stainings. Primary antibody conditions were determined by following the manufacturer's instructions and subsequently optimised where necessary. Details of the recommended primary antibody dilutions and incubations conditions can be found in Table 2.2. Host species- and concentration-matched IgG isotopes were used as negative controls. All primary antibodies and IgG controls were diluted to the optimised concentration in 0.05mol/L Tris buffer (pH 7.2-7.6) containing 1% (w/v) Bovine Serum Albumin (BSA). Following primary antibody incubation, slides were washed for 5 minutes in TBS-T three times and then incubated with the appropriate biotinylated secondary antibody. Three TBS-T washes were repeated on the slides again before subsequently developing each tissue section in 3, 3-diaminobenzidine tetrahydrochloride (DAB) for 5 minutes. The reaction was then quenched by immersing the slides in dH2O for 5 minutes. Slides were counterstained with hematoxylin (Sigma Aldrich) for 3 minutes. Immediately afterwards, slides were washed under gentle running tap water for 5 minutes. The slides were gradually dehydrated by immersing in increasing concentrations of industrial methylated spirits (IMS, 70% once, 100% twice) and in xylene two times, each at 3 minute intervals. Lastly, slides were allow to fully dry before applying them each with DPX mountant (Sigma Aldrich) and a cover slip.

Table 2.2: IHC primary antibody conditions

Target protein	1° Antibody and supplier	Working 1° Antibody dilutions	Antigen Retrieval	2° Antibody
Ki67	Mouse mAb, Dako clone MIB-1, M2740, #A97064	1 in 100	Sodium Citrate	Anti-mouse IgG
ER	Mouse mAb, novacastra leica, NCL-L-ER-6F11, #6043537	1 in 50	Sodium Citrate	Anti-mouse IgG
PanCK	Mouse mAb, novacastra leica, NCL-L-AE1/AE3, #6038590	1 in 50	Sodium Citrate	Anti-rabbit IgG
HER2	Mouse mAb novacastra leica, NCL-L-CB11, #6046036	1 in 40	Sodium Citrate	Anti-mouse IgG
RET	Rabbit polyclonal, Sigma Prestige Antibodies, #A97064	1 in 150	Sodium Citrate	Anti-rabbit IgG
EGFR	Rabbit mAb, D38B1, Cell signalling, #4267	1 in 100	EDTA	Anti-rabbit IgG
HER3	Rabbit mAb, D22C5, Cell Signalling, #12708	1 in 200	EDTA	Anti-rabbit IgG
HER4	Rabbit mAb, 111B2, Cell Signalling, #4795	1 in 200	EDTA	Anti-rabbit IgG
pHER2 (Tyr1221/1222)	Rabbit mAb, 6B12, Cell Signalling, #2243	1 in 200	EDTA	Anti-mouse IgG
pRET(Y1062)	Rabbit polyclonal, Abcam, #ab51103	1 in 400	EDTA	Anti-rabbit IgG
pEGFR (Tyr1068)	Rabbit mAb, D7A5, Cell Signalling, #3777	1 in100	EDTA	Anti-rabbit IgG
pHER3 (Tyr1289)	Rabbit mAb, D1B5, Cell Signalling, #2842	1 in 500	EDTA	Anti-rabbit IgG
pHER4 (Tyr1284)	Rabbit mAb, 21A9, Cell Signalling, #4757	1 in 200	Sodium Citrate	Anti-rabbit IgG
p-AKT (Ser473)	Rabbit polyclonal, D9E, Cell Signalling, #4060S	1 in 50	Sodium Citrate	Anti-rabbit IgG
p-p70 S6 Kinase (Thr389)	Rabbit polyclonal, Cell Signalling, #9205	1 in 100	Sodium Citrate	Anti-rabbit IgG
p-ERK (T202/Y204)	Rabbit polyclonal, , Cell Signalling, #2105S	1 in 400	Sodium Citrate	Anti-rabbit IgG
p-RAF (Ser259)	Rabbit polyclonal, Cell Signalling, #9421S	1 in 50	Sodium Citrate	Anti-rabbit IgG
p-MTOR (Ser2448)	Rabbit polyclonal, 49F9, Cell signalling, #2976S	1 in 50	Sodium Citrate	Anti-rabbit IgG

2.5.1. Analysis of IHC data

All IHC analysis and scoring was conducted independently by two researchers. Slides were viewed by light microscopy on an Olympus IX51 inverted microscope. High resolution Images were captured at either 10x, 20x or 40x magnifications.

2.5.1.1. IHC evaluation of HER2 positivity

Interpretation of HER2 staining followed validated scoring diagnostic criteria according to the 2013 ASCO/CAP HER-2 testing guidelines (Wolff et al., 2013). This method of HER2 scoring is established on a 0-3 scale which considers both the intensity and completeness of membrane staining as well as the coverage of stained tumour cells. The scoring system is summarised in Table 2.3 below. Examples of staining patterns for tissue scored 0, 1+, 2+, and 3+, can be found in Appendix I, Figure 8.1.

Table 2.3: HER2 IHC positivity scoring criteria

Staining Pattern	**Intensity Score**	**Assessment**
No staining in cells	0	Negative
Weak incomplete membranous/cytoplasmic in >10% of tumour cells	1+	Weak
Weak to moderate membrane/cytoplasmic staining in >10%	2+	Equivocal
Strong membrane/cytoplasmic staining in >10%	3+	Strong

2.5.1.2. IHC scoring system for total/phosphorylated RET and HER family members

RET and HER family IHC scoring was evaluated based on (1) staining intensity (ie. 0=Negative; 1=Weak; 2=Moderate, 3=Strong, 4=Very Strong) cellular location (cytoplasmic, membranous, nuclear), and coverage (ie. 2= <40%; 3 <60%; 4 =<80%). EGFR and pEGFR immunostaining data was predominantly membranous, whilst HER3, HER4 and RET and their phosphorylated forms were cytoplasmic. The same scoring criteria was used to assess pHER2 staining This scoring system was similar in principle to several methods already published in literature and was originally adapted from them (Kodack et al., 2017c; Saunus et al., 2015). The modified scoring system followed in this study is indicated in Table 2.4. Positive reference staining of total and phospho- RET/HER family can be found in Appendix I, Figure 8.1, Figure 8.2, respectively.

Table 2.4: Scoring criteria of RET and HER family IHC assay

Staining Pattern	Intensity Score	Assessment
No staining in cells	0	Negative
Weak incomplete membranous	1+	Weak
Weak staining +/- <40% positive	2+	Moderate
Heterogenous or moderate to strong in <60%	3+	Strong
Strong staining in >80% of cells	4+	Very Strong

2.5.1.3. Ki67 quantification analysis

Ki67 calling was performed according to the following recommended guidelines (Dowsett et al., 2011). Only nuclear ki67 staining was counted and incorporated into a Ki67 score (= % ki67 positive stained tumour cell nuclei among total number cell nuclei) where staining intensity was considered irrelevant. A minimum of 500 cells were counted to give a score, Quantitative analysis was performed on 3 non-consecutive tissue sections that were at least 10 cuts apart and a total of 5-10 images were analysed per treatment group.

2.5.1.4. Downstream signalling quantification analysis

Downstream pathway analysis of pAKT, p70S6K, pSRC, pERK and pRaf were quantified using the Aperio Digital Pathology imaging software. 5-10 images were analysed per treatment group. To evaluate the amount IHC staining present in each image, the Aperio Positive Pixel Count Algorithm was applied using the ImageScope program which quantifies both the number and intensity of positive pixels. The algorithm is pre-configured with a set of input parameters for staining quantification: brown colour staining was selected for as positive pixels which are measured in three intensity ranges (weak, positive and strong). The sum of positive pixels are quantified in each intensity range as well as the average intensity, ratio of strong/total number and average intensity of weak+positive pixels. Pixels that do not meet the set colour specification are deemed as negative staining but are still counted for by the algorithm in order to determine the % of positive to total stained areas.

2.6. *In vitro* cell culture

2.6.1. Cell culture environment

All routine cell culture work was carried within a sterile environment using a laminar flow hood. All cells were maintained in a humid 5% (v/v) CO_2 atmosphere at 37 ˚C. All cell culture work was performed using standard aseptic techniques.

2.6.2. Cell culture maintenance

All used tissue culture reagents can be found in Appendix I, Table 8.1. BC and primary cell lines were cultured in T-75 cm^2 filtered tissue culture flasks (Sarstedt, Germany). Cell were passaged at approximately 70%-80% confluency by washing them in 5 ml of phosphate buffer saline (PBS; Oxoid Limited, Basginstoke, Hampshire, England) followed by incubation with 2 ml of 0.05% trypsin (v/v)/0.02% EDTA (v/v) solution (Sigma Aldrich) for 3 minutes at 37 ˚C. Trypsin was subsequently quenched with 8mls of appropriate cell culture media before transferring the cell suspension into a 15ml conical tube (Greiner Bio-One, Germany) and centrifuged at

1200rpm for 3 minutes. The supernatant was discard and the cell pellet was resuspended in the required volume of cell culture medium. The final cell suspension was sub-divided into a new T-75 cm^2 flask at a lower confluency.

2.6.3. Culturing of cells from cryo-storage

Cryovials containing frozen cells were removed from liquid nitrogen and allowed to defrost rapidly at room temperature before transferring contents into a 15ml conical tube containing 7 ml of cell culture medium. Cell suspension was centrifuged at 1200 rpm for 3 minutes. The supernatant was discarded and the cell pellet was resuspended in 2mls of fresh medium. This suspension was transferred into a T-75 cm^2 flask to which a further 8mls of fresh cell culture medium was added. The cells were incubated at 37˚C for 4 hours before checking cells for viability. Once the majority of the cells had adhered the cell culture medium was refreshed.

2.6.4. Cell counting

To seed cells according to the recommended seeding density for each functional assay, cells were manually counted using a haemocytometer (Neubauer, Germany). After cells had been trypsinised, 20 µL of cell suspension was mixed with 20 µL of Trypan blue (Sigma Aldrich) and 10 µL of this solution was pipetted onto the haemocytometer. The cells were counted in the two square grids on the left and on the right, before obtaining an average and multiplying this by $2x10^4$ to obtain the number of cells per ml of cell suspension. Counting was performed in duplicate and an average count per ml was calculated. The require volume of cell suspension was calculated and seeded into the appropriate cell culture vessel.

2.6.5. Breast cancer cell lines

For *in vitro* comparative studies, specialised brain seeking ER-positive and triple negative breast (TNBC) cancer cells in addition to PDX cell culture models established from resected brain metastatic tumours were utilised to evaluate the anti-tumour efficacy of cabozantinib and afatinib.

2.6.5.1. LY2 cell line

LY2 cells were a kind gift from Dr. Robert Clarke, Department of Oncology, Georgetown University, Washington DC, USA. These cells were initially derived as stable variants of the MCF-7 cell line and are resistant to LY117018, a potent anti-oestrogen (A. Bronzert et al., 1985). LY2 cells were maintained in phenol red-free modified eagle medium (PRF-MEM) which was supplemented with 10% fetal calf serum (FCS) (Sigma Aldrich), 1% L-glutamine (L-Glut), 1% penicillin-streptomycin (PS). They are an ER-positive and HER2-negaitve endocrine therapy-resistant cell line and our lab have previously demonstrated their ability to readily metastasise to distant organs, including the brain (Figure 2.1A, Figure 2.1D, Figure 2.1F) (McBryan et al., 2015).

2.6.5.2. MDA-231-BrM2 cell line

MDA-231-BrM2 cell line was obtained from the Massagué Lab, MSKCC, New York. It is a highly metastatic derivative of the triple negative MDA-MB-231 cell line with brain-seeking selectivity (Figure 2.1B, Figure 2.1D) (Bos et al., 2009a). This subline was initially established from the parental cells after repeated rounds of intracardiac injection, brain resection, tumour cell dissociation and re-injection into mice, generating a clonal population of cells that have been demonstrated to specifically metastasise to the brain (Figure 2.1F). MDA-231-BrM2 cells were cultured in Dulbecco's MEM with supplemented with 10% FCS, 1% L-Glut, 1% PS.

2.6.5.3. T347-2c primary cell line

The T347-2c brain metastatic primary cell line was initially derived from an ER-positive, PR-negative and HER2-positive patient tumour, which had been expanded in NOD-SCID mice as previously described (Figure 2.1C, Figure 2.1D) (Ward et al., 2018b) . T347-2c primary culture cell line was derived from T347x brain metastasis tumour. The cell line was cultured in human breast epithelial cell culture (HBEC) media. (Vareslija et al., 2017).

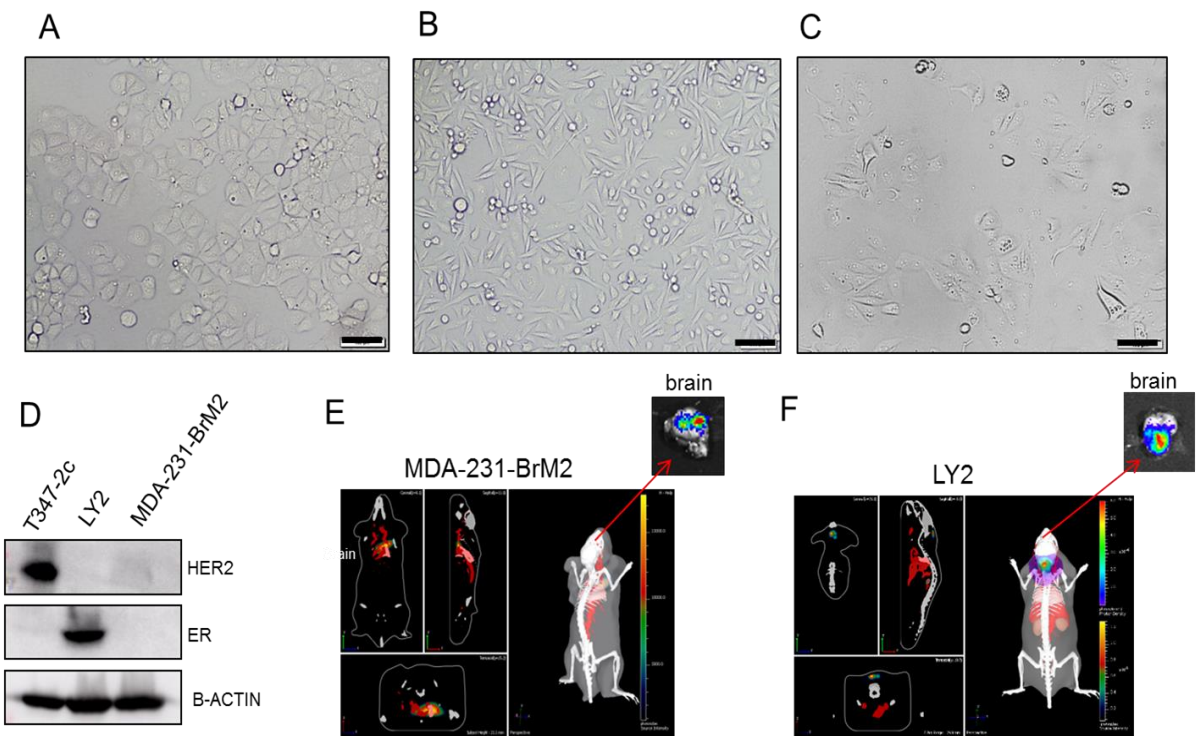

Figure 2.1: *In vitro* cell line models of breast cancer brain metastases.

Light microscopic images showing the morphology of (A) LY2 cells, (B) MDA-231-BrM2 cells (C) T347-2c cells. All Images were captured at 10x magnifications; scale bars correspond to 100µm. (D) Western blotting of key biomarkers represented in our cell line models (E; F) Representative *in vivo* and *ex vivo* bioluminescence images of mice following intracardiac injection of luciferase labelled brain seeking MDA-231-BrM2 and LY2 breast cancer cell lines.

2.6.6. Cell culture treatment conditions

For 24 hours prior to any *in vitro* cytotoxic assays, all cells were cultured at reduced serum levels (3% FCS) in their appropriate cell culture mediums. The T347-2c primary cell line was grown for 24 hours in Hyclone DMEM/F12 (1:1) containing 3% FCS, 1M HEPES and 1% (L-Glut). Drug treatments were prepared at the required concentration for each cell line by diluting in appropriate reduced serum media. For all *in vitro* functional assays, following seeding at the appropriate densities, cells were then incubated with treatment conditions outlined in Table 2.5. Concentrations of afatinib and cabozantinib were determined from publically available IC50 values

obtained from the Genomics of Drug Sensitivity in Cancer (GDSC) database and were based on the levels required for inhibiting the ERRB2 and RET receptor, respectively (Iorio et al., 2016). The same concentrations were also used for the *ex vivo* studies as mentioned in Section 2.8.2.

Table 2.5: Treatment conditions for *in vitro* drug efficacy study

Treatment	**Final concentration**	**Treatment time**
DMSO (Sigma-Aldrich)	0.001%	24 hours (Cell motility assay) 72 hours (Cell proliferation assay)
Cabozantinib (CT-XL184, Chemietek, USA)	10 nM	24 hours (Cell motility assay) 72 hours (Cell proliferation assay)
Afatinib (#CT-BW2992, Chemietek, USA)	25 nM	24 hours (Cell motility assay) 72 hours (Cell proliferation assay)

2.7. *In vitro* functional assays

2.7.1. Cell motility assay

Cell motility plays an essential role in several biological and pathological events including embryogenesis, wound healing and angiogenesis. This cellular behaviour is also a key characteristic of cancer cell invasion, metastasis and angiogenesis. The ability of cells to move is dependent on complex interactions between cell adhesion molecules, the cytoskeleton and a large network of signalling molecules. Thus, evaluating cell motility has become a fundamental tool in determining the aggressive nature and metastatic ability of cancer cells. To assess individual movement per cell the Cellomics® cell motility kit (Thermo Scientific, K0800011) was employed.

The wells of a 96 well plate were coated with collagen (Sigma Aldrich) and incubated for 1hr at room temperature (RT). Wells were then washed with 100 ul of sterile PBS. 75µl of fluorescent beads (supplied in the Cellomics® kit) were added to each well before wrapping the plate in tinfoil and incubating it for 1hr at 37°C in the incubator. During this time, all cell lines were harvested, trypsinised and a cell suspension of 5000 cell/ml was prepared. Wells were washed five times in 1x Wash Buffer (supplied in the Cellomics® kit) before adding 50 µl of prepared cell suspension to each well. The plate was then wrapped in tinfoil and incubated for 24hr at 37°C. In order to fix the cells, 200µl of a formaldehyde solution was added to each well and incubated for 1 hr. The formaldehyde was aspirated and 100µl of 1x Permeabilisation Buffer (Kit) was pipetted into each well and left at RT for 15 min. Wells were carefully washed and stained for 30 minutes with Rhodamine Phalloidin. Wells were washed four times with 1x Wash Buffer and images were taken on an inverted microscope. Track areas were measured using Olympus cellF imaging software and compared with a Student t test.

2.7.2. Cell proliferation assay

The MTS CellTiter 96® Aqueous reagent (Promega) system was utilised to assess cell proliferation in LY2, MDA-231-BrM2 and T347-2c cell lines. This is a time-effective and dependable colorimetric method for determining the efficacy of drugs on various cancer cell lines by quantifying the number of metabolically viable cells after treatments.

The procedure was performed in a 96-well plate and each cell line was seeded at 2000 cells per well. Cells were incubated overnight to allow adherence at the bottom of the well before exchanging the normal media with serum depleted media cells for 24 hours. The media was then then removed with care to prevent any disturbance to the bottom cell monolayer and replaced with serum-free media containing the appropriate drug treatment concentrations. Each treatment condition was carried out in triplicate wells of which cells were grown in at 37°C for 72 hrs. 30 µL of MTS solution was then added into each well. As this is a light-sensitive reagent, this step was performed in a dark laminar flow hood and the plate was wrapped in

tinfoil before incubating the reaction for 4 hrs at 37°C. The reagent also contains the active tetrazolium 3-(4,5-Dimethylthiazol-2-yl)-5-(3-carboxymethoxyphenyl)-2-(4-sulfophenyl)-2H tetrazolium, inner salt; MTS] and an electron coupling reagent (phenazine methosulfate) PMS. MTS is bioreduced by cells into a brown-coloured formazan product that is soluble in tissue culture medium. The quantity of formazan product in each well can be determined by measuring their absorbance values at 490 nm in a spectrophotometer machine (Perkin Elmer, USA) which is directly proportional to the number of metabolically active cells within. The average was obtained for each triplicate treatment and results were normalised to the vehicle control.

2.8. *Ex vivo* cell culture of patient breast cancer brain metastases

2.8.1. Patient sample collection for *ex vivo* work

Ethical approval for all studies on human samples was acquired from the Medical Ethics Committee, Beaumont Hospital. Biological samples were only used from patients who provided written informed consent for the use of their tissue in any subsequent research. Detailed information about each patient can be found in Appendix I, Table 7.4. A Unique Identifier Number (UIN) was applied to each patient to maintain anonymity and confidentiality. Patient databases were stored securely in an encrypted Microsoft Excel file. Brain metastatic tumour samples were obtained from patients undertaking neurosurgery under the RCSI Institutional Review Board approved protocol (#13/09; ICORG09/07).

2.8.2. Establishment and culture of *ex vivo* models

On the day of patient neurosurgery, *ex vivo* culture conditions were prepared in advance. Under sterile conditions, 1 cm^3 hemostatic gelatin dental sponges (Vetspon, Novartis) were hydrated in complete HBEC media at 37°C as described previously (Dean et al., 2012). To culture brain metastatic tissue, this breast supporting media was also supplemented with B27 (Life Technologies), N2 (Life Technologies) to

facilitate neural cell growth. Fresh intact tumour tissue was collected, de-identified and placed in DMEM/F12 on ice immediately after surgical resection from the brain. The tumour sample was dissected into approximately 2-4mm^3 fragments in size as indicated in Figure 2.2 and placed on the pre-soaked dental sponges. These were maintained at 37 °C and 5% CO_2 and treated with cabozantinib (10 nM), afatinib (25 nM) or vehicle (% DMSO) for 72 hrs. At the end of experimental treatments, tumour samples were fixed in 10% formalin overnight before paraffin embedded them for sectioning and IHC staining.

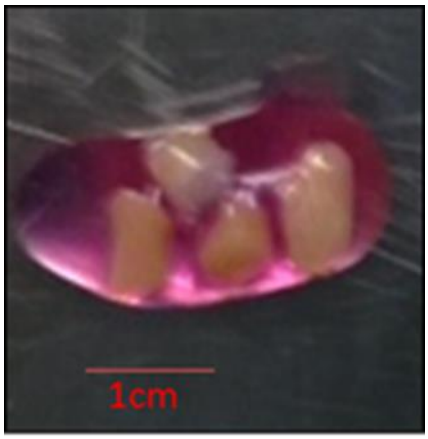

Figure 2.2: Fresh patient brain metastatic tissue prior to establishing *ex vivo* culture.

Following retrieval of fresh patient tumour tissue the sample was maccrodissected into approximately 2-4 mm^3 fragments.

2.9 Animals and *In vivo* experimental protocols

All experimental procedures using live animals were reviewed and approved by American Association for Laboratory Animal Science (IACUC). *In vivo* work was conducted in collaboration with Champions Oncology, using Champions Oncology BC BrM PDX model CTG-1520. Immune-compromised female mice (Harlan; nu/nu) between 5-8 weeks of age were housed on irradiated, Alpha-twist-enriched 1/8" corncob bedding (Sheperd) in individual HEPA ventilated cages (Innocage® IVC, Innovive USA) on a 12-hour light-dark cycle at 68-74°F (20-23°C) and 30-70%

humidity. Animals were given water (reverse osmosis, 2 ppm Cl2) and an irradiated test rodent diet (Teklad 2919; 19% protein, 9% fat, and 4% fibre) ad libitum.

Pre-study stock mice were implanted unilaterally on the left flank with stock tumour fragments. Seven-ten days after implantation, tumour growth was measured twice a week using digital callipers and the tumour volume was determined using the formula (0.52 x [length x width)]. When pre-study tumour volumes (TV) reached an average volume of approximately 150-300 mm^3, animals were matched by tumour and assorted into control or treatment groups for dosing with a total number of 4 study mice per group. A summary highlighting the conditions used for the *in vivo* drug efficacy study can be found in Table 2.6. Dosing initiated on Day 0. For 5 days, mice were given a once daily treatment of vehicle, 20 mg/kg afatinib or 30 mg/kg cabozantinib through oral administration followed by 2 days off (QDx5 on, 2 off). Concentrations were selected based on previous preclinical studies showing these doses to be the highest nontoxic oral levels (Zhao et al., 2016; Tanaka et al., 2014). This treatment cycle was carried out 4 times for a total duration of 28 days. Tumour volumes and body weight were taken twice weekly. The study endpoint was when the mean TV of the control group reached approximately 1500mm^3. If the control groups had reached maximum TV before Day 28, treatment groups and individual mice were still dosed and measured up to Day 28. Any animal showing adverse treatment related side-affects, substantial weight loss or signs of distress due to tumour burden were humanely euthanised, of which there were none. At study completion, percent tumour growth inhibition (%TGI) values were calculated and reported for each treatment group (T) versus control (C) using initial (i) and final (f) tumour measurements by the formula (2): $\%TGI = 1 - (T_f - T_i) / (C_f - C_i)$. Additionally, tumours were collected from all animals in each group. The tumours were split; half flash frozen and stored at -80°C and the other half fixed in 10% formalin for 18-24 hours and stored at room temperature in 70% ethanol. After formalin fixation, samples were then paraffin-embedded and stored at 4°C.

Table 2.6: Treatment conditions for *in vivo* drug efficacy study

Group	-n-	Agent	Dose (mg/kg/dose)	Dose Volume (mL/kg)	ROA	Schedule	Total Number of Doses
1	4	Vehicle Control[1]	-	10	PO	Qd5 on, 2offx4	20
2	4	Afatinib	20	10	PO	Qd5 on, 2offx4	20
3	4	Cabozantinib	30	10	PO	Qd5 on, 2offx4	20

Vehicle control[1] - 0.5% Methyl Cellulose (MC), 0.4%

2.9. Statistical analysis

All results are shown as mean +/- s.e.m. A two-way student's t-test was used to compare treatment groups to the vehicle unless otherwise stated. A *p*-value of less than 0.05 was deemed to be statistically significant. The investigators were blinded to allocation for *ex vivo* and IHC analyses. All *in vitro* experiments are representative of the mean of three independent experiments (n=3), with a technical replicate of three for each cell-line treatment. For the *in vivo* experiment, tumour-bearing mice of similar tumour burden were randomise into control and experimental groups and all treatments were not blinded. The calculated mean and the +/- s.e.m, for the measured tumour volume and body weight of each group are provided in Appendix I, Table 8.3 and Table 8.4, respectively. Statistical comparisons of tumour volumes were conducted using one-way ANOVA followed by Newman-Keuls multiple comparison test (GraphPad Prism). All IHC analysis and scoring for *in vivo* and *ex vivo* study was conducted independently by two researchers both of whom were blinded to allocation. While no statistical tests were applied to calculate the sample size for the *in vivo* study, all efforts were made to achieve the scientific aims using the minimum number of animals. Deviations in PDX tumour growth were also considered in interpreting the therapeutic tumour drug response data. HER2 and

RET gene expression differences between patient-matched primary and brain metastatic tumour samples were plotted and statistically assessed using paired Wilcoxon-signed ranked tests (primary vs. metastasis) on log2normCPM values.

3. RET and HER2 expression gains are commonly acquired characteristics in breast cancer brain metastasis

3.1. Introduction

Approximately 20-30% of patients with BC will eventually develop metastasis (Redig and McAllister, 2013). While substantial improvements have been achieved in the treatments of patients with MBC, 15-30% are still diagnosed with BrM, a clinical complication that is indicative of poor outcome with a short median survival time (Leone and Leone, 2015). Furthermore, BrM presents a major cause of neurologic morbidity and severely impacts on patient quality of life. As current treatment options are predominantly limited to local interventions including surgical resection and radiation therapy, the disease management strategies for BrM still pose a major clinical challenge.

On the other hand, targeted therapies have made significant progress over the years, yet many still fail to achieve optimal disease control when it comes to BrM. Recently, small molecule TKIs of HER2 have emerged as favourable alternatives in HER2-positive disease due to their ability to cross the BBB. However, while such anti-HER2 agents have shown promising clinical activity in HER2-positive BrM (Lin et al., 2011; Bachelot et al., 2013; Freedman et al., 2017), effective targeted therapies still remain unavailable for HER2 negative BrM. Thus, there is a critical need to uncover molecular alterations that contribute to brain-specific metastasis in order to ultimately identify novel therapeutic targets.

3.2. Brain metastasis genomic studies

Within recent years, targeted gene expression analyses across longitudinal breast and BrM samples have revealed a number of differentially expressed genes between both neoplastic sites, with metastases often manifesting a larger assortment of gene alterations than the parent tumour. Indeed, these comparative expression profiling studies have illuminated BrM-acquired aberrations including an overexpression of DNA-repair genes in addition well-established oncogenes such as HER2 and TP53 (Woditschka et al., 2014; Brastianos et al., 2015; Priedigkeit et al., 2017a; Lee et al., 2015b). These metastasis-associated modifications are driven by the highly adaptive

nature of MBC cells in response to the highly specialised features of the brain microenvironment and different adjuvant treatments. At the DNA-level, targeted mutational analysis of longitudinal breast and BrM samples have uncovered acquired mutations predicting sensitivity to the PI3K/AKT/mTOR pathway (Brastianos et al., 2015). Similarly, using smaller cohorts of breast-to-brain metastases, other gene expression profiling studies have demonstrated that BrM were more enriched for somatic mutations in several BC genes including EGFR and PTEN (Da Silva et al., 2010; Wikman et al., 2012). Altogether these findings reveal BrM acquire molecular alterations that are unique from their corresponding primary tumours. The identification of such BrM-specific features are of major clinical importance as some may be crucial for the brain metastatic process and hence represent exploitable vulnerabilities that could be targeted to treat this disease. However, a large-scale study on the global transcriptional profile of BrM is still in demand. Furthermore, the therapeutic significance of clinically actionable alterations to improve BrM treatment remains poorly investigated and mandates attention for functional validation.

3.3. Preliminary work

To address these deficiencies, our lab further expanded on these previous studies in a collaborative effort with researchers at the University of Pittsburgh. To achieve this, genome-wide exome capture RNA-Seq analysis was conducted on 21 patient-matched FFPE samples of breast tumours and their associated resected BrM. All bioinformatics analysis was carried out in collaboration with Dr. Nolan Priedigkeit (University of Pittsburgh). While such archival specimens are highly susceptible to RNA degradation, an FFPE-specific sequencing approach was employed for this study. The reliability of this method has been supported by several reports in maintaining transcript integrity, demonstrating high levels of concordance with matched frozen tissue (Priedigkeit et al., 2017b; Van Allen et al., 2014; Munchel et al., 2015). The clinical characteristics of the patient cohort is illustrative of the molecular diversity within BC as seen by their varying tumour features and hormone receptor status. The full clinicopathological data of the study cohort is given in

Appendix I, Table 8.2. From this patient collection, a comprehensive characterisation on the transcriptional landscape of BrM was obtained and recurrent patterns of shifting transcriptomes were identified. Following gene set enrichment analysis (GSEA) of the data, we observed common expression differences in those associated with BC proto-oncogenes including KRAS and ALK (Figure 3.1A) (Hanzelmann et al., 2013). In particular, BrM–acquired aberrant enrichment was also detected in multiple receptor tyrosine kinase (RTK) driven signalling pathways which are key adaptive mechanisms in driving brain metastatic colonisation and outgrowth. Further comparative transcriptomic analysis between matched tumour pairs using an established mTOR/AKT gene signature (Ni et al., 2016) revealed an elevated score in 19/21 BrM (Figure 3.1B).

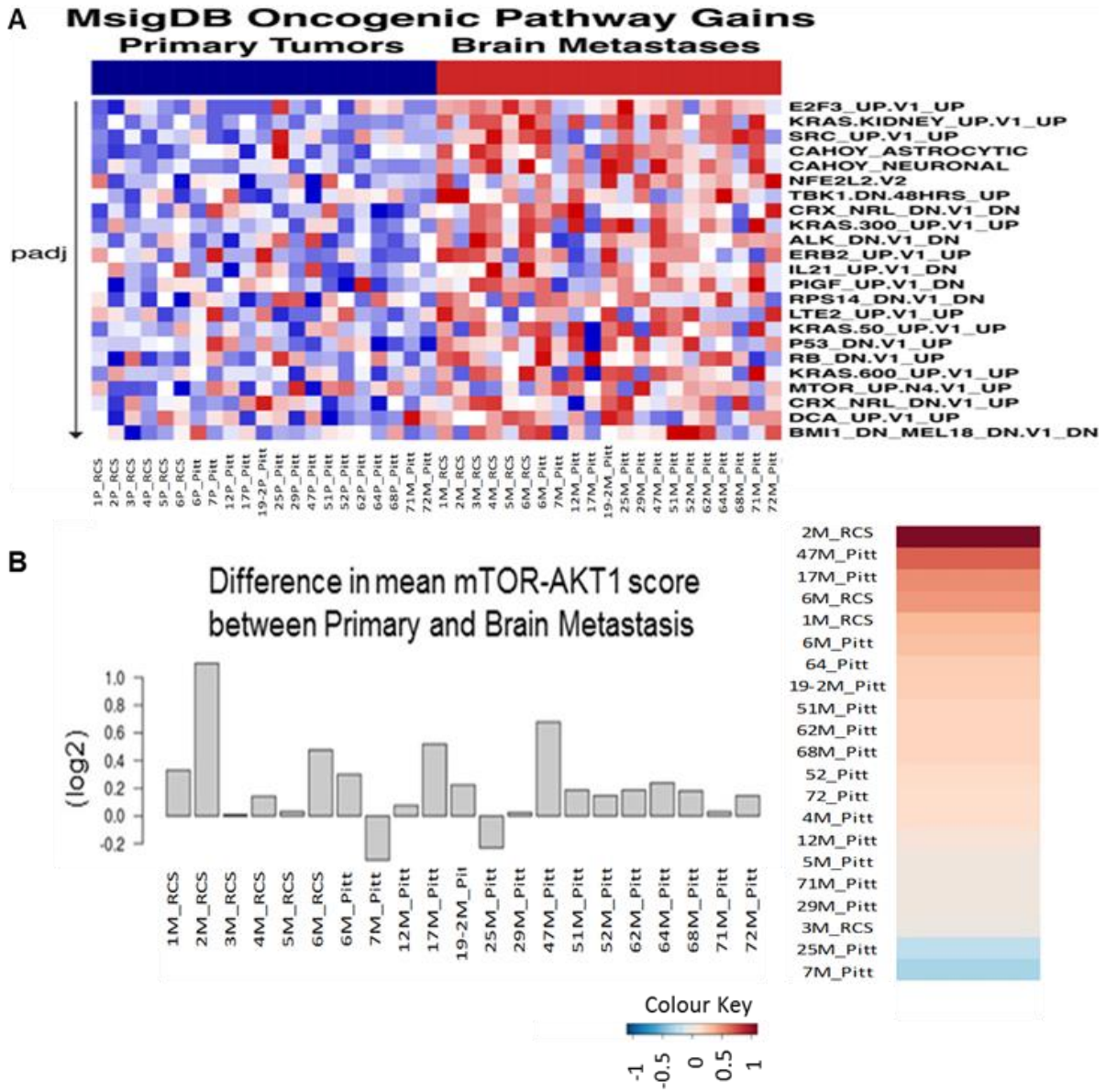

Figure 3.1: Oncogenic pathway enrichments in breast cancer brain metastases. (A) GSEA analysis of the RNA-Seq data using oncogenic pathway relevant gene sets from the Molecular Signatures Database (MSigDB). Gene expression differences between 21 patient-matched brain metastases vs. primaries is visualised as a heatmap and highlights brain metastasis enriched pathways (FDR adjusted Wilcoxon signed-ranked P-value <0.05) (B) Transcriptomic analysis of established AKT-MTOR dependent signature genes in matched tumour samples (n=21). Box blots correspond to difference in mean signature score (log2) in mTOR-AKT1 score gained in brain metastasis over patient-matched primary.

The HER2 pathway was also enriched which is consistent with the previously reported elevation of HER2 expression in up to 35% of BrM relative to matched primaries (Priedigkeit et al., 2017a). In light of this, a thorough examination of HER2 pathway activation was performed by drawing on a pre-defined gene set associated with HER2 signature (Desmedt et al., 2008). This work revealed an enriched HER2 signature score in 15/21 pairs of BrM compared with matched primary breast tumours (Figure 3.2A). Furthermore, HER2 pathway enrichment was also observed to be correlated with downregulation of estrogen receptor 1 (ESR1), a well-established determinate of hormone therapy resistant disease (Figure 3.2B). Interestingly, HER2 signalling was upregulated in cases that were HER2-negative in the primary tumour, three of which scored an intermediate HER2 signature gain and were reclassified as HER2-positive in BrM as a result (Figure 3.2C). These findings may bear immediate clinical implications as some patients might be underdiagnosed as HER2 negative according to the status of the primary tumour yet could potentially receive benefit from anti-HER2 therapies.

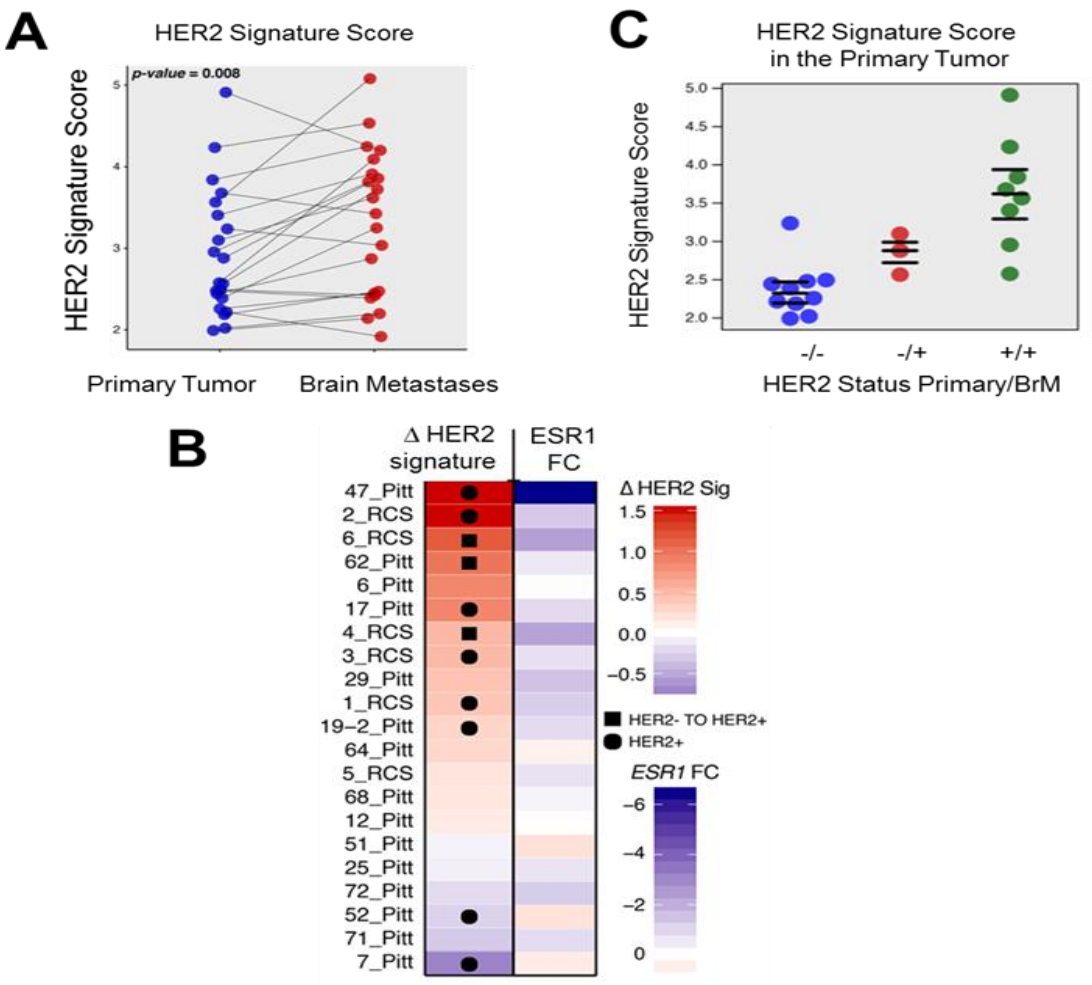

Figure 3.2: HER2 pathway enrichment in breast cancer brain metastases.

(A) Paired ladder plot of established genes represented in the HER2 signature depicts the expression change in patient matched cases ($p<0.008$; Wilcoxon signed-rank test; primaries vs. brain metastases). Blue dots represent primary tumour signature scores and red dots represent metastatic tumour signature scores. (B) Scatter plot of HER2 signature score in primary tumours. Blue dots (-/-) represent patient-matched are HER2 negative in both the primary and metastatic tumours, red dots (-/+) represent patient-matched cases that switched from HER2 negative to positive whereas green dots (+/+) represent HER2 positive tumours that have further activation in HER2 pathway. (C) Tile plot representing increases in HER2 signature or loss of ESR1 expression. HER2 subtype switching from negative to positive is indicated by squares whereas circles denote originally HER2 positive tumours that have additional activation in HER2 pathways.

Given the strikingly enriched kinase landscape, the transcriptomic data was further examined and prioritised on the basis of clinically targetable kinases (Wagner et al., 2016). “Expression gains” were marked as any log2-transformed expression fold-changes greater than the 95th percentile (log2FoldChange = 1.198) of all gene and case fold-changes. All expression fold-change values can be found in Appendix I, Table 8.2. Among these, top recurrent alterations were found in RET and ERRB2, both of which had a 2-fold or greater increase in 38% of BrM (Figure 3.3). Other notable targets include EPHA3 and members of the PI3K family (PIK3C2G and PIK3R1/2) whose oncogenic activation has been implicated to play critical roles in the pathogenesis of GBM and BrM, respectively (Day et al., 2013; Adamo et al., 2011; Da Silva et al., 2010).

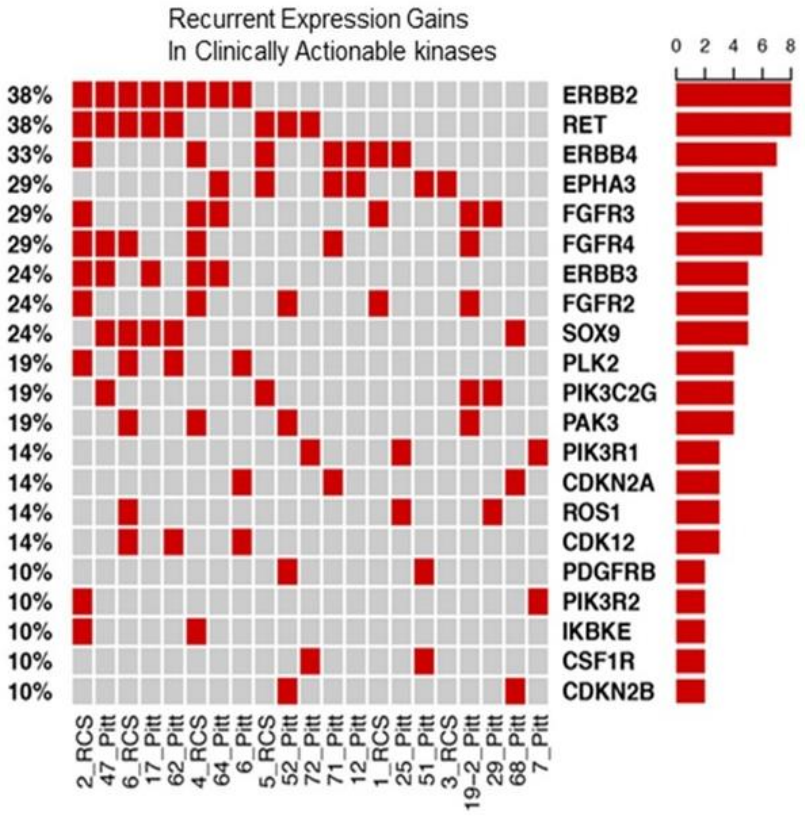

Figure 3.3 Identification of recurrent expression gains of clinically actionable kinases in brain metastases

OncoPrint of clinically actionable kinases (DGIdb) with discrete expression gains in brain metastases.

3.4. Multi-targeted tyrosine kinase inhibitors

Following this extensive preliminary work, there was strong rationale for investigating these alterations as clinically actionable therapeutic targets for BrM. HER2 and RET have FDA-approved drugs that are currently being explored as a therapy for numerous tumour types, including BC (Modjtahedi et al., 2014; Lin et al., 2012; Elisei et al., 2013; Drilon et al., 2013; Tolaney et al., 2016). Furthermore, given RET and HER2 had the most recurrent expression gains from the clinical cohort of BrM, both RTKs were selected for further functional investigation in this study.

Afatinib (BIBW 2992) is an orally bioavailable irreversible HER family blocker that has been tested in several tumour types and was initially approved as a first line treatment of EGFR-mutated NSCLC. It inhibits HER family signalling via covalent binding with the intracellular tyrosine kinase domains of EGFR, HER2 and HER4. This subsequently prevents their auto-phosphorylation as well as trans-phosphorylation of HER3, thereby interrupting downstream signalling cascades and reducing proliferation and tumour growth. Its broad spectrum inhibitory activity has the potential efficacy to significantly disrupt HER2 homo and heterodimerization and its ability to do so may perhaps offer improved clinical activity over HER2-directed monoclonal antibodies and mono or dual- targeted HER-TKIs (Modjtahedi et al., 2014).

For RET targeting, cabozantinib was selected. Cabozantinib is orally bioavailable multi-kinase inhibitor that was recently approved for the treatment of medullary thyroid cancer (MTC). It has potent activity against RET and other RTKs that are associated with tumour progression including MET and VEGFR (Grullich, 2014).

3.5. Aims

The aim of this chapter was to:

- Validate the observed transcriptomic changes of HER2 and RET by assessing their IHC profiles from available FFPE samples of the 21 patient-matched cases.
- Determine the functional efficacy of small molecule TKIs, cabozantinib and afatinib, to inhibit tumour progression using *in vitro* models of BC BrM.

3.6. Results

3.6.1. Validation of recurrent RET and HER2 transcriptomic alterations in primary breast cancers and matched brain metastases.

RNA-Seq profiling of 21 paired primary breast tumour and BrM revealed a substantial increase in HER2 and RET expression in BrM (Figure 3.4). The raw sequencing counts were transformed to log2 counts per million (CPM) values and normalised using the TMM method. This accounts for any underlying discrepancies between samples such as library size differences, thus providing better adjusted data for differential expression analysis. Genes were defined as significantly upregulated if fold-changes were greater than 1.5 and the P values were <0.05. According to this set threshold, both genes showed increased expression in 8 of 21 BrM.

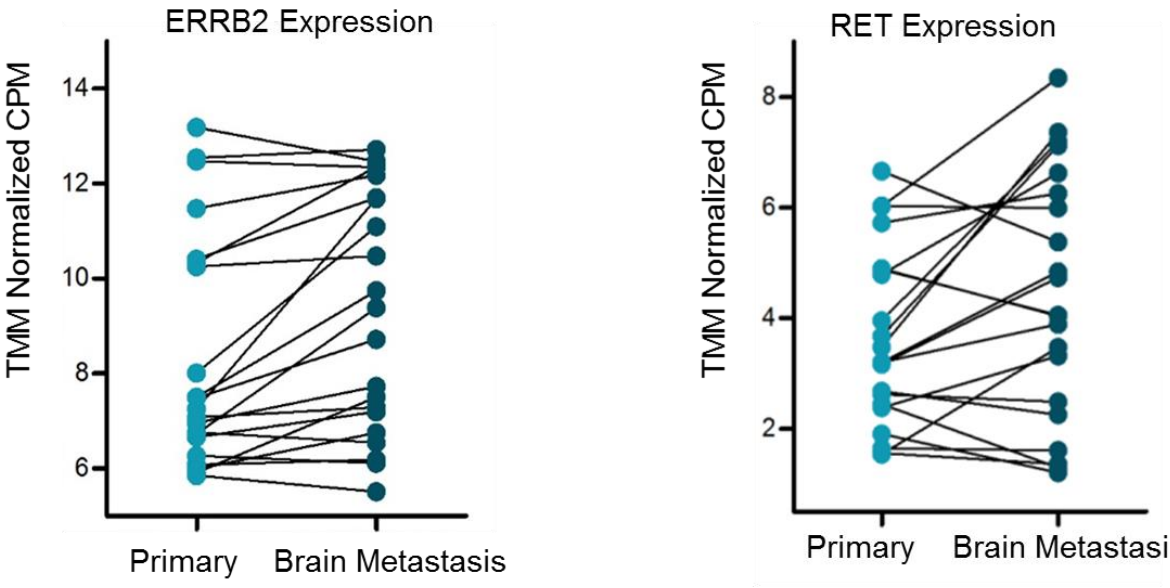

Figure 3.4: Recurrent expression gains of HER2 and RET in breast cancer brain metastases.

Paired ladder plots representing expression of the two most recurrent upregulated clinically actionable genes HER2 and RET in each patient matched case. Light green dots represent primary tumour expression values and dark green dots represent metastatic tumour expression values (log2norm CPM).

With respect to the enriched RET mRNA expression between matched sample pairs, RET IHC analysis was performed on all available cases (18/21) to validate this at the protein level. Due to limited availability, not all matching cases were retrievable for staining (Figure 3.5).

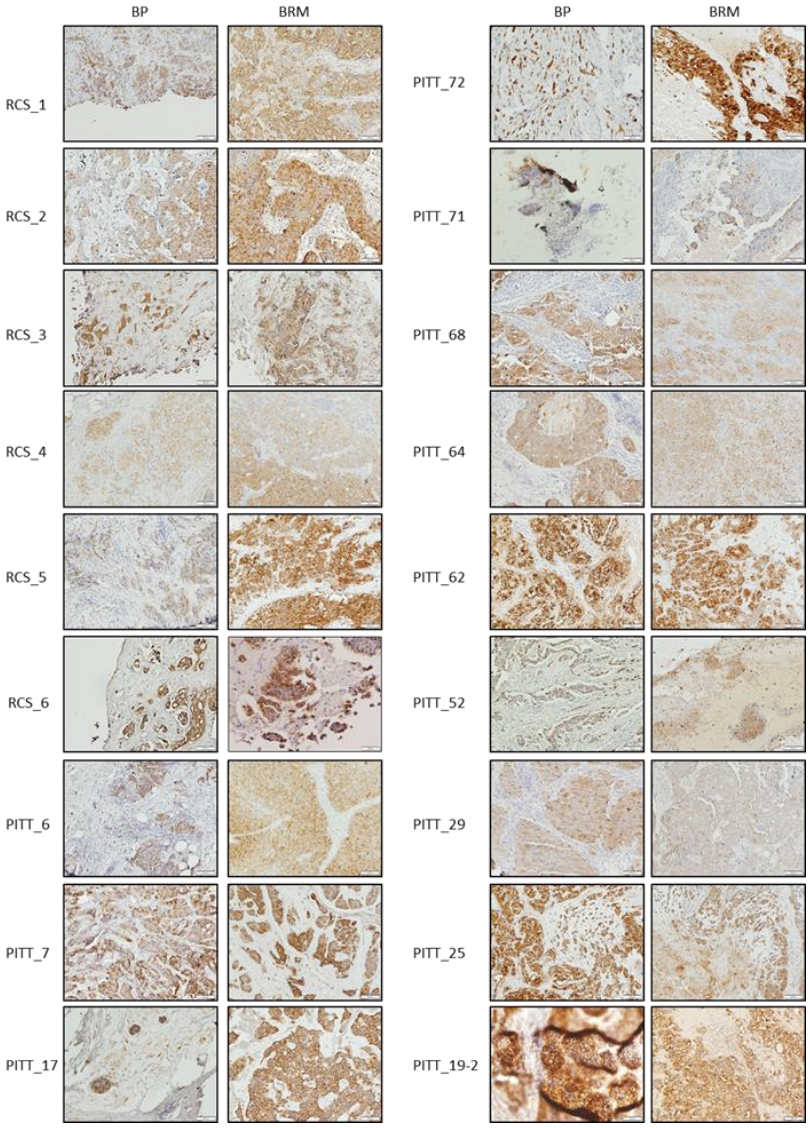

Figure 3.5 RET protein expression is altered between matched primary and brain metastases

IHC staining and analysis for RET was conducted in matched brain metastatic vs primary breast tumours for cases that were available (n=18) from the 21 patient cohort study. Images shown are all taken at 20x magnification. All scale bars correspond to 50 μm.

A comprehensive RET scoring system was defined and applied to evaluate RET IHC positivity in all of the profiled paired cases. The adopted scoring approach is summarised in Table 2.4 of the Material and Methods chapter. Alterations in RET protein expression was detected in 13/18 paired patient tumours. In addition, the observed differences in RET IHC positivity between paired primary and metastatic samples faithfully paralleled their mRNA expression changes. For instance, cases with RET mRNA gains also demonstrated a RET IHC positivity score that was higher in BrM - RCS_2; 2+ in primary, 3+ in BrM, PITT_72; 3+ in primary, 4+ in BrM, and RCS_5; 1-2+ in primary, 3+ in BrM (Figure 3.6). Comparative differences in RET protein expression between matched primary and metastatic tumours were also correlative with cases that revealed no expression fold-changes and metastasis-specific downregulation of RET mRNA; RCS_4 and PITT_25, respectively (Figure 3.6). Overall, the alterations that had been observed in RET mRNA between matched patient tumours and BrM were confirmed at a protein level by IHC. Furthermore, these findings also indicate that the RNA-Seq analysis that was applied to this study is an effective and accurate method of detecting true expression levels in FFPE samples.

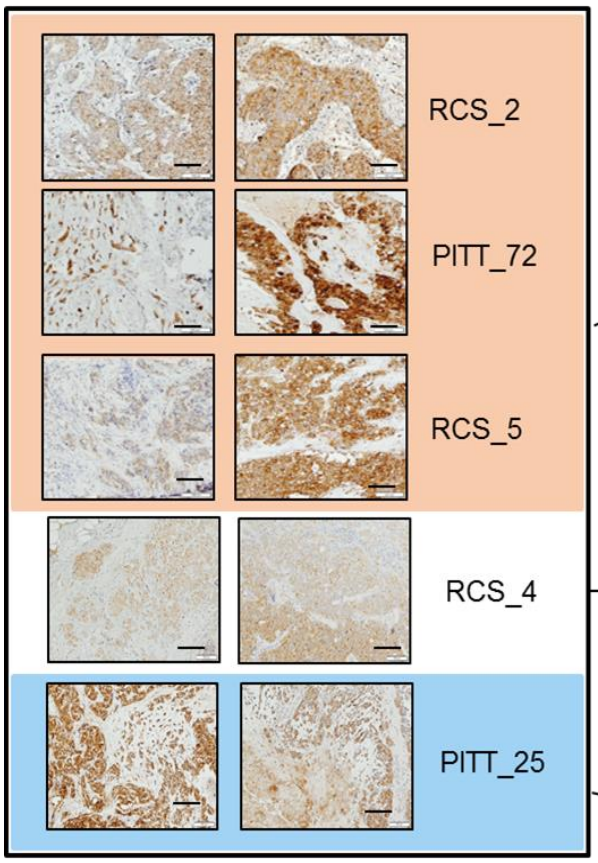

		RET IHC SCORE	RNA-SEQ
	Case	Primary	Brain Metastasis	log2FC >
UP	2_RCS	2	3	1.831
	5_RCS	1-2	3	1.564
	6_RCS	3	3-4	3.238
	17_Pitt	2	4	3.450
	47_Pitt	n/a	n/a	3.892
	52_Pitt	2	2-3	1.931
	62_Pitt	2-3	4	1.639
	72_Pitt	3	4	2.319
UNCHANGED	6_Pitt	1-2	1-2	0.936
	7_Pitt	2-3	3	0.684
	51_Pitt	n/a	n/a	0.525
	29_Pitt	1-2	1-2	-0.032
	19-2_Pitt	3	3	-0.032
	4_RCS	2-3	2-3	-0.430
	12_Pitt	n/a	n/a	-0.199
	64_Pitt	2	1-2	-0.136
DOWN	1_RCS	1-2	2	-0.852
	71_Pitt	0-1	0-1	-0.700
	25_Pitt	3-4	2-3	-0.827
	68_Pitt	2-3	2	-1.151
	3_RCS	3-4	3	-1.280

Figure 3.6: RET IHC protein analysis is highly concordant with RET mRNA levels in both matched primary and metastatic samples.

Representative RET IHC images of matched primary and brain metastases from example cases that showed upregulated, unchanged and downregulated RET mRNA in BrM; along with a graphic presenting RET IHC scores for 19/21 cases and their corresponding log2 fold change RET mRNA scores.

As previously mentioned, comparative analysis of the transcriptomic data revealed that the HER2 status in three patient cases had changed from negative to positive in the BrM. To validate this at a protein expression level, HER2 IHC analysis and pathological scoring was performed for one of these patient-matched cases, 4_RCS. From the RNA-Seq analysis, this case demonstrated a ~2-fold expression increase for ERRB2 mRNA in BrM relative to the matching primary (Figure 3.7A). Consistently, IHC results show that HER2 protein expression altered from 1+ positivity score in the primary, to 3+ score in the BrM (Figure 3.7B). Again, due to limited availability of matching primary tumours HER2 staining could not be performed on all other 20 matched pairs of samples.

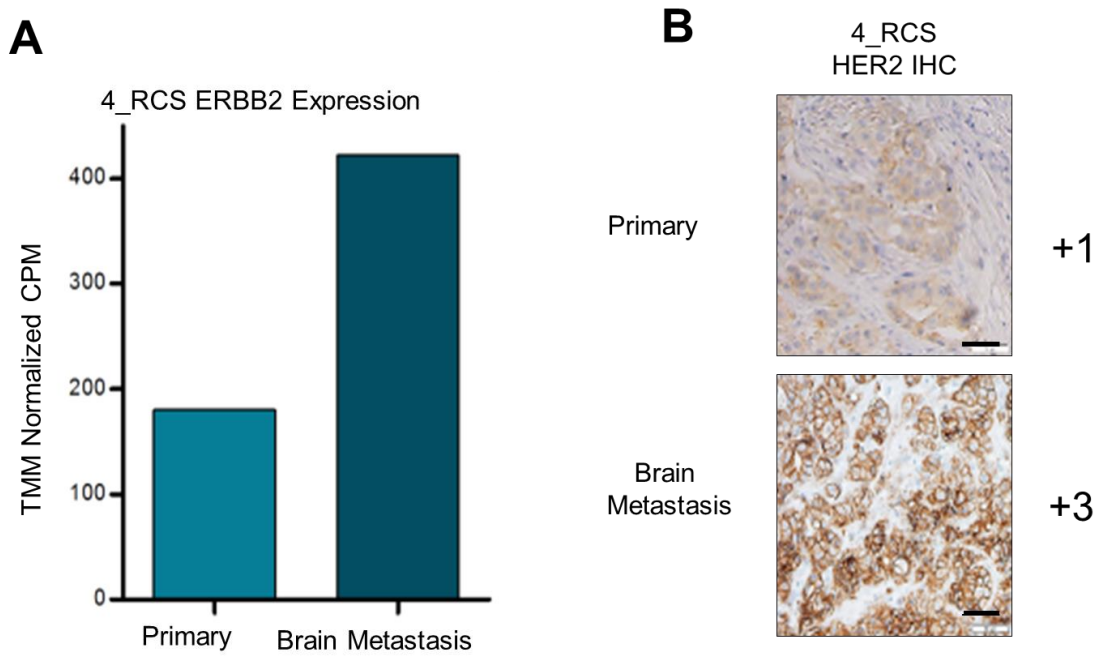

Figure 3.7: Case specific protein analysis and validation of HER2 expression gain in BrM.

(A) TMM Normalised CPM counts of ERBB2 in patient matched primary and BrM tumour samples from case 4 _RCS. RNA sequencing counts were transformed to log2 counts per million (CPM) values and TMM normalised. (B) IHC analysis of HER2 in patient-matched primary and BrM tumour samples from case 4 _RCS. Images shown are 20x; scale bars correspond to 50μm.

Given the IHC confirmation of HER2 subtype switching in case 4_RCS, NanoString nCounter CNV assay or FISH analysis was employed on all samples that were available to investigate if gained DNA mutational alterations were responsible for the observed increases in HER2 expression. Nanostring was carried out in collaboration with Dr. Nolan Priedigkeit and FISH analysis was carried out using the pathology services in Beaumont Hospital.

Nanostring was employed to evaluate the HER2 amplification status of 13/21 primary and metastatic paired BC samples from the Pittsburgh cohort of patients (PITT), where sufficient DNA was already available. A copy number cut-off value of ≥5 was selected for HER2 amplification. As a result, HER2 copy number alterations were detected in 2/12 primary tumours and 3/12 metastatic tumours. Interestingly, 1 HER2-negative patient case, 62_PITT, gained HER2 amplification with metastatic disease (Table 3.1).

FISH was used to evaluate the selected cases from the RCSI cohort (RCS) that had changed from negative to positive in the BrM from the RNA-Seq analysis, 4_RCS and 6_RCS. The FISH results showed that 4_RCS was non-amplified (HER2:cep17 ratio 1.33; HER2 count 4.1) whereas 6_RCS acquired HER2 amplification in the BrM compared to the primary. With regards to 4_RCS, the observed HER2 expression gains and enriched signalling in BrM may alternatively be caused by the acquisition of somatic activating mutations or else, perhaps even beyond DNA-level modifications such as epigenetic mechanisms driving transcriptional expression.

Table 3.1: Evaluation of HER2 amplification using NanoString assay in matched tumour pairs from the Pittsburgh cases

Case	Primary Breast Tumour		Brain Metastases	
	HER2 copy number	HER2 amplification	HER2 copy number	HER2 amplification
6_Pitt_BP	na	na	na	na
7_Pitt _BM	91.39	AMP	36.1	AMP
12_Pitt	1.2	NOT AMP	1.43	NOT AMP
17_Pitt	na	na	na	na
19-2_Pitt	na	na	na	na
25_Pitt	3.48	NOT AMP	2.83	NOT AMP
29_Pitt	2.76	NOT AMP	2.6	NOT AMP
47_Pitt	2.84	NOT AMP	2.18	NOT AMP
51_Pitt	2.14	NOT AMP	1.67	NOT AMP
52_Pitt	34.28	AMP	14.68	AMP
62_Pitt	**3.58**	**NOT AMP**	**20.85**	**AMP**
64_Pitt	2.56	NOT AMP	1.98	NOT AMP
68_Pitt	2.68	NOT AMP	3.44	NOT AMP
71_Pitt	2.83	NOT AMP	1.69	NOT AMP
72_Pitt	1.57	NOT AMP	2.3	NOT AMP

3.6.2. Inhibition of RET and HER2 effectively inhibits the growth of brain metastatic breast cancer cell lines *in vitro*

Given RET and HER2 had the most recurrent expression gains, and their altered expression had been confirmed at protein level, the effect of inhibiting both RTKs was next investigated in a preclinical setting. For this, the efficacy of two FDA-approved agents; a multi-kinase RET inhibitor, cabozantinib, and a pan-HER family inhibitor, afatinib, was examined *in vitro*. The inhibitory activity of both drugs on cell proliferation was assessed in three cell line models of BC BrM. ER-positive, tamoxifen resistant model LY2 cells have previously demonstrated the capacity to metastasise to several organs, including the brain (Figure 3.8A). T347-2c is a primary culture cell line that was derived from an ER-positive/PR-negative/HER2-positive patient BrM tumour, T347x (Ward et al., 2018a). MDA-231-BrM2 cells is a well-

established brain colonising derivative of TNBC parental line, MDA-MB-231(Bos et al., 2009b).

For cell proliferation assays, cells were treated with vehicle (% DMSO) cabozantinib (10 nM), afatinib (25 nM) or else a combination of cabozantinib and afatinib. After treatment with either single or combined agents, cell viability was evaluated by using the MTS assay after 72 hours. A significant decrease in cell proliferation was observed in LY2 cells after treatment with cabozantinib (n=3; p=0.0107), afatinib (n=3; p=0.0016) and a combination of both agents (n=3; p=0.0055) by 1.7-fold, 2.9-fold and 2.8-fold, respectively (Figure 3.8A). A significant ~2-fold reduction in cell viability was also detected in MDA-231-BR cells in response to cabozantinib (n=3; p=.0007), afatinib (n=3; p=0.0016) and combined drug treatment (n=3; p=0.0009). (Figure 3.8B). T347-2C cells demonstrated significant drug sensitivity to both cabozantinib (n=3; p<0.0001) and afatinib (n=3; p<0.0001) as well as dual drug treatment (n=3; p=0.0004) leading to a 3.1-fold, 10.5-fold and 3.1-fold decrease in cell proliferation, respectively (Figure 3.8C). Given this cell line has been characterised to overexpress HER2, as shown in the Material and Methods section, the larger anti-proliferative effect observed from afatinib treatment may be due to the inhibition of this RTK. Co-treatment with cabozantinib and afatinib in all cell lines showed no synergistic inhibition of cell growth compared to single drug treatment. Therefore, it is possible that either RET and HER2 may serve as sufficient targets alone to treat some cases of BrM. Overall, the *in vitro* results indicate that cabozantinib and afatinib can decrease cell growth in BC cells that either have brain metastatic potential or have previously colonised the brain.

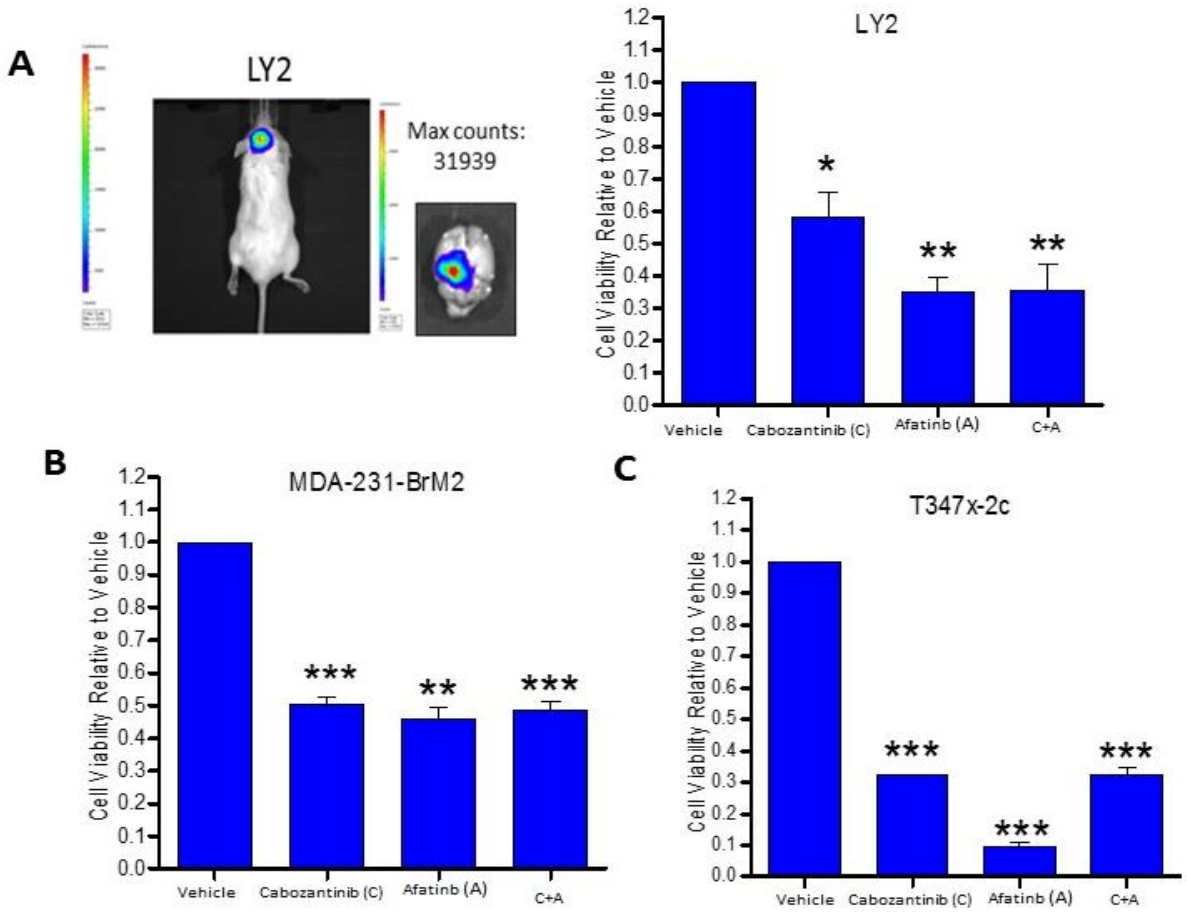

Figure 3.8: Cabozantinib and afatinib demonstrates significant *in vitro* anti-proliferative activity in cell line models of breast cancer brain metastases.

(A) An *ex vivo* bioluminescent IVIS image a NON-SCID mouse with BrM following 8 weeks post-intracardiac injection of luciferase tagged ER-positive BC endocrine resistance LY2 cells; alongside a bar chart illustrating the significant anti-proliferative effect of cabozantinib (10 nM)(p=0.0107) and afatinib (25 nM)(p=0.0016) on LY2 cells relative to vehicle-treated cells (DMSO). (B) A bar chart illustrating the significant anti-proliferative effect of cabozantinib (10 nM)(p=0.0007) and afatinib (25 nM) (p=0.0014) on brain-colonising MDA-231-BrM2 relative to vehicle-treated cells (% DMSO). (C) A bar chart illustrating the significant effect of cabozantinib (10 nM)(p<0.0001) and afatinib (25 nM)(p<0.0001) in brain metastasis PDX-derived cell line ,T347x-2c, relative to vehicle-treated cells (% DMSO). All error bars represent mean ± S.E.M., n=3. P value compares treatments versus vehicle and is obtained using two-way paired student t-test where ***p<0.001, **p<0.01, *p<0.05.

Cell motility is a critical parameter for tumour progression and dissemination, as metastasis formation implies the migration of cancer cells from the original tumour location to distant sites (Yilmaz & Christofori, 2010). Thus, the effects of either cabozantinib or afatinib was examined on cell movement in the highly migratory MDA-231-BrM cell line following 24 hours of treatments. Vehicle-treated MDA-231-BrM2 cells maintained a high level of motility. However, cells that were treated with afatinib (25 nM) had significantly decreased levels of motility (2.8-fold; n=3; $p=0.0018$) and were even slower in response to cabozantinib (10 nM) (1.5-fold; n=3; $p<0.0001$) (Figure 3.9). These observations suggest that cabozantinib and afatinib can inhibit growth and migration in a BC brain colonising cell line model.

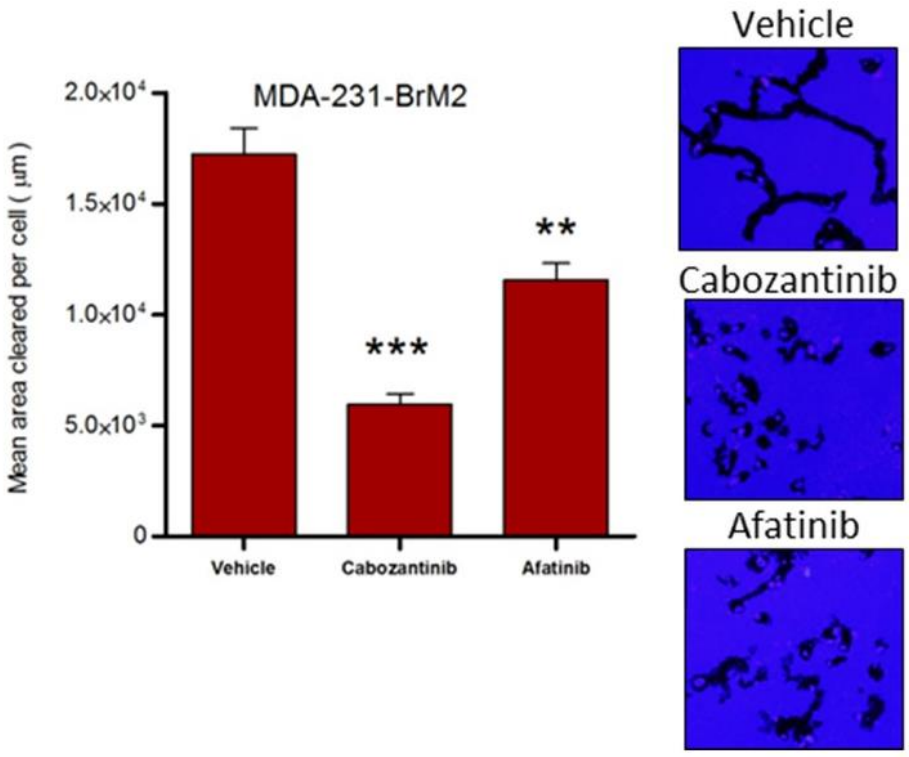

Figure 3.9 Afatinib and Cabozantinib demonstrates significant *in vitro* anti-tumour activity in brain seeking breast cancer cell line, MDA-231-BrM2.

A bar chart illustrating the significant anti-migratory effect of cabozantinib (10 nM)($p<0.0001$) and afatinib (25 nM)($p=0.0018$) on MDA-231-BrM2 cells. Histogram shows mean migratory area per cell (μm^2). Representative images of the cellular migration tracks for each treated group is shown staining with DAPI and rhodamine phalloidin. All error bars represent mean ± S.E.M., n=3. P value compares treatments versus vehicle and is obtained using two-way paired student t-test where ***$p<0.001$, **$p<0.01$, *$p<0.05$.

3.7. Discussion

The incidence of BrM is increasing among patients with BC, which typically manifests years after primary BC diagnosis. However, this clinical latency can vastly differ between patients as the development of BrM is relatively short among patients with TNBC (Hines et al., 2008). Early events of brain relapse might be driven by rapid tumour cell clonal evolution, as intra-tumour heterogeneity is a major underlying cause of disease recurrence, especially for TNBC cases. According to this theory, it is hypothesised that a very rare subpopulation of clones with inherent metastatic potential are pre-existent in BC cells. These then become subjected to various selection pressures within the progressing primary tumour, giving rise to an evolved group of sub-clones that harbour the necessary molecular perquisites for brain colonisation (Nowell, 1976).

By contrast, a much longer interval of metastatic latency is reported in patients with luminal BC. For these cases, an alternative course for metastatic brain tumours has been suggested whereby, during this dormancy period, BC cells experience gradual evolutionary changes as an adaptive mechanism to both the selection pressures of intervening therapy and the surrounding host microenvironment. McBryan and colleagues previously observed that the degree of these genetic divergences were correspondent with the duration of disease latency as demonstrated by the larger transcriptome changes between primary breast tumours and liver metastases than primary and nodal tumours (McBryan et al., 2015). Indeed, in the context of BrM, several genomic analysis studies revealed that tumour cells continue undergoing genetic changes after dissemination into the brain parenchyma, acquiring clinically informative alterations distinct from their respective primary tumours. BrM from these reports were shown to harbour unique oncogenic aberrations affecting the PI3K/AKT/mTOR pathway as well as members of the HER family (Brastianos et al., 2015; Da Silva et al., 2010). However, to date, a full comprehensive characterisation of the global transcriptional landscape of BrM and its divergence from primary BC remains incomplete and alterations specific to BrM have not yet been defined.

The objective of this work was to explore the role of abnormal transcriptional regulation in the development and progression of BrM with the ultimate goal of identifying potential therapeutic targets. For this, comparative RNA-Seq analysis was performed on a set of 21 patient-matched primary tumours and their corresponding BrM. The results reported here constitute important progress to our understanding of the molecular evolutionary shift from primary BC to BrM, revealing valuable information on alterations that may offer potential improvements to clinical outcomes. Recurrent patterns of gene enrichment in several RTKs were detected in BrM many of which were druggable. Among these, RET and HER2 expression were identified as the most recurrent acquired expression gains in BrM.

In this chapter, IHC was carried on all available patient-matched FFPE tumour samples to validate the reported observed expression changes of RET and HER2 at a protein level. IHC analysis results show conclusive upregulation of HER2 expression in BrM, through confirmation of *a* HER2-negative-to-positive conversion in one of the paired cases, 4_RCS. Consistently with these findings, in an expression analysis study of unmatched BrM from multiple cancer types, Saunus et al. reported a higher expression of HER2 in BC BrM compared to BrM originating from other sites (Saunus et al., 2015). Furthermore, previous studies have also reported receptor discordances between matched primary breast and BrM tumours with common shifts being gains in HER2 and loss of ER status (Priedigkeit et al., 2017a; Duchnowska et al., 2012; Jung et al., 2018; Thomson et al., 2016). Similar changes in ESR1 were also observed from the preliminary patient RNA-Seq data, as mentioned in the introductory section to this chapter, which was inversely correlated with increased HER2 gene signature scores. This negative relationship has also been suggested in other distant metastases of BC (Hoefnagel et al., 2010). Indeed the biological phenomena of subtype switching bear massive clinical implications since such receptor profile alterations could affect patient prognosis. For example, BrM patients whom are diagnosed as non-HER2 amplified on the basis of their primary tumour status may potentially benefit from anti-HER2 therapies. Therefore, future therapeutic

decisions for advanced BC should be guided by sampling the metastatic tumour where available.

HER2 gains by DNA-level alterations are also frequently observed in BrM. One previous study demonstrated that 22.2% of BrM harboured ERBB2 amplifications and/or mutations while analysis of 7,884 BCs revealed a significant enrichment for DNA level ERBB2 mutations in BrM versus local disease (13% local vs 24% brain metastasis) (Priedigkeit et al., 2017a). Thus, the potential attribution of these molecular mechanisms to the observed increases in HER2 gene expression was not excluded in this study. Upon evaluation of HER2 gene amplification, BrM-acquired copy number gains was confirmed in 2/3 cases that had changed from negative to positive in the BrM from the results of the RNA-Seq analysis. While a gain in HER2-positive status was validated by IHC in the other subtype altered case, it was clinically designated as non-amplified by FISH. Therefore, in this scenario, enrichments of HER2 expression and signalling in BrM may be explained by acquired activating mutations. Alternatively, perhaps the observed increases in HER2 mRNA may be accounted for beyond genomic aberrations and instead by a mechanism involving epigenetic reprogramming leading to transcriptional enrichment. Such a proposed possibility will need to be explored in future studies, given the reported epigenetic instability often seen in tumours found in the brain (Nagarajan and Costello, 2009).

Recurrent upregulation of RET mRNA was also shown to be unique to BrM (Vareslija et al., 2018). Indeed, no such enrichments for RET were found in similar transcriptome analysis of patient-matched longitudinal cases that included primaries and other metastatic sites, indicating that responses to RET are potentially specific to the brain (Priedigkeit et al., 2017b). IHC was performed on the majority of available matched cases and confirmed consistency with the RNA-Seq data results. Oncogenic activation of RET has been shown to be involved in disease progression for various cancers and is reported to show a strong association with the development of endocrine resistance in luminal BC (Drilon et al., 2017a; Morandi et

al., 2013; Plaza-Menacho et al., 2010b). Interestingly, RET inhibition in cell line models of endocrine resistant BC that harbour high expression of RET was demonstrated to lead to decreased growth and metastasis (Plaza-Menacho et al., 2010b). Hence, RET was deemed as a potential molecular target for treating BC BrM.

The role of deregulated RTKs in multiple cancer types has been well-established in literature and are recognised as effective targets for therapeutic intervention. Small molecule TKIs have proven to be valuable clinical tools for such targeted cancer therapies (Arora and Scholar, 2005). Drug compounds of this class offer particularly promising treatment strategies against BrM, as several have indicated an ability to penetrate the BBB (Ahn et al., 2017; Bachelot et al., 2013).

In this present study, the TKIs, cabozantinib and afatinib, were selected to target RET and HER2, respectively. Clinical observations would suggest these molecules possess favourable BBB permeability properties, as they have previously displayed intracranial activities in patients with glioblastomas, as well as NSCLC patients with BrM (Hoffknecht et al., 2015; Cloughesy et al., 2018; Schuler et al., 2016). As single agents, both demonstrated significant anti-proliferative effects in specialised cell line models of BrM that feature brain-seeking and brain-colonising traits. However, no synergy or additional activity was observed when cabozantinib and afatinib were combined. As both drugs are known to target functionally overlapping pathways, the combination treatments may only yield an anti-proliferative effect similar to either single agent alone. Furthermore, other works have shown that additive cytotoxicity from anti-cancer drug combinations can vary within patient populations (Palmer and Sorger, 2017).

HER2 and RET inhibition also caused a striking decrease in cell migration, which performs an essential function in the metastatic cascade. Stimulation of either RTK can trigger signalling along the PI3K/AKT and MAPK pathways, both of which are central to mediating many downstream responses, including cell migration (Hynes and MacDonald, 2009; Morandi et al., 2011). Furthermore, aberrant activation of these pathways has been frequently associated with metastatic colonisation and

sustained tumour outgrowth in the brain (Da Silva et al., 2010; Brastianos et al., 2015). Therefore, such findings would suggest that the observed cell motility responses to cabozantinib and afatinib may have been due to disruptions of these two downstream signalling pathways.

Taken together, the above *in vitro* preclinical data define both HER2 and RET as potential actionable targets for BrM.

4. Inhibition of RET and HER2 demonstrates significant anti-tumour activity in breast cancer brain metastases *in vivo*

4.1. Introduction

Over the years, the extensive application of BC cell lines have served as valuable and informative tools for preclinical drug testing due to their well-defined characteristics. Granted, these models can provide useful preliminary indications of drug efficacy *in vivo*, this data cannot be relied on in predicting patient outcome. Moreover, one of the main shortcomings of traditional *in vitro* cell culture models is that they do not portray an entirely adequate representation of BC heterogeneity and morphology, with some showing a significant degree of divergence from the patient tumours that they had been originally derived from. As cancer cell lines are cultured in conditions that deviate from their natural tumour microenvironment they will inevitably encounter various growth selection pressures which have the potential to reduce gene complexity and introduce bias. Therefore, translatability of *in vitro* cell lines model to the clinic is often poor due to their unreliability in predicting patients responsiveness to targeted agents (Siolas and Hannon, 2013).

In contrast, PDX models have yielded superior predictive value in the efficacy of novel anticancer therapeutics. Thus, employment of this pre-clinical platform as a route to study personalised treatment strategies has become increasingly popular over recent years. Typically, PDXs are developed by engrafting dissociated cells or freshly resected tissue from a patient's tumour into immunocompromised and once fully established, PDXs can serve as a renewable resource of human tumour tissue. Unlike cell lines, these models can faithfully recapitulate patient tumour heterogeneity and stably retain the clinical and histopathological features of their donor tumour across multiple generations (Vareslija et al., 2017). Moreover, PDXs also mimic the disease biology of specific patient tumours as they have shown capacity to metastasise to the same sites as their original patient tumour and mirror their treatment responses (Marangoni et al., 2007; DeRose et al., 2011). They also have the added benefit of exhibiting slower progression rates than cell lines which makes them more ideally suited to serve as preclinical models to evaluate new target-directed drugs for patients with BC BrM of drugs in therapeutic settings (Contreras-Zarate et al., 2017). Such predicative and therapeutically powerful model systems of BrM have been markedly underrepresented in preclinical research studies leading to

a serious deficiency in the development of novel targeted therapies against this disease. Here, in this chapter, HER2 and RET were explored as potential therapeutic targets based on a PDX tumour established from a BC BrM. The following work was conducted in collaboration with Champions Oncology, who executed the therapeutic intervention study.

4.2. Aims

The aim of this chapter was:

- To determine the efficacy of targeting RET and HER2 receptor tyrosine kinases to inhibit tumour growth in an *in vivo* PDX model of BC BrM
- To extensively characterise the RET and HER family expression profile of our PDX tumour material using IHC
- To subsequently evaluate the effect of both inhibitors on key phosphorylated nodes downstream of HER2 and RET in order to determine downstream signalling impact of therapeutic interventions on the BrM PDX model

4.3. Results

4.3.1. Characterisation of triple negative breast cancer BrM PDX

This study was conducted to evaluate the *in vivo* antitumour activity of afatinib alone and cabozantinib alone in female immunocompromised mice bearing a low-passage tumour model, CTG-1520, representing human BC BrM. The xenograft was derived from an ER-negative/PR-negative/HER2-negative BC brain metastatic tumour and the patient was originally diagnosed with TNBC prior to adjuvant chemotherapy and brain relapse. A brief summary of the patient's clinical history is summarised in Figure 4.1A and full details are given in Appendix I, Table 8.5. Tumour section slides were stained with hematoxylin and eosin (H&E) to examine their basic histomorphological features and establishment of PDX tumours was verified by staining for human-specific epithelial marker, pan-cytokeratin (PanCK) (Figure 4.1B)

IHC was subsequently employed to gain a comprehensive expression profile of all HER family receptors and RET as well as their phosphorylated states in the BrM PDX model. RET and HER2 IHC staining was quantitatively determined according to staining intensity, location and coverage. Full details of the adopted scoring system can be viewed in Table 2.3 and Table 2.4 in the Material and Methods section. Activated RET signalling was detected as shown by the strong and tumour specific protein expression of total RET and pRET (Y^{1062}). IHC results confirmed the HER2 negative status of CTG-1520 which had been clinically validated as non-amplified (1+). Furthermore, the PDX model expressed strong total levels of EGFR, HER4 and HER3. Interestingly, despite the low levels of HER2 protein expression, our phosphorylation analysis revealed that pHER2 expression was still elevated, in addition to pEGFR and pHER4 while pHER3 protein staining was relatively weak. These findings therefore suggest that HER2 signalling may be occurring through heterodimerization with EGFR and HER4, hence their concurrent activated states.

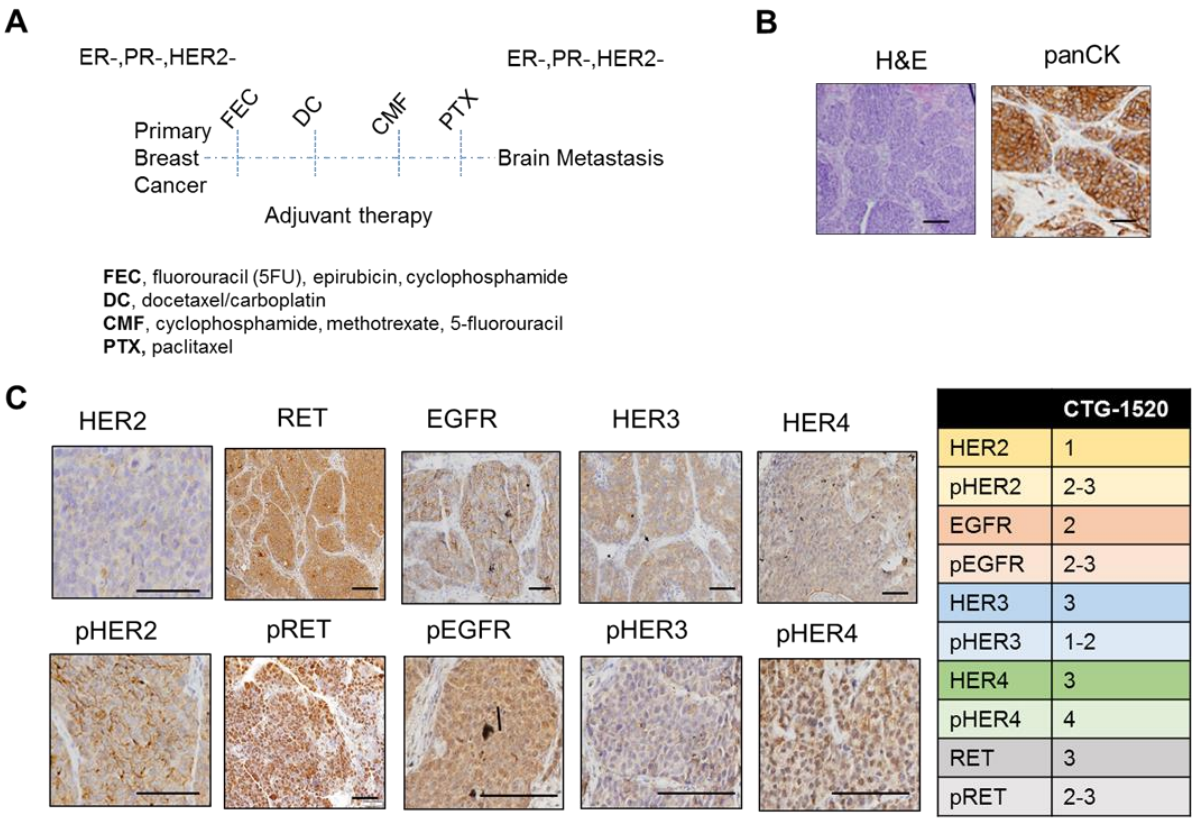

Figure 4.1: IHC characterisation of BrM patient-derived xenograft *in vivo* model

(A) Summarised clinical information of the patient from which the tumour xenograft, CTG-1520, was derived from. ER, PR and HER2 status in primary and BrM are indicated alongside adjuvant treatment received prior to resection (B). Representative images of PDX tumour sections after Hematoxylin & Eosin *(*H&E) and IHC staining for pan-cytokeratin (C) Representative IHC staining for RET and HER family members alongside key phosphorylated proteins pEGFR (Y^{1068}), pHER2 (Y^{1221}), pHER3 (Y^{1289}) and pHER4 (Y^{1284}) and pRET (Y^{1062}) alongside a chart displaying their assigned IHC intensity scores. Images shown were captured at 20x or 40x magnifications; scale bars correspond to 50μm or to 20μm. HER2 and all HER family members are 40x; scale bars correspond to 20μm. All other images were captured at 20x magnifications; scale bars correspond to 50μm

4.3.2. Inhibition of RET and HER2 demonstrates significant anti-tumour activity in breast cancer brain metastases *in vivo*

To determine the efficacy of RET and HER2 inhibition *in vivo*, the drug effect of cabozantinib and afatinib on tumour growth was evaluated in BrM PDX CTG-1520, in collaboration with Champion Oncology. All PDX tumours were transplanted subcutaneously as tumour fragments into immunocompromised mice before being allowed to grow to a volume of 150–300 mm^3. PDX implanted mice were then randomly assigned to treatment groups and orally administered with either cabozantinib (30 mg/kg), afatinib (20 mg/kg) or vehicle control over a period 20 days (5 days on/ 2 days off; n=12, 4 mice per treatment group). Throughout the treatment course, tumour growth was monitored by recording tumour volume twice a week via caliper measurements and the study was terminated when the mean tumour volume in the control group reached approximately 1500 mm^3. The workflow of this *in vivo* study is summarised in Figure 4.2A. The effect of drug treatments on tumour growth were determined by the % of tumour growth inhibition (TGI). At the conclusion of the study (Day 20), both cabozantinib, afatinib and vehicle treated group showed a mean tumour volume of 389 mm^3 ± 47, 326 ± 49 and 1503 ± 218, respectively. The mean tumour volumes ± SEM can be found in Table 8.3, Appendix I. Cabozantinib and afatinib showed significant anti-tumour activity leading to disease stabilisation compared to vehicle treatment in the BrM PDX model ($p < 0.001$, 86%TGI and $p < 0.01$; 91%TGI, respectively) (Figure 4.2B).

In order to assess mouse toxicity to drug treatments, variations in weight were monitored throughout the treatment course. The mean ± SD animal body weights for all groups be can be found in Table 8.4, Appendix I. As shown in Figure 4.2C, transient mean weight loss was only observed in the afatinib-treated group as compared to Day 0. However, groups receiving this line of treatment had recovered their weight loss and reached a positive weight gain at the end of the study. These observed drug responses would suggest that treatment studies with cabozantinib or afatinib has no adverse side effects on the welfare of mice in vivo. Altogether, these

encouraging results suggest the potential utility and safety of both agents in treating BrM in the clinic.

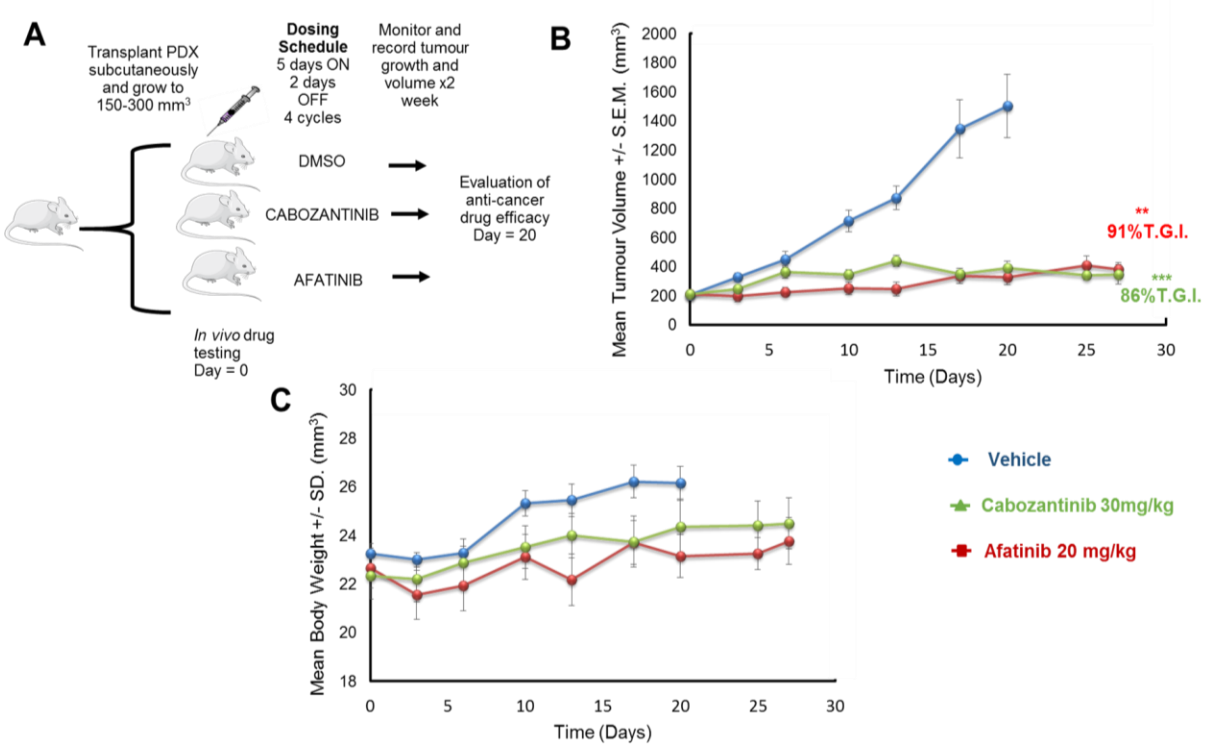

Figure 4.2: Inhibition of HER2 and RET significantly reduced tumour burden in breast cancer brain metastases *in vivo* model.

(A) Schematic of the experimental design of the *in vivo* experiment and treatment schedule followed. (B) Growth curve of CTG1520 xenograft tumour in mice receiving oral administration of vehicle (blue line) 30 mg/kg cabozantinib (green line) and 20 mg/kg afatinib (Red line). Tumour growth was evaluated by tumour volume via caliper measurements. Tumour response to cabozantinib and afatinib is represented by the red and blue line, respectively. Effects on tumour growth were evaluated with % tumour growth inhibition (RGI). The tumour growth curve shows mean tumour volume ± SEM (n=4 treatment group). The difference in the tumour volumes between treatments was compared using one-way ANOVA, followed by Newman-Keuls test. (C) Weight change curves of mice in CTG1520 xenograft tumour models during the course of the treatments. Each point represents the mean weight (g) values ± SEM from each treatment group.

4.3.3. Afatinib and cabozantinib deactivates signalling components downstream of RET/HER2 pathway in *in vivo* BrM model

A pharmacodynamics assessment of afatinib and cabozantinib treatment in PDX tumours was performed in order to better understand the drug responses observed. To explain the mechanisms underlying the anti-proliferative effects of both TKIs in the *in vivo* BrM tumour model, downstream effectors and key signalling nodes were examined using IHC. A significant reduction of ~7-fold in pRET(Y^{1062}) ($p<0.0001$) positivity was observed in cabozantinib treated PDXs versus vehicle treated PDXs (Figure 4.3B).

Interestingly, it was noted that afatinib had showed similar efficacy to cabozantinib independent of the HER2 negative status of the PDX tumour. Given that afatinib is a pan-HER family inhibitor we conducted a full interrogation of their expression and phosphorylated states in treated tumours. pEGFR ($p<0.0001$) and pHER4 ($p=0.0342$) was significantly diminished in afatinib treated group compared to vehicle by 20-fold and 6-fold, respectively (Figure 4.3A). Furthermore, a significant 4-fold reduction was detected in major downstream mediator of the HER family, pERK ($p=0.0003$), upon treatment with afatinib (Figure 4.3A). These results, therefore, show that inhibition of pEGFR and pHER4 may be responsible for the observed durable responses to afatinib treatment.

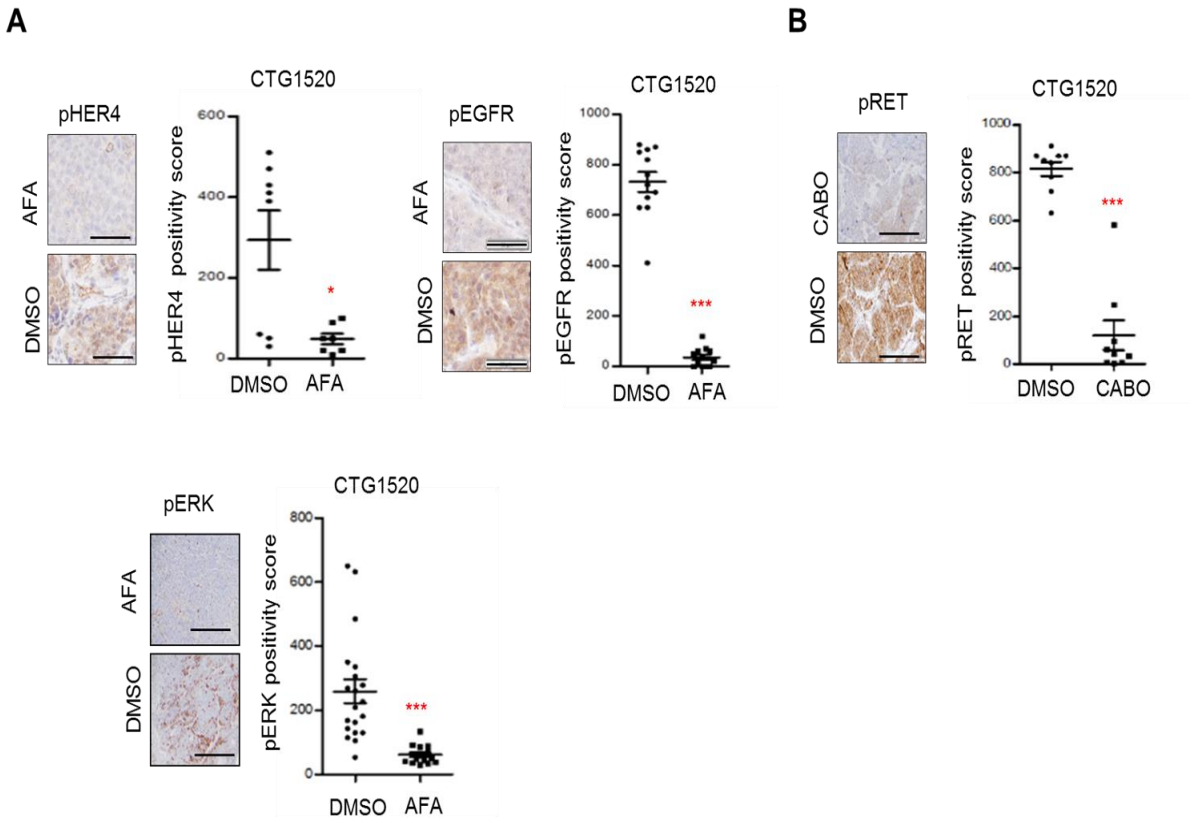

Figure 4.3: IHC analysis of signalling pathways downstream of RET/HER2 in BrM PDX CTG-1520.

(A) IHC analysis and quantification of pRET(Y^{1062}) expression in vehicle (DMSO) and cabozantinib (CABO) treated samples. (B) IHC analysis and quantification of pEGFR (Y^{1068}), pHER4 (Y^{1284}) and pERK(T^{202}/Y^{204}) expression in vehicle (V) and afatinib (AFA) treated samples. Representative images of IHC analyses of the tumours treated at the conclusion of *in vivo* experiment are shown. IHC quantification of all phosphorylated proteins was performed using the Aperio Digital Pathology imaging software. Representative images of IHC analyses of the tumours analysed at the conclusion of experiment. All scale bars correspond to 50 μm. Error bars represent mean ± s.e.m. (n = 5–10 images per group). P value compares treatments versus vehicle and is obtained using two-way paired student t-test where ***p<0.001, **p<0.01, *p<0.05.

4.4. Discussion

In this chapter, the efficacy of two multi-kinase inhibitors, cabozantinib and afatinib against tumour growth was assessed in an *in vivo* PDX model of BC BrM. These xenograft platforms have been widely renowned for their translational value into the clinic as demonstrated by multiple studies (Gao et al., 2015; Townsend et al., 2016). Moreover, given the significantly high incidence of BrM among patients with advanced TNBC, the molecular subtype of the PDX model is clinically relevant to large subset of the BrM patient population (Smid et al., 2008). In addition, while anti-HER2 therapies exhibit beneficial effects in HER2-positive patients, targeted therapies remain an unmet need for HER2-negative cases (Priedigkeit et al., 2017a). Interestingly, significant sensitivity to afatinib treatment was observed in the PDX model CTG-1520 despite being non-HER2 amplified.

There is substantial evidence that HER family members are aberrantly overexpressed in BC BrM which strongly suggest their involvement in facilitating brain colonisation and metastatic outgrowth. Deregulated expression of the HER family members, most notably, EGFR and HER2, contributes to disease progression in BC and have also been associated in colonisation of BrM (Sirkisoon et al., 2016). Previous studies have also reported a higher burden of HER3 and HER4 alterations in BrM relative to unmatched primary breast tumours (Da Silva et al., 2010; Saunus et al., 2015). This is also consistent with the preliminary RNA-Seq results where recurrent HER3 and HER4 expression gains had been observed in 33% and 24% of BrM, respectively. The nature of these receptors to heterodimerise with HER2 has been shown to play an important role in the development of resistance to anti-HER2 therapies suggesting that dual targeting of different receptor combinations could potentially be more efficacious, even for cases without HER2 amplification (Roskoski, 2014b). Therefore, a full co-expression profile analysis was conducted for all HER family members and their phosphorylated forms in the BrM PDX model. High expression levels of total EGFR, HER3 and HER4 were detected, together with significant activation of EGFR and HER4.

The EGFR IHC positive status of the BrM PDX model is consistent with the frequent reports of EGFR overexpression in TNBC subtypes (Nakai et al., 2016). Although some cell line models are sensitive *in vivo* to EGFR inhibition, clinical trials of EGFR inhibitors for treating TNBC have been fairly disappointing with poor response rates (Quesnelle et al., 2012; Nakai et al., 2016). However, in the treated BrM PDX tumour model, afatinib had significantly reduced both EGFR and HER4 activity. Consistent with this drug response, a strong decrease in phosphorylated ERK was shown, a key downstream module of the Ras–Raf–MEK cascade which is a primary effector of EGFR signalling. Dysregulation of this pathway is implicated in several oncogenic processes such as cancer cell proliferation, migration and survival (Roskoski, 2014b).

One of the possible molecular mechanisms underlying the sensitivity of our PDX model to afatinib could be the potential existence of HER family activating mutations. Indeed, other clinical trials have demonstrated afatinib efficacy in BrM harbouring EGFR mutations from patients with NSCLC (Schuler et al., 2016; Hoffknecht et al., 2015). Alternatively, activation of EGFR and HER4 could also be occurring through the formation of heterodimers with other HER family members, as suggested by their synchronised phosphorylation activity, including pHER2 despite having weak HER2 expression (1+). These findings are clinically significant, demonstrating that clinically HER2 negative BrM patients may benefit from treatment with pan-HER inhibitors.

RET targeting had also induced significant anti-tumour effects in the BrM PDX model. High levels of RET signalling were observed in this model as demonstrated by the strong RET and pRET IHC positivity. As previously mentioned, cabozantinib is an inhibitor of multiple tyrosine kinases including VEGFR, MET and AXL, all of which have been also implicated in metastasis and angiogenesis. Although the clinical activity of this TKI is hypothesised to be driven by RET inhibition the inhibitory effects of these other targets cannot be excluded. To provide more supporting evidence that the observed anti-tumour responses are indeed contributed to by the effects RET inhibition, the activation status of this receptor was further investigated in treated tumours. Cabozantinib treatment caused a significant disruption to the

phosphorylation of RET tyrosine 1062. Y^{1062} serves as a key docking site in RET for several intracellular adapters, namely SHC, which can recruit GRB2 and lead to subsequent activation of RAS/ERK and PI3K/AKT signalling (Putzer and Drosten, 2004) Therefore it can be concluded that the observed anti-tumour growth response is contributed to by the inhibition of RET signalling.

While PDXs represent indispensable preclinical model systems for testing novel therapeutic strategies, it is still worth acknowledging some of its main limitations related to this investigation. Firstly, it is noted that it would have been desirable to have a larger therapeutic dataset that included HER2-positive BrM PDX models and matched primary tumours. However, creating PDX models can be labour intensive and time-consuming and the establishment of such a collection would have been a tremendous rate-limiting step for this investigation.

Secondly, the PDX tumour employed in study had been subcutaneously transplanted into mice. However, there is evidence to suggest that such tumour models may respond differently to therapies compared with orthotopic BrM tumour xenografts. Indeed, this is well-reflected in clinic by the evident discordance between intracranial and extracranial tumour responses to HER2-directed therapies (Dagogo-Jack et al., 2017). More importantly, the host organ microenvironment has been shown to play crucial role in facilitating the growth pattern of transplanted tumour xenografts (Chung et al., 2005) and can also mediate treatment responses by compromising the efficacy of targeted therapies. Using orthotopic CDX mouse models of HER2-positive BrM, several recent cases studies have demonstrated how the neural niche can support drug resistance in BrM through adaptive signalling mechanisms. Two independent studies have revealed that these tumour models had differential responses to drug treatments compared with matched cell lines implanted in the mammary fat pad and were much less sensitive to HER2 and PI3K inhibitors (Ni et al., 2016; Kodack et al., 2017b; Kodack et al., 2012). One study was further extended to show that, relative to the heterotopic counterpart, orthotopic BrM CDXs had increased expression of HER3 and that activation of this RTK was driving resistance to PI3K inhibitors. Given the

enrichment of HER3 ligands, neuregulin-1/2, in normal brain tissue it was hypothesised that the brain microenvironment may be indirectly responsible for this. The addition of HER3 agonist to treatments with either HER2 or PI3K leads to a significant increase in mouse survival compared with single agent alone. Altogether these studies' findings suggest that the brain microenvironment influences treatment outcomes for BrM which must also be considered when interpreting drug efficacy data from extracranial model PDX model systems.

Hence, in order to include the potential molecular impact of metastatic tumour cell-brain microenvironment interaction on therapeutic intervention and, an intracranial PDX will need to be tested in future preclinical target validation studies. This could also provide invaluable information on the involvement of activated astrocytes and their neuro-inflammatory responses to these novel therapies. While this may be quite a challenging task, the aforementioned studies and others have demonstrated success in establishing these models (Contreras-Zarate et al., 2017; Fei et al., 2010; Ni et al., 2016).

Nevertheless, these limitations do not undermine the clinical relevance of the presented work here on the BrM PDX model which supports the sensitivity and specificity of targeting RET in BrM. Furthermore, the finding from this chapter show that pan-HER inhibitors may potentially provide therapeutic benefit for non-amplified HER2 BrM.

5. HER2 and RET inhibition demonstrates drug efficacy in *ex vivo* models of breast cancer brain metastases

5.1. Introduction

From the previous comparative RNA-Seq analysis, a considerable level of transcriptional heterogeneity was observed between clinically sampled patient-matched breast tumours and their corresponding resected BrM. Importantly, common transcriptional differences were observed in oncogenic pathways, with notable patterns of recurrent enrichments in RTKs that were unique to brain metastatic lesions. As previously mentioned, these BrM-specific alterations are attributable to the selection pressures of both adjuvant treatment regimens and the brain microenvironment against highly adaptive MBC cells.

Although, the BrM PDX model from the previous chapter constituted a valuable *in vivo* system for preclinical drug evaluation it may lose some original features of the brain microenvironment which, as described, can be a major determining factor of therapy response. The development of preclinical models that emulate the complex biology of BrM are imperative to fully understand the pathophysiology of this disease and validate RET and HER2 as clinically actionable targets. Therefore to address and bridge these gaps between preclinical and translational research, this section of the study sought to explore a more innovative model system that could incorporate this additional dimension into the evaluation of BrM tumour response to anti-RET and anti-HER2 therapies.

Organotypic explants of intact brain tumour resections are a clinically relevant and efficient *ex vivo* modelling tool for evaluating specific patient response to new drug therapies. Furthermore, it facilitates rapid investigations of individual tumour biopsies and, most importantly, ensures minimal tissue manipulation. This essentially allows patient intratumour heterogeneity and architecture to be almost entirely preserved while maintaining the original brain-tumour microenvironment. Thus, for this study, these models systems can re-enact important tumour-brain stromal cell interactions that transpire during therapeutic intervention which ultimately improves the accuracy for predicting patient outcome. Furthermore, the reliability of assessing drug responses in *ex vivo* explants of patient tumour biopsies has already been validated

by several studies in different cancers (Karekla et al., 2017; Novo et al., 2017; Vaira et al., 2010). However, to date no such approaches have been employed in in the context of exploring new drug targets against BrM. Here, we established 3-dimensional *ex vivo* models of BC BrM by acquiring fresh tumour biopsies from patients undergoing surgical BrM resection in order to determine the efficacy of cabozantinib and afatinib in a more patient individualised treatment context.

5.2. Aims

The aim of this chapter was to:

- Characterise the RET and HER family expression profile in all *ex vivo* models using IHC
- Determine the anti-tumour efficacy of cabozantinib and afatinib in *ex vivo* models through IHC quantification of ki67 cell proliferation marker
- Evaluate the potential mechanism of action of both inhibitors in treated *ex vivo* models by mutational analysis of their multiple target genes.
- Evaluate the potential mechanism of action of both inhibitors in treated *ex vivo* models by IHC analysis of phosphorylated signalling modules downstream of HER2 and RET

5.3. Results

5.3.1. Establishment of BrM *ex vivo* explants

To further support the potential therapeutic benefit of targeting RET and HER2 in treating BrM, the efficacy of cabozantinib and afatinib was next examined in patient-derived *ex vivo* models of the disease (n=4). These tumour explants were generated by acquiring fresh viable BrM from patients undergoing neurosurgery. Once obtained, the tissue sample was immediately macrodissected into smaller fragments before culturing them on media pre-soaked semi-solid scaffolds. This unique model system preserves both the unique cellular and molecular components of the original human brain microenvironment as well as the heterogeneity and histological properties of BrM. In doing so, crucial tumour-stromal interactions that may affect drug responses can be reproduced and be integrated into this study. The *ex vivo* brain tumours were then treated with vehicle, cabozantinib (10nM) and afatinib (25nM) for 72 hours followed by fixing, paraffin embedding and IHC analysis (Figure 5.1A). BrM specimens were amenable to explant culture as tumour tissue architecture was still intact at the end of treatments (Figure 5.1B)

Overall, fresh tumour from 4 BrM patients were analysed in this *ex vivo* experiment. The clinical information for each patient is outlined in Appendix I, Table 4. Notably, the pathology of these metastatic tumours reiterates the key receptor subtype alterations that we have previously observed from our sequencing study. *Ex vivo* Patient 1 (xBrM-T606) had endocrine resistant ER-positive BC but had lost ER expression resulting in a triple negative brain metastatic tumour. Patient 2 (xBrM-T347) and Patient 3 (xBrM-T638) are both cases of ER+/HER2- primary tumours that had switched to HER2 positivity in the BrM. PR expression was also lost in Patient 2. *Ex vivo* Patient 4 (xBrM-T681) was treatment naïve and had an ER-positive/HER2-positive primary tumour whose status was maintained in BrM. The *ex vivo* samples were also evaluated for HER2 amplification using FISH.

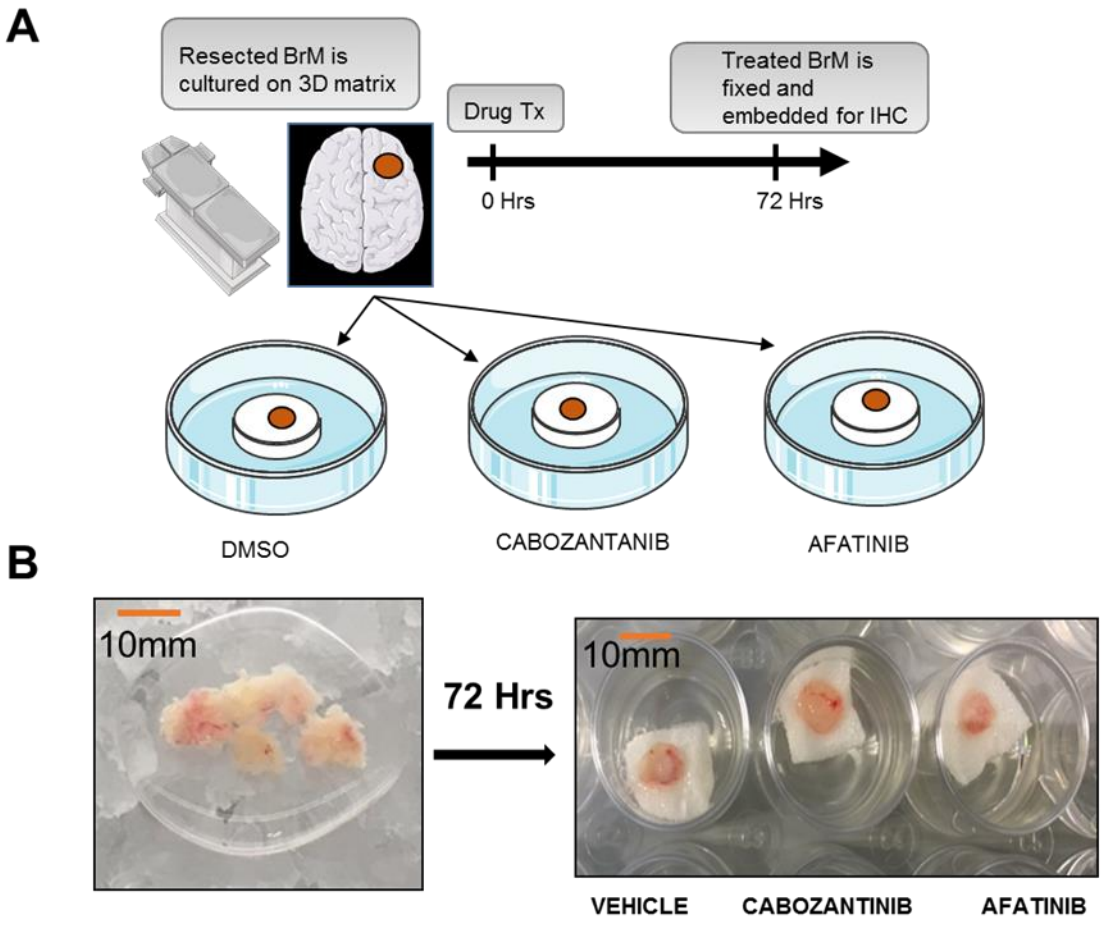

Figure 5.1: Illustration of *ex vivo* experimental design.

(A) A schematic workflow of the study. To establish patient-derived brain metastatic *ex vivo* models, resected BrM tumour tissue from patients were cultured and each treated with either drugs or vehicle for 72hrs after which were then paraffin embedded and IHC stained. (B) Image represents an example and the process of preparing BrM explant cultures. Brain metastatic tissue was dissected into smaller fragments and cultured on pre-soaked 1 cm^3 hemostatic gelatin dental sponges in breast/brain supporting media before receiving drug treatments.

5.3.2. Expression profile analysis of RET, HER family and their activated states in each brain metastatic tumour tissues utilised in *ex vivo* study

The expression and activation profile of both RET and all members of the HER family were concomitantly determined in uncultured samples of the BrM by means of IHC (Figure 5.2A; Figure 5.2B). Tumour specific RET and pRET expression was detected in all tumour samples. Strong HER2 expression was also observed in T347, T638 and T681, whereas T606 was clinically validated as HER2 negative. Interestingly, T347 and T638 switched from HER2 negative in the primary to HER2 positive in the BrM. FISH analysis was applied to these *ex vivo* specimens to determine if increased HER2 expression and altered status was accompanied by a gain in gene copy number. T347 was shown to be amplified by FISH (HER2:cep17 ratio 1.01; HER2 count 7.15) yet despite this, had only moderate levels of pHER2 expression. However, IHC results suggest that functional signalling may be predominantly occurring via EGFR instead as it had also demonstrated strong expression and activation of EGFR protein. While T638 was clinically designated as FISH equivocal (HER2:cep17 ratio 1.77; HER2 count 4.1), yet HER2 was still highly expressed at protein level, along with EGFR, HER3 and HER4. However, only the phosphorylation status of HER2 and HER4 was elevated in this patient model. Similarly, T681 showed high expression all of HER family members, together with their activated states. In the HER2-negative BrM model, T606, EGFR and HER4 were shown to be co-expressed, together with their activated forms. Notably, despite low levels of HER2 protein expression in this model, phosphorylation of HER2 was still detected suggesting that its activation status is possibly being maintained by dimerising with EGFR and/or HER4. Taken together, the IHC data confirms potent activation of both RET and HER family signalling in all of the *ex vivo* models.

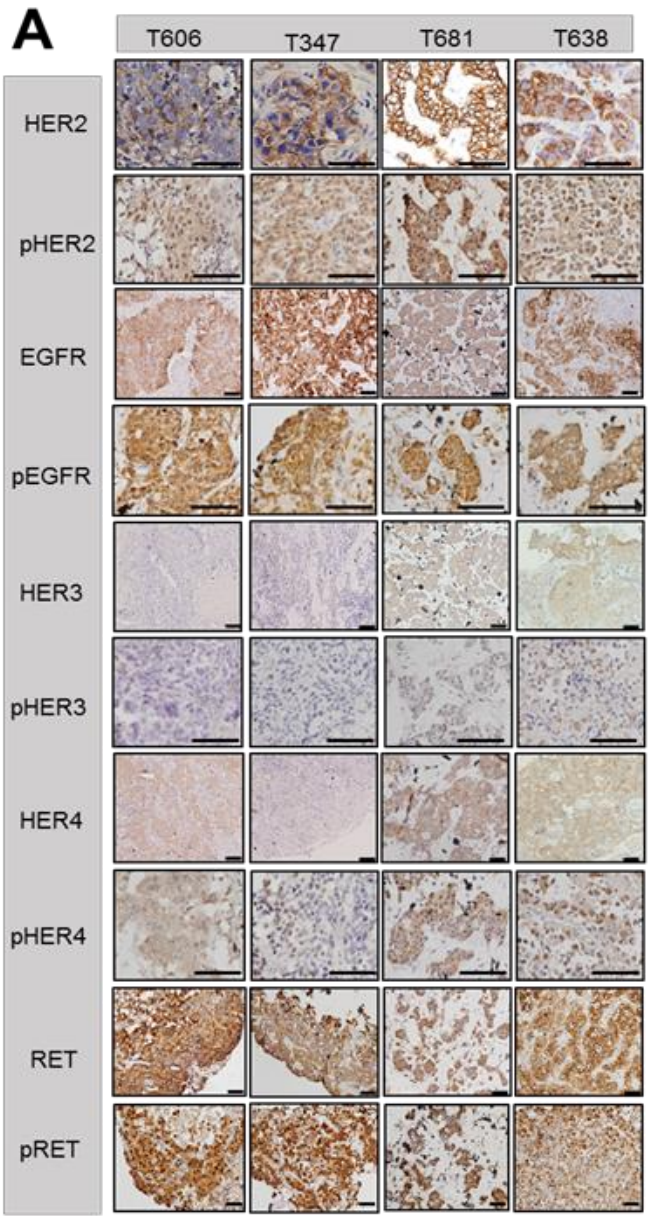

B

xBrM	T606	T347	T681	T638
HER2	1	2	3	3
pHER2	2-3	2	3-4	2-3
EGFR	3	4	3	3
pEGFR	2-3	3-4	2-3	1-2
HER3	0	1	2	2
pHER3	0	0	1	1
HER4	2	1	4	3
pHER4	2	1	3	3
RET	4	3	2	3
pRET	4	3	2-3	2-3

Figure 5.2: IHC expressing profiling of HER2 and RET signalling in *ex vivo* BrM models

(A) Representative IHC images of the RET/HER family members together with key phosphorylated proteins pEGFR (Y^{1068}), pHER2 (Y^{1221}), pHER3 (Y^{1289}) and pHER4 (Y^{1284}) and pRET (Y^{1062}). Images shown were captured at 20x or 40x magnifications; scale bars correspond to 50μm or to 20μm. (B) IHC scores that were assigned to each of the tumour explants and tumour PDXs.

5.3.2 RET and HER2 expression gains in brain metastasis is demonstrated in a patient-matched case.

Matched primary tumour tissue was available for one of the patient cases, T638. At the protein level, by IHC analysis, HER2 and RET levels were conclusively demonstrated to be higher in BrM relative to the primary (Figure 5.3A). These expression changes were also observed and confirmed at the mRNA level for RET as determined by TaqMan RT-qPCR (Figure 5.3B). With regards to the other patient BrM tumours, matching primary tumours were unavailable. Indeed, such longitudinal studies across patient-matched samples can be quite challenging as tumour specimens are rare and difficult to collect.

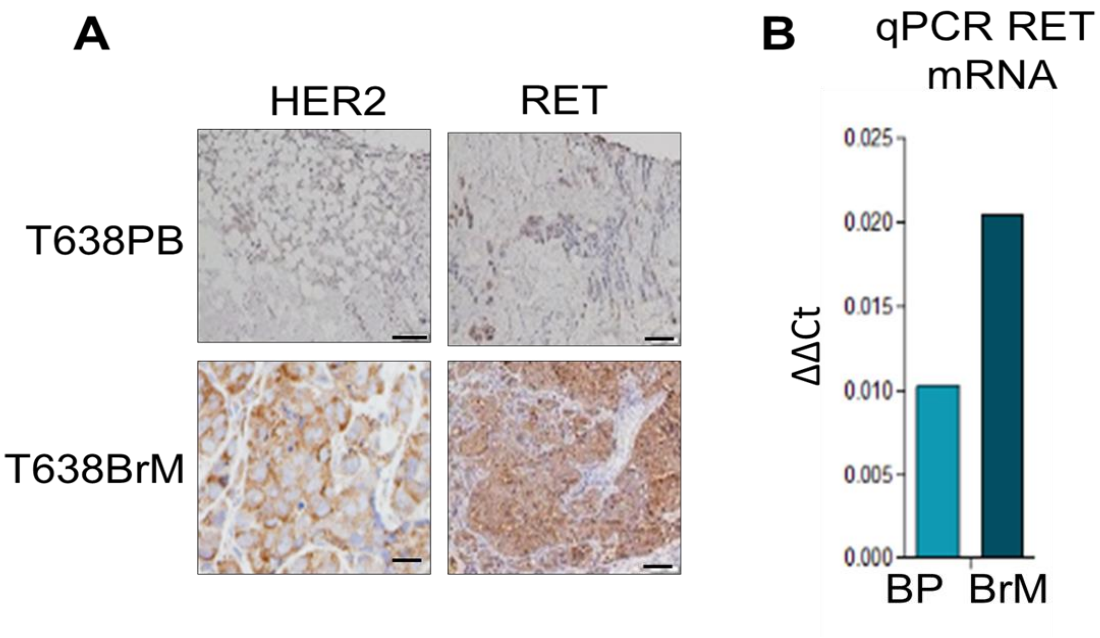

Figure 5.3: Expression gains of HER2 and RET in xBrM-T638 compared with matched primary tumour.

(A) Primary and metastatic IHC staining and protein analysis of RET/HER2 from case T638PB (Primary Breast) and patient matched T638 BrM (Brain Metastasis).Images shown are 20x; scale bars correspond to 50 μm (B) mRNA expression levels of RET as analysed by Taqman PCR. Bar chart displays ΔΔCt values.

5.3.3. Therapeutic response to RET and HER2 inhibition in *ex vivo* BrM models

Analysis of ki67 IHC expression was performed on 5 µM paraffin sections to assess the rate of cell proliferation in all FFPE embedded tumour explants that had been treated with cabozantinib, afatinib and vehicle control for 72 hours. The ki67 proliferation index is a well-established tool for assessing tumour aggressiveness in BC and high levels are strongly associated with poor prognosis (Dowsett et al., 2011). Cabozantinib had a substantial anti-tumour effect on x-BrM models T606 (p= 0.0008), T347 (=0.0014), T681 (p=0.0253)and T638 (p=0.0003), as demonstrated by a significant decrease in proliferating cells (ki67+) relative to vehicle treated tumours by 93.9%, 73.75%, 66.76% and 65.24%, respectively (Figure 5.4). Similarly, afatinib treatment also lead to a significant suppression of ki67 in x-BrM models T606 (p=0.0046), T347 (p=0.0005), T681 (p=0.021) and T638 (p<0.0001) relative to the vehicle control by 83.6%, 76.2%, 74.3% and 88.74%, respectively (Figure 5.4). Altogether, our data validates that targeting RET and HER2 induces significant anti-tumour effects in all of the BC BrM *ex vivo* models. Moreover, similarly to the PDX model from chapter 4, afatinib had also demonstrated an anti-proliferative effect independent of HER2 amplification in one of the treated explant cases, xBrM-T606. This could most likely be due to inhibition of EGFR or/and HER4-mediated signalling as both receptors were previously shown to be expressed and activated (Figure 5.2A; Figure 5.2B).

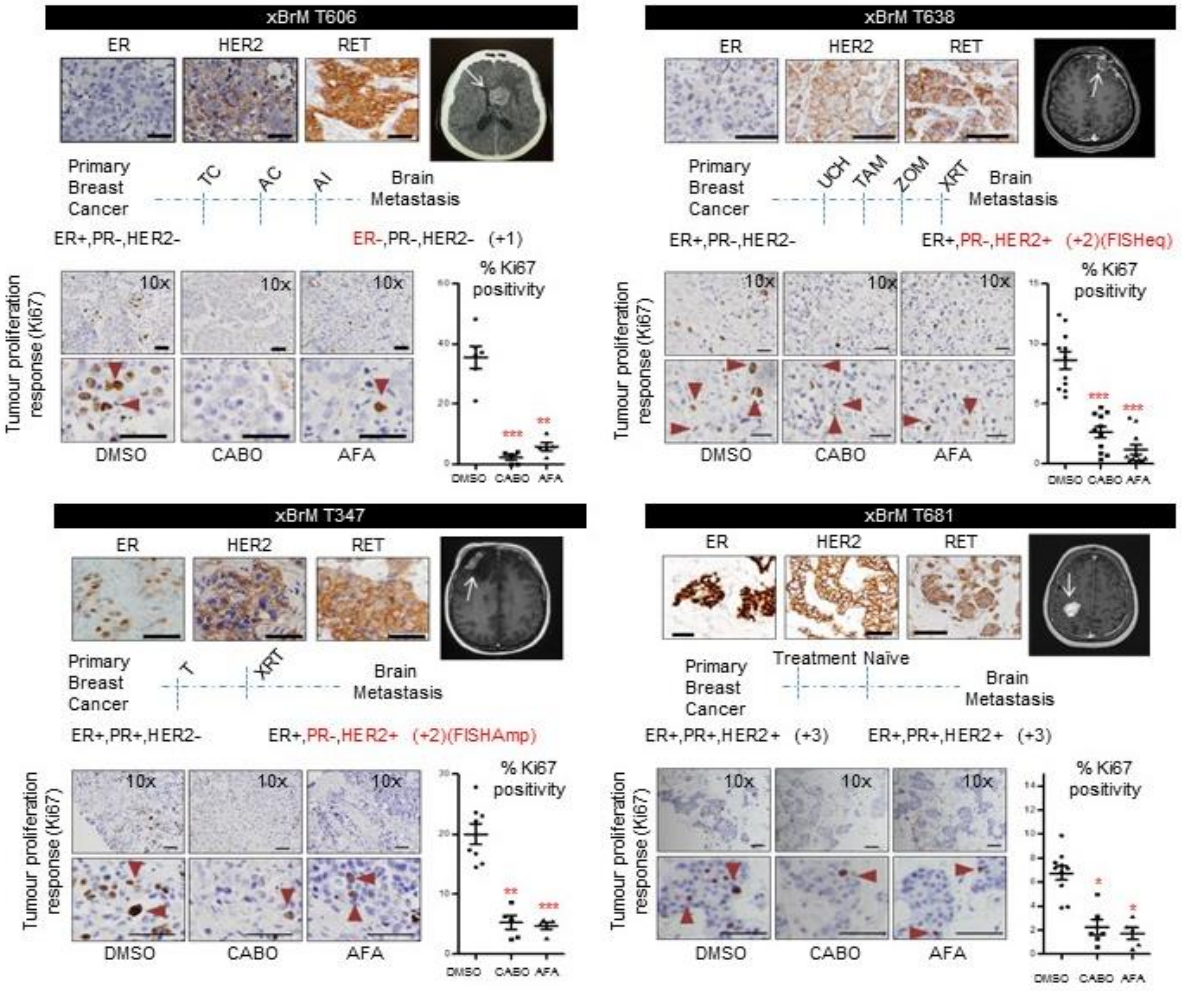

Figure 5.4: IHC analysis of Ki67 in treated *ex vivo* models of breast cancer brain metastasis

Ex vivo models (x-BrMT606, T347, T638 and T681) were treated with vehicle (0.1% DMSO), 10 nM cabozantinib and 25 nM afatinib and processed as previously described. MRI/CTI images of the brain metastases resected for each patient case are shown together with their ER, HER2 and RET IHC expression profile. Accompanied below each case is a diagram summarising the adjuvant treatment received prior to BrM resection as well as the hormone receptor status of both the primary breast and BrM tumours. Representative images of ki67 IHC staining analyses and quantification in treated and processed tumour explants (red triangles indicate ki67+ cells). All scale bars, 50 μm. Error bars represent mean ± s.e.m. (n = 5–10 images per group). P value compares treatments versus vehicle and is obtained using two-way paired student t-test where ***p<0.001, **p<0.01, *p<0.05.

5.3.4. Identification of somatic HER2 and RET mutations in *ex vivo* BrM models

To investigate the anti-tumourigenic responses to both TKI treatments, a mutational analysis of cabozantinib and afatinib target genes was conducted on the BrM samples by WES (Table 5.1). Multiple variants were identified in several targeted kinase receptors, but their functional effects have not been previously characterised. Other types of mutations were also detected, including missense mutations (n=5) and silent mutations (n=6). Notably, DNA alterations relating to the kinase domain of HER2 were not detected or any other region previously associated with constitutive HER2 activation (Bose et al., 2013; Hyman et al., 2018). Furthermore, only 1 of the 4 tumour samples, T606, harboured a missense RET mutation whose oncogenic activity is still unknown. However, this variant may be of clinical significance, as this case exhibited the strongest RET and pRET expression by IHC and highest anti-proliferative response to cabozantinib out of all the *ex vivo* models.

Taken together, these results reveal the presence of several mutations in the BrM tumour samples which may possess biological importance and be responsible for the drug responses observed. However, given the uncertainty of their oncogenic properties, further investigations were performed in this study to better define the nature of cabozantinib and afatinib activity in the treated explants.

Table 5.1: Somatic mutations identified by whole exome sequencing in brain metastasis tumours used in the *ex vivo* study

Sample ID	Func	Gene	Exonic|Biotype	Transcript	Codon_Change	Impact	COSMIC	1000G_ALL
Afatinib targeted genes								
T347BrM	intron_variant	ERBB3	protein_coding	NM_001982.3:c.2617-73delA		MODIFIER		
T347BrM	intron_variant	ERBB4	protein_coding	NM_005235.2:c.2719+164delA		MODIFIER		
T638BrM	synonymous_variant	ERBB3	SILENT	NM_001982.3:p.Arg1116Arg/c.3348G>A	agG/agA	LOW		0.252196
T638BrM	intron_variant	ERBB4	protein_coding	NM_005235.2:c.2644-70_2644-69insGTTAACTGC		MODIFIER		
T638BrM	intron_variant	ERBB4	protein_coding	NM_005235.2:c.2643+79dupA		MODIFIER		0.285543
T638BrM	intron_variant	ERBB4	protein_coding	NM_005235.2:c.1947-24_1947-23insA		MODIFIER	COSN17139814	0.0315495
T638BrM	intron_variant	ERBB4	protein_coding	NM_005235.2:c.1622+84_1622+85delTT		MODIFIER		
T606BrM	missense_variant	EGFR	MISSENSE	NM_005228.3:p.Ala1210Val/c.3629C>T	gCa/gTa	MODERATE		0.000199681
T606BrM	missense_variant	ERBB2	MISSENSE	NM_001289936.1:p.Pro8Thr/c.22C>A	Cca/Aca	MODERATE	3	0.0658946
T606BrM	missense_variant	ERBB2	MISSENSE	NM_004448.3:p.Ile654Val/c.1960A>G	Atc/Gtc	MODERATE		0.00259585
T606BrM	intron_variant	ERBB3	protein_coding	NM_001982.3:c.2938-40_2938-39insAGTTCTTTAAA		MODIFIER		
T606BrM	intron_variant	ERBB3	protein_coding	NM_001982.3:c.3202-97delA		MODIFIER		
T606BrM	intron_variant	ERBB4	protein_coding	NM_005235.2:c.1622+83_1622+85delTTT		MODIFIER		
T681BrM	synonymous_variant	EGFR	SILENT	NM_005228.3:p.Ala613Ala/c.1839C>T	gcC/gcT	LOW	COSM5019978(2)	0.0421326
T681BrM	synonymous_variant	ERBB3	SILENT	NM_001982.3:p.Arg1116Arg/c.3348G>A	agG/agA	LOW		0.252196
T681BrM	synonymous_variant	ERBB3	SILENT	NM_001982.3:p.Gly1297Gly/c.3891G>T	ggG/ggT	LOW		
T681BrM	intron_variant	EGFR	protein_coding	NM_005228.3:c.629-329delG		MODIFIER		0.0123802
T681BrM	intron_variant	EGFR	protein_coding	NM_005228.3:c.1880+737dupA		MODIFIER		
T681BrM	intron_variant	ERBB4	protein_coding	NM_005235.2:c.2643+79dupA		MODIFIER		0.285543
Cabozantinib targeted genes								
Sample ID	Func	Gene	Exonic|Biotype	Transcript	Codon_Change	Impact	COSMIC	1000G_ALL
T347BrM	missense_variant	KDR	MISSENSE	NM_002253.2:p.Gln472His/c.1416A>T	caA/caT	MODERATE	COSM149673(20)	0.211861
T606BrM	missense_variant	RET	MISSENSE	NM_020975.4:p.Arg189Cys/c.565C>T	Cgc/Tgc	MODERATE		
T606BrM	synonymous_variant	RET	SILENT	NM_020975.4:p.Ser836Ser/c.2508C>T	agC/agT	LOW		0.0359425
T681BrM	synonymous_variant	RET	SILENT	NM_020975.4:p.Ser904Ser/c.2712C>G	tcC/tcG	LOW	COSM3751779(7)	0.172524

5.3.5. Cabozantinib and afatinib deactivates signalling components downstream of RET/HER2 pathway in *ex vivo* models

To explore the mechanisms underlying the anti-proliferative effects of both TKIs in our *ex vivo* models, downstream effectors and key signalling nodes were examined via IHC and quantified using Aperio Digital Pathology ImageScope software. Cabozantinib and afatinib significantly attenuated the activation of several downstream signalling proteins in treated explants, including pmTOR, pAKT, pP70S6k, pRaf and pERK, providing mechanism of action and further evidence for the functionality of both RTKs.

HER3 has been reported to be the more favoured dimerization partner of HER2 and that it is frequently co-expressed in HER2 positive tumours which was previously demonstrated in patient xBrM-T638 and xBrM-T681. In xBrM-T638, pHER2 was significantly reduced in the afatinib treated explants compared to the vehicle by ~5.5 fold ($p<0.0001$) in addition to downstream mediators of the PI3K/AKT pathway, pmTOR and pP70S6k ($p=0.0032$ and $p=0.0025$, respectively) (Figure 5.5). A decrease in pERK signalling was also noted ($p=0.0042$) (Figure 5.5).

Following cabozantinib treatment, pmTOR was also reduced compared to vehicle control (p=0.0032). In relation to the signalling activity of RET in cabozantinib treated explants versus the vehicle, a significant reduction in pRET positivity was observed (p=0.0004) by ~1.5 fold (Figure 5.5).

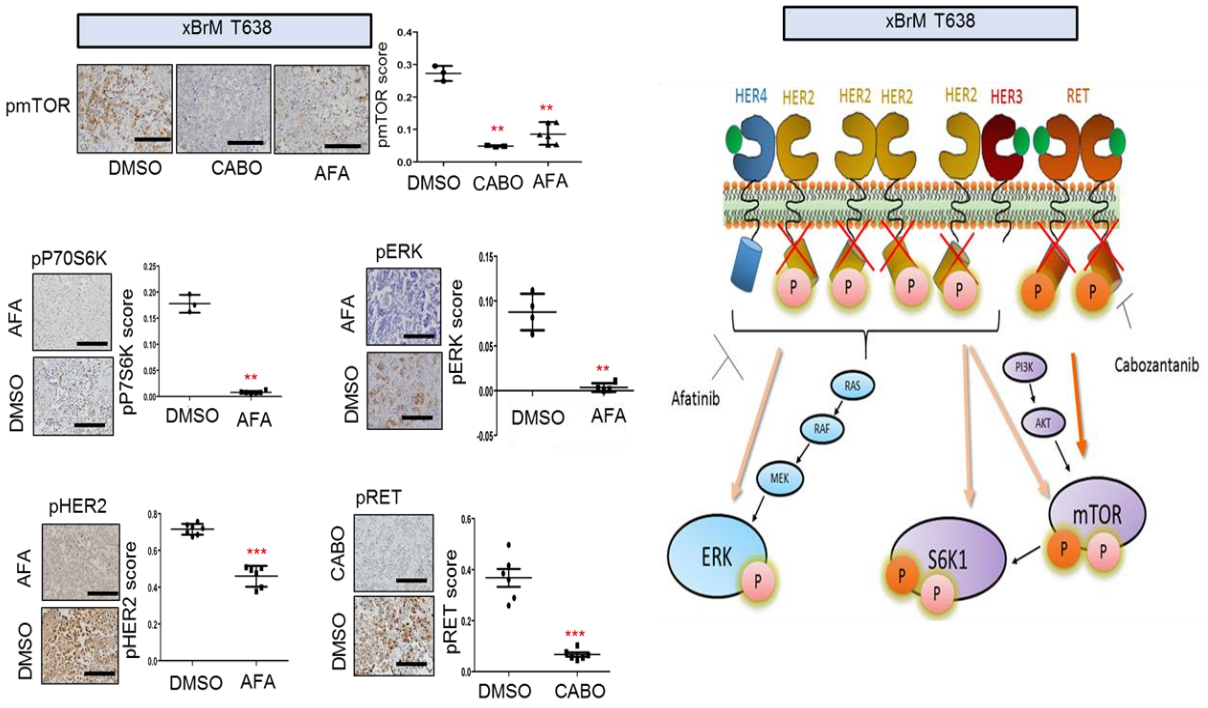

Figure 5.5: Downstream signalling analysis of xBrM-T638 in response to afatinib or cabozantinib treatment.

Quantitative IHC was carried out to profile, pERK, p70S6K, pmTOR as well as proteins pHER2 (Y^{1221}), and pRET (Y^{1062}) in all of the treated *ex vivo* samples. All images are representative of IHC analyses performed on tumour explants receiving indicated treatments for 72 hrs. All scale bars, 50 μm. Error bars represent mean ± s.e.m. (n = 5–10 images per group). P value compares treatments versus vehicle and is obtained using two-way paired student t-test where ***p<0.001, **p<0.01. Accompanied beside the scores is a schematic summary diagram explaining potential mechanism of drug effect in treated *ex vivo* model, xBrM-T638.

In xBrM-T681, pHER2 (p=0.004) and pAKT (p=0.01) were also downregulated in the afatinib treated explants compared to vehicle. Furthermore, a strong reduction in pHER4 signalling was observed in this model (p=0.04), which is another RTK that can potentially dimerise with HER2 and activate downstream signalling (Figure 5.6). Additionally, pAKT was also decreased in the cabozantinib treated explants compared to vehicle control (p=0.01).

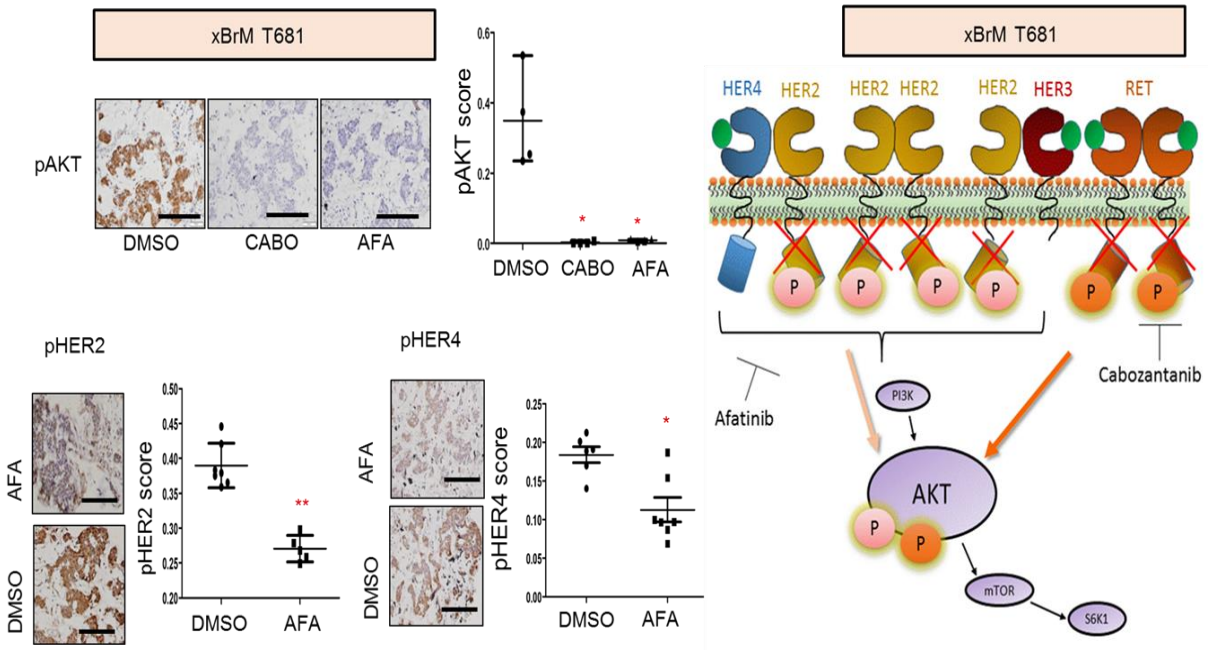

Figure 5.6: Downstream signalling analysis of xBrM-T681 in response to afatinib or cabozantinib treatment.

Quantitative IHC was carried out to profile, pRAF as well as proteins pEGFR (Y^{1068}), and pRET (Y^{1062}) in all of the treated ex vivo samples. All images are representative of IHC analyses performed on tumour explants receiving indicated treatments for 72 hrs. All scale bars, 50 μm. Error bars represent mean ± s.e.m. (n = 5–10 images per group). P value compares treatments versus vehicle and is obtained using two-way paired student t-test where **p<0.01, *p<0.05. Accompanied beside the scores is a schematic summary diagram explaining potential mechanism of drug effect in treated ex vivo model, xBrM-T681.

In the EGFR-overexpressed and HER2-amplified model, xBrM-T347, pEGFR was shown to decrease when treated with afatinib, although not significantly ($p=0.1119$). Nevertheless, a reduction was observed in pRAF ($p=0.0065$) when treated with afatinib, a key player of RAS signalling which is a major downstream pathway of activated EGFR (Lowenstein et al., 1992). Therefore, in this model, afatinib may be inhibiting the oncogenic activity resulting from EGFR/HER2 heterodimerization. Cabozantinib also successfully disrupted RET signalling as indicated by a significant reduction in both pRET ($p<0.0001$) and pRAF. ($p<0.0001$) by 3-fold and 2-fold, respectively (Figure 5.7*)*.

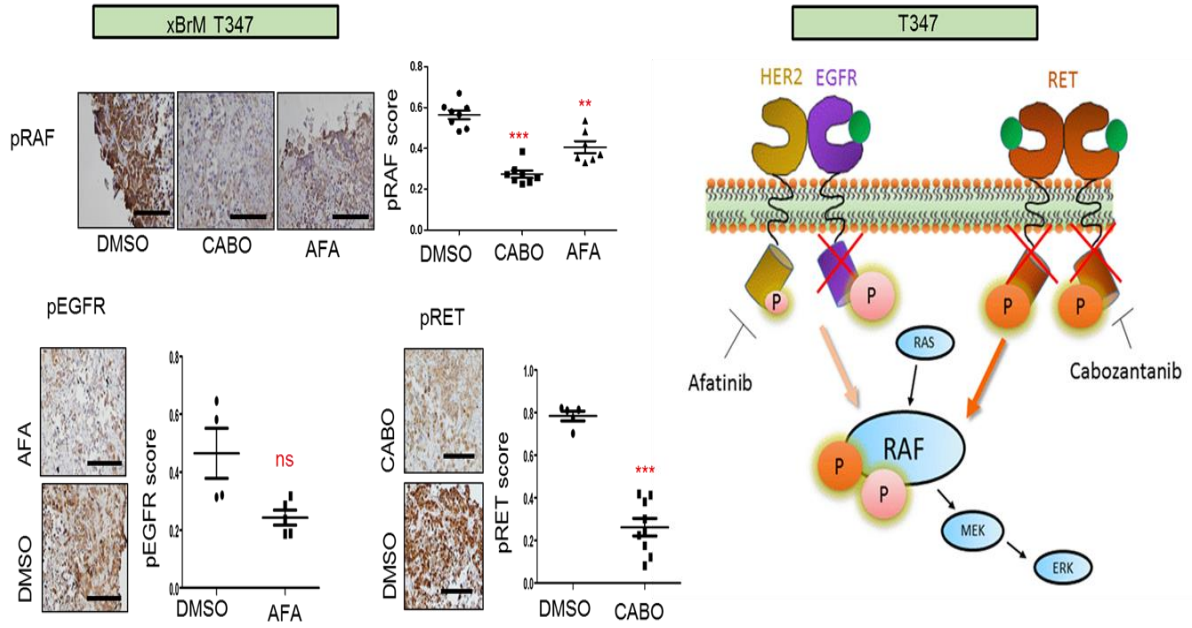

Figure 5.7: Downstream signalling analysis of xBrM-T347 in response to afatinib or cabozantinib treatment:

Quantitative IHC was carried out to profile, pRAF as well as proteins pEGFR (Y^{1068}), and pRET (Y^{1062}) in all of the treated *ex vivo* samples. All images are representative of IHC analyses performed on tumour explants receiving indicated treatments for 72 hrs. All scale bars, 50 μm. Error bars represent mean ± s.e.m. (n = 5–10 images per group). P value compares treatments versus vehicle and is obtained using two-way paired student t-test where ***p<0.001, **p<0.01, *p<0.05, n.s. not significant. Accompanied beside the scores is a schematic summary diagram explaining potential mechanism of drug effect in treated *ex vivo* model, xBrM-T347.

Finally, in xBrM-T606, a significant 3.5-fold decrease in pRET was observed post cabozantinib treatment, relative to the vehicle control ($p=0.0005$). A reduction in several intracellular signalling pathways was also observed following cabozantinib treatment as demonstrated in Figure 5.8. AKT signalling was abrogated as indicated by a decrease in pAKT and pP70SK6, relative to the vehicle control ($p=0.0156$ and $p=0.012$, respectively). A significant inhibitory effect was also observed on signalling modules along the MAPK pathway, including pERK and pRAF ($p<0.0001$ and $p=0.0052$, respectively).

While this model previously demonstrated weak HER2 expression, sensitivity to afatinib was still observed. The blocking effect of afatinib against other members of the HER family was therefore further investigated by assessing their activation profiles in treated *ex vivo* samples. Positive expression of EGFR and its activated form was previously demonstrated in this model. Treatment of tumour explants with afatinib lead to a significant 3.3-fold reduction in pEGFR relative to the vehicle control ($p<0.0001$). Despite low HER2 expression levels, its phosphorylated form was still previously observed in this model and, significantly, was almost completed suppressed upon afatinib treatment ($p<0.0001$). The co-inhibition of both HER receptors was accompanied by a decrease in pAKT levels relative the vehicle control ($p=0.0157$). Furthermore, inactivation of the MAPK pathway was also detected following afatinib treatment, as shown by an inhibition of pRAF and a significant decreased in pERK by 3.6-fold relative to the vehicle control ($p=0.0093$ and $p<0.0001$, respectively). Overall, downstream signalling analysis of the afatinib treated explants suggests that the observed anti-tumourigenic effects may be due to inhibition of pEGFR and pHER2 (Figure 5.8).

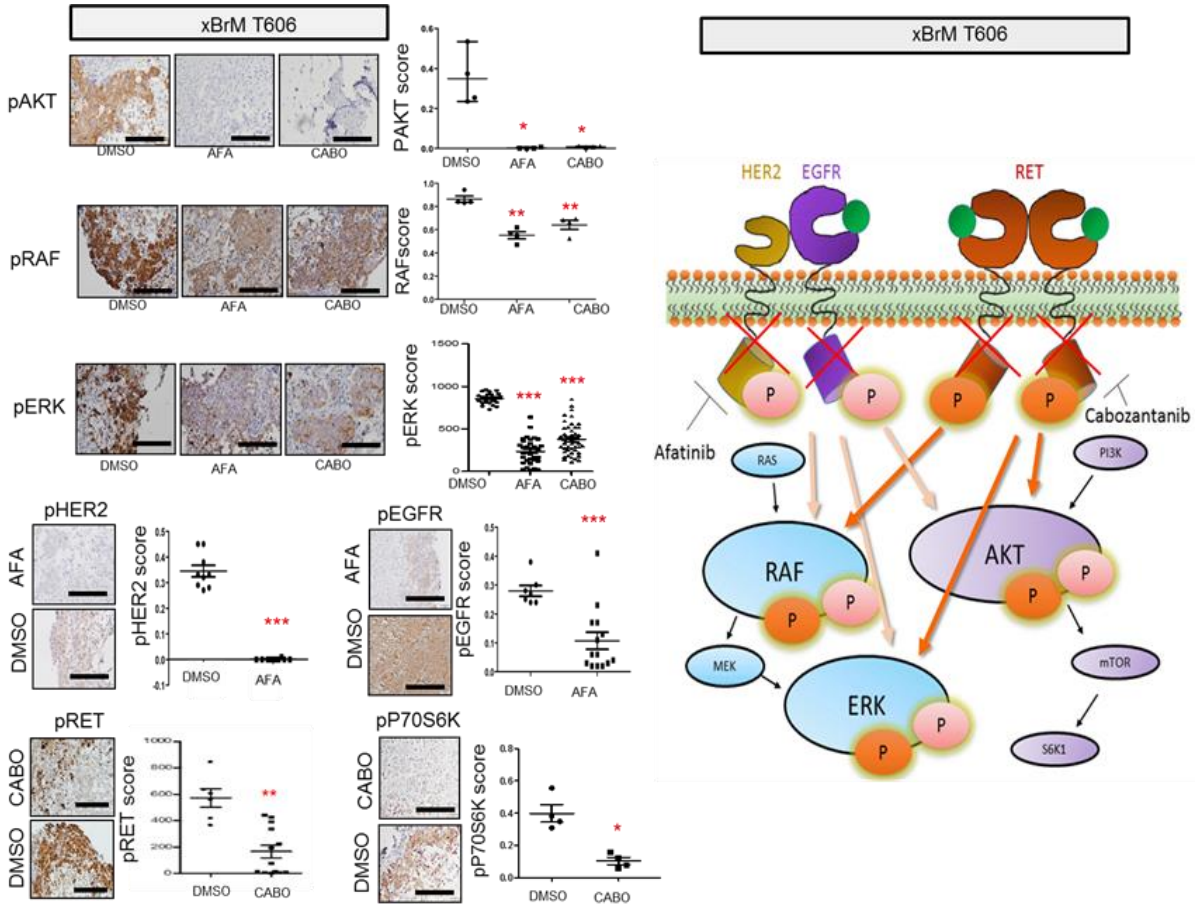

Figure 5.8: Downstream signalling analysis of xBrM-T606 in response to afatinib or cabozantinib treatment

(A) Quantitative IHC was carried out to profile pAKT, p70S6K, pERK, pRAF as well as proteins pEGFR (Y^{1068}), pHER2 (Y^{1221}), and pRET (Y^{1062}) in all of the treated *ex vivo* samples. All images are representative of IHC analyses performed on tumour explants receiving indicated treatments for 72 hrs. All scale bars, 50 μm. Error bars represent mean ± s.e.m. (n = 5–10 images per group). P value compares treatments versus vehicle and is obtained using two-way paired student t-test where ***p<0.001, **p<0.01, *p<0.05, n.s. not significant. Accompanied beside the scores is a schematic summary diagram explaining potential mechanism of drug effect in treated *ex vivo* model, xBrM-T606.

5.4. Discussion

Currently, there are still insufficient preclinical models that can adequately predict patient individual response to novel therapeutics and this is especially true in BrM. A common limitation with many existing platforms is their inability to mimic the intricate tumour-stroma interplay that transpires within the host microenvironment. Indeed, a plethora of unique cell populations reside within the unique brain milieu including astrocytes and microglia, many of which have been reported to promote tumour growth and survival (Fitzgerald et al., 2008) . Therefore, in order to better translate the reported findings to clinic, *ex vivo* explant culture models derived from fresh resections of human BrM tumour tissue was employed. This method presents an ideal system for evaluating the efficacy of cabozantinib and afatinib in individual patient BrM whilst simultaneously incorporating key physiological and micro environmental parameters into the study.

A diverse cohort of BC BrM patients was recruited to this study providing a deeper insight into differential patient responses. WES was subsequently performed for each surgical specimen to detect alterations in TKI target genes in order to explain the observed tumour sensitivity to treatments. From this gene expression analysis, no known activating mutations were identified in either HER2 or HER3. These results are unsurprising given that the frequency of such mutations have been reported to be relatively low in MBC patients (Nik-Zainal et al., 2016). However, this mutation frequency may be higher if investigated in large-scale screening analyses of brain metastatic patients. Furthermore, missense alterations in other regions besides the kinase domains of HER family members were observed whose exact functions are not currently defined

To characterise the mechanism of action of both TKI treatments, the scope of this study was expanded further by dissecting the expression profiles and activation status of the entire HER family repertoire and RET in each of the BrM models. IHC analyses revealed strong RET and pRET staining specifically in the tumour cells of all clinical BrM specimens. High levels of EGFR and pEGFR was also detected at the

cytoplasmic and membrane levels of malignant cells. These results are consistent with several findings that EGFR signalling is critical in BrM tumourigenesis. Furthermore, studies have also shown that the % increase of EGFR expression is higher in brain metastatic tumours (41%) in comparison to primary breast tumours (16%) (Gaedcke et al., 2007).

HER3 expression was detected in both cases that were defined as HER2-positive by IHC (3+), xBrM-T681 and xBrM-T683, albeit had relatively weak HER3 activation. Both RTKs have been previously reported to be frequently co-expressed in many BCs, most likely due to their preferred dimerization with one another out of all the HER family members (Bieche et al., 2003; deFazio et al., 2000). Of all the receptor paired combinations, the HER3/HER2 signalling complex is the most potent activator of the PI3K/AKT pathway due to the presence of several phospho-tyrosine docking sites in HER3 for PI3K (Roskoski, 2014b). Consistent with this, both xBrM-T681 and xBrM-T683 demonstrated strong activation of AKT and mTOR, respectively. Moreover, overexpression of HER3 has been established in both independent matched and unmatched BrM cohorts from BC and has also been linked with BrM-associated HER2 expression gains (Saunus et al., 2015; Da Silva et al., 2010). Given the wide abundance of the HER3 ligand, NRG-1, in the brain, HER3 activation has been implicated to play a role both in brain colonisation and in the acquired resistance of HER2-positive BC BrM to anti-HER2 therapies (Da Silva et al., 2010). This is believed to occur through oncogenic heterodimerization with HER2 and subsequent hyper-activation of the PI3K-AKT-mTOR signalling pathway. One recent study by Kodack et al. showed that resistance to PI3K inhibitors in HER2-amplified BrM can be circumvented by targeting HER3 (Kodack et al., 2017b). Thus, it would be interesting to evaluate if a dual combination of afatinib and a PI3K/MTOR inhibitor such as gedatolisib has a more synergistic effect in cases of HER2-positive/HER3-positive BrM tumours.

IHC studies were also extended to analyse key phosphorylation nodes of downstream target RTK pathways in order to determine the signalling impact of therapeutic intervention. Treatment with cabozantinib or afatinib in tumour explants

caused a downregulation in several regulatory effectors along the PI3K/AKT/mTOR and Ras-Raf-MEK-ERK cascade, which play major roles in cell proliferation and survival, respectively (Roskoski, 2014b). These preclinical findings are significant as aberrant expression of these signalling pathways may play pivotal roles in BrM biology (Da Silva et al., 2010). In particular, activated PI3K signalling is becoming an emerging hallmark of BrM. Recurrent genomic alterations along this pathway have been reported by several molecular characterisation studies of BrM (Brastianos et al., 2015; Bollig-Fischer et al., 2015; Adamo et al., 2011) with one notable multi-omic integration analysis revealing an enrichment of aberrations in 54.5% of BrM (Saunus et al., 2015). Similar to the aforementioned study above, an increasing body of evidence suggests that deregulation of this pathway may be a key adaptive mechanism underpinning BrM resistance to HER2-directed therapies (Dagogo-Jack et al., 2017; Kodack et al., 2015). In IHC analyses of matched primary breast and BrM, Da Silva et al. also demonstrated similar elevated activation of both AKT and Ras-Raf-MEK-ERK pathways in BrM in addition to activating mutations in upstream effectors such as PIK3CA and NRAS, HRAS and KRAS (Da Silva et al., 2010).

A critical negative mediator of the PI3K/AKT cascade is the tumour suppressor gene, PTEN. Downregulation of PTEN expression has been shown to be a recurrent genomic feature in BrM (Saunus et al., 2015; Ni et al., 2016). In a comparative target gene expression analysis between unmatched pairs of BrM and primary breast tumours, Wikman et al. observed that chromosomal aberrations in PTEN were more detectable in BrM by 52% (Wikman et al., 2012). Furthermore, while loss of PTEN is not typically found in the majority of epithelial carcinomas, it represents one of the most frequently observed aberrations in GBM and other CNS-related malignancies. These findings indicate that PTEN suppression may be a BrM-acquired feature for BC cell survival in the brain microenvironment via adaptive PI3K/AKT signalling. However, Adamo et al. previously reported a high concordance of PTEN expression between patient-matched tumour samples, alternatively suggesting that PTEN loss could perhaps facilitate earlier stages of brain metastatic progression. Furthermore, PTEN may be a prognostic marker for the development of BrM as lower expression levels in primary tumours has been associated with shorter time to disease

recurrence. (Adamo et al., 2011). Consistently, in the earlier mentioned study by Wikman et al., the frequency of PTEN chromosomal aberrations was also higher in primary tumours from patients that had suffered from BrM relative to patients without brain relapse. Taken together, loss of PTEN expression may represent an innate and/or acquired mechanism for PI3K/AKT activation in BrM.

Overall, the extensive IHC analysis of both RET and HER family expression profiles as well as their downstream signalling pathways provides a mechanistic insight into the anti-tumourigenic responses of each BrM tumour to both cabozantinib and afatinib. Characterising different patient tumour responses to the anti-tumour efficacy to TKI treatments is fundamental as evidence from the clinic suggests that not all BrM patients will respond to tyrosine kinase inhibition (Brastianos et al., 2015; Priedigkeit et al., 2016). This is believed to be primarily due to a number of oncogenic drivers that appears exclusively in BrM versus extracranial metastasis of the same patient. Similarly, the previous findings together with the work presented here, confirm discordances in expression profiles between primary breast and BrM tumours. Therefore, such individual patient profiling work can help inform rational drug selection and make refinements to approaches in treatment strategies for a unique cohort of responders. Of clinical relevance, two of the tumour specimens recruited to *ex vivo* study had originated from HER2-negative primary breast tumours but were reclassified as positive in their BrM by either IHC as well as FISH analysis. Several studies have described similar events of HER2 subtype switching during tumour progression from primary breast tumour to distant BrM or else increased HER2 amplifications and mutation in BrM that are undetected in patient-matched primary tumours (Priedigkeit et al., 2017a; Saunus et al., 2015). Furthermore, these observed expression differences are reported to be more common in BC BrM compared with BrM of tumours originating from different primary sites (Saunus et al., 2015).

The findings from this *ex vivo* therapeutic intervention study suggest that small molecule TKI pan-HER inhibitors are a promising treatment strategy for BrM. Interestingly, noteworthy anti-tumour activity was observed, independent of HER2

status, as demonstrated by the significant inhibitory effect of afatinib in HER2 low-expressing model xBrM-T606. This case demonstrated high activation levels of EGFR and in addition phosphorylated HER2 implicating functional signalling through EGFR-HER2 heterodimers. Indeed, there is currently a growing curiosity as to whether HER2 targeted therapies can confer clinical benefit to BCs presenting with lower HER2 expression, that is, patients that are FISH negative but have an IHC score of 1+ or 2+. Disappointingly, a recent phase lll clinical trial, NSABP B47 had demonstrated that trastuzumab was not effective in treating HER2 in early non-amplified tumours. However, the clinical potential of pan-HER inhibitors in treating this class are now being explored and their assessment in clinical trials are currently underway. One such study, SUMMIT, investigating non-HER2 amplified patients harbouring HER2/HER3 somatic activating mutations has reported significant responses, neratinib, which is a much more potent irreversible pan-HER TKI quite similar to afatinib (Hyman et al., 2018). These results indicate that a subset of low HER2 expressing patients could benefit from such therapeutic approaches. Given that both HER2-positive BrM patients, T347 and T683, had not received HER2 targeted drugs due to the negative HER2 status of their primary tumour this is certainly a clinical strategy worth considering.

In a recent randomised phase II study, both afatinib as a monotherapy and in conjunction with chemotherapy showed disappointing results in HER2-positive BC patients with progressive BrM (Cortés et al., 2015). There are a number of possible explanations for these poor patient responses. (1) Firstly, the trial was conducted in patients that had progressed after or during treatment with either trastuzumab, lapatinib or both. A greater clinical response may have been observed in a cohort whom were not previously exposed to HER2-targeting drugs. Patients of the *ex vivo* BrM tumours had no prior anti-HER2-based therapies which may explain their increased sensitivity to afatinib treatment. (2) Secondly, patient eligibility for the trial study was restricted to those defined as HER2-positive in their primary BC. The two HER2-positive switched BrM cases from the *ex vivo* study, T347 and T683, had not received HER2-targeted drugs due to the negative HER2 status of their primary

tumour yet both responded well to afatinib treatment. This again highlights the importance of characterising the molecular profile of both the primary and metastatic tumours in patients. Perhaps, afatinib may have been more efficacious if conducted in a clinical cohort that are selected for HER2 positivity in the BrM. (3) Thirdly, a greater CNS response may have been achieved at higher dosages, yet adverse events were already quite frequent at the administered drug concentration. Sensitivity to afatinib may have been observed in the *ex vivo* tumour explants at treatment concentrations that may not have been achievable in patients without significant toxicity.

On the other hand, more potent pan-HER inhibitor, neratinib, has shown greater clinical promise in treating HER2-positive BC with progressive BrM and has an acceptable safety profile in humans. While the CNS ORR are only modest as a single agent (8%), a significant improvement is obtained in combination with chemotherapy with a reported CNS ORR of 49% (Freedman et al., 2016; Freedman et al., 2017)., Dual EGFR/HER2 reversible TKI, lapatinib, demonstrated similar monotherapy outcomes with a response rate of 6% in patients with CNS metastases, implicating a possible intrinsic tumour resistance to both anti-HER2 drugs (Lin et al., 2009a). Similarly again, encouraging activity is observed when delivered in conjunction with capecitabine with a CNS response of 38%, suggesting that BrM resistance to HER2-directed therapies may possibly be circumvented with combination therapy (Lin et al., 2011). While lapatinib did surpass neratinib in another recent combination trial study with a response rate of 66%, it must be noted that the selected patient cohort were newly diagnosed with BrM (Bachelot et al., 2013). Perhaps the same or even greater response rates may be achieved with neratinib and chemotherapy if conducted in a similar clinical cohort of previously untreated BrM. Importantly, from a drug toxicity perspective, neratinib was also much more tolerated by patients than lapatinib in both the monotherapy and combination clinical trial studies. The results from these clinical trial studies is summarised in

Table 5.2. Taken together with these supportive studies, the work from this thesis strengthens the potential promise of small molecule TKIs of HER2 in treating BC BrM, in particular pan-HER inhibitors.

Table 5.2: Summary of clinical trials testing dual EGFR/HER2 and pan-HER inhibitors in HER2-positive BC with BrM

Treatment Regimen	HER Targets	Prior anti-HER2 therapy	Cohort (N)	CNS response rate	No. of grade ≥3 adverse events	No. of serious adverse events
Monotherapy						
Afatinib (Cortés et al., 2015)	HER2/EGFR/ HER4	Lapatinib and/or Trastuzumab	40	0%	46	5
Lapatinib (Lin et al., 2009a)	HER2/EGFR	Trastuzumab	242	6%	31	18
Neratinib (Freedman et al., 2016)	HER2/EGFR/ HER4,	Lapatinib and/or Trastuzumab	40	8%	16	0
In conjunction with chemotherapy						
Afatinib + Vinorelibine (Cortés et al., 2015)	HER2/EGFR/ HER4, antimetabolite	Lapatinib and/or Trastuzumab	37	3%	72	11
Lapatinib + Capecitabine (Lin et al., 2011)	HER2/EGFR, antimetabolite	Trastuzumab (treated for brain metastasis)	13	38%	65	16
Neratainib + Capecitabine (Freedman et al., 2017)	HER2/EGFR/ HER4, antimetabolite	Trastuzumab	39	49%	18	6
Lapatinib + Capecitabine (Bachelot et al., 2013)	HER2/EGFR/ HER4, antimetabolite	Trastuzumab (untreated for brain metastasis)	44	66%	22	14

Lastly, the results from this chapter demonstrate the feasibility of exploiting RET as a novel therapeutic target to treat BC BrM. Oncogenic activation of RET mediates tumour progression in multiple tumour types which is mainly achieved through activating rearrangements and mutations. Many of these molecular RET alterations have been viewed as clinically actionable in these patient populations as reflected by their confirmed responses to RET-directed multi-kinase inhibitors, including BrM in patients with RET-rearranged NSCLC (Tolaney et al., 2016; Takeuchi et al., 2012b; Drilon et al., 2013; Drilon et al., 2016; Subbiah et al., 2015). However, although a RET missense mutation had been detected in one of the *ex vivo* tumour models, this mechanism of oncogenic RET activity is not commonly reported in advanced BC (Nik-Zainal et al., 2016).

Despite the rarity of RET mutations in BC populations, a large body of evidence has shown that a significant subset, particularly ER-positive subtypes, exhibit abnormally high levels of RET. In alignment with these findings, a recent clinical study reported that cabozantinib had shown efficacy as a single agent against RET-driven tumours in ER-positive BC patients with extra-cranial metastasis (Tolaney et al., 2016). Furthermore, cross-talk between RET and ER has been well-established and several preclinical studies have implicated that aberrant signalling through this RTK may also mediate resistance to anti-estrogen therapies (Horibata et al., 2017; Morandi et al., 2013). One study showed that in tamoxifen-resistant MCF7 cells, targeting RET restored tamoxifen sensitivity (Plaza-Menacho et al., 2010a). Another independent study demonstrated that the cell growth of luminal BC cells is more significantly inhibited by combined anti-estrogen and anti-RET therapy than either therapy alone (Spanheimer et al., 2014).

Currently there are several ongoing trials assessing whether these inhibitors are effective in sensitising ER-positive/RET-positive BC to endocrine therapy and/or preventing the acquisition of endocrine therapy resistance (NCT03168074; NCT02562118). These findings are relevant to this work given that 3 of 4 patient study cases had retained ER expression in BrM and that the *ex vivo* models showed significant anti-proliferative responses to anti-RET treatments. Although the majority of patients with ER-positive BC develop endocrine refractory disease by the time

metastases are detected in the brain, anti-estrogen sensitivity may potentially be restored through RET inhibition. While this study suggests that RET inhibitors may be sufficiently effective as a single agent alone for the treatment of BrM, responses to cabozantinib may be more improved by the inclusion of anti-estrogens. Furthermore, no prospective trials have been performed to assess the effectiveness of endocrine therapy in the setting of BC BrM despite the reports of some responses to hormonal agents (Colomer et al., 1988; Lien et al., 1991; Pors et al., 1991; Salvati et al., 1993; Madhup et al., 2006). The efficacy of cabozantinib is also currently being evaluated in a clinical trial as either a single agent alone or in combination with trastuzumab for HER2-positive BC BrM (NCT02260531). Given the demonstrated anti-proliferative effect of cabozantinib in all of the HER2-positive *ex vivo* models, positive trial outcomes may be anticipated.

In summary, the findings from this *ex vivo* study provides functional evidence for the suitability of RET and HER2 as potential therapeutic targets against BrM and provides a unique preclinical platform system for evaluating novel anticancer drugs.

.

6. General Discussion

6.1. Transcriptomic characterisation of breast cancer brain metastases reveals clinically targetable alterations.

Although metastatic disease contributes significantly to mortality in BC, the current understanding of it is largely limited, especially with regards to BrM. Approximately 30% of BC patients will develop a secondary malignancy in the brain and the incidence is steadily rising, due to longer survival from improved systemic therapies (Leone and Leone, 2015). As chemotherapy is remarkably ineffective against metastatic brain tumours, the only available therapeutic options are surgical resection and radiotherapy (Venur and Ahluwalia, 2016). Given the severe lack of disease treatment strategies, BrM are an unmet clinical need.

Genomic and transcriptomic analyses of BrM have revealed several clinically informative molecular alterations that are distinct from primary tumour sites, bearing testament to the adaptive evolutionary nature of MBC cells upon colonisation of the unique brain microenvironment (Da Silva et al., 2010; Brastianos et al., 2015; Saunus et al., 2015). However, this fundamental area of research is still in its infancy, hindered by the lack of tissue availability. Hence, the vast genomic landscape of BrM remains largely unknown. In an attempt to address this void in research, genome-wide RNA-Seq was employed to chart the global transcriptional landscape of a large cohort of patient-matched primary BCs and their associated BrM. Further detailed analyses revealed transcriptional aberrations in a variety of key oncogenic pathways, most of which were more abundantly expressed in BrM. In particular, BrM-acquired abnormal enrichments were identified in multiple RTKs. The most notable recurrent alterations were upregulations in RET and HER2, both of which are clinically actionable and could provide potential therapeutic targets for treating BrM. Furthermore, the clinical potential of molecular target-based therapies against BrM is quite promising, as several small molecule TKIs have been reported to achieve effective CNS penetration and anti-tumour activity in patients harbouring metastatic brain lesions (Bachelot et al., 2013; Lin et al., 2009b; Geyer et al., 2006; Ceresoli et al., 2004; Popat et al., 2007; Kim et al., 2015). It should be noted, however, that the majority of TKIs are unable to cross the BBB as single agents (Pardridge, 2005), and

a number have been shown to display poor distribution in the brain tissue (Kast and Focosi, 2010; Kinoshita et al., 2013). Indeed, the BBB permeability profile of these drug compounds can considerably vary, which is influenced by a number of key molecular properties such as their substrate nature for drug efflux transporters, molecular weight, polar surface area (PSA) and lipophilicity index (LogP) (Di et al., 2013). Nevertheless, as discussed in the previous chapter, strategies to improve the delivery of these agents can be significantly achieved through combination with chemotherapy. With this rationale, the central work of this thesis, therefore, focused on validating RET and HER2 as viable therapeutic targets against BrM through the employment of TKIs, cabozantinib an afatinib, respectively. To explore this in a preclinical setting, patient derived *ex vivo* and brain metastatic PDX models were utilised which recapitulate characteristics of the patients from the RNA-Seq analysis. The principle findings from this work is discussed below and their implications for the clinical management of BrM.

6.2. Pan-HER inhibitors may be more superior to other current HER2 targeting agents in patients with breast cancer brain metastases

The HER2 proto-oncogene is overexpressed or/and gene amplified in approximately 20-30% of BCs and is a major therapeutic target for both early and advanced stages of this disease subtype (Slamon et al., 1989). Trastuzumab plus chemotherapy is the current first-line treatment option for HER2 positive MBC patients and has resulted in significantly improved OS (Inoue et al., 2010; Hamberg et al., 2011). However, after initial treatment there is a high risk of succumbing to BrM among this population, despite systemic control of the disease (Olson et al., 2013)**.** Historically, it was widely perceived that this was owing to the restricted penetration of large molecule drugs across the BBB such as trastuzumab, thereby failing to prevent brain relapse (Stemmler et al., 2007). However, poor brain distribution of these anti-HER2 agents is not the only factor governing drug sensitivity in BrM, as both clinical and preclinical studies show supporting evidence for the accumulation of these drugs in brain tumour lesions (Askoxylakis et al., 2016; Tamura et al., 2013). Furthermore, despite

the reported anti-tumour activity of highly BBB-penetrant dual HER2/EGFR TKI, lapatinib, in both recurrent and progressive cases of BrM, brain tumour growth was still uncontrolled, suggesting additional resistance mechanisms at play to HER2-targeted therapies (Lin et al., 2009b; Geyer et al., 2006).

In addition to aberrant activation of HER2, there is a growing body of evidence implicating the deregulation of other HER family members in brain colonisation and BrM outgrowth (Sirkisoon et al., 2016; Da Silva et al., 2010; Momeny et al., 2015; Bos et al., 2009a). These receptors become activated on the cell membrane through specific ligand binding, resulting in homo- and hetero-dimerization with other fellow family members. This interaction leads to the phosphorylation of each receptor's tyrosine kinases, which in turn activates several downstream effector modules (Roskoski, 2014a). Cross-talk signalling via different HER receptor pathways may effectively bypass the inhibitory effect of mono- or dual- targeted HER-TKIs which has previously been shown to mediate resistance to anti-HER2 therapies in BC (Sergina et al., 2007). Furthermore, in the setting of breast-to-brain metastatic disease, this compensatory signalling mechanism was even recently reported to be mediated by the brain microenvironment itself (Kodack et al., 2017a). This, together with the necessity for HER family receptors to heterodimerise for activation, suggests that BrM may therefore be more sensitive to pan-HER inhibitors.

Using an irreversible pan-HER TKI, afatinib, the impact of targeting HER2 was evaluated in different models of BC BrM which demonstrated significant anti-tumour efficacy. Given that this inhibitory effect may be due, at least in part, to activation of other HER family members, the impact of afatinib was therefore examined in both HER2-amplified and non-amplified cases. Strong activation of HER family members were observed in both *in vivo* and *ex vivo* BrM tumour models, which were significantly abrogated following treatment with the pan-HER inhibitor.

Furthermore, WES analysis of the *ex vivo* BrM tumour models revealed somatic mutations in HER family receptors. While the functional significance of these alterations have not been elucidated, it is plausible that they may contribute to the increased expression of the native and activated HER family members in these models. Indeed, the therapeutic potential of such unknown HER mutations

can be supported by a recent 'basket' trial study, SUMMIT, whereby pan-HER inhibitor, neratinib demonstrated clinical activity in different HER2-negative BC harbouring either kinase or extracellular domain missense mutations in HER2/HER3 (Hyman et al., 2018). Taken together with the findings from this present study, concomitant targeting HER family receptors with pan-HER TKIs could offer a promising treatment strategy for BrM.

6.3. Additional challenges in defining HER2 positivity

From the preliminary RNA-Seq study, HER2 was identified to be one of the two most recurrently upregulated protein kinases in BrM among the clinical patient cohort. This is an important finding given that Priedigkeit et al. previously reported significant enrichments for HER2 mutations/amplifications in BrM versus local disease (Priedigkeit et al., 2017a). Even more remarkably, these transcriptional alterations led to a negative-to-positive HER2 status conversion in some patient-matched cases which reinforces previous studies' observations (Duchnowska et al., 2012; Thomson et al., 2016; Priedigkeit et al., 2017a).

Upon further inspection of HER2-subtype switching in BrM, the observed expression gains were demonstrated to be was governed by amplification of the ERBB2 locus in two of the patient-matched cases from the RNA-Seq study. In contrast, another case that had undergone HER2-switching exhibited no BrM-acquired copy number gains for HER2 but had increased HER2 protein levels, as determined by IHC. HER2 amplification analysis revealed that, asides from two patient cases, there appears to be no underlying mutation level changes that are driving this transcriptomic shift which leads to the conclusion that the acquisition of HER2 enrichment in BrM is achieved by more than one mechanism. These scenarios demonstrate how analysing tumour specimens by FISH can potentially result in false negatives. These misclassifications may be due to the extensive intra-tumoural heterogeneity of HER2 that is commonly observed in BC (Buckley et al., 2016). Alternatively there may be an unexpected mechanism at play here that increases HER2 expression at the transcript or protein level, which is not uncommon. Indeed, tumourigenic transcriptional changes can also be driven by alterations of key

epigenetic modulators such as transcription factors which can reprogram the chromatin landscape and potentiate metastatic events (Morrow et al., 2018; Malladi et al., 2016). Therefore, considering the IHC data in relation to HER2-negative BrM patients is crucial, especially those in borderline categories, and additional HER2 testing strategies should be incorporated into routine BC pathology.

Similarly, aberrant HER2 transcriptional regulation and its peculiar subtype-switching behaviour was observed in the *ex vivo* models. Interestingly, one of these patient cases was confirmed as IHC HER2-negative yet had full HER2 pathway activation and functional signalling through HER2-EGFR heterodimerization. In line with these observations, HER3/HER4/EGFR activation are known to drive HER2 phosphorylation and its downstream signalling independent from total HER2 expression (Contreras-Zarate et al., 2017; Wulfkuhle et al., 2012). This is not surprising given the ligand independent nature of HER2 activation and that it is the preferred dimerization partner of all other HER family members (Roskoski, 2014c). While there was no evidence of activating HER2 mutations in these tumour models from WES analysis, there were somatic variants in other HER members which could be responsible for their elevated native and phosphorylated expression levels.

Taken together, this work demonstrates that the HER2 expression profile can alter between primary and metastatic sites. These findings bear massive clinical and diagnostic implications which are important especially given the recent ASCO guideline recommendations pertaining to HER2 retesting (Wolff et al., 2013). Indeed, in some cases BrM patients may be falsely classified as HER2 negative according to the status of their primary tumour biopsies, resulting in suboptimal treatments by denying them the potential benefits of HER2-targeted therapy. These research findings further suggest that HER2-negative BrM, of which there are still no targeted therapies for, may also receive positive results from anti-HER2 therapy.

6.4. Oncogenic activation of RET as a novel therapeutic target for breast cancer brain metastases

Although the brain represents one of most common sites of BC metastasis, BrM patients are typically excluded from clinical trials. Thus, there is an extreme lack of molecular targeted therapies for the treatment of HER2-negative BrM. Furthermore, given the worse clinical outcomes of TNBC BrM patient the discovery of novel actionable genomic alterations beyond HER2 aberrations require urgent attention. Addressing this clinical gap, recurrent enrichments of RET were identified in BrM which was further explored as a potential novel therapeutic target to treat this progressive disease. Through parallel meta-analysis with public microarray gene expression datasets in primary BC tumours and other metastatic sites previous bioinformatic work revealed that these transcriptional events associated specifically with BrM. Other studies have also reported RET overexpression in GBM, implicating a possible role for RET in promoting tumour progression in the brain (Ng et al., 2009; Gil et al., 2010). Additionally, the importance of dysregulated RET signalling in brain-related cancers is also highlighted by the strikingly high incidence of BrM in patients with RET-altered NSCLC (Drilon et al., 2017b).

RET is a major proto-oncogene that contributes to tumour progression in a diverse range of cancers. The most common mechanism of RET-mediated oncogenesis among these diseases are either mutations or fusions, most of which are commonly observed in sporadic medullary thyroid carcinoma (MTC) and papillary thyroid carcinomas (PTC), respectively. However, these gain-of-function alterations are quite rare in BC and have only been reported at low frequencies from several high throughput studies (Kato et al., 2017; Kan et al., 2010a). By contrast, RET amplification and overexpression has been identified in BCs instead (Morandi et al., 2011). Many of these RET-driven tumours are the focus of several molecularly targeted FDA-approved drugs and drugs under current clinical trial investigation; these could be redirected to treat metastatic brain tumours. In turn, the design of new treatment strategies may be rapidly achieved, sparing substantial time investment in the development of novel therapeutic agents.

Several multi-kinase RET inhibitors have confirmed modest yet durable responses in patients with RET-rearranged or RET mutant cancers (Elisei et al., 2013; Wells et al., 2012; Velcheti et al., 2016). In particular, cabozantinib, a multi-kinase RET inhibitor, has shown efficacy against solid tumours with oncogenic RET activity, including extra-cranial metastatic BC disease (Drilon et al., 2013; Lipson et al., 2012; Takeuchi et al., 2012b; Tolaney et al., 2016). This agent was used to target RET for the therapeutic intervention studies, demonstrating significant anti-tumour efficacy in *in vitro*, *in vivo* and *ex vivo* models of BrM.

The incidence of BrM is reported to be lower in patients with luminal BC relative to other HER2-positive and TNBC subtypes. Contrary to this, a considerable proportion of the clinical cases from the 21-patient cohort study were ER-positive (39%). While many had experienced a decrease in ER transcript levels during the process of acquiring BrM, it is noteworthy that 5/9 total ER-positive brain metastatic tumours experienced significant transcriptional gains in RET, suggesting a possible association between the ER status and RET expression. Similarly, the patient BrM samples that were used in the *ex vivo* study exhibited high levels of RET and had originated from ER-positive BCs, one of which lost ER expression upon brain colonisation and switched to a triple negative tumour phenotype. In agreement with these observations, recent expression profiling studies have indicated increased RET expression being strongly associated with ER-positive BCs as well as poorer metastasis-free survival (Tozlu et al., 2006; Boulay et al., 2008; Gattelli et al., 2013). The functional significance of RET-ER interactions have been previously described with RET being shown to be a direct transcriptional target of ER. Consistent with this, RET expression has also been shown to become enhanced in response to estrogen treatment. (Horibata et al., 2017). More importantly, several ER/RET-positive BC cell lines and primary tumour models have suggested that oncogenic RET signalling may be necessary to mediate resistance to endocrine therapies (Gattelli et al., 2013; Morandi et al., 2013; Plaza-Menacho et al., 2010b; Andreucci et al., 2016). This was

demonstrated to occur via estrogen-independent ER activation in response to treatment with RET activating ligand, GDNF (Plaza-Menacho et al., 2010b).

Evidence suggests that the brain microenvironment may play a role in mediating this resistance via GDNF-RET signalling. One particular report demonstrated that astrocytes can promote the invasive properties of RET-expressing glioma cells in GBM through secretion of GDNF, leading to subsequent activation of RET signalling (Shabtay-Orbach et al., 2015). Indeed, activated astrocytes have been demonstrated to be highly abundant in brain tumours (Zhang and Olsson, 1995). Similarly to the context of this study, ER-positive brain-colonising BC cells may evolve to acquire an increase in RET expression in order to exploit the GDNF-rich brain tumour microenvironment that consequently stimulates ER and RET cross talk signalling. Taken together with the findings from this thesis, there is strong evidence to believe that inhibition of RET with cabozantinib in conjunction with anti-estrogens may be effective in re-sensitising BrM to endocrine therapy. In this disease setting, no prospective trials have been performed to assess the effectiveness of endocrine therapy despite there being anecdotal reports of patients with BrM responding well to such treatments (Lien et al., 1991; Colomer et al., 1988; Pors et al., 1991; Salvati et al., 1993). Additionally, treatment with cabozantinib could also be more efficacious through combined mTOR pathway inhibition (Ni et al., 2016; Gild et al., 2013; Subbiah et al., 2015).

Elevated levels of RET and its physiological relevance has also been reported in a subset of triple negative and HER2-positive breast tumours (Gattelli et al., 2013; Hatem et al., 2016; Nguyen et al., 2015). Similarly, high expression of total and activated RET had been observed in all preclinical models of TNBC and HER2-positive BrM from the previous chapters of this thesis. Furthermore, their downstream signalling became significantly attenuated following treatment with cabozantinib. Hence, these findings suggests that RET targeting within these subtypes may also provide a potential treatment option for BrM irrespective of molecular subtype.

6.5. A new era of anti-RET therapies

Whilst cabozantinib decreased RET activation and achieved durable tumour regression in all BrM models it is important to note that these observed anti-tumourigenic effects may also be mediated in part by the inhibition of other target RTKs. Until recent times, only multi-kinase RET inhibitors have been explored in RET-altered cancers. While these non-selective anti-RET agents have demonstrated clinical activity in cases of RET-fusion positive lung cancers with BrM (Subbiah et al., 2015; Drilon et al., 2016), the objective response rates were a little lacklustre, especially in comparison to those observed from targeted therapies for ALK- and ROS1-driven cases (Shaw et al., 2013; Lim et al., 2017).

As significant toxicities are associated with inhibition of other off-target kinases, including KDR, frequent dose reductions of MKIs have been made in clinical trials (Drilon et al., 2013; Elisei et al., 2013; Wells et al., 2012) which could be compromising the potency and full therapeutic potential of RET-specific inhibition (Drilon et al., 2017a). These disappointing trial reports have raised uncertainties regarding the impact of deregulated RET signalling in disease oncogenesis and whether the currently available MKIs are sufficient for RET inhibition. Perhaps, response rates may be improved with more potent and selective RET inhibitors which are being developed and undergoing clinical investigations at present. The initial prospects already appear quite promising, as recently seen by the therapeutic outcomes of two highly selective RET inhibitors, RXDX-105 and LOXO-292. Both agents have demonstrated encouraging activity in a broad range of advanced RET-altered cancers, including confirmed intracranial responses in a proportion of NSCLC patients with BrM, with no significant signs of toxicity observed (Subbiah et al., 2018b; Li et al., 2017). BLU-667 is another RET-specific antagonist that has also shown notable anti-tumour activity in NSCLC patients harbouring RET rearrangements, without any noticeable signs of adverse toxicity (Subbiah et al., 2018a). Therefore, as work from this thesis demonstrates RET to be a novel and specific target in treating BrM, the effectiveness of more RET-focused inhibitors should be investigated in future preclinical studies. However, given the expression of RET in the adult central nervous system and its reported requirement for the survival

of mature neurons, there have been concerns as to whether long-term treatments could potentially lead to neuronal degradation (Jain et al., 2006; Kramer et al., 2007). These potential long-term side-effects from prolonged RET inhibition should be strictly monitored in future clinical trial studies.

6.6. Conclusion

Taken together, these results demonstrate profound and recurrent transcriptional remodelling events in BC BrM. Such transcriptomic shifts are illustrative of the adaptive nature of BrM, suggesting breast-to-brain metastases acquire therapeutic vulnerabilities that are unique from their matched primary tumours. Clinically relevant alterations independent of the primary site were identified in multiple receptor kinase-driven signalling pathways, most notably, recurrent enrichments in HER2 and RET which has clear implications for clinical management. In summary, this study reports RET and HER2 as candidate targets to treat BrM offering new approaches to therapy that may not otherwise be apparent from the molecular analysis of clinically sampled primary tumours. Critically, these findings show that primary biopsies alone are insufficient to inform individualised treatment decisions for patients with BrM and instead comprehensive genomic profiling of resectable BrM should be integrated in paving management strategies moving forward. As proven, such underutilised tools could reveal additional candidates that may meet the criteria for trial eligibility and potentially unveil new targeted therapies for treating this disease.

7. References

2012. Comprehensive molecular portraits of human breast tumours. *Nature*, 490**,** 61-70.

A. BRONZERT, D., GREENE, G. & LIPPMAN, M. 1985. *Selection and Characterization of a Breast Cancer Cell Line Resistant to the Antiestrogen LY 117018*.

ABBOTT, N. J., RÖNNBÄCK, L. & HANSSON, E. 2006. Astrocyte–endothelial interactions at the blood–brain barrier. *Nature Reviews Neuroscience*, 7, 41.

ABD EL-REHIM, D. M., PINDER, S. E., PAISH, C. E., BELL, J. A., RAMPAUL, R. S., BLAMEY, R. W., ROBERTSON, J. F., NICHOLSON, R. I. & ELLIS, I. O. 2004. Expression and co-expression of the members of the epidermal growth factor receptor (EGFR) family in invasive breast carcinoma. *Br J Cancer*, 91**,** 1532-42.

ADAMO, B., DEAL, A. M., BURROWS, E., GERADTS, J., HAMILTON, E., BLACKWELL, K. L., LIVASY, C., FRITCHIE, K., PRAT, A., HARRELL, J. C., EWEND, M. G., CAREY, L. A., MILLER, C. R. & ANDERS, C. K. 2011. Phosphatidylinositol 3-kinase pathway activation in breast cancer brain metastases. *Breast Cancer Res*, 13**,** R125.

AHN, M.-J., KIM, D.-W., CHO, B. C., KIM, S.-W., LEE, J. S., AHN, J.-S., KIM, T. M., LIN, C.-C., KIM, H. R., JOHN, T., KAO, S., GOLDMAN, J. W., SU, W.-C., NATALE, R., RABBIE, S., HARROP, B., OVEREND, P., YANG, Z. & YANG, J. C.-H. 2017. Activity and safety of AZD3759 in EGFR-mutant non-small-cell lung cancer with CNS metastases (BLOOM): a phase 1, open-label, dose-escalation and dose-expansion study. *The Lancet Respiratory Medicine*, 5, 891-902.

ANDREUCCI, E., FRANCICA, P., FEARNS, A., MARTIN, L. A., CHIARUGI, P., ISACKE, C. M. & MORANDI, A. 2016. Targeting the receptor tyrosine kinase RET in combination with aromatase inhibitors in ER positive breast cancer xenografts. *Oncotarget*, 7**,** 80543-80553.

ANTONIOU, A. C. & EASTON, D. F. 2006. Models of genetic susceptibility to breast cancer. *Oncogene*, 25**,** 5898-905.

ARORA, A. & SCHOLAR, E. M. 2005. Role of Tyrosine Kinase Inhibitors in Cancer Therapy. *Journal of Pharmacology and Experimental Therapeutics*, 315**,** 971-979.

ARTEAGA, C. L. & ENGELMAN, J. A. 2014. ERBB receptors: from oncogene discovery to basic science to mechanism-based cancer therapeutics. *Cancer Cell*, 25**,** 282-303.

ASATI, V., MAHAPATRA, D. K. & BHARTI, S. K. 2016. PI3K/Akt/mTOR and Ras/Raf/MEK/ERK signaling pathways inhibitors as anticancer agents: Structural and pharmacological perspectives. *Eur J Med Chem*, 109**,** 314-41.

ASKOXYLAKIS, V., FERRARO, G. B., KODACK, D. P., BADEAUX, M., SHANKARAIAH, R. C., SEANO, G., KLOEPPER, J., VARDAM, T., MARTIN, J. D., NAXEROVA, K., BEZWADA, D., QI, X., SELIG, M. K., BRACHTEL, E., DUDA, D. G., HUANG, P., FUKUMURA, D., ENGELMAN, J. A. & JAIN, R. K. 2016. Preclinical Efficacy of Ado-trastuzumab Emtansine in the Brain Microenvironment. *J Natl Cancer Inst*, 108.

BACHELOT, T., ROMIEU, G., CAMPONE, M., DIÉRAS, V., CROPET, C., DALENC, F., JIMENEZ, M., LE RHUN, E., PIERGA, J.-Y., GONÇALVES, A., LEHEURTEUR, M., DOMONT, J., GUTIERREZ, M., CURÉ, H., FERRERO, J.-M. & LABBE-DEVILLIERS, C. Lapatinib plus capecitabine in patients with previously untreated brain metastases from HER2-positive metastatic breast cancer (LANDSCAPE): a single-group phase 2 study. *The Lancet Oncology*, 14**,** 64-71.

BACHELOT, T., ROMIEU, G., CAMPONE, M., DIERAS, V., CROPET, C., DALENC, F., JIMENEZ, M., LE RHUN, E., PIERGA, J. Y., GONCALVES, A., LEHEURTEUR, M., DOMONT, J., GUTIERREZ, M., CURE, H., FERRERO, J. M. & LABBE-DEVILLIERS, C. 2013. Lapatinib plus capecitabine in patients with previously untreated brain metastases from HER2-positive metastatic breast cancer (LANDSCAPE): a single-group phase 2 study. *Lancet Oncol*, 14**,** 64-71.

BARTSCH, R., BERGHOFF, A. S., VOGL, U., RUDAS, M., BERGEN, E., DUBSKY, P., DIECKMANN, K., PINKER, K., BAGO-HORVATH, Z., GALID, A., OEHLER, L., ZIELINSKI, C. C., GNANT, M., STEGER,

G. G. & PREUSSER, M. 2015. Activity of T-DM1 in Her2-positive breast cancer brain metastases. *Clinical & Experimental Metastasis*, **32,** 729-737.

BARTSCH, R., ROTTENFUSSER, A., WENZEL, C., DIECKMANN, K., PLUSCHNIG, U., ALTORJAI, G., RUDAS, M., MADER, R. M., POETTER, R., ZIELINSKI, C. C. & STEGER, G. G. 2007. Trastuzumab prolongs overall survival in patients with brain metastases from Her2 positive breast cancer. *J Neurooncol*, **85,** 311-7.

BASELGA, J. & SWAIN, S. M. 2009. Novel anticancer targets: revisiting ERBB2 and discovering ERBB3. *Nature Reviews Cancer*, **9,** 463.

BENDELL, J. C., DOMCHEK, S. M., BURSTEIN, H. J., HARRIS, L., YOUNGER, J., KUTER, I., BUNNELL, C., RUE, M., GELMAN, R. & WINER, E. 2003. Central nervous system metastases in women who receive trastuzumab-based therapy for metastatic breast carcinoma. *Cancer*, **97,** 2972-7.

BERGERS, G. & BENJAMIN, L. E. 2003. Tumorigenesis and the angiogenic switch. *Nat Rev Cancer*, **3,** 401-10.

BIECHE, I., ONODY, P., TOZLU, S., DRIOUCH, K., VIDAUD, M. & LIDEREAU, R. 2003. Prognostic value of ERBB family mRNA expression in breast carcinomas. *Int J Cancer*, **106,** 758-65.

BOLLIG-FISCHER, A., MICHELHAUGH, S. K., WIJESINGHE, P., DYSON, G., KRUGER, A., PALANISAMY, N., CHOI, L., ALOSH, B., ALI-FEHMI, R. & MITTAL, S. 2015. Cytogenomic profiling of breast cancer brain metastases reveals potential for repurposing targeted therapeutics. *Oncotarget*, **6,** 14614-24.

BOS, P. D., ZHANG, X. H., NADAL, C., SHU, W., GOMIS, R. R., NGUYEN, D. X., MINN, A. J., VAN DE VIJVER, M. J., GERALD, W. L., FOEKENS, J. A. & MASSAGUE, J. 2009a. Genes that mediate breast cancer metastasis to the brain. *Nature*, **459,** 1005-9.

BOS, P. D., ZHANG, X. H. F., NADAL, C., SHU, W., GOMIS, R. R., NGUYEN, D. X., MINN, A. J., VAN DE VIJVER, M. J., GERALD, W. L., FOEKENS, J. A. & MASSAGUÉ, J. 2009b. Genes that mediate breast cancer metastasis to the brain. *Nature*, **459,** 1005.

BOSE, R., KAVURI, S. M., SEARLEMAN, A. C., SHEN, W., SHEN, D., KOBOLDT, D. C., MONSEY, J., GOEL, N., ARONSON, A. B., LI, S., MA, C. X., DING, L., MARDIS, E. R. & ELLIS, M. J. 2013. Activating HER2 mutations in HER2 gene amplification negative breast cancer. *Cancer Discov*, **3,** 224-37.

BOULAY, A., BREULEUX, M., STEPHAN, C., FUX, C., BRISKEN, C., FICHE, M., WARTMANN, M., STUMM, M., LANE, H. A. & HYNES, N. E. 2008. The Ret receptor tyrosine kinase pathway functionally interacts with the ERalpha pathway in breast cancer. *Cancer Res*, **68,** 3743-51.

BOYD, N. F., MARTIN, L. J., BRONSKILL, M., YAFFE, M. J., DURIC, N. & MINKIN, S. 2010. Breast tissue composition and susceptibility to breast cancer. *J Natl Cancer Inst*, **102,** 1224-37.

BRASTIANOS, P. K., CARTER, S. L., SANTAGATA, S., CAHILL, D. P., TAYLOR-WEINER, A., JONES, R. T., VAN ALLEN, E. M., LAWRENCE, M. S., HOROWITZ, P. M., CIBULSKIS, K., LIGON, K. L., TABERNERO, J., SEOANE, J., MARTINEZ-SAEZ, E., CURRY, W. T., DUNN, I. F., PAEK, S. H., PARK, S. H., MCKENNA, A., CHEVALIER, A., ROSENBERG, M., BARKER, F. G., 2ND, GILL, C. M., VAN HUMMELEN, P., THORNER, A. R., JOHNSON, B. E., HOANG, M. P., CHOUEIRI, T. K., SIGNORETTI, S., SOUGNEZ, C., RABIN, M. S., LIN, N. U., WINER, E. P., STEMMER-RACHAMIMOV, A., MEYERSON, M., GARRAWAY, L., GABRIEL, S., LANDER, E. S., BEROUKHIM, R., BATCHELOR, T. T., BASELGA, J., LOUIS, D. N., GETZ, G. & HAHN, W. C. 2015. Genomic Characterization of Brain Metastases Reveals Branched Evolution and Potential Therapeutic Targets. *Cancer Discov*, **5,** 1164-1177.

BUCKLEY, N. E., FORDE, C., MCART, D. G., BOYLE, D. P., MULLAN, P. B., JAMES, J. A., MAXWELL, P., MCQUAID, S. & SALTO-TELLEZ, M. 2016. Quantification of HER2 heterogeneity in breast cancer–implications for identification of sub-dominant clones for personalised treatment. *Scientific Reports*, **6,** 23383.

BULLITT, E., LIN, N. U., SMITH, J. K., ZENG, D., WINER, E. P., CAREY, L. A., LIN, W. & EWEND, M. G. 2007. Blood Vessel Morphologic Changes Depicted with MR Angiography during Treatment of Brain Metastases: A Feasibility Study. *Radiology*, 245**,** 824-830.

CERESOLI, G. L., CAPPUZZO, F., GREGORC, V., BARTOLINI, S., CRINO, L. & VILLA, E. 2004. Gefitinib in patients with brain metastases from non-small-cell lung cancer: a prospective trial. *Ann Oncol*, 15**,** 1042-7.

CHAMBERLAIN, M. C. 2011. Bevacizumab for the treatment of recurrent glioblastoma. *Clin Med Insights Oncol*, 5**,** 117-29.

CHAMBERLAIN, M. C., BAIK, C. S., GADI, V. K., BHATIA, S. & CHOW, L. Q. 2017. Systemic therapy of brain metastases: non-small cell lung cancer, breast cancer, and melanoma. *Neuro Oncol*, 19**,** i1-i24.

CHEN, Q., BOIRE, A., JIN, X., VALIENTE, M., ER, E. E., LOPEZ-SOTO, A., JACOB, L., PATWA, R., SHAH, H., XU, K., CROSS, J. R. & MASSAGUE, J. 2016. Carcinoma-astrocyte gap junctions promote brain metastasis by cGAMP transfer. *Nature*, 533**,** 493-498.

CHIANG, A. C. & MASSAGUE, J. 2008. Molecular basis of metastasis. *N Engl J Med*, 359**,** 2814-23.

CHUNG, L. W., BASEMAN, A., ASSIKIS, V. & ZHAU, H. E. 2005. Molecular insights into prostate cancer progression: the missing link of tumor microenvironment. *J Urol*, 173**,** 10-20.

CLOUGHESY, T. F., DRAPPATZ, J., DE GROOT, J., PRADOS, M. D., REARDON, D. A., SCHIFF, D., CHAMBERLAIN, M., MIKKELSEN, T., DESJARDINS, A., PING, J., HOLLAND, J., WEITZMAN, R. & WEN, P. Y. 2018. Phase II study of cabozantinib in patients with progressive glioblastoma: subset analysis of patients with prior antiangiogenic therapy. *Neuro Oncol*, 20**,** 259-267.

COLOMER, R., COSOS, D., DEL CAMPO, J. M., BOADA, M., RUBIO, D. & SALVADOR, L. 1988. Brain metastases from breast cancer may respond to endocrine therapy. *Breast Cancer Res Treat*, 12**,** 83-6.

CONTRERAS-ZARATE, M. J., ORMOND, D. R., GILLEN, A. E., HANNA, C., DAY, N. L., SERKOVA, N. J., JACOBSEN, B. M., EDGERTON, S. M., THOR, A. D., BORGES, V. F., LILLEHEI, K. O., GRANER, M. W., KABOS, P. & CITTELLY, D. M. 2017. Development of Novel Patient-Derived Xenografts from Breast Cancer Brain Metastases. *Front Oncol*, 7**,** 252.

CORTÉS, J., DIERAS, V., RO, J., BARRIERE, J., BACHELOT, T., HURVITZ, S., LE RHUN, E., ESPIÉ, M., KIM, S.-B., SCHNEEWEISS, A., SOHN, J. H., NABHOLTZ, J.-M., KELLOKUMPU-LEHTINEN, P.-L., TAGUCHI, J., PIACENTINI, F., CIRUELOS, E., BONO, P., OULD-KACI, M., ROUX, F. & JOENSUU, H. 2015. Afatinib alone or afatinib plus vinorelbine versus investigator's choice of treatment for HER2-positive breast cancer with progressive brain metastases after trastuzumab, lapatinib, or both (LUX-Breast 3): a randomised, open-label, multicentre, phase 2 trial. *The Lancet Oncology*, 16**,** 1700-1710.

CURTIS, C., SHAH, S. P., CHIN, S.-F., TURASHVILI, G., RUEDA, O. M., DUNNING, M. J., SPEED, D., LYNCH, A. G., SAMARAJIWA, S., YUAN, Y., GRÄF, S., HA, G., HAFFARI, G., BASHASHATI, A., RUSSELL, R., MCKINNEY, S., GROUP, M., LANGERØD, A., GREEN, A., PROVENZANO, E., WISHART, G., PINDER, S., WATSON, P., MARKOWETZ, F., MURPHY, L., ELLIS, I., PURUSHOTHAM, A., BØRRESEN-DALE, A.-L., BRENTON, J. D., TAVARÉ, S., CALDAS, C. & APARICIO, S. 2012. The genomic and transcriptomic architecture of 2,000 breast tumours reveals novel subgroups. *Nature*, 486**,** 346.

DA SILVA, L., SIMPSON, P. T., SMART, C. E., COCCIARDI, S., WADDELL, N., LANE, A., MORRISON, B. J., VARGAS, A. C., HEALEY, S., BEESLEY, J., PAKKIRI, P., PARRY, S., KURNIAWAN, N., REID, L., KEITH, P., FARIA, P., PEREIRA, E., SKALOVA, A., BILOUS, M., BALLEINE, R. L., DO, H., DOBROVIC, A., FOX, S., FRANCO, M., REYNOLDS, B., KHANNA, K. K., CUMMINGS, M., CHENEVIX-TRENCH, G. & LAKHANI, S. R. 2010. HER3 and downstream pathways are involved in colonization of brain metastases from breast cancer. *Breast Cancer Res*, 12**,** R46.

DAGOGO-JACK, I., GILL, C. M., CAHILL, D. P., SANTAGATA, S. & BRASTIANOS, P. K. 2017. Treatment of brain metastases in the modern genomic era. *Pharmacol Ther*, 170, 64-72.

DAI, X., XIANG, L., LI, T. & BAI, Z. 2016. Cancer Hallmarks, Biomarkers and Breast Cancer Molecular Subtypes. *J Cancer*, 7, 1281-94.

DAY, BRYAN W., STRINGER, BRETT W., AL-EJEH, F., TING, MICHAEL J., WILSON, J., ENSBEY, KATHLEEN S., JAMIESON, PAUL R., BRUCE, ZARA C., LIM, YI C., OFFENHÄUSER, C., CHARMSAZ, S., COOPER, LEANNE T., ELLACOTT, JENNIFER K., HARDING, A., LEVEQUE, L., INGLIS, P., ALLAN, S., WALKER, DAVID G., LACKMANN, M., OSBORNE, G., KHANNA, KUM K., REYNOLDS, BRENT A., LICKLITER, JASON D. & BOYD, ANDREW W. 2013. EphA3 Maintains Tumorigenicity and Is a Therapeutic Target in Glioblastoma Multiforme. *Cancer Cell*, 23, 238-248.

DE GROOT, J. W. B., LINKS, T. P., PLUKKER, J. T. M., LIPS, C. J. M. & HOFSTRA, R. M. W. 2006. RET as a Diagnostic and Therapeutic Target in Sporadic and Hereditary Endocrine Tumors. *Endocrine Reviews*, 27, 535-560.

DEAN, J. L., MCCLENDON, A. K., HICKEY, T. E., BUTLER, L. M., TILLEY, W. D., WITKIEWICZ, A. K. & KNUDSEN, E. S. 2012. Therapeutic response to CDK4/6 inhibition in breast cancer defined by ex vivo analyses of human tumors. *Cell Cycle*, 11, 2756-61.

DEFAZIO, A., CHIEW, Y. E., SINI, R. L., JANES, P. W. & SUTHERLAND, R. L. 2000. Expression of c-erbB receptors, heregulin and oestrogen receptor in human breast cell lines. *Int J Cancer*, 87, 487-98.

DEPRISTO, M. A., BANKS, E., POPLIN, R., GARIMELLA, K. V., MAGUIRE, J. R., HARTL, C., PHILIPPAKIS, A. A., DEL ANGEL, G., RIVAS, M. A., HANNA, M., MCKENNA, A., FENNELL, T. J., KERNYTSKY, A. M., SIVACHENKO, A. Y., CIBULSKIS, K., GABRIEL, S. B., ALTSHULER, D. & DALY, M. J. 2011. A framework for variation discovery and genotyping using next-generation DNA sequencing data. *Nat Genet*, 43, 491-8.

DEROSE, Y. S., WANG, G., LIN, Y. C., BERNARD, P. S., BUYS, S. S., EBBERT, M. T., FACTOR, R., MATSEN, C., MILASH, B. A., NELSON, E., NEUMAYER, L., RANDALL, R. L., STIJLEMAN, I. J., WELM, B. E. & WELM, A. L. 2011. Tumor grafts derived from women with breast cancer authentically reflect tumor pathology, growth, metastasis and disease outcomes. *Nat Med*, 17, 1514-20.

DESMEDT, C., HAIBE-KAINS, B., WIRAPATI, P., BUYSE, M., LARSIMONT, D., BONTEMPI, G., DELORENZI, M., PICCART, M. & SOTIRIOU, C. 2008. Biological processes associated with breast cancer clinical outcome depend on the molecular subtypes. *Clin Cancer Res*, 14, 5158-65.

DI, L., RONG, H. & FENG, B. 2013. Demystifying brain penetration in central nervous system drug discovery. Miniperspective. *J Med Chem*, 56, 2-12.

DOWSETT, M., NIELSEN, T. O., A'HERN, R., BARTLETT, J., COOMBES, R. C., CUZICK, J., ELLIS, M., HENRY, N. L., HUGH, J. C., LIVELY, T., MCSHANE, L., PAIK, S., PENAULT-LLORCA, F., PRUDKIN, L., REGAN, M., SALTER, J., SOTIRIOU, C., SMITH, I. E., VIALE, G., ZUJEWSKI, J. A., HAYES, D. F. & INTERNATIONAL KI-67 IN BREAST CANCER WORKING, G. 2011. Assessment of Ki67 in breast cancer: recommendations from the International Ki67 in Breast Cancer working group. *J Natl Cancer Inst*, 103, 1656-64.

DRILON, A., HU, Z. I., LAI, G. G. Y. & TAN, D. S. W. 2017a. Targeting RET-driven cancers: lessons from evolving preclinical and clinical landscapes. *Nature Reviews Clinical Oncology*, 15, 151.

DRILON, A., REKHTMAN, N., ARCILA, M., WANG, L., NI, A., ALBANO, M., VAN VOORTHUYSEN, M., SOMWAR, R., SMITH, R. S., MONTECALVO, J., PLODKOWSKI, A., GINSBERG, M. S., RIELY, G. J., RUDIN, C. M., LADANYI, M. & KRIS, M. G. 2016. Cabozantinib in patients with advanced RET-rearranged non-small-cell lung cancer: an open-label, single-centre, phase 2, single-arm trial. *Lancet Oncol*, 17, 1653-1660.

DRILON, A., WANG, L., HASANOVIC, A., SUEHARA, Y., LIPSON, D., STEPHENS, P., ROSS, J., MILLER, V., GINSBERG, M., ZAKOWSKI, M. F., KRIS, M. G., LADANYI, M. & RIZVI, N. 2013. Response to

Cabozantinib in patients with RET fusion-positive lung adenocarcinomas. *Cancer Discov*, 3**,** 630-5.

DRILON, A. E., FILLERON, T., BERGAGNINI, I., MILIA, J., HATZOGLOU, V., VELCHETI, V., BESSE, B., MOK, T., AWAD, M. M., WOLF, J., CARBONE, D. P., CAMIDGE, D. R., RIELY, G. J., PELED, N., MAZIERES, J., KRIS, M. G., GAUTSCHI, O. & INVESTIGATORS, G. M. R. R. 2017b. Baseline frequency of brain metastases and outcomes with multikinase inhibitor therapy in patients with RET-rearranged lung cancers. *Journal of Clinical Oncology*, 35**,** 9069-9069.

DUCHNOWSKA, R., DZIADZIUSZKO, R., TROJANOWSKI, T., MANDAT, T., OCH, W., CZARTORYSKA-ARLUKOWICZ, B., RADECKA, B., OLSZEWSKI, W., SZUBSTARSKI, F., KOZLOWSKI, W., JAROSZ, B., ROGOWSKI, W., KOWALCZYK, A., LIMON, J., BIERNAT, W. & JASSEM, J. 2012. Conversion of epidermal growth factor receptor 2 and hormone receptor expression in breast cancer metastases to the brain. *Breast Cancer Res*, 14**,** R119.

EDGE, S. B. & COMPTON, C. C. 2010. The American Joint Committee on Cancer: the 7th edition of the AJCC cancer staging manual and the future of TNM. *Ann Surg Oncol*, 17**,** 1471-4.

EICHLER, A. F. & LOEFFLER, J. S. 2007. Multidisciplinary management of brain metastases. *Oncologist*, 12**,** 884-98.

ELISEI, R., SCHLUMBERGER, M. J., MÜLLER, S. P., SCHÖFFSKI, P., BROSE, M. S., SHAH, M. H., LICITRA, L., JARZAB, B., MEDVEDEV, V., KREISSL, M. C., NIEDERLE, B., COHEN, E. E. W., WIRTH, L. J., ALI, H., HESSEL, C., YARON, Y., BALL, D., NELKIN, B. & SHERMAN, S. I. 2013. Cabozantinib in Progressive Medullary Thyroid Cancer. *Journal of Clinical Oncology*, 31**,** 3639-3646.

ESSEGHIR, S., TODD, S. K., HUNT, T., POULSOM, R., PLAZA-MENACHO, I., REIS-FILHO, J. S. & ISACKE, C. M. 2007. A role for glial cell derived neurotrophic factor induced expression by inflammatory cytokines and RET/GFR alpha 1 receptor up-regulation in breast cancer. *Cancer Res*, 67**,** 11732-41.

FEELEY, L. P., MULLIGAN, A. M., PINNADUWAGE, D., BULL, S. B. & ANDRULIS, I. L. 2014. Distinguishing luminal breast cancer subtypes by Ki67, progesterone receptor or TP53 status provides prognostic information. *Mod Pathol*, 27**,** 554-561.

FEHRENBACHER, L., JEONG, J.-H., RASTOGI, P., GEYER, C. E., PAIK, S., GANZ, P. A., LAND, S. R., COSTANTINO, J. P., SWAIN, S. M., MAMOUNAS, E. P. & WOLMARK, N. 2012. NSABP B-47: A phase III trial of adjuvant therapy comparing chemotherapy alone (six cycles of docetaxel plus cyclophosphamide or four cycles of doxorubicin plus cyclophosphamide followed by weekly paclitaxel) to chemotherapy plus trastuzumab in women with node-positive or high-risk, node-negative, HER2-low invasive breast cancer. *Journal of Clinical Oncology*, 30**,** TPS1142-TPS1142.

FEI, X. F., ZHANG, Q. B., DONG, J., DIAO, Y., WANG, Z. M., LI, R. J., WU, Z. C., WANG, A. D., LAN, Q., ZHANG, S. M. & HUANG, Q. 2010. Development of clinically relevant orthotopic xenograft mouse model of metastatic lung cancer and glioblastoma through surgical tumor tissues injection with trocar. *J Exp Clin Cancer Res*, 29**,** 84.

FERLAY, J., SOERJOMATARAM, I., DIKSHIT, R., ESER, S., MATHERS, C., REBELO, M., PARKIN, D. M., FORMAN, D. & BRAY, F. 2015. Cancer incidence and mortality worldwide: sources, methods and major patterns in GLOBOCAN 2012. *Int J Cancer*, 136**,** E359-86.

FIDLER, I. J., YANO, S., ZHANG, R. D., FUJIMAKI, T. & BUCANA, C. D. 2002. The seed and soil hypothesis: vascularisation and brain metastases. *Lancet Oncol*, 3**,** 53-7.

FITZGERALD, D. P., PALMIERI, D., HUA, E., HARGRAVE, E., HERRING, J. M., QIAN, Y., VEGA-VALLE, E., WEIL, R. J., STARK, A. M., VORTMEYER, A. O. & STEEG, P. S. 2008. Reactive glia are recruited by highly proliferative brain metastases of breast cancer and promote tumor cell colonization. *Clin Exp Metastasis*, 25**,** 799-810.

FREEDMAN, R. A., GELMAN, R. S., MELISKO, M. E., ANDERS, C. K., MOY, B., BLACKWELL, K. L., CONNOLLY, R. M., NIRAVATH, P. A., POZNAK, C. H. V., PUHALLA, S., FAROOQ, S., CROPP, A., COTTER, C. M., LIU, M. C., KROP, I. E., NANGIA, J. R., TUNG, N. M., WOLFF, A. C., WINER, E. P. & LIN, N. U. 2017. TBCRC 022: Phase II trial of neratinib + capecitabine for patients (Pts) with human epidermal growth factor receptor 2 (HER2+) breast cancer brain metastases (BCBM). *Journal of Clinical Oncology*, **35**, 1005-1005.

FREEDMAN, R. A., GELMAN, R. S., WEFEL, J. S., MELISKO, M. E., HESS, K. R., CONNOLLY, R. M., POZNAK, C. H. V., NIRAVATH, P. A., PUHALLA, S. L., IBRAHIM, N., BLACKWELL, K. L., MOY, B., HEROLD, C., LIU, M. C., LOWE, A., AGAR, N. Y. R., RYABIN, N., FAROOQ, S., LAWLER, E., RIMAWI, M. F., KROP, I. E., WOLFF, A. C., WINER, E. P. & LIN, N. U. 2016. Translational Breast Cancer Research Consortium (TBCRC) 022: A Phase II Trial of Neratinib for Patients With Human Epidermal Growth Factor Receptor 2–Positive Breast Cancer and Brain Metastases. *Journal of Clinical Oncology*, **34**, 945-952.

FUCHS, I. B., LOEBBECKE, M., BUHLER, H., STOLTENBURG-DIDINGER, G., HEINE, B., LICHTENEGGER, W. & SCHALLER, G. 2002. HER2 in brain metastases: issues of concordance, survival, and treatment. *J Clin Oncol*, 20, 4130-3.

GABOS, Z., SINHA, R., HANSON, J., CHAUHAN, N., HUGH, J., MACKEY, J. R. & ABDULKARIM, B. 2006. Prognostic significance of human epidermal growth factor receptor positivity for the development of brain metastasis after newly diagnosed breast cancer. *J Clin Oncol*, 24, 5658-63.

GAEDCKE, J., TRAUB, F., MILDE, S., WILKENS, L., STAN, A., OSTERTAG, H., CHRISTGEN, M., VON WASIELEWSKI, R. & KREIPE, H. H. 2007. Predominance of the basal type and HER-2/neu type in brain metastasis from breast cancer. *Mod Pathol*, 20, 864-70.

GAO, H., KORN, J. M., FERRETTI, S., MONAHAN, J. E., WANG, Y., SINGH, M., ZHANG, C., SCHNELL, C., YANG, G., ZHANG, Y., BALBIN, O. A., BARBE, S., CAI, H., CASEY, F., CHATTERJEE, S., CHIANG, D. Y., CHUAI, S., COGAN, S. M., COLLINS, S. D., DAMMASSA, E., EBEL, N., EMBRY, M., GREEN, J., KAUFFMANN, A., KOWAL, C., LEARY, R. J., LEHAR, J., LIANG, Y., LOO, A., LORENZANA, E., ROBERT MCDONALD, E., 3RD, MCLAUGHLIN, M. E., MERKIN, J., MEYER, R., NAYLOR, T. L., PATAWARAN, M., REDDY, A., ROELLI, C., RUDDY, D. A., SALANGSANG, F., SANTACROCE, F., SINGH, A. P., TANG, Y., TINETTO, W., TOBLER, S., VELAZQUEZ, R., VENKATESAN, K., VON ARX, F., WANG, H. Q., WANG, Z., WIESMANN, M., WYSS, D., XU, F., BITTER, H., ATADJA, P., LEES, E., HOFMANN, F., LI, E., KEEN, N., COZENS, R., JENSEN, M. R., PRYER, N. K., WILLIAMS, J. A. & SELLERS, W. R. 2015. High-throughput screening using patient-derived tumor xenografts to predict clinical trial drug response. *Nat Med*, 21, 1318-25.

GARRETT, J. T., SUTTON, C. R., KURUPI, R., BIALUCHA, C. U., ETTENBERG, S. A., COLLINS, S. D., SHENG, Q., WALLWEBER, J., DEFAZIO-ELI, L. & ARTEAGA, C. L. 2013. Combination of antibody that inhibits ligand-independent HER3 dimerization and a p110alpha inhibitor potently blocks PI3K signaling and growth of HER2+ breast cancers. *Cancer Res*, 73, 6013-23.

GATTELLI, A., NALVARTE, I., BOULAY, A., ROLOFF, T. C., SCHREIBER, M., CARRAGHER, N., MACLEOD, K. K., SCHLEDERER, M., LIENHARD, S., KENNER, L., TORRES-ARZAYUS, M. I. & HYNES, N. E. 2013. Ret inhibition decreases growth and metastatic potential of estrogen receptor positive breast cancer cells. *EMBO Mol Med*, 5, 1335-50.

GEYER, C. E., FORSTER, J., LINDQUIST, D., CHAN, S., ROMIEU, C. G., PIENKOWSKI, T., JAGIELLO-GRUSZFELD, A., CROWN, J., CHAN, A., KAUFMAN, B., SKARLOS, D., CAMPONE, M., DAVIDSON, N., BERGER, M., OLIVA, C., RUBIN, S. D., STEIN, S. & CAMERON, D. 2006. Lapatinib plus capecitabine for HER2-positive advanced breast cancer. *N Engl J Med*, 355, 2733-43.

GHOSH, R., NARASANNA, A., WANG, S. E., LIU, S., CHAKRABARTY, A., BALKO, J. M., GONZÁLEZ-ANGULO, A. M., MILLS, G. B., PENUEL, E., WINSLOW, J., SPERINDE, J., DUA, R., PIDAPARTHI,

S., MUKHERJEE, A., LEITZEL, K., KOSTLER, W. J., LIPTON, A., BATES, M. & ARTEAGA, C. L. 2011. Trastuzumab Has Preferential Activity against Breast Cancers Driven by HER2 Homodimers. *Cancer Research*, 71, 1871-1882.

GIL, Z., CAVEL, O., KELLY, K., BRADER, P., REIN, A., GAO, S. P., CARLSON, D. L., SHAH, J. P., FONG, Y. & WONG, R. J. 2010. Paracrine regulation of pancreatic cancer cell invasion by peripheral nerves. *J Natl Cancer Inst*, 102, 107-18.

GILD, M. L., LANDA, I., RYDER, M., GHOSSEIN, R. A., KNAUF, J. A. & FAGIN, J. A. 2013. Targeting mTOR in RET mutant medullary and differentiated thyroid cancer cells. *Endocr Relat Cancer*, 20, 659-67.

GRADISHAR, W. J. 2013. Emerging approaches for treating HER2-positive metastatic breast cancer beyond trastuzumab. *Ann Oncol*, 24, 2492-500.

GRAUS-PORTA, D., BEERLI, R. R., DALY, J. M. & HYNES, N. E. 1997. ErbB-2, the preferred heterodimerization partner of all ErbB receptors, is a mediator of lateral signaling. *Embo j*, 16, 1647-55.

GROOTHUIS, D. R. 2000. The blood-brain and blood-tumor barriers: A review of strategies for increasing drug delivery. *Neuro-Oncology*, 2, 45-59.

GRULLICH, C. 2014. Cabozantinib: a MET, RET, and VEGFR2 tyrosine kinase inhibitor. *Recent Results Cancer Res*, 201, 207-14.

GU, Z., EILS, R. & SCHLESNER, M. 2016. Complex heatmaps reveal patterns and correlations in multidimensional genomic data. *Bioinformatics*, 32, 2847-9.

HAMBERG, P., BOS, M. M., BRAUN, H. J., STOUTHARD, J. M., VAN DEIJK, G. A., ERDKAMP, F. L., VAN DER STELT-FRISSEN, I. N., BONTENBAL, M., CREEMERS, G. J., PORTIELJE, J. E., PRUIJT, J. F., LOOSVELD, O. J., SMIT, W. M., MULLER, E. W., SCHMITZ, P. I., SEYNAEVE, C. & KLIJN, J. G. 2011. Randomized phase II study comparing efficacy and safety of combination-therapy trastuzumab and docetaxel vs. sequential therapy of trastuzumab followed by docetaxel alone at progression as first-line chemotherapy in patients with HER2+ metastatic breast cancer: HERTAX trial. *Clin Breast Cancer*, 11, 103-13.

HANZELMANN, S., CASTELO, R. & GUINNEY, J. 2013. GSVA: gene set variation analysis for microarray and RNA-seq data. *BMC Bioinformatics*, 14, 7.

HATEM, R., LABIOD, D., CHATEAU-JOUBERT, S., DE PLATER, L., EL BOTTY, R., VACHER, S., BONIN, F., SERVELY, J. L., DIERAS, V., BIECHE, I. & MARANGONI, E. 2016. Vandetanib as a potential new treatment for estrogen receptor-negative breast cancers. *Int J Cancer*, 138, 2510-21.

HICKS, D. G., SHORT, S. M., PRESCOTT, N. L., TARR, S. M., COLEMAN, K. A., YODER, B. J., CROWE, J. P., CHOUEIRI, T. K., DAWSON, A. E., BUDD, G. T., TUBBS, R. R., CASEY, G. & WEIL, R. J. 2006. Breast cancers with brain metastases are more likely to be estrogen receptor negative, express the basal cytokeratin CK5/6, and overexpress HER2 or EGFR. *Am J Surg Pathol*, 30, 1097-104.

HINES, S. L., VALLOW, L. A., TAN, W. W., MCNEIL, R. B., PEREZ, E. A. & JAIN, A. 2008. Clinical outcomes after a diagnosis of brain metastases in patients with estrogen- and/or human epidermal growth factor receptor 2-positive versus triple-negative breast cancer. *Annals of Oncology*, 19, 1561-1565.

HOEFNAGEL, L. D., VAN DE VIJVER, M. J., VAN SLOOTEN, H. J., WESSELING, P., WESSELING, J., WESTENEND, P. J., BART, J., SELDENRIJK, C. A., NAGTEGAAL, I. D., OUDEJANS, J., VAN DER VALK, P., VAN DER GROEP, P., DE VRIES, E. G., VAN DER WALL, E. & VAN DIEST, P. J. 2010. Receptor conversion in distant breast cancer metastases. *Breast Cancer Res*, 12, R75.

HOFFKNECHT, P., TUFMAN, A., WEHLER, T., PELZER, T., WIEWRODT, R., SCHUTZ, M., SERKE, M., STOHLMACHER-WILLIAMS, J., MARTEN, A., MARIA HUBER, R. & DICKGREBER, N. J. 2015. Efficacy of the irreversible ErbB family blocker afatinib in epidermal growth factor receptor

(EGFR) tyrosine kinase inhibitor (TKI)-pretreated non-small-cell lung cancer patients with brain metastases or leptomeningeal disease. *J Thorac Oncol*, 10**,** 156-63.

HORIBATA, S., RICE, E. J., ZHENG, H., ANGUISH, L. J., COONROD, S. & DANKO, C. G. 2017. ER-positive breast cancer cells are poised for RET-mediated endocrine resistance. *bioRxiv*

HSU, F., DE CALUWE, A., ANDERSON, D., NICHOL, A., TORIUMI, T. & HO, C. 2016. EGFR mutation status on brain metastases from non-small cell lung cancer. *Lung Cancer*, 96**,** 101-107.

HU, Z., FAN, C., OH, D. S., MARRON, J. S., HE, X., QAQISH, B. F., LIVASY, C., CAREY, L. A., REYNOLDS, E., DRESSLER, L., NOBEL, A., PARKER, J., EWEND, M. G., SAWYER, L. R., WU, J., LIU, Y., NANDA, R., TRETIAKOVA, M., RUIZ ORRICO, A., DREHER, D., PALAZZO, J. P., PERREARD, L., NELSON, E., MONE, M., HANSEN, H., MULLINS, M., QUACKENBUSH, J. F., ELLIS, M. J., OLOPADE, O. I., BERNARD, P. S. & PEROU, C. M. 2006. The molecular portraits of breast tumors are conserved across microarray platforms. *BMC Genomics*, 7**,** 96.

HUNG, M. H., LIU, C. Y., SHIAU, C. Y., HSU, C. Y., TSAI, Y. F., WANG, Y. L., TAI, L. C., KING, K. L., CHAO, T. C., CHIU, J. H., SU, C. H., LO, S. S., TZENG, C. H., SHYR, Y. M. & TSENG, L. M. 2014. Effect of age and biological subtype on the risk and timing of brain metastasis in breast cancer patients. *PLoS One*, 9**,** e89389.

HYMAN, D. M., PIHA-PAUL, S. A., WON, H., RODON, J., SAURA, C., SHAPIRO, G. I., JURIC, D., QUINN, D. I., MORENO, V., DOGER, B., MAYER, I. A., BONI, V., CALVO, E., LOI, S., LOCKHART, A. C., ERINJERI, J. P., SCALTRITI, M., ULANER, G. A., PATEL, J., TANG, J., BEER, H., SELCUKLU, S. D., HANRAHAN, A. J., BOUVIER, N., MELCER, M., MURALI, R., SCHRAM, A. M., SMYTH, L. M., JHAVERI, K., LI, B. T., DRILON, A., HARDING, J. J., IYER, G., TAYLOR, B. S., BERGER, M. F., CUTLER JR, R. E., XU, F., BUTTURINI, A., ELI, L. D., MANN, G., FARRELL, C., LALANI, A. S., BRYCE, R. P., ARTEAGA, C. L., MERIC-BERNSTAM, F., BASELGA, J. & SOLIT, D. B. 2018. HER kinase inhibition in patients with HER2- and HER3-mutant cancers. *Nature*, 554**,** 189.

HYNES, N. E. & MACDONALD, G. 2009. ErbB receptors and signaling pathways in cancer. *Curr Opin Cell Biol*, 21**,** 177-84.

INOUE, K., NAKAGAMI, K., MIZUTANI, M., HOZUMI, Y., FUJIWARA, Y., MASUDA, N., TSUKAMOTO, F., SAITO, M., MIURA, S., EGUCHI, K., SHINKAI, T., ANDO, M., WATANABE, T., MASUDA, N., OHASHI, Y., SANO, M. & NOGUCHI, S. 2010. Randomized phase III trial of trastuzumab monotherapy followed by trastuzumab plus docetaxel versus trastuzumab plus docetaxel as first-line therapy in patients with HER2-positive metastatic breast cancer: the JO17360 Trial Group. *Breast Cancer Res Treat*, 119**,** 127-36.

IORIO, F., KNIJNENBURG, T. A., VIS, D. J., BIGNELL, G. R., MENDEN, M. P., SCHUBERT, M., ABEN, N., GONCALVES, E., BARTHORPE, S., LIGHTFOOT, H., COKELAER, T., GRENINGER, P., VAN DYK, E., CHANG, H., DE SILVA, H., HEYN, H., DENG, X., EGAN, R. K., LIU, Q., MIRONENKO, T., MITROPOULOS, X., RICHARDSON, L., WANG, J., ZHANG, T., MORAN, S., SAYOLS, S., SOLEIMANI, M., TAMBORERO, D., LOPEZ-BIGAS, N., ROSS-MACDONALD, P., ESTELLER, M., GRAY, N. S., HABER, D. A., STRATTON, M. R., BENES, C. H., WESSELS, L. F. A., SAEZ-RODRIGUEZ, J., MCDERMOTT, U. & GARNETT, M. J. 2016. A Landscape of Pharmacogenomic Interactions in Cancer. *Cell*, 166**,** 740-754.

JAIN, S., GOLDEN, J. P., WOZNIAK, D., PEHEK, E., JOHNSON, E. M., JR. & MILBRANDT, J. 2006. RET is dispensable for maintenance of midbrain dopaminergic neurons in adult mice. *J Neurosci*, 26**,** 11230-8.

JUNG, J., LEE, S. H., PARK, M., YOUN, J. H., SHIN, S. H., GWAK, H. S. & YOO, H. 2018. Discordances in ER, PR, and HER2 between primary breast cancer and brain metastasis. *J Neurooncol*, 137**,** 295-302.

KALKANIS, S. N., KONDZIOLKA, D., GASPAR, L. E., BURRI, S. H., ASHER, A. L., COBBS, C. S., AMMIRATI, M., ROBINSON, P. D., ANDREWS, D. W., LOEFFLER, J. S., MCDERMOTT, M., MEHTA, M. P.,

MIKKELSEN, T., OLSON, J. J., PALEOLOGOS, N. A., PATCHELL, R. A., RYKEN, T. C. & LINSKEY, M. E. 2010. The role of surgical resection in the management of newly diagnosed brain metastases: a systematic review and evidence-based clinical practice guideline. *J Neurooncol*, 96**,** 33-43.

KAN, Z., JAISWAL, B. S., STINSON, J., JANAKIRAMAN, V., BHATT, D., STERN, H. M., YUE, P., HAVERTY, P. M., BOURGON, R., ZHENG, J., MOORHEAD, M., CHAUDHURI, S., TOMSHO, L. P., PETERS, B. A., PUJARA, K., CORDES, S., DAVIS, D. P., CARLTON, V. E., YUAN, W., LI, L., WANG, W., EIGENBROT, C., KAMINKER, J. S., EBERHARD, D. A., WARING, P., SCHUSTER, S. C., MODRUSAN, Z., ZHANG, Z., STOKOE, D., DE SAUVAGE, F. J., FAHAM, M. & SESHAGIRI, S. 2010a. Diverse somatic mutation patterns and pathway alterations in human cancers. *Nature*, 466**,** 869-73.

KAN, Z., JAISWAL, B. S., STINSON, J., JANAKIRAMAN, V., BHATT, D., STERN, H. M., YUE, P., HAVERTY, P. M., BOURGON, R., ZHENG, J., MOORHEAD, M., CHAUDHURI, S., TOMSHO, L. P., PETERS, B. A., PUJARA, K., CORDES, S., DAVIS, D. P., CARLTON, V. E. H., YUAN, W., LI, L., WANG, W., EIGENBROT, C., KAMINKER, J. S., EBERHARD, D. A., WARING, P., SCHUSTER, S. C., MODRUSAN, Z., ZHANG, Z., STOKOE, D., DE SAUVAGE, F. J., FAHAM, M. & SESHAGIRI, S. 2010b. Diverse somatic mutation patterns and pathway alterations in human cancers. *Nature*, 466**,** 869.

KAREKLA, E., LIAO, W. J., SHARP, B., PUGH, J., REID, H., QUESNE, J. L., MOORE, D., PRITCHARD, C., MACFARLANE, M. & PRINGLE, J. H. 2017. Ex Vivo Explant Cultures of Non-Small Cell Lung Carcinoma Enable Evaluation of Primary Tumor Responses to Anticancer Therapy. *Cancer Res*, 77**,** 2029-2039.

KAST, R. E. & FOCOSI, D. 2010. Three paths to better tyrosine kinase inhibition behind the blood-brain barrier in treating chronic myelogenous leukemia and glioblastoma with imatinib. *Transl Oncol*, 3**,** 13-5.

KATO, S., SUBBIAH, V., MARCHLIK, E., ELKIN, S. K., CARTER, J. L. & KURZROCK, R. 2017. RET Aberrations in Diverse Cancers: Next-Generation Sequencing of 4,871 Patients. *Clinical Cancer Research*, 23**,** 1988-1997.

KENNECKE, H., YERUSHALMI, R., WOODS, R., CHEANG, M. C. U., VODUC, D., SPEERS, C. H., NIELSEN, T. O. & GELMON, K. 2010. Metastatic Behavior of Breast Cancer Subtypes. *Journal of Clinical Oncology*, 28**,** 3271-3277.

KHUNTIA, D., BROWN, P., LI, J. & MEHTA, M. P. 2006. Whole-brain radiotherapy in the management of brain metastasis. *J Clin Oncol*, 24**,** 1295-304.

KIM, D.-W., YANG, J. C.-H., CHEN, K., CHENG, Z., YIN, L., MARTIN, P. D., YANG, Z., JIANG, H. & AHN, M.-J. 2015. AZD3759, an EGFR inhibitor with blood brain barrier (BBB) penetration for the treatment of non-small cell lung cancer (NSCLC) with brain metastasis (BM): Preclinical evidence and clinical cases. *Journal of Clinical Oncology*, 33**,** 8016-8016.

KIM, L. S., HUANG, S., LU, W., LEV, D. C. & PRICE, J. E. 2004. Vascular endothelial growth factor expression promotes the growth of breast cancer brain metastases in nude mice. *Clin Exp Metastasis*, 21**,** 107-18.

KIM, S. J., KIM, J. S., PARK, E. S., LEE, J. S., LIN, Q., LANGLEY, R. R., MAYA, M., HE, J., KIM, S. W., WEIHUA, Z., BALASUBRAMANIAN, K., FAN, D., MILLS, G. B., HUNG, M. C. & FIDLER, I. J. 2011. Astrocytes upregulate survival genes in tumor cells and induce protection from chemotherapy. *Neoplasia*, 13**,** 286-98.

KINOSHITA, Y., KOGA, Y., SAKAMOTO, A. & HIDAKA, K. 2013. Long-lasting response to crizotinib in brain metastases due to EML4-ALK-rearranged non-small-cell lung cancer. *BMJ Case Rep*, 2013.

KODACK, D. P., ASKOXYLAKIS, V., FERRARO, G. B., FUKUMURA, D. & JAIN, R. K. 2015. Emerging strategies for treating brain metastases from breast cancer. *Cancer Cell*, **27**, 163-75.

KODACK, D. P., ASKOXYLAKIS, V., FERRARO, G. B., SHENG, Q., BADEAUX, M., GOEL, S., QI, X., SHANKARAIAH, R., CAO, Z. A., RAMJIAWAN, R. R., BEZWADA, D., PATEL, B., SONG, Y., COSTA, C., NAXEROVA, K., WONG, C. S. F., KLOEPPER, J., DAS, R., TAM, A., TANBOON, J., DUDA, D. G., MILLER, C. R., SIEGEL, M. B., ANDERS, C. K., SANDERS, M., ESTRADA, M. V., SCHLEGEL, R., ARTEAGA, C. L., BRACHTEL, E., HUANG, A., FUKUMURA, D., ENGELMAN, J. A. & JAIN, R. K. 2017a. The brain microenvironment mediates resistance in luminal breast cancer to PI3K inhibition through HER3 activation. *Science Translational Medicine*, 9,

KODACK, D. P., ASKOXYLAKIS, V., FERRARO, G. B., SHENG, Q., BADEAUX, M., GOEL, S., QI, X., SHANKARAIAH, R., CAO, Z. A., RAMJIAWAN, R. R., BEZWADA, D., PATEL, B., SONG, Y., COSTA, C., NAXEROVA, K., WONG, C. S. F., KLOEPPER, J., DAS, R., TAM, A., TANBOON, J., DUDA, D. G., MILLER, C. R., SIEGEL, M. B., ANDERS, C. K., SANDERS, M., ESTRADA, M. V., SCHLEGEL, R., ARTEAGA, C. L., BRACHTEL, E., HUANG, A., FUKUMURA, D., ENGELMAN, J. A. & JAIN, R. K. 2017b. The brain microenvironment mediates resistance in luminal breast cancer to PI3K inhibition through HER3 activation. *Sci Transl Med*, 9.

KODACK, D. P., ASKOXYLAKIS, V., FERRARO, G. B., SHENG, Q., BADEAUX, M., GOEL, S., QI, X. L., SHANKARAIAH, R., CAO, Z. A., RAMJIAWAN, R. R., BEZWADA, D., PATEL, B., SONG, Y. C., COSTA, C., NAXEROVA, K., WONG, C. S. F., KLOEPPER, J., DAS, R., TAM, A., TANBOON, J., DUDA, D. G., MILLER, C. R., SIEGEL, M. B., ANDERS, C. K., SANDERS, M., ESTRADA, M. V., SCHLEGEL, R., ARTEAGA, C. L., BRACHTEL, E., HUANG, A., FUKUMURA, D., ENGELMAN, J. A. & JAIN, R. K. 2017c. The brain microenvironment mediates resistance in luminal breast cancer to PI3K inhibition through HER3 activation. *Science Translational Medicine*, 9,

KODACK, D. P., CHUNG, E., YAMASHITA, H., INCIO, J., DUYVERMAN, A. M., SONG, Y., FARRAR, C. T., HUANG, Y., AGER, E., KAMOUN, W., GOEL, S., SNUDERL, M., LUSSIEZ, A., HIDDINGH, L., MAHMOOD, S., TANNOUS, B. A., EICHLER, A. F., FUKUMURA, D., ENGELMAN, J. A. & JAIN, R. K. 2012. Combined targeting of HER2 and VEGFR2 for effective treatment of HER2-amplified breast cancer brain metastases. *Proc Natl Acad Sci U S A*, 109, E3119-27.

KOHNO, T., ICHIKAWA, H., TOTOKI, Y., YASUDA, K., HIRAMOTO, M., NAMMO, T., SAKAMOTO, H., TSUTA, K., FURUTA, K., SHIMADA, Y., IWAKAWA, R., OGIWARA, H., OIKE, T., ENARI, M., SCHETTER, A. J., OKAYAMA, H., HAUGEN, A., SKAUG, V., CHIKU, S., YAMANAKA, I., ARAI, Y., WATANABE, S., SEKINE, I., OGAWA, S., HARRIS, C. C., TSUDA, H., YOSHIDA, T., YOKOTA, J. & SHIBATA, T. 2012. KIF5B-RET fusions in lung adenocarcinoma. *Nat Med*, 18, 375-7.

KRAMER, E. R., ARON, L., RAMAKERS, G. M., SEITZ, S., ZHUANG, X., BEYER, K., SMIDT, M. P. & KLEIN, R. 2007. Absence of Ret signaling in mice causes progressive and late degeneration of the nigrostriatal system. *PLoS Biol*, 5, e39.

KROP, I. E., SAURA, C., AHNERT, J. R., BECERRA, C., BRITTEN, C. D., ISAKOFF, S. J., DEMANSE, D., HACKL, W., QUADT, C., SILVA, A. P., BURRIS, H. A., ABU-KHALAF, M. M. & BASELGA, J. 2012. A phase I/IB dose-escalation study of BEZ235 in combination with trastuzumab in patients with PI3-kinase or PTEN altered HER2+ metastatic breast cancer. *Journal of Clinical Oncology*, 30, 508-508.

LEE-HOEFLICH, S. T., CROCKER, L., YAO, E., PHAM, T., MUNROE, X., HOEFLICH, K. P., SLIWKOWSKI, M. X. & STERN, H. M. 2008. A central role for HER3 in HER2-amplified breast cancer: implications for targeted therapy. *Cancer Res*, 68, 5878-87.

LEE, J. J., LOH, K. & YAP, Y. S. 2015a. PI3K/Akt/mTOR inhibitors in breast cancer. *Cancer Biol Med*, 12, 342-54.

LEE, J. Y., PARK, K., LEE, E., AHN, T., JUNG, H. H., LIM, S. H., HONG, M., DO, I.-G., CHO, E. Y., KIM, D.-H., KIM, J.-Y., AHN, J. S., IM, Y.-H. & PARK, Y. H. 2016. Gene Expression Profiling of Breast Cancer Brain Metastasis. *Scientific Reports*, **6**, 28623.

LEE, J. Y., PARK, K., LIM, S. H., KIM, H. S., YOO, K. H., JUNG, K. S., SONG, H. N., HONG, M., DO, I. G., AHN, T., LEE, S. K., BAE, S. Y., KIM, S. W., LEE, J. E., NAM, S. J., KIM, D. H., JUNG, H. H., KIM, J. Y., AHN, J. S., IM, Y. H. & PARK, Y. H. 2015b. Mutational profiling of brain metastasis from breast cancer: matched pair analysis of targeted sequencing between brain metastasis and primary breast cancer. *Oncotarget*, **6**, 43731-42.

LEE, S. S., AHN, J. H., KIM, M. K., SYM, S. J., GONG, G., AHN, S. D., KIM, S. B. & KIM, W. K. 2008. Brain metastases in breast cancer: prognostic factors and management. *Breast Cancer Res Treat*, 111**,** 523-30.

LEMMON, M. A. & SCHLESSINGER, J. 2010. Cell signaling by receptor tyrosine kinases. *Cell*, 141**,** 1117-34.

LEONE, J. P. & LEONE, B. A. 2015. Breast cancer brain metastases: the last frontier. *Exp Hematol Oncol*, 4**,** 33.

LESTER, S. C., BOSE, S., CHEN, Y. Y., CONNOLLY, J. L., DE BACA, M. E., FITZGIBBONS, P. L., HAYES, D. F., KLEER, C., O'MALLEY, F. P., PAGE, D. L., SMITH, B. L., TAN, L. K., WEAVER, D. L. & WINER, E. 2009. Protocol for the examination of specimens from patients with invasive carcinoma of the breast. *Arch Pathol Lab Med*, 133**,** 1515-38.

LI, C. I., URIBE, D. J. & DALING, J. R. 2005. Clinical characteristics of different histologic types of breast cancer. *Br J Cancer*, 93**,** 1046-52.

LI, G. G., SOMWAR, R., JOSEPH, J., SMITH, R. S., HAYASHI, T., MARTIN, L., FRANOVIC, A., SCHAIRER, A., MARTIN, E., RIELY, G. J., HARRIS, J., YAN, S., WEI, G., OLIVER, J. W., PATEL, R., MULTANI, P., LADANYI, M. & DRILON, A. 2017. Antitumor Activity of RXDX-105 in Multiple Cancer Types with RET Rearrangements or Mutations. *Clinical Cancer Research*, 23**,** 2981-2990.

LI, H. & DURBIN, R. 2009. Fast and accurate short read alignment with Burrows-Wheeler transform. *Bioinformatics*, 25**,** 1754-60.

LIEN, E. A., WESTER, K., LØNNING, P. E., SOLHEIM, E. & UELAND, P. M. 1991. Distribution of tamoxifen and metabolites into brain tissue and brain metastases in breast cancer patients. *British Journal of Cancer*, 63**,** 641-645.

LIGIBEL, J. 2011. Obesity and breast cancer. *Oncology (Williston Park)*, 25**,** 994-1000.

LIM, E. & LIN, N. U. 2014. Updates on the management of breast cancer brain metastases. *Oncology (Williston Park)*, 28**,** 572-8.

LIM, S. M., KIM, H. R., LEE, J. S., LEE, K. H., LEE, Y. G., MIN, Y. J., CHO, E. K., LEE, S. S., KIM, B. S., CHOI, M. Y., SHIM, H. S., CHUNG, J. H., LA CHOI, Y., LEE, M. J., KIM, M., KIM, J. H., ALI, S. M., AHN, M. J. & CHO, B. C. 2017. Open-Label, Multicenter, Phase II Study of Ceritinib in Patients With Non-Small-Cell Lung Cancer Harboring ROS1 Rearrangement. *J Clin Oncol*, 35**,** 2613-2618.

LIN, N. U. 2013. Breast cancer brain metastases: new directions in systemic therapy. *Ecancermedicalscience*, 7**,** 307.

LIN, N. U., DIÉRAS, V., PAUL, D., LOSSIGNOL, D., CHRISTODOULOU, C., STEMMLER, H.-J., ROCHÉ, H., LIU, M. C., GREIL, R., CIRUELOS, E., LOIBL, S., GORI, S., WARDLEY, A., YARDLEY, D., BRUFSKY, A., BLUM, J. L., RUBIN, S. D., DHARAN, B., STEPLEWSKI, K., ZEMBRYKI, D., OLIVA, C., ROYCHOWDHURY, D., PAOLETTI, P. & WINER, E. P. 2009a. Multicenter Phase II Study of Lapatinib in Patients with Brain Metastases from HER2-Positive Breast Cancer. *Clinical Cancer Research*, 15**,** 1452-1459.

LIN, N. U., DIERAS, V., PAUL, D., LOSSIGNOL, D., CHRISTODOULOU, C., STEMMLER, H. J., ROCHE, H., LIU, M. C., GREIL, R., CIRUELOS, E., LOIBL, S., GORI, S., WARDLEY, A., YARDLEY, D., BRUFSKY, A., BLUM, J. L., RUBIN, S. D., DHARAN, B., STEPLEWSKI, K., ZEMBRYKI, D., OLIVA, C.,

ROYCHOWDHURY, D., PAOLETTI, P. & WINER, E. P. 2009b. Multicenter phase II study of lapatinib in patients with brain metastases from HER2-positive breast cancer. *Clin Cancer Res*, 15**,** 1452-9.

LIN, N. U., EIERMAN, W., GREIL, R., CAMPONE, M., KAUFMAN, B., STEPLEWSKI, K., LANE, S. R., ZEMBRYKI, D., RUBIN, S. D. & WINER, E. P. 2011. Randomized phase II study of lapatinib plus capecitabine or lapatinib plus topotecan for patients with HER2-positive breast cancer brain metastases. *J Neurooncol*, 105**,** 613-20.

LIN, N. U., GELMAN, R. S., YOUNGER, W. J., SOHL, J., FREEDMAN, R. A., SORENSEN, A. G., BULLITT, E., HARRIS, G. J., MORGANSTERN, D., SCHNEIDER, B. P., KROP, I. E. & WINER, E. P. 2013. Phase II trial of carboplatin (C) and bevacizumab (BEV) in patients (pts) with breast cancer brain metastases (BCBM). *Journal of Clinical Oncology*, 31**,** 513-513.

LIN, N. U., WINER, E. P., WHEATLEY, D., CAREY, L. A., HOUSTON, S., MENDELSON, D., MUNSTER, P., FRAKES, L., KELLY, S., GARCIA, A. A., CLEATOR, S., UTTENREUTHER-FISCHER, M., JONES, H., WIND, S., VINISKO, R. & HICKISH, T. 2012. A phase II study of afatinib (BIBW 2992), an irreversible ErbB family blocker, in patients with HER2-positive metastatic breast cancer progressing after trastuzumab. *Breast Cancer Res Treat*, 133**,** 1057-65.

LIN, Q., BALASUBRAMANIAN, K., FAN, D., KIM, S. J., GUO, L., WANG, H., BAR-ELI, M., ALDAPE, K. D. & FIDLER, I. J. 2010. Reactive astrocytes protect melanoma cells from chemotherapy by sequestering intracellular calcium through gap junction communication channels. *Neoplasia*, 12**,** 748-54.

LIPSON, D., CAPELLETTI, M., YELENSKY, R., OTTO, G., PARKER, A., JAROSZ, M., CURRAN, J. A., BALASUBRAMANIAN, S., BLOOM, T., BRENNAN, K. W., DONAHUE, A., DOWNING, S. R., FRAMPTON, G. M., GARCIA, L., JUHN, F., MITCHELL, K. C., WHITE, E., WHITE, J., ZWIRKO, Z., PERETZ, T., NECHUSHTAN, H., SOUSSAN-GUTMAN, L., KIM, J., SASAKI, H., KIM, H. R., PARK, S. I., ERCAN, D., SHEEHAN, C. E., ROSS, J. S., CRONIN, M. T., JANNE, P. A. & STEPHENS, P. J. 2012. Identification of new ALK and RET gene fusions from colorectal and lung cancer biopsies. *Nat Med*, 18**,** 382-4.

LOCKMAN, P. R., MITTAPALLI, R. K., TASKAR, K. S., RUDRARAJU, V., GRIL, B., BOHN, K. A., ADKINS, C. E., ROBERTS, A., THORSHEIM, H. R., GAASCH, J. A., HUANG, S., PALMIERI, D., STEEG, P. S. & SMITH, Q. R. 2010. Heterogeneous blood-tumor barrier permeability determines drug efficacy in experimental brain metastases of breast cancer. *Clin Cancer Res*, 16**,** 5664-78.

LOWENSTEIN, E. J., DALY, R. J., BATZER, A. G., LI, W., MARGOLIS, B., LAMMERS, R., ULLRICH, A., SKOLNIK, E. Y., BAR-SAGI, D. & SCHLESSINGER, J. 1992. The SH2 and SH3 domain-containing protein GRB2 links receptor tyrosine kinases to ras signaling. *Cell*, 70**,** 431-42.

LU, Y. S., CHEN, T. W., LIN, C. H., YEH, D. C., TSENG, L. M., WU, P. F., RAU, K. M., CHEN, B. B., CHAO, T. C., HUANG, S. M., HUANG, C. S., SHIH, T. T. & CHENG, A. L. 2015. Bevacizumab preconditioning followed by Etoposide and Cisplatin is highly effective in treating brain metastases of breast cancer progressing from whole-brain radiotherapy. *Clin Cancer Res*, 21**,** 1851-8.

MADHUP, R., KIRTI, S., BHATT, M. L., SRIVASTAVA, P. K., SRIVASTAVA, M. & KUMAR, S. 2006. Letrozole for brain and scalp metastases from breast cancer--a case report. *Breast*, 15**,** 440-2.

MALHOTRA, G. K., ZHAO, X., BAND, H. & BAND, V. 2010. Histological, molecular and functional subtypes of breast cancers. *Cancer Biol Ther*, 10**,** 955-60.

MALLADI, S., MACALINAO, D. G., JIN, X., HE, L., BASNET, H., ZOU, Y., DE STANCHINA, E. & MASSAGUE, J. 2016. Metastatic Latency and Immune Evasion through Autocrine Inhibition of WNT. *Cell*, 165**,** 45-60.

MARANGONI, E., VINCENT-SALOMON, A., AUGER, N., DEGEORGES, A., ASSAYAG, F., DE CREMOUX, P., DE PLATER, L., GUYADER, C., DE PINIEUX, G., JUDDE, J. G., REBUCCI, M., TRAN-PERENNOU, C.,

SASTRE-GARAU, X., SIGAL-ZAFRANI, B., DELATTRE, O., DIERAS, V. & POUPON, M. F. 2007. A new model of patient tumor-derived breast cancer xenografts for preclinical assays. *Clin Cancer Res*, 13**,** 3989-98.

MASSAGUE, J. & OBENAUF, A. C. 2016. Metastatic colonization by circulating tumour cells. *Nature*, 529**,** 298-306.

MASUDA, H., ZHANG, D., BARTHOLOMEUSZ, C., DOIHARA, H., HORTOBAGYI, G. N. & UENO, N. T. 2012. Role of epidermal growth factor receptor in breast cancer. *Breast Cancer Res Treat*, 136**,** 331-45.

MCBRYAN, J., FAGAN, A., MCCARTAN, D., BANE, F. T., VARESLIJA, D., COCCHIGLIA, S., BYRNE, C., BOLGER, J., MCILROY, M., HUDSON, L., TIBBITTS, P., GAORA, P. O., HILL, A. D. & YOUNG, L. S. 2015. Transcriptomic Profiling of Sequential Tumors from Breast Cancer Patients Provides a Global View of Metastatic Expression Changes Following Endocrine Therapy. *Clin Cancer Res*, 21**,** 5371-9.

MCTIERNAN, A., KOOPERBERG, C., WHITE, E., WILCOX, S., COATES, R., ADAMS-CAMPBELL, L. L., WOODS, N. & OCKENE, J. 2003. Recreational physical activity and the risk of breast cancer in postmenopausal women: the Women's Health Initiative Cohort Study. *Jama*, 290**,** 1331-6.

MENARD, S., BALSARI, A., CASALINI, P., TAGLIABUE, E., CAMPIGLIO, M., BUFALINO, R. & CASCINELLI, N. 2002. HER-2-positive breast carcinomas as a particular subset with peculiar clinical behaviors. *Clin Cancer Res*, 8**,** 520-5.

METZGER-FILHO, O., BARRY, W. T., KROP, I. E., YOUNGER, W. J., LAWLER, E. S., WINER, E. P. & LIN, N. U. 2014. Phase I dose-escalation trial of ONT-380 in combination with trastuzumab in participants with brain metastases from HER2+ breast cancer. *Journal of Clinical Oncology*, 32**,** TPS660-TPS660.

MILES, D. W., DIERAS, V., CORTES, J., DUENNE, A. A., YI, J. & O'SHAUGHNESSY, J. 2013. First-line bevacizumab in combination with chemotherapy for HER2-negative metastatic breast cancer: pooled and subgroup analyses of data from 2447 patients. *Ann Oncol*, 24**,** 2773-80.

MILLER, K., WANG, M., GRALOW, J., DICKLER, M., COBLEIGH, M., PEREZ, E. A., SHENKIER, T., CELLA, D. & DAVIDSON, N. E. 2007. Paclitaxel plus bevacizumab versus paclitaxel alone for metastatic breast cancer. *N Engl J Med*, 357**,** 2666-76.

MILLIS, S. Z., GATALICA, Z., WINKLER, J., VRANIC, S., KIMBROUGH, J., REDDY, S. & O'SHAUGHNESSY, J. A. 2015. Predictive Biomarker Profiling of > 6000 Breast Cancer Patients Shows Heterogeneity in TNBC, With Treatment Implications. *Clin Breast Cancer*, 15**,** 473-481.e3.

MODJTAHEDI, H., CHO, B. C., MICHEL, M. C. & SOLCA, F. 2014. A comprehensive review of the preclinical efficacy profile of the ErbB family blocker afatinib in cancer. *Naunyn Schmiedebergs Arch Pharmacol*, 387**,** 505-21.

MOMENY, M., SAUNUS, J. M., MARTURANA, F., MCCART REED, A. E., BLACK, D., SALA, G., IACOBELLI, S., HOLLAND, J. D., YU, D., DA SILVA, L., SIMPSON, P. T., KHANNA, K. K., CHENEVIX-TRENCH, G. & LAKHANI, S. R. 2015. Heregulin-HER3-HER2 signaling promotes matrix metalloproteinase-dependent blood-brain-barrier transendothelial migration of human breast cancer cell lines. *Oncotarget*, 6**,** 3932-46.

MONSKY, W. L., MOUTA CARREIRA, C., TSUZUKI, Y., GOHONGI, T., FUKUMURA, D. & JAIN, R. K. 2002. Role of host microenvironment in angiogenesis and microvascular functions in human breast cancer xenografts: mammary fat pad versus cranial tumors. *Clin Cancer Res*, 8**,** 1008-13.

MORANDI, A., MARTIN, L. A., GAO, Q., PANCHOLI, S., MACKAY, A., ROBERTSON, D., ZVELEBIL, M., DOWSETT, M., PLAZA-MENACHO, I. & ISACKE, C. M. 2013. GDNF-RET signaling in ER-positive breast cancers is a key determinant of response and resistance to aromatase inhibitors. *Cancer Res*, 73**,** 3783-95.

MORANDI, A., PLAZA-MENACHO, I. & ISACKE, C. M. 2011. RET in breast cancer: functional and therapeutic implications. *Trends Mol Med*, 17, 149-57.

MORROW, J. J., BAYLES, I., FUNNELL, A. P. W., MILLER, T. E., SAIAKHOVA, A., LIZARDO, M. M., BARTELS, C. F., KAPTEIJN, M. Y., HUNG, S., MENDOZA, A., DHILLON, G., CHEE, D. R., MYERS, J. T., ALLEN, F., GAMBAROTTI, M., RIGHI, A., DIFEO, A., RUBIN, B. P., HUANG, A. Y., MELTZER, P. S., HELMAN, L. J., PICCI, P., VERSTEEG, H. H., STAMATOYANNOPOULOS, J. A., KHANNA, C. & SCACHERI, P. C. 2018. Positively selected enhancer elements endow osteosarcoma cells with metastatic competence. *Nat Med*, 24, 176-185.

MUNCHEL, S., HOANG, Y., ZHAO, Y., COTTRELL, J., KLOTZLE, B., GODWIN, A. K., KOESTLER, D., BEYERLEIN, P., FAN, J. B., BIBIKOVA, M. & CHIEN, J. 2015. Targeted or whole genome sequencing of formalin fixed tissue samples: potential applications in cancer genomics. *Oncotarget*, 6, 25943-61.

MURTHY, R., BORGES, V. F., CONLIN, A., CHAVES, J., CHAMBERLAIN, M., GRAY, T., VO, A. & HAMILTON, E. 2018. Tucatinib with capecitabine and trastuzumab in advanced HER2-positive metastatic breast cancer with and without brain metastases: a non-randomised, open-label, phase 1b study. *The Lancet Oncology*, 19, 880-888.

MUSGROVE, E. A. & SUTHERLAND, R. L. 2009. Biological determinants of endocrine resistance in breast cancer. *Nat Rev Cancer*, 9, 631-43.

NAGARAJAN, R. P. & COSTELLO, J. F. 2009. Epigenetic mechanisms in glioblastoma multiforme. *Semin Cancer Biol*, 19, 188-97.

NAKAI, K., HUNG, M. C. & YAMAGUCHI, H. 2016. A perspective on anti-EGFR therapies targeting triple-negative breast cancer. *Am J Cancer Res*, 6, 1609-23.

NCRI 2016. Cancer in Ireland 2016: Annual report of the National Cancer Registry.

NEMAN, J., CHOY, C., KOWOLIK, C. M., ANDERSON, A., DUENAS, V. J., WALIANY, S., CHEN, B. T., CHEN, M. Y. & JANDIAL, R. 2013. Co-evolution of breast-to-brain metastasis and neural progenitor cells. *Clin Exp Metastasis*, 30, 753-68.

NG, W. H., WAN, G. Q., PENG, Z. N. & TOO, H. P. 2009. Glial cell-line derived neurotrophic factor (GDNF) family of ligands confer chemoresistance in a ligand-specific fashion in malignant gliomas. *Journal of Clinical Neuroscience*, 16, 427-436.

NGUYEN, D. X., BOS, P. D. & MASSAGUE, J. 2009. Metastasis: from dissemination to organ-specific colonization. *Nat Rev Cancer*, 9, 274-84.

NGUYEN, M., MIYAKAWA, S., KATO, J., MORI, T., ARAI, T., ARMANINI, M., GELMON, K., YERUSHALMI, R., LEUNG, S., GAO, D., LANDES, G., HAAK-FRENDSCHO, M., ELIAS, K. & SIMMONS, A. D. 2015. Preclinical Efficacy and Safety Assessment of an Antibody-Drug Conjugate Targeting the c-RET Proto-Oncogene for Breast Carcinoma. *Clin Cancer Res*, 21, 5552-62.

NI, J., RAMKISSOON, S. H., XIE, S., GOEL, S., STOVER, D. G., GUO, H., LUU, V., MARCO, E., RAMKISSOON, L. A., KANG, Y. J., HAYASHI, M., NGUYEN, Q. D., LIGON, A. H., DU, R., CLAUS, E. B., ALEXANDER, B. M., YUAN, G. C., WANG, Z. C., IGLEHART, J. D., KROP, I. E., ROBERTS, T. M., WINER, E. P., LIN, N. U., LIGON, K. L. & ZHAO, J. J. 2016. Combination inhibition of PI3K and mTORC1 yields durable remissions in mice bearing orthotopic patient-derived xenografts of HER2-positive breast cancer brain metastases. *Nat Med*, 22, 723-6.

NIE, F., YANG, J., WEN, S., AN, Y.-L., DING, J., JU, S.-H., ZHAO, Z., CHEN, H.-J., PENG, X.-G., WONG, S. T. C., ZHAO, H. & TENG, G.-J. 2012. Involvement of epidermal growth factor receptor overexpression in the promotion of breast cancer brain metastasis. *Cancer*, 118, 5198-5209.

NIK-ZAINAL, S., DAVIES, H., STAAF, J., RAMAKRISHNA, M., GLODZIK, D., ZOU, X., MARTINCORENA, I., ALEXANDROV, L. B., MARTIN, S., WEDGE, D. C., VAN LOO, P., JU, Y. S., SMID, M., BRINKMAN, A. B., MORGANELLA, S., AURE, M. R., LINGJÆRDE, O. C., LANGERØD, A., RINGNÉR, M., AHN, S.-M., BOYAULT, S., BROCK, J. E., BROEKS, A., BUTLER, A., DESMEDT, C., DIRIX, L., DRONOV,

S., FATIMA, A., FOEKENS, J. A., GERSTUNG, M., HOOIJER, G. K. J., JANG, S. J., JONES, D. R., KIM, H.-Y., KING, T. A., KRISHNAMURTHY, S., LEE, H. J., LEE, J.-Y., LI, Y., MCLAREN, S., MENZIES, A., MUSTONEN, V., O'MEARA, S., PA RAMAKRISHNAN, K., RODRÍGUEZ-GONZÁLEZ, F. G., ROMIEU, G., SIEUWERTS, A. M., SIMPSON, P. T., SHEPHERD, R., STEBBINGS, L., STEFANSSON, O. A., TEAGUE, J., TOMMASI, S., TREILLEUX, I., VAN DEN EYNDEN, G. G., VERMEULEN, P., VINCENT-SALOMON, A., YATES, L., CALDAS, C., VEER, L. V. T., TUTT, A., KNAPPSKOG, S., TAN, B. K. T., JONKERS, J., BORG, Å., UENO, N. T., SOTIRIOU, C., VIARI, A., FUTREAL, P. A., CAMPBELL, P. J., SPAN, P. N., VAN LAERE, S., LAKHANI, S. R., EYFJORD, J. E., THOMPSON, A. M., BIRNEY, E., STUNNENBERG, H. G., VAN DE VIJVER, M. J., MARTENS, J. W. M., BØRRESEN-DALE, A.-L., RICHARDSON, A. L., KONG, G., THOMAS, G. & STRATTON, M. R. 2016. Landscape of somatic mutations in 560 breast cancer whole-genome sequences. *Nature*, 534**,** 47.

NOVO, S. M., WEDGE, S. R. & STARK, L. A. 2017. Ex vivo treatment of patient biopsies as a novel method to assess colorectal tumour response to the MEK1/2 inhibitor, Selumetinib. *Scientific Reports*, 7**,** 12020.

NOWELL, P. C. 1976. The clonal evolution of tumor cell populations. *Science*, 194**,** 23-8.

O'BRIEN, E., HOWARTH, C. & SIBSON, N. 2013. The role of astrocytes in CNS tumors: pre-clinical models and novel imaging approaches. *Frontiers in Cellular Neuroscience*, 7**,**

O'DONOVAN, N. & CROWN, J. 2007. EGFR and HER-2 antagonists in breast cancer. *Anticancer Res*, 27**,** 1285-94.

OLSON, E. M., ABDEL-RASOUL, M., MALY, J., WU, C. S., LIN, N. U. & SHAPIRO, C. L. 2013. Incidence and risk of central nervous system metastases as site of first recurrence in patients with HER2-positive breast cancer treated with adjuvant trastuzumab. *Ann Oncol*, 24**,** 1526-33.

PAGET, S. 1989. The distribution of secondary growths in cancer of the breast. 1889. *Cancer Metastasis Rev*, 8**,** 98-101.

PALMER, A. C. & SORGER, P. K. 2017. Combination Cancer Therapy Can Confer Benefit via Patient-to-Patient Variability without Drug Additivity or Synergy. *Cell*, 171**,** 1678-1691.e13.

PALMIERI, D., BRONDER, J. L., HERRING, J. M., YONEDA, T., WEIL, R. J., STARK, A. M., KUREK, R., VEGA-VALLE, E., FEIGENBAUM, L., HALVERSON, D., VORTMEYER, A. O., STEINBERG, S. M., ALDAPE, K. & STEEG, P. S. 2007. Her-2 overexpression increases the metastatic outgrowth of breast cancer cells in the brain. *Cancer Res*, 67**,** 4190-8.

PARDRIDGE, W. M. 2005. The blood-brain barrier: bottleneck in brain drug development. *NeuroRx*, 2**,** 3-14.

PATANAPHAN, V., SALAZAR, O. M. & RISCO, R. 1988. Breast cancer: metastatic patterns and their prognosis. *South Med J*, 81**,** 1109-12.

PATRO, R., DUGGAL, G., LOVE, M. I., IRIZARRY, R. A. & KINGSFORD, C. 2017. Salmon provides fast and bias-aware quantification of transcript expression. *Nat Methods*

PEREZ, E. A., ROMOND, E. H., SUMAN, V. J., JEONG, J.-H., DAVIDSON, N. E., JR, C. E. G., MARTINO, S., MAMOUNAS, E. P., KAUFMAN, P. A. & WOLMARK, N. 2011. Four-Year Follow-Up of Trastuzumab Plus Adjuvant Chemotherapy for Operable Human Epidermal Growth Factor Receptor 2–Positive Breast Cancer: Joint Analysis of Data From NCCTG N9831 and NSABP B-31. *Journal of Clinical Oncology*, 29**,** 3366-3373.

PEROU, C. M., SORLIE, T., EISEN, M. B., VAN DE RIJN, M., JEFFREY, S. S., REES, C. A., POLLACK, J. R., ROSS, D. T., JOHNSEN, H., AKSLEN, L. A., FLUGE, O., PERGAMENSCHIKOV, A., WILLIAMS, C., ZHU, S. X., LONNING, P. E., BORRESEN-DALE, A. L., BROWN, P. O. & BOTSTEIN, D. 2000. Molecular portraits of human breast tumours. *Nature*, 406**,** 747-52.

PLAZA-MENACHO, I., MORANDI, A., ROBERTSON, D., PANCHOLI, S., DRURY, S., DOWSETT, M., MARTIN, L. A. & ISACKE, C. M. 2010a. Targeting the receptor tyrosine kinase RET sensitizes

breast cancer cells to tamoxifen treatment and reveals a role for RET in endocrine resistance. *Oncogene*, 29**,** 4648.

PLAZA-MENACHO, I., MORANDI, A., ROBERTSON, D., PANCHOLI, S., DRURY, S., DOWSETT, M., MARTIN, L. A. & ISACKE, C. M. 2010b. Targeting the receptor tyrosine kinase RET sensitizes breast cancer cells to tamoxifen treatment and reveals a role for RET in endocrine resistance. *Oncogene*, 29**,** 4648-57.

POPAT, S., HUGHES, S., PAPADOPOULOS, P., WILKINS, A., MOORE, S., PRIEST, K., MEEHAN, L., NORTON, A. & O'BRIEN, M. 2007. Recurrent responses to non-small cell lung cancer brain metastases with erlotinib. *Lung Cancer*, 56**,** 135-7.

PORS, H., VON EYBEN, F. E., SORENSEN, O. S. & LARSEN, M. 1991. Longterm remission of multiple brain metastases with tamoxifen. *J Neurooncol*, 10**,** 173-7.

PRIEDIGKEIT, N., HARTMAIER, R. J., CHEN, Y., VARESLIJA, D., BASUDAN, A., WATTERS, R. J., THOMAS, R., LEONE, J. P., LUCAS, P. C., BHARGAVA, R., HAMILTON, R. L., CHMIELECKI, J., PUHALLA, S. L., DAVIDSON, N. E., OESTERREICH, S., BRUFSKY, A. M., YOUNG, L. & LEE, A. V. 2016. Intrinsic Subtype Switching and Acquired ERBB2/HER2 Amplifications and Mutations in Breast Cancer Brain Metastases. *JAMA Oncol*

PRIEDIGKEIT, N., HARTMAIER, R. J., CHEN, Y., VARESLIJA, D., BASUDAN, A., WATTERS, R. J., THOMAS, R., LEONE, J. P., LUCAS, P. C., BHARGAVA, R., HAMILTON, R. L., CHMIELECKI, J., PUHALLA, S. L., DAVIDSON, N. E., OESTERREICH, S., BRUFSKY, A. M., YOUNG, L. & LEE, A. V. 2017a. Intrinsic Subtype Switching and Acquired ERBB2/HER2 Amplifications and Mutations in Breast Cancer Brain Metastases. *JAMA Oncol*, 3**,** 666-671.

PRIEDIGKEIT, N., WATTERS, R. J., LUCAS, P. C., BASUDAN, A., BHARGAVA, R., HORNE, W., KOLLS, J. K., FANG, Z., ROSENZWEIG, M. Q., BRUFSKY, A. M., WEISS, K. R., OESTERREICH, S. & LEE, A. V. 2017b. Exome-capture RNA sequencing of decade-old breast cancers and matched decalcified bone metastases. *JCI Insight*, 2.

PUTZER, B. M. & DROSTEN, M. 2004. The RET proto-oncogene: a potential target for molecular cancer therapy. *Trends Mol Med*, 10**,** 351-7.

QUESNELLE, K. M., WHEELER, S. E., RATAY, M. K. & GRANDIS, J. R. 2012. Preclinical modeling of EGFR inhibitor resistance in head and neck cancer. *Cancer Biol Ther*, 13**,** 935-45.

REDIG, A. J. & MCALLISTER, S. S. 2013. Breast cancer as a systemic disease: a view of metastasis. *J Intern Med*, 274**,** 113-26.

ROBINSON, M. D., MCCARTHY, D. J. & SMYTH, G. K. 2010. edgeR: a Bioconductor package for differential expression analysis of digital gene expression data. *Bioinformatics*, 26**,** 139-40.

ROBINSON, M. D. & OSHLACK, A. 2010. A scaling normalization method for differential expression analysis of RNA-seq data. *Genome Biology*, 11**,** R25.

ROMOND , E. H., PEREZ , E. A., BRYANT , J., SUMAN , V. J., GEYER , C. E. J., DAVIDSON , N. E., TAN-CHIU , E., MARTINO , S., PAIK , S., KAUFMAN , P. A., SWAIN , S. M., PISANSKY , T. M., FEHRENBACHER , L., KUTTEH , L. A., VOGEL , V. G., VISSCHER , D. W., YOTHERS , G., JENKINS , R. B., BROWN , A. M., DAKHIL , S. R., MAMOUNAS , E. P., LINGLE , W. L., KLEIN , P. M., INGLE , J. N. & WOLMARK , N. 2005. Trastuzumab plus Adjuvant Chemotherapy for Operable HER2-Positive Breast Cancer. *New England Journal of Medicine*, 353**,** 1673-1684.

ROSKOSKI, R. 2014a. The ErbB/HER family of protein-tyrosine kinases and cancer. *Pharmacological Research*, 79**,** 34-74.

ROSKOSKI, R. 2014b. The ErbB/HER family of protein-tyrosine kinases and cancer. *Pharmacological Research*, 79**,** 34-74.

ROSKOSKI, R., JR. 2014c. The ErbB/HER family of protein-tyrosine kinases and cancer. *Pharmacol Res*, 79**,** 34-74.

SAHA, A., GHOSH, S. K., ROY, C., CHOUDHURY, K. B., CHAKRABARTY, B. & SARKAR, R. 2013. Demographic and clinical profile of patients with brain metastases: A retrospective study. *Asian J Neurosurg*, **8**, 157-61.

SALHIA, B., KIEFER, J., ROSS, J. T., METAPALLY, R., MARTINEZ, R. A., JOHNSON, K. N., DIPERNA, D. M., PAQUETTE, K. M., JUNG, S., NASSER, S., WALLSTROM, G., TEMBE, W., BAKER, A., CARPTEN, J., RESAU, J., RYKEN, T., SIBENALLER, Z., PETRICOIN, E. F., LIOTTA, L. A., RAMANATHAN, R. K., BERENS, M. E. & TRAN, N. L. 2014. Integrated genomic and epigenomic analysis of breast cancer brain metastasis. *PLoS One*, **9**, e85448.

SALVATI, M., CERVONI, L., INNOCENZI, G. & BARDELLA, L. 1993. Prolonged stabilization of multiple and single brain metastases from breast cancer with tamoxifen. Report of three cases. *Tumori*, 79, 359-62.

SARIOLA, H. & SAARMA, M. 2003. Novel functions and signalling pathways for GDNF. *Journal of Cell Science*, 116, 3855-3862.

SAUNUS, J. M., MCCART REED, A. E., LIM, Z. L. & LAKHANI, S. R. 2017. Breast Cancer Brain Metastases: Clonal Evolution in Clinical Context. *Int J Mol Sci*, 18.

SAUNUS, J. M., QUINN, M. C., PATCH, A. M., PEARSON, J. V., BAILEY, P. J., NONES, K., MCCART REED, A. E., MILLER, D., WILSON, P. J., AL-EJEH, F., MARIASEGARAM, M., LAU, Q., WITHERS, T., JEFFREE, R. L., REID, L. E., DA SILVA, L., MATSIKA, A., NILAND, C. M., CUMMINGS, M. C., BRUXNER, T. J., CHRIST, A. N., HARLIWONG, I., IDRISOGLU, S., MANNING, S., NOURSE, C., NOURBAKHSH, E., WANI, S., ANDERSON, M. J., FINK, J. L., HOLMES, O., KAZAKOFF, S., LEONARD, C., NEWELL, F., TAYLOR, D., WADDELL, N., WOOD, S., XU, Q., KASSAHN, K. S., NARAYANAN, V., TAIB, N. A., TEO, S. H., CHOW, Y. P., KCONFAB, JAT, P. S., BRANDNER, S., FLANAGAN, A. M., KHANNA, K. K., CHENEVIX-TRENCH, G., GRIMMOND, S. M., SIMPSON, P. T., WADDELL, N. & LAKHANI, S. R. 2015. Integrated genomic and transcriptomic analysis of human brain metastases identifies alterations of potential clinical significance. *J Pathol*, 237, 363-78.

SAXENA, R. & DWIVEDI, A. 2012. ErbB family receptor inhibitors as therapeutic agents in breast cancer: Current status and future clinical perspective. *Medicinal Research Reviews*, **32**, 166-215.

SCHLESSINGER, J. 2002. Ligand-Induced, Receptor-Mediated Dimerization and Activation of EGF Receptor. *Cell*, 110, 669-672.

SCHULER, M., WU, Y. L., HIRSH, V., O'BYRNE, K., YAMAMOTO, N., MOK, T., POPAT, S., SEQUIST, L. V., MASSEY, D., ZAZULINA, V. & YANG, J. C. 2016. First-Line Afatinib versus Chemotherapy in Patients with Non-Small Cell Lung Cancer and Common Epidermal Growth Factor Receptor Gene Mutations and Brain Metastases. *J Thorac Oncol*, 11, 380-90.

SERGINA, N. V., RAUSCH, M., WANG, D., BLAIR, J., HANN, B., SHOKAT, K. M. & MOASSER, M. M. 2007. Escape from HER-family tyrosine kinase inhibitor therapy by the kinase-inactive HER3. *Nature*, 445, 437-41.

SEVENICH, L., BOWMAN, R. L., MASON, S. D., QUAIL, D. F., RAPAPORT, F., ELIE, B. T., BROGI, E., BRASTIANOS, P. K., HAHN, W. C., HOLSINGER, L. J., MASSAGUE, J., LESLIE, C. S. & JOYCE, J. A. 2014. Analysis of tumour- and stroma-supplied proteolytic networks reveals a brain-metastasis-promoting role for cathepsin S. *Nat Cell Biol*, 16, 876-88.

SHABTAY-ORBACH, A., AMIT, M., BINENBAUM, Y., NA'ARA, S. & GIL, Z. 2015. Paracrine regulation of glioma cells invasion by astrocytes is mediated by glial-derived neurotrophic factor. *Int J Cancer*, 137, 1012-20.

SHAO, M. M., LIU, J., VONG, J. S., NIU, Y., GERMIN, B., TANG, P., CHAN, A. W., LUI, P. C., LAW, B. K., TAN, P. H. & TSE, G. M. 2011. A subset of breast cancer predisposes to brain metastasis. *Med Mol Morphol*, 44, 15-20.

SHAW, A. T., KIM, D.-W., NAKAGAWA, K., SETO, T., CRINÓ, L., AHN, M.-J., DE PAS, T., BESSE, B., SOLOMON, B. J., BLACKHALL, F., WU, Y.-L., THOMAS, M., O'BYRNE, K. J., MORO-SIBILOT, D., CAMIDGE, D. R., MOK, T., HIRSH, V., RIELY, G. J., IYER, S., TASSELL, V., POLLI, A., WILNER, K. D. & JÄNNE, P. A. 2013. Crizotinib versus Chemotherapy in Advanced ALK-Positive Lung Cancer. *New England Journal of Medicine*, **368**, 2385-2394.

SIOLAS, D. & HANNON, G. J. 2013. Patient-Derived Tumor Xenografts: Transforming Clinical Samples into Mouse Models. *Cancer Research*, **73**, 5315-5319.

SIRKISOON, S. R., CARPENTER, R. L., RIMKUS, T., MILLER, L., METHENY-BARLOW, L. & LO, H. W. 2016. EGFR and HER2 signaling in breast cancer brain metastasis. *Front Biosci (Elite Ed)*, **8**, 245-63.

SLAMON, D. J., GODOLPHIN, W., JONES, L. A., HOLT, J. A., WONG, S. G., KEITH, D. E., LEVIN, W. J., STUART, S. G., UDOVE, J., ULLRICH, A. & ET AL. 1989. Studies of the HER-2/neu proto-oncogene in human breast and ovarian cancer. *Science*, **244**, 707-12.

SMID, M., WANG, Y., ZHANG, Y., SIEUWERTS, A. M., YU, J., KLIJN, J. G., FOEKENS, J. A. & MARTENS, J. W. 2008. Subtypes of breast cancer show preferential site of relapse. *Cancer Res*, **68**, 3108-14.

SMITH, J. S., TACHIBANA, I., PASSE, S. M., HUNTLEY, B. K., BORELL, T. J., ITURRIA, N., O'FALLON, J. R., SCHAEFER, P. L., SCHEITHAUER, B. W., JAMES, C. D., BUCKNER, J. C. & JENKINS, R. B. 2001. PTEN Mutation, EGFR Amplification, and Outcome in Patients With Anaplastic Astrocytoma and Glioblastoma Multiforme. *JNCI: Journal of the National Cancer Institute*, **93**, 1246-1256.

SONESON, C., LOVE, M. I. & ROBINSON, M. D. 2015. Differential analyses for RNA-seq: transcript-level estimates improve gene-level inferences. *F1000Res*, **4**, 1521.

SONI, A., REN, Z., HAMEED, O., CHANDA, D., MORGAN, C. J., SIEGAL, G. P. & WEI, S. 2015. Breast cancer subtypes predispose the site of distant metastases. *Am J Clin Pathol*, **143**, 471-8.

SORLIE, T., PEROU, C. M., TIBSHIRANI, R., AAS, T., GEISLER, S., JOHNSEN, H., HASTIE, T., EISEN, M. B., VAN DE RIJN, M., JEFFREY, S. S., THORSEN, T., QUIST, H., MATESE, J. C., BROWN, P. O., BOTSTEIN, D., LONNING, P. E. & BORRESEN-DALE, A. L. 2001. Gene expression patterns of breast carcinomas distinguish tumor subclasses with clinical implications. *Proc Natl Acad Sci U S A*, **98**, 10869-74.

SORLIE, T., TIBSHIRANI, R., PARKER, J., HASTIE, T., MARRON, J. S., NOBEL, A., DENG, S., JOHNSEN, H., PESICH, R., GEISLER, S., DEMETER, J., PEROU, C. M., LONNING, P. E., BROWN, P. O., BORRESEN-DALE, A. L. & BOTSTEIN, D. 2003. Repeated observation of breast tumor subtypes in independent gene expression data sets. *Proc Natl Acad Sci U S A*, **100**, 8418-23.

SPANHEIMER, P. M., CYR, A. R., GILLUM, M. P., WOODFIELD, G. W., ASKELAND, R. W. & WEIGEL, R. J. 2014. Distinct pathways regulated by RET and estrogen receptor in luminal breast cancer demonstrate the biological basis for combination therapy. *Ann Surg*, **259**, 793-9.

STEEG, P. S., CAMPHAUSEN, K. A. & SMITH, Q. R. 2011. Brain metastases as preventive and therapeutic targets. *Nat Rev Cancer*, **11**, 352-63.

STEMMLER, H. J., SCHMITT, M., WILLEMS, A., BERNHARD, H., HARBECK, N. & HEINEMANN, V. 2007. Ratio of trastuzumab levels in serum and cerebrospinal fluid is altered in HER2-positive breast cancer patients with brain metastases and impairment of blood-brain barrier. *Anticancer Drugs*, **18**, 23-8.

SUBBIAH, V., BERRY, J., ROXAS, M., GUHA-THAKURTA, N., SUBBIAH, I. M., ALI, S. M., MCMAHON, C., MILLER, V., CASCONE, T., PAI, S., TANG, Z. & HEYMACH, J. V. 2015. Systemic and CNS activity of the RET inhibitor vandetanib combined with the mTOR inhibitor everolimus in KIF5B-RET re-arranged non-small cell lung cancer with brain metastases. *Lung Cancer*, **89**, 76-9.

SUBBIAH, V., GAINOR, J. F., RAHAL, R., BRUBAKER, J. D., KIM, J. L., MAYNARD, M., HU, W., CAO, Q., SHEETS, M. P., WILSON, D., WILSON, K. J., DIPIETRO, L., FLEMING, P., PALMER, M., HU, M. I., WIRTH, L., BROSE, M. S., OU, S.-H. I., TAYLOR, M., GARRALDA, E., MILLER, S., WOLF, B.,

LENGAUER, C., GUZI, T. & EVANS, E. K. 2018a. Precision Targeted Therapy With BLU-667 for RET-Driven Cancers. *Cancer Discovery*

SUBBIAH, V., VELCHETI, V., TUCH, B. B., EBATA, K., BUSAIDY, N. L., CABANILLAS, M. E., WIRTH, L. J., STOCK, S., SMITH, S., LAURIAULT, V., CORSI-TRAVALI, S., HENRY, D., BURKARD, M., HAMOR, R., BOUHANA, K., WINSKI, S., WALLACE, R. D., HARTLEY, D., RHODES, S., REDDY, M., BRANDHUBER, B. J., ANDREWS, S., ROTHENBERG, S. M. & DRILON, A. 2018b. Selective RET kinase inhibition for patients with RET-altered cancers. *Annals of Oncology*, mdy137-mdy137.

TABOURET, E., CHINOT, O., METELLUS, P., TALLET, A., VIENS, P. & GONCALVES, A. 2012. Recent trends in epidemiology of brain metastases: an overview. *Anticancer Res*, 32**,** 4655-62.

TAKEUCHI, K., SODA, M., TOGASHI, Y., SUZUKI, R., SAKATA, S., HATANO, S., ASAKA, R., HAMANAKA, W., NINOMIYA, H., UEHARA, H., LIM CHOI, Y., SATOH, Y., OKUMURA, S., NAKAGAWA, K., MANO, H. & ISHIKAWA, Y. 2012a. RET, ROS1 and ALK fusions in lung cancer. *Nature Medicine*, 18**,** 378.

TAKEUCHI, K., SODA, M., TOGASHI, Y., SUZUKI, R., SAKATA, S., HATANO, S., ASAKA, R., HAMANAKA, W., NINOMIYA, H., UEHARA, H., LIM CHOI, Y., SATOH, Y., OKUMURA, S., NAKAGAWA, K., MANO, H. & ISHIKAWA, Y. 2012b. RET, ROS1 and ALK fusions in lung cancer. *Nat Med*, 18**,** 378-81.

TAMURA, K., KURIHARA, H., YONEMORI, K., TSUDA, H., SUZUKI, J., KONO, Y., HONDA, N., KODAIRA, M., YAMAMOTO, H., YUNOKAWA, M., SHIMIZU, C., HASEGAWA, K., KANAYAMA, Y., NOZAKI, S., KINOSHITA, T., WADA, Y., TAZAWA, S., TAKAHASHI, K., WATANABE, Y. & FUJIWARA, Y. 2013. 64Cu-DOTA-trastuzumab PET imaging in patients with HER2-positive breast cancer. *J Nucl Med*, 54**,** 1869-75.

TANAKA, H., HIRATA, M., SHINONOME, S., WADA, T., IGUCHI, M., DOHI, K., INOUE, M., ISHIOKA, Y., HOJO, K., YAMADA, T., SUGIMOTO, T., MASUNO, K., NEZASA, K., SATO, N., MATSUO, K., YONEZAWA, S., FRENKEL, E. P. & SHICHIJO, M. 2014. Preclinical antitumor activity of S-222611, an oral reversible tyrosine kinase inhibitor of epidermal growth factor receptor and human epidermal growth factor receptor 2. *Cancer Sci*, 105**,** 1040-8.

TEBBUTT, N., PEDERSEN, M. W. & JOHNS, T. G. 2013. Targeting the ERBB family in cancer: couples therapy. *Nature Reviews Cancer*, 13**,** 663.

THAM, Y. L., SEXTON, K., KRAMER, R., HILSENBECK, S. & ELLEDGE, R. 2006. Primary breast cancer phenotypes associated with propensity for central nervous system metastases. *Cancer*, 107**,** 696-704.

THOMSON, A. H., MCGRANE, J., MATHEW, J., PALMER, J., HILTON, D. A., PURVIS, G. & JENKINS, R. 2016. Changing molecular profile of brain metastases compared with matched breast primary cancers and impact on clinical outcomes. *Br J Cancer*, 114**,** 793-800.

TOLANEY, S. M., NECHUSHTAN, H., RON, I. G., SCHOFFSKI, P., AWADA, A., YASENCHAK, C. A., LAIRD, A. D., O'KEEFFE, B., SHAPIRO, G. I. & WINER, E. P. 2016. Cabozantinib for metastatic breast carcinoma: results of a phase II placebo-controlled randomized discontinuation study. *Breast Cancer Res Treat*, 160**,** 305-312.

TOWNSEND, E. C., MURAKAMI, M. A., CHRISTODOULOU, A., CHRISTIE, A. L., KOSTER, J., DESOUZA, T. A., MORGAN, E. A., KALLGREN, S. P., LIU, H., WU, S. C., PLANA, O., MONTERO, J., STEVENSON, K. E., RAO, P., VADHI, R., ANDREEFF, M., ARMAND, P., BALLEN, K. K., BARZAGHI-RINAUDO, P., CAHILL, S., CLARK, R. A., COOKE, V. G., DAVIDS, M. S., DEANGELO, D. J., DORFMAN, D. M., EATON, H., EBERT, B. L., ETCHIN, J., FIRESTONE, B., FISHER, D. C., FREEDMAN, A. S., GALINSKY, I. A., GAO, H., GARCIA, J. S., GARNACHE-OTTOU, F., GRAUBERT, T. A., GUTIERREZ, A., HALILOVIC, E., HARRIS, M. H., HERBERT, Z. T., HORWITZ, S. M., INGHIRAMI, G., INTLEKOFER, A. M., ITO, M., IZRAELI, S., JACOBSEN, E. D., JACOBSON, C. A., JEAY, S., JEREMIAS, I., KELLIHER, M. A., KOCH, R., KONOPLEVA, M., KOPP, N., KORNBLAU, S. M., KUNG, A. L., KUPPER, T. S.,

LEBOEUF, N. R., LACASCE, A. S., LEES, E., LI, L. S., LOOK, A. T., MURAKAMI, M., MUSCHEN, M., NEUBERG, D., NG, S. Y., ODEJIDE, O. O., ORKIN, S. H., PAQUETTE, R. R., PLACE, A. E., RODERICK, J. E., RYAN, J. A., SALLAN, S. E., SHOJI, B., SILVERMAN, L. B., SOIFFER, R. J., STEENSMA, D. P., STEGMAIER, K., STONE, R. M., TAMBURINI, J., THORNER, A. R., VAN HUMMELEN, P., WADLEIGH, M., WIESMANN, M., WENG, A. P., WUERTHNER, J. U., WILLIAMS, D. A., WOLLISON, B. M., LANE, A. A., LETAI, A., BERTAGNOLLI, M. M., RITZ, J., BROWN, M., LONG, H., ASTER, J. C., SHIPP, M. A., GRIFFIN, J. D. & WEINSTOCK, D. M. 2016. The Public Repository of Xenografts Enables Discovery and Randomized Phase II-like Trials in Mice. *Cancer Cell*, 29, 574-586.

TOZLU, S., GIRAULT, I., VACHER, S., VENDRELL, J., ANDRIEU, C., SPYRATOS, F., COHEN, P., LIDEREAU, R. & BIECHE, I. 2006. Identification of novel genes that co-cluster with estrogen receptor alpha in breast tumor biopsy specimens, using a large-scale real-time reverse transcription-PCR approach. *Endocr Relat Cancer*, 13, 1109-20.

UNGER, K., WIENBERG, J., RICHES, A., HIEBER, L., WALCH, A., BROWN, A., O'BRIEN, P. C., BRISCOE, C., GRAY, L., RODRIGUEZ, E., JACKL, G., KNIJNENBURG, J., TALLINI, G., FERGUSON-SMITH, M. & ZITZELSBERGER, H. 2010. Novel gene rearrangements in transformed breast cells identified by high-resolution breakpoint analysis of chromosomal aberrations. *Endocr Relat Cancer*, 17, 87-98.

VAIRA, V., FEDELE, G., PYNE, S., FASOLI, E., ZADRA, G., BAILEY, D., SNYDER, E., FAVERSANI, A., COGGI, G., FLAVIN, R., BOSARI, S. & LODA, M. 2010. Preclinical model of organotypic culture for pharmacodynamic profiling of human tumors. *Proceedings of the National Academy of Sciences*, 107, 8352-8356.

VALASTYAN, S. & WEINBERG, R. A. 2011. Tumor metastasis: molecular insights and evolving paradigms. *Cell*, 147, 275-92.

VALIENTE, M., OBENAUF, A. C., JIN, X., CHEN, Q., ZHANG, X. H., LEE, D. J., CHAFT, J. E., KRIS, M. G., HUSE, J. T., BROGI, E. & MASSAGUE, J. 2014. Serpins promote cancer cell survival and vascular co-option in brain metastasis. *Cell*, 156, 1002-16.

VAN ALLEN, E. M., WAGLE, N., STOJANOV, P., PERRIN, D. L., CIBULSKIS, K., MARLOW, S., JANE-VALBUENA, J., FRIEDRICH, D. C., KRYUKOV, G., CARTER, S. L., MCKENNA, A., SIVACHENKO, A., ROSENBERG, M., KIEZUN, A., VOET, D., LAWRENCE, M., LICHTENSTEIN, L. T., GENTRY, J. G., HUANG, F. W., FOSTEL, J., FARLOW, D., BARBIE, D., GANDHI, L., LANDER, E. S., GRAY, S. W., JOFFE, S., JANNE, P., GARBER, J., MACCONAILL, L., LINDEMAN, N., ROLLINS, B., KANTOFF, P., FISHER, S. A., GABRIEL, S., GETZ, G. & GARRAWAY, L. A. 2014. Whole-exome sequencing and clinical interpretation of formalin-fixed, paraffin-embedded tumor samples to guide precision cancer medicine. *Nat Med*, 20, 682-8.

VARESLIJA, D., COCCHIGLIA, S., BYRNE, C. & YOUNG, L. 2017. Patient-Derived Xenografts of Breast Cancer. *Methods Mol Biol*, 1501, 327-336.

VARESLIJA, D., FAGAN, A., GREEN, M., HILL, A. & YOUNG, L. 2016. Abstract P2-05-03: Whole genome transcriptome analysis of sequential breast to brain metastasis uncovers new signalling pathways and druggable targets. *Cancer Research*, 76, P2-05-03-P2-05-03.

VARESLIJA, D., PRIEDIGKEIT, N., FAGAN, A., PURCELL, S., COSGROVE, N., O'HALLORAN, P. J., WARD, E., COCCHIGLIA, S., HARTMAIER, R., CASTRO, C. A., ZHU, L., TSENG, G. C., LUCAS, P. C., PUHALLA, S. L., BRUFSKY, A. M., HAMILTON, R. L., MATHEW, A., LEONE, J. P., BASUDAN, A., HUDSON, L., DWYER, R., DAS, S., O'CONNOR, D. P., BUCKLEY, P. G., FARRELL, M., HILL, A. D. K., OESTERREICH, S., LEE, A. V. & YOUNG, L. S. 2018. Transcriptome Characterization of Matched Primary Breast and Brain Metastatic Tumors to Detect Novel Actionable Targets. *J Natl Cancer Inst*

VELCHETI, V., HIDA, T., RECKAMP, K. L., YANG, J. C., NOKIHARA, H., SACHDEV, P., FEIT, K., KUBOTA, T., NAKADA, T., DUTCUS, C. E., REN, M. & TAMURA, T. 2016. Phase 2 study of lenvatinib (LN) in patients (Pts) with RET fusion-positive adenocarcinoma of the lung. *Annals of Oncology*, **27**, 1204PD-1204PD.

VENUR, V. A. & AHLUWALIA, M. S. 2016. Targeted Therapy in Brain Metastases: Ready for Primetime? *Am Soc Clin Oncol Educ Book*, **35**, e123-30.

VERMA, S., MILES, D., GIANNI, L., KROP, I. E., WELSLAU, M., BASELGA, J., PEGRAM, M., OH, D. Y., DIERAS, V., GUARDINO, E., FANG, L., LU, M. W., OLSEN, S. & BLACKWELL, K. 2012. Trastuzumab emtansine for HER2-positive advanced breast cancer. *N Engl J Med*, **367**, 1783-91.

VIALE, G., ROTMENSZ, N., MAISONNEUVE, P., BOTTIGLIERI, L., MONTAGNA, E., LUINI, A., VERONESI, P., INTRA, M., TORRISI, R., CARDILLO, A., CAMPAGNOLI, E., GOLDHIRSCH, A. & COLLEONI, M. 2009. Invasive ductal carcinoma of the breast with the "triple-negative" phenotype: prognostic implications of EGFR immunoreactivity. *Breast Cancer Res Treat*, **116**, 317-28.

VODUC, K. D., CHEANG, M. C. U., TYLDESLEY, S., GELMON, K., NIELSEN, T. O. & KENNECKE, H. 2010. Breast Cancer Subtypes and the Risk of Local and Regional Relapse. *Journal of Clinical Oncology*, **28**, 1684-1691.

VREDENBURGH, J. J., DESJARDINS, A., HERNDON, J. E., 2ND, MARCELLO, J., REARDON, D. A., QUINN, J. A., RICH, J. N., SATHORNSUMETEE, S., GURURANGAN, S., SAMPSON, J., WAGNER, M., BAILEY, L., BIGNER, D. D., FRIEDMAN, A. H. & FRIEDMAN, H. S. 2007. Bevacizumab plus irinotecan in recurrent glioblastoma multiforme. *J Clin Oncol*, **25**, 4722-9.

WAGNER, A. H., COFFMAN, A. C., AINSCOUGH, B. J., SPIES, N. C., SKIDMORE, Z. L., CAMPBELL, K. M., KRYSIAK, K., PAN, D., MCMICHAEL, J. F., ELDRED, J. M., WALKER, J. R., WILSON, R. K., MARDIS, E. R., GRIFFITH, M. & GRIFFITH, O. L. 2016. DGIdb 2.0: mining clinically relevant drug-gene interactions. *Nucleic Acids Res*, **44**, D1036-44.

WARD, E., VARESLIJA, D., CHARMSAZ, S., FAGAN, A., BROWNE, A. L., COSGROVE, N., COCCHIGLIA, S., PURCELL, S. P., HUDSON, L., DAS, S., O'CONNOR, D., O'HALLORAN, P. J., SIMS, A. H., HILL, A. D. & YOUNG, L. S. 2018a. Epigenome-wide SRC-1-Mediated Gene Silencing Represses Cellular Differentiation in Advanced Breast Cancer. *Clin Cancer Res*.

WARD, E., VARESLIJA, D., CHARMSAZ, S., FAGAN, A., BROWNE, A. L., COSGROVE, N. S., COCCHIGLIA, S., PURCELL, S. P., HUDSON, L., DAS, S., O'CONNOR, D., O'HALLORAN, P. J., SIMS, A. H., HILL, A. D. & YOUNG, L. S. 2018b. Epigenome-wide SRC-1 mediated gene silencing represses cellular differentiation in advanced breast cancer. *Clinical Cancer Research*

WEIGELT, B., BAEHNER, F. L. & REIS-FILHO, J. S. 2010. The contribution of gene expression profiling to breast cancer classification, prognostication and prediction: a retrospective of the last decade. *The Journal of Pathology*, **220**, 263-280.

WELLS, S. A., JR., ROBINSON, B. G., GAGEL, R. F., DRALLE, H., FAGIN, J. A., SANTORO, M., BAUDIN, E., ELISEI, R., JARZAB, B., VASSELLI, J. R., READ, J., LANGMUIR, P., RYAN, A. J. & SCHLUMBERGER, M. J. 2012. Vandetanib in patients with locally advanced or metastatic medullary thyroid cancer: a randomized, double-blind phase III trial. *J Clin Oncol*, **30**, 134-41.

WIKMAN, H., LAMSZUS, K., DETELS, N., USLAR, L., WRAGE, M., BENNER, C., HOHENSEE, I., YLSTRA, B., EYLMANN, K., ZAPATKA, M., SAUTER, G., KEMMING, D., GLATZEL, M., MULLER, V., WESTPHAL, M. & PANTEL, K. 2012. Relevance of PTEN loss in brain metastasis formation in breast cancer patients. *Breast Cancer Res*, **14**, R49.

WITZEL, I., OLIVEIRA-FERRER, L., PANTEL, K., MULLER, V. & WIKMAN, H. 2016. Breast cancer brain metastases: biology and new clinical perspectives. *Breast Cancer Res*, **18**, 8.

WODITSCHKA, S., EVANS, L., DUCHNOWSKA, R., REED, L. T., PALMIERI, D., QIAN, Y., BADVE, S., SLEDGE, G., JR., GRIL, B., ALADJEM, M. I., FU, H., FLORES, N. M., GOKMEN-POLAR, Y.,

BIERNAT, W., SZUTOWICZ-ZIELINSKA, E., MANDAT, T., TROJANOWSKI, T., OCH, W., CZARTORYSKA-ARLUKOWICZ, B., JASSEM, J., MITCHELL, J. B. & STEEG, P. S. 2014. DNA double-strand break repair genes and oxidative damage in brain metastasis of breast cancer. *J Natl Cancer Inst*, 106.

WOLFF, A. C., HAMMOND, M. E., HICKS, D. G., DOWSETT, M., MCSHANE, L. M., ALLISON, K. H., ALLRED, D. C., BARTLETT, J. M., BILOUS, M., FITZGIBBONS, P., HANNA, W., JENKINS, R. B., MANGU, P. B., PAIK, S., PEREZ, E. A., PRESS, M. F., SPEARS, P. A., VANCE, G. H., VIALE, G., HAYES, D. F., AMERICAN SOCIETY OF CLINICAL, O. & COLLEGE OF AMERICAN, P. 2013. Recommendations for human epidermal growth factor receptor 2 testing in breast cancer: American Society of Clinical Oncology/College of American Pathologists clinical practice guideline update. *J Clin Oncol*, 31**,** 3997-4013.

WORTHYLAKE, R., OPRESKO, L. K. & WILEY, H. S. 1999. ErbB-2 amplification inhibits down-regulation and induces constitutive activation of both ErbB-2 and epidermal growth factor receptors. *J Biol Chem*, 274**,** 8865-74.

WULFKUHLE, J. D., BERG, D., WOLFF, C., LANGER, R., TRAN, K., ILLI, J., ESPINA, V., PIEROBON, M., DENG, J., DEMICHELE, A., WALCH, A., BRONGER, H., BECKER, I., WALDHOR, C., HOFLER, H., ESSERMAN, L., LIOTTA, L. A., BECKER, K. F. & PETRICOIN, E. F., 3RD 2012. Molecular analysis of HER2 signaling in human breast cancer by functional protein pathway activation mapping. *Clin Cancer Res*, 18**,** 6426-35.

YATES, J. W., CHALMER, B. & MCKEGNEY, F. P. 1980. Evaluation of patients with advanced cancer using the Karnofsky performance status. *Cancer*, 45**,** 2220-4.

YERSAL, O. & BARUTCA, S. 2014. Biological subtypes of breast cancer: Prognostic and therapeutic implications. *World J Clin Oncol*, 5**,** 412-24.

YONEMORI, K., TSUTA, K., ONO, M., SHIMIZU, C., HIRAKAWA, A., HASEGAWA, T., HATANAKA, Y., NARITA, Y., SHIBUI, S. & FUJIWARA, Y. 2010. Disruption of the blood brain barrier by brain metastases of triple-negative and basal-type breast cancer but not HER2/neu-positive breast cancer. *Cancer*, 116**,** 302-8.

ZHANG, C. & YU, D. 2011. Microenvironment determinants of brain metastasis. *Cell Biosci*, 1**,** 8.

ZHANG, L., RIDGWAY, L. D., WETZEL, M. D., NGO, J., YIN, W., KUMAR, D., GOODMAN, J. C., GROVES, M. D. & MARCHETTI, D. 2013. The identification and characterization of breast cancer CTCs competent for brain metastasis. *Sci Transl Med*, 5**,** 180ra48.

ZHANG, M. & OLSSON, Y. 1995. Reactions of astrocytes and microglial cells around hematogenous metastases of the human brain. Expression of endothelin-like immunoreactivity in reactive astrocytes and activation of microglial cells. *J Neurol Sci*, 134**,** 26-32.

ZHAO, Z., ZHU, X., CUI, K., MANCUSO, J., FEDERLEY, R., FISCHER, K., TENG, G., MITTAL, V., GAO, D., ZHAO, H. & WONG, S. T. 2016. In Vivo Visualization and Characterization of Epithelial-Mesenchymal Transition in Breast Tumors. *Cancer Res*, 76**,** 2094-2104.

ZHOU, W., CHEN, C., SHI, Y., WU, Q., GIMPLE, R. C., FANG, X., HUANG, Z., ZHAI, K., KE, S. Q., PING, Y. F., FENG, H., RICH, J. N., YU, J. S., BAO, S. & BIAN, X. W. 2017. Targeting Glioma Stem Cell-Derived Pericytes Disrupts the Blood-Tumor Barrier and Improves Chemotherapeutic Efficacy. *Cell Stem Cell*, 21**,** 591-603.e4.

8. Appendix I

IHC Reagents

Sodium Citrate buffer

1.47g sodium citrate in 300ml dH2O. Adjust pH to 6 with concentrated HCL. Bring up the volume to 500ml with dH2O (make up fresh on day).

10x EDTA Buffer

12.1g Tris base, 3.7g EDTA. Adjust pH to 9.0 with concentrated HCL. Bring up the volume to 1L with dH2O.

EDTA solution

10mM Tris Base, 1mM EDTA Solution, 0.05% Tween 20, pH 9.0

0.5M Tris-HCl buffer

181.65 g Tris Base in 700ml dH2O. Adjust pH to 7.4 with concentrated HCL. Bring up the volume to 1L with dH2O

Antibody Diluent

0.05mol/l Tris-HCl buffer (pH 7.2-7.6) containing 1% BSA

Phosphate buffered saline

Dissolve one PBS tablet per 100 ml dH2O Each PBS tablet contains: 0.1 M phosphate buffer 0.0027 M potassium chloride 0.137 M sodium chloride

Table 8.1: List of cell culture reagents.

Cell culture reagents	Cat #	Supplier
Modified Eagle Medium (no glutamine, no phenol red)	#51200-038	Thermo Scientific
Dulbecco's Modified Eagle Medium (1.0g/L Glucose, no glutamine with HEPES)	#12-708F	Lonza
HyClone™ DMEM/F12 1:1 Media with HEPES	# SH30023.01	Thermo Scientific
L-Glutamine	G7513	
FCS	F7524	Sigma
Trypsin-EDTA 10X	T4174	Sigma
PBS tablets	11058	Oxoid
1M HEPES solution	#H3537	Sigma
Bovine Serum Albumin	#A7906	Sigma
Insulin-Transferrin-Selenium-X Supplement(100X)	#51500-056	Invitrogen
Hydrocortisone	#H0888	Sigma
Gentamycin	3V30080.01	HyClone
Fungizone	#SV30078.01	HyClone

Table 8.2: Clinical Information for the patient-matched brain metastasis cohort

	Primary Breast Tumor					Pre Brain Metastases Treatment					Brain Metastases			Post Brain Metastases Treatment					Progression (months)			
Case	Histology	Dx.Age	ER	PR	HER2	Endocrine	Radiotherapy	Chemotherapy	HER2	Recurrence.Prior.To.BrM	ER	PR	HER2	Endocrine	HER2	Radiotherapy	Chemotherapy	Status	DFS	BMFS	SPBM	OS
1_RCS	IDC	49	Neg	Neg	Pos	No	No	Yes	Yes	No	Neg	Neg	Pos	No	Yes	Yes	Yes	Dead	20	20	11	32
2_RCS	IDC	58	Neg	Neg	Pos	No	Yes	Yes	Yes	Yes	Neg	Neg	Pos	No	Yes	Yes	No	Dead	61	67	48	108
3_RCS	IDC	61	Pos	Neg	Pos	No	No	Yes	Yes	No	Pos	Neg	Pos	Yes	No	Yes	No	Alive	37	37	67	76
4_RCS	IDC	53	Pos	Neg	Neg	Yes	Yes	Yes	No	No	Pos	Neg	Pos	No	No	Yes	No	Dead	66	66	24	90
5_RCS	IDC	38	Neg	Neg	Neg	No	No	No	No	No	Neg	Neg	Neg	No	No	Yes	Yes	Dead	23	23	17	40
6_RCS	IDC	45	Pos	Neg	Neg	Yes	No	No	No	Yes	Pos	Neg	Pos	No	No	Yes	No	Dead	53	53	21	74
6_Pitt	IDC	66	Neg	Neg	Neg	No	Yes	Yes	No	Yes	Neg	Neg	Neg	No	No	Yes	Yes	Dead	23	25	12	37
7_Pitt	IDC	40	Pos	Neg	Pos	Yes	Yes	Yes	Yes	-	Pos	NA	Pos	NA	Yes	Yes	Yes	Dead	0	5	13	18
12_Pitt	IDC	38	Neg	Neg	Neg	No	Yes	Yes	No	-	Neg	Neg	Neg	No	No	Yes	Yes	Dead	0	31	14	46
17_Pitt	MDC	36	Pos	Neg	Pos	No	Yes	Yes	Yes	No	Pos	Pos	Pos	Yes	Yes	Yes	No	Dead	12	12	30	42
19-2_Pitt	IDC	57	Neg	Neg	Pos	No	Yes	Yes	No	No	Neg	NA	Pos	NA	NA	Yes	Yes	Dead	17	17	16	33
25_Pitt	IDC	66	Neg	Neg	Neg	No	Yes	Yes	No	Yes	Neg	NA	Neg	No	No	No	Yes	Dead	24	40	3	43
29_Pitt	IDC	52	Neg	Neg	Neg	No	Yes	Yes	No	No	Neg	NA	Neg	NA	NA	NA	NA	Dead	22	22	5	28
47_Pitt	IDC/ILC	53	Pos	Pos	Pos	Yes	Yes	Yes	No	Yes	Pos	Neg	Pos	Yes	Yes	Yes	Yes	Dead	83	151	74	225
51_Pitt	IDC	60	Pos	Neg	Neg	Yes	Yes	Yes	No	Yes	Pos	Pos	Neg	No	No	Yes	Yes	Dead	18	57	9	66
52_Pitt	IDC	62	Neg	Pos	Pos	No	Yes	Yes	Yes	Yes	Neg	Pos	Pos	No	Yes	Yes	Yes	Dead	36	55	7	63
62_Pitt	IDC	63	Pos	Pos	Neg	Yes	No	Yes	Yes	Yes	Pos	NA	Pos	No	Yes	Yes	Yes	Dead	39	53	6	60
64_Pitt	IDC	39	Neg	Neg	Neg	Yes	Yes	Yes	No	Yes	Neg	Neg	Neg	No	No	Yes	Yes	Dead	75	89	5	94
68_Pitt	IDC	51	Neg	Neg	Neg	Yes	Yes	Yes	No	No	Neg	NA	Neg	Yes	No	Yes	No	Dead	20	20	114	135
71_Pitt	IDC	26	Neg	Neg	Neg	No	Yes	Yes	No	No	Neg	Neg	Neg	No	No	Yes	Yes	Alive	25	25	147	173
72_Pitt	ILC	55	Pos	Pos	Neg	Yes	Yes	Yes	No	-	Pos	Pos	Neg	NA	No	Yes	Yes	Dead	0	31	5	37

Dx.Age, age at primary breast diagnosis; IDC, invasive ductal carcinoma; ILC, invasive lobular carcinoma; MDC, Mucinous Ductal Carcinoma; ER, estrogen receptor; PR, progesterone receptor; HER2, human epidermal growth factor receptor 2; pos, positive; neg, negative; -,not determined; NA, not available; BrM, brain metastasis; DFS, disease free survival, time from primary diagnosis to first recurrence; BMFS, brain metastases free survival, time from primary diagnosis to death or last follow-up; SPBM, survival post brain metastasis, time from brain metastasis to death or last follow-up; OS, overall survival, time from primary diagnosis to death or last follow up.

Table 8.3: Mean tumour volumes of each treatment group per measurement day from the *in vivo* study

Tumour Volume - Mean									
Day of Treatment	**0**	**3**	**6**	**10**	**13**	**17**	**20**	**25**	**27**
Vehicle Control	207	328	451	714	872	1347	1503		
Afatinib	212	199	227	252	247	338	326	410	382
Cabozantinib	211	246	365	346	440	349	389	343	347
Tumour Volume - SEM									
Day of Treatment	**0**	**3**	**6**	**10**	**13**	**17**	**20**	**25**	**27**
Vehicle Control	20.885	28.539	54.251	74.483	80.667	199.371	218.274		
Afatinib	29.005	38.864	32.374	43.691	47.423	51.54	48.636	64.577	47.254
Cabozantinib	24.634	18.281	42.517	35.595	37.443	25.461	47.026	34.586	66.49
Tumour Growth Inhibition (%)									
Day of Treatment	**0**	**3**	**6**	**10**	**13**	**17**	**20**	**25**	**27**
Vehicle Control	0	0	0	0	0	0	0		
Afatinib	0	110.74	93.85	92.11	94.74	88.95	91.2	0	0
Cabozantinib	0	71.07	36.89	73.37	65.56	87.89	86.27	0	0

Table 8.4: Measured body weights of all mice from *in vivo* experiment during the treatment course with vehicle, afatinib or cabozantinib.

Body Weight - Mean									
Treatment	**0**	**3**	**6**	**10**	**13**	**17**	**20**	**25**	**27**
Vehicle Control	23.242	23	23.275	25.325	25.45	26.225	26.15		
Afatinib	22.67	21.55	21.925	23.125	22.175	23.7	23.15	23.25	23.775
Cabozantinib	22.328	22.2	22.875	23.525	24	23.75	24.35	24.4	24.5
Body Weight - SEM									
Treatment	**0**	**3**	**6**	**10**	**13**	**17**	**20**	**25**	**27**
Vehicle Control	0.426	0.302	0.275	0.526	0.676	0.679	0.693		
Afatinib	0.822	1.008	1.026	0.927	1.054	0.903	0.893	0.652	0.978
Cabozantinib	0.949	0.919	0.983	0.867	0.91	1.043	1.159	1.017	1.051

Table 8.5: Clinical Information for the brain metastases cohort utilised in *ex vivo* and *in vivo* experiments

	Primary Breast Tumour					**Pre Brain Metastases Treatment**				**Brain Metastases**			**Post Brain Metastases Treatment**			
Case	Histology	Dx.Age	ER	PR	HER2	Endocrine	Radiotherapy	Chemotherapy	Anti-HER2 therapy	ER	PR	HER2	Endocrine	Radiotherapy	Chemotherapy	Status
xBrM T606	IDC	58	Pos	Neg	Neg	Yes	Yes	Yes	No	Neg	Neg	Neg	No	Yes	No	Alive
xBrM T347	IDC	43	Pos	Pos	Neg	No	Yes	Yes	No	Pos	Neg	Pos	No	Yes	No	Alive
xBrM T681	ILC	60	Pos	Neg	Pos	No	No	No	No	Pos	Neg	Pos	No	Yes	No	Alive
xBrM T638	ILC/IDC	74	Pos	Neg	Neg	Yes	No	Yes	No	Pos	Neg	Pos	No	Yes	No	Alive
CTG-1520	IDC	57	Neg	Neg	Neg	No	No	Yes	-	Neg	Neg	Neg	No	NA	Yes	NA

Table 8.6: Case-fold changes and expression gains in clinically actionable kinases

Clinically Actionable Kinase	1_RCS	2_RCS	3_RCS	4_RCS	5_RCS	6_RCS	6_Pitt	7_Pitt	12_Pitt	17_Pitt	19-2_Pitt	25_Pitt	29_Pitt	47_Pitt	51_Pitt	52_Pitt	62_Pitt	64_Pitt	68_Pitt	71_Pitt	72_Pitt
ATM	-0.802	-1.694	0.100	-0.117	-1.020	-0.821	-0.374	0.623	-0.429	-0.809	-0.284	1.117	0.247	-0.866	-0.155	0.021	0.017	-0.136	-0.513	-0.134	-0.126
CHEK1	0.251	1.076	-0.290	-1.267	0.321	-0.397	0.001	0.727	0.796	0.956	1.385	0.578	-0.210	0.783	-0.973	-0.328	0.065	0.030	-0.381	-0.114	-0.631
PIK3R1	0.024	-0.457	-0.758	0.242	0.360	-0.834	-0.730	1.283	-0.051	-0.618	0.346	2.458	-0.462	-0.616	-0.476	-0.486	0.051	-1.615	-0.034	-0.556	1.395
ARAF	-0.107	-0.094	0.233	-0.018	-0.035	-0.370	0.289	0.306	-0.648	0.281	-0.126	-0.575	0.703	0.471	0.339	0.796	0.010	0.553	0.998	-0.332	-0.071
MTOR	0.087	0.958	-0.002	0.107	-0.044	0.079	-0.201	-0.340	0.470	0.241	-0.264	-0.065	-0.051	0.636	0.208	0.577	0.180	-0.252	0.231	-0.017	-0.065
PRKAR1A	0.180	-0.179	0.388	-1.058	0.412	1.831	0.104	-0.364	-0.064	1.038	0.174	0.309	-0.055	0.397	0.061	-0.799	-0.057	-0.268	0.329	-0.165	-0.139
CDK8	0.316	-1.296	0.120	-0.732	-0.512	-0.194	-0.353	0.414	0.417	0.955	0.057	0.948	0.562	-0.071	0.132	-0.670	0.217	-0.617	-1.001	0.126	0.227
PLK2	-0.796	2.390	0.025	-2.034	-0.605	2.210	1.319	0.306	-0.025	-1.469	0.558	-0.574	-0.228	0.706	0.272	-0.276	2.934	-0.218	-1.370	-0.960	0.180
EPHA3	-1.822	-1.314	1.420	-1.207	2.299	-0.833	-0.114	1.096	1.310	-0.347	-1.538	0.556	0.940	0.277	1.954	0.889	-1.687	1.919	-0.411	1.688	0.470
CARD11	-1.449	-1.817	0.493	-0.830	-1.322	-1.007	-1.121	-0.450	-0.581	-1.138	-1.309	-0.298	-1.786	-1.807	0.929	0.324	-1.453	-1.330	0.725	-1.013	0.352
BCR	0.089	1.300	0.317	0.225	0.305	0.424	-0.038	0.552	0.095	-0.080	0.048	0.190	-0.229	0.210	0.374	0.327	0.301	-0.528	0.509	0.306	-0.157
MAPK1	0.412	-0.328	-0.071	-0.929	-0.502	0.210	-0.014	0.076	0.124	-0.350	0.376	0.088	0.130	0.666	0.181	-0.020	0.076	-0.503	-0.287	0.275	0.410
PIK3CB	0.341	-1.363	0.065	0.250	0.315	-0.049	0.027	-0.214	-0.189	0.497	0.506	-0.356	0.711	0.036	-0.415	0.006	0.195	-0.296	-0.283	-0.330	-0.086
CDKN1A	-0.688	-0.605	1.165	-0.974	0.440	2.333	-0.098	-1.067	-0.841	1.197	-0.045	0.039	0.747	-0.088	0.908	-0.599	-1.278	0.310	-0.162	-0.596	0.364
MAP3K13	-0.067	0.699	0.380	0.730	-0.088	1.055	0.160	-0.181	0.178	0.752	0.322	0.065	0.520	0.554	-0.765	0.221	0.736	0.345	0.042	-0.215	-0.061
FLT1	-0.221	1.449	1.144	1.073	0.841	0.104	-0.226	-0.121	0.209	0.011	0.430	0.853	0.203	0.205	1.017	0.906	-0.779	1.179	-1.657	-0.138	-0.546
LATS1	-0.227	-1.749	-0.335	-0.575	-0.353	0.024	-0.184	-0.029	0.060	-0.351	-0.076	0.213	0.136	-0.448	-1.247	-0.163	-0.160	-0.067	-0.935	-0.627	-0.497
AURKB	0.471	2.127	0.098	0.065	0.658	0.603	0.038	0.822	-0.022	0.741	0.959	-0.733	-0.037	-0.141	-0.305	0.337	0.133	-0.097	0.038	-0.473	-0.498
ERBB4	2.070	1.373	-0.063	3.056	1.408	-0.582	0.126	-2.056	1.202	0.298	1.008	2.101	0.307	-0.392	-1.029	-0.640	-0.310	0.295	0.556	1.277	-1.038
BRAF	-0.444	-0.629	0.439	0.347	-0.130	0.250	0.498	0.209	0.255	-0.122	0.212	0.531	0.196	-0.028	-0.418	0.474	0.846	0.214	-0.993	-0.145	0.038
PAK1	1.094	-0.437	0.193	-1.321	-0.113	0.842	0.308	-0.236	-0.219	-0.240	0.467	0.602	0.454	0.367	-0.363	-0.212	0.314	0.446	0.668	-0.408	0.380
BMPR1A	-0.012	-0.622	0.088	-0.507	0.371	-0.615	0.205	-0.153	-0.364	0.393	0.424	0.003	-0.039	0.027	0.221	0.199	0.286	0.121	-0.404	-0.462	0.232
ERBB2	0.174	2.019	0.694	1.233	0.535	4.436	2.656	-0.718	-0.343	1.294	0.225	0.206	0.772	2.241	0.765	-0.132	3.084	1.592	-0.218	0.108	-0.159
PIK3R3	0.654	0.918	1.058	0.871	0.736	0.963	0.183	-0.285	0.583	1.419	0.223	0.309	-1.536	0.841	-0.534	-0.211	0.291	0.629	-0.816	-0.254	0.107
AKT3	-0.510	-1.701	0.049	-1.053	-0.454	0.496	-0.585	-0.294	0.293	-2.391	0.152	-0.026	1.321	-0.243	0.523	0.102	-0.772	-0.823	0.092	0.018	0.249
CCND1	-0.880	1.452	0.145	-1.374	-2.138	-1.040	-0.001	0.501	-0.141	0.926	-0.144	-1.041	1.017	-3.038	0.017	-0.372	-0.065	-0.634	0.441	0.970	-0.150
IGF1R	-0.413	0.944	-3.940	-2.088	-0.238	-4.709	0.975	1.071	-1.341	0.800	0.048	0.409	0.851	-3.318	-0.080	0.981	1.056	-0.958	-2.846	-1.742	-0.224
PIK3CD	-1.435	-1.191	0.227	-0.500	-0.992	-1.641	-0.705	-0.567	-0.694	-1.930	-1.296	-0.990	-2.224	-1.306	0.522	1.153	-1.612	-0.811	0.602	-0.567	-0.365
MAP3K1	-0.268	-0.435	-0.166	-1.933	-0.853	0.502	-0.362	-0.077	-0.392	-1.085	-0.367	-0.341	-1.291	0.026	-0.780	-0.218	0.865	-1.901	0.441	-0.780	0.279
EGFR	0.728	0.388	-0.065	1.803	-0.011	-1.294	0.968	-1.233	-1.137	-3.814	0.563	0.008	-0.511	0.398	0.281	-0.337	-0.975	0.785	0.623	-1.308	0.674
PDGFRA	-1.518	-4.218	-1.569	-3.811	-0.364	-2.413	-1.548	-3.853	-0.574	-3.439	-2.525	-1.243	-0.811	-1.002	-0.927	-0.819	-3.035	-1.477	-2.390	-0.699	0.775
TGFBR2	-0.735	-1.013	0.037	-2.197	-0.620	-1.839	-0.789	-0.717	-0.707	-3.561	-0.905	0.559	-0.382	-0.941	1.217	0.266	-2.282	-0.687	-0.183	-0.168	1.160
CDK6	-1.290	1.520	-0.402	0.939	-0.536	-0.114	0.149	-0.859	-0.396	-1.753	-1.148	-1.294	0.381	-0.796	-0.096	0.453	-1.182	-0.541	0.880	0.841	-0.101
ABL1	0.154	0.630	0.050	-0.436	-0.216	-1.306	-0.182	-1.368	0.018	-0.625	-0.470	-0.026	-0.759	-0.342	0.131	0.042	-0.610	-0.079	0.190	-0.316	-0.092
INSR	-0.212	3.376	0.189	0.984	0.373	-0.805	0.425	-1.354	0.080	0.135	0.072	0.672	-0.592	0.044	0.617	0.470	0.111	0.707	0.113	-0.478	-0.264
CDKN2C	-0.099	-0.400	0.355	-1.044	0.062	-0.482	-0.003	0.595	0.095	-0.641	-0.513	0.077	0.096	-1.162	-0.618	0.832	0.667	0.263	0.139	0.366	-0.779
PDGFRB	-0.776	-0.081	0.140	-0.964	1.190	-1.428	-0.458	-1.313	-0.522	-2.171	-1.771	-0.483	-0.893	-0.290	2.133	1.548	-2.139	-0.045	-0.824	-0.652	0.168
KIT	1.917	-3.197	-1.061	-1.146	0.755	-1.302	-1.464	0.110	-0.503	-4.698	-0.588	-0.455	-0.357	-1.569	-1.692	0.759	-1.991	-1.785	1.113	0.049	-0.559
CDKN1B	0.093	0.539	0.231	-0.310	-0.185	-0.101	-0.192	0.257	-0.010	-0.690	0.037	-0.046	-0.352	-0.785	-0.946	-0.474	-0.237	-0.508	-0.033	-0.302	-0.052
PIK3R2	0.136	1.282	-0.386	0.076	-0.274	0.776	0.314	1.411	0.591	1.079	-0.184	0.057	0.539	0.771	-0.733	0.030	0.521	0.426	-0.484	-0.076	-0.057
ERBB3	0.185	2.095	0.544	1.249	1.112	0.807	0.675	0.088	-0.495	1.355	0.427	-0.778	0.186	1.209	-0.813	0.082	0.222	1.216	0.249	0.262	-0.340
RPS6KB2	0.111	1.495	0.043	0.993	-0.442	-0.259	-0.086	0.466	0.365	0.651	0.058	-0.379	-0.245	0.923	0.299	0.009	-0.050	-0.094	0.243	0.289	-0.239
PIK3CG	-1.890	-3.440	-0.369	-2.599	-1.349	-1.501	-1.564	-0.168	-1.080	-2.010	-1.445	-0.401	-2.069	-1.929	0.408	-0.027	-2.141	-1.544	-0.075	-0.543	-0.639
JAK2	-0.533	-2.839	-0.284	-0.414	-0.897	-0.297	-0.814	-0.045	-0.577	-0.372	-0.539	0.775	-2.047	-1.231	0.275	0.013	-0.943	-0.604	-0.408	-0.361	0.440
LATS2	-0.954	-0.707	-0.422	-0.793	-0.536	-1.429	-0.623	-1.115	-0.253	-2.045	-0.630	1.000	1.078	-1.116	0.772	0.697	-1.399	-0.592	-0.377	-0.460	0.062
BRD4	0.227	-0.638	-0.408	0.212	-0.046	-0.359	-0.406	0.195	-0.152	-0.338	0.041	0.293	0.686	-0.581	-0.159	-0.607	-0.294	-0.505	0.042	-0.455	0.038
NTRK1	-0.283	0.834	0.196	0.841	-0.099	-0.941	-0.457	0.123	0.267	-2.406	0.090	-0.282	-0.580	-1.534	0.354	-0.435	-0.044	-0.351	0.223	-0.670	-0.497
BTK	-1.478	-3.310	-0.279	-1.817	-1.046	-1.384	-1.073	0.219	-0.707	-2.088	-0.496	0.189	-1.495	-1.228	0.919	1.054	-1.704	-0.890	0.212	0.399	-0.058
PDPK1	-0.041	0.649	0.045	0.933	0.220	-0.103	0.068	0.013	-0.153	0.423	0.290	0.038	-0.040	0.402	-0.253	-0.106	0.510	-0.469	0.471	0.142	-0.147

Table 8.6: Case-fold changes and expression gains in clinically actionable kinases (Continued)

Clinically Actionable Kinase	1_RCS	2_RCS	3_RCS	4_RCS	5_RCS	6_RCS	6_Pitt	7_Pitt	12_Pitt	17_Pitt	19-2_Pitt	25_Pitt	29_Pitt	47_Pitt	51_Pitt	52_Pitt	62_Pitt	64_Pitt	68_Pitt	71_Pitt	72_Pitt
JAK1	-0.434	-0.567	0.117	-1.469	-0.262	-0.437	-0.054	-0.552	0.272	-0.810	-0.130	0.622	-0.015	-1.008	0.764	0.541	0.046	-0.406	-0.103	-0.334	0.590
NTRK3	2.681	-1.094	2.211	3.922	1.983	2.886	1.903	0.842	3.363	-1.131	2.050	0.818	1.394	2.548	1.788	2.796	2.415	2.396	0.815	2.307	3.532
ATR	-0.070	0.093	0.220	0.427	0.277	-0.179	-0.083	0.075	-0.006	0.294	-0.020	-0.410	0.292	0.185	-0.536	0.572	0.393	0.177	-0.598	-0.688	-0.023
PIK3C3	0.003	-0.184	0.271	-0.092	-0.209	0.380	-0.125	0.677	0.110	0.220	0.008	0.628	0.450	-0.364	-0.283	-0.038	-0.116	0.450	-0.055	0.043	0.299
PIK3C2G	-0.363	-1.910	-0.570	-2.078	1.837	-0.700	0.042	-0.300	0.764	-1.071	1.233	-4.008	1.522	2.276	-2.533	0.665	0.833	0.215	-3.816	0.564	0.477
AKT1	0.227	0.990	-0.083	0.042	0.024	0.512	0.106	-0.167	0.223	1.030	-0.076	-0.991	0.406	0.441	0.745	0.713	0.003	-0.127	0.458	0.092	0.023
EPHB1	0.149	0.046	-0.115	0.291	-1.411	1.136	-1.025	0.320	0.737	-0.615	-0.368	-0.709	-0.053	0.371	-0.335	0.061	0.511	-0.272	-0.682	0.512	-0.795
CDKN2A	-0.704	1.072	-0.400	-0.694	-0.848	-1.087	1.420	0.265	-0.808	-0.150	0.149	-1.208	-0.085	-0.373	-0.451	-0.603	-1.784	1.165	2.383	1.246	-0.188
MAP2K4	0.356	-0.837	0.085	-0.524	0.194	0.493	-0.122	-1.308	-0.177	0.100	0.238	0.392	-0.202	0.233	-0.039	-0.013	0.093	-0.183	-0.807	-0.001	-0.112
MAP2K1	-0.168	0.113	0.035	-0.816	-0.245	0.793	0.229	0.137	-0.197	0.021	0.485	0.634	-1.027	0.160	0.202	-0.325	0.273	0.240	0.292	-0.107	0.585
RAF1	0.494	0.720	-0.049	0.155	0.074	-0.328	0.233	0.108	0.392	-0.291	0.061	0.282	-0.462	0.014	0.016	0.534	0.155	0.753	-0.371	-0.092	-0.002
ERCC2	0.271	1.538	-0.156	0.534	-0.373	-0.268	0.076	-0.205	-0.006	0.691	-0.149	-0.556	-0.173	-0.053	0.089	0.765	0.082	-0.051	0.189	0.652	0.143
PIK3CA	-0.025	-1.738	0.031	-0.838	0.091	-0.317	-0.270	-0.056	-0.057	0.328	0.006	0.065	0.525	-0.502	0.120	-0.280	0.186	-0.216	-0.476	-0.240	0.334
CCND3	0.082	0.943	0.655	-0.181	-0.085	0.035	0.114	-0.122	-0.764	0.425	0.279	-0.132	0.333	0.483	1.217	0.682	-0.047	-0.008	0.822	-0.400	0.548
FGFR3	1.215	2.851	0.071	2.369	0.955	-0.599	-0.067	-1.272	1.132	0.457	1.863	0.880	2.032	-2.001	0.535	0.405	-1.322	1.309	1.171	0.624	-1.082
YES1	0.896	-1.179	-0.282	-1.336	0.151	-0.617	0.266	-0.307	-0.197	0.919	0.416	-0.193	-0.130	-0.467	-0.656	-0.339	-0.182	0.755	-0.370	-0.941	0.293
PRKDC	1.031	0.395	-0.051	-1.020	0.006	-0.138	-0.599	0.077	-0.900	0.583	0.375	-0.328	-0.260	0.410	-1.230	-1.033	-0.558	-0.881	-0.416	0.555	-0.214
MAP2K2	0.284	1.103	0.127	0.728	-0.123	-0.194	0.287	-0.369	0.473	0.191	0.116	-0.436	0.102	0.511	0.697	0.430	0.168	0.143	0.646	0.201	0.128
JAK3	-1.887	-3.374	-0.537	-1.763	-1.581	-1.279	-1.428	-0.991	-1.001	-1.251	-1.460	-1.249	-0.279	-2.638	0.098	0.409	-2.701	-1.065	-0.250	-0.991	-1.455
FLT4	-1.390	1.244	0.103	0.791	-0.342	0.687	-0.784	-0.016	-0.309	-0.464	-1.506	-0.387	-0.460	-0.244	0.342	0.114	-1.353	-1.007	-0.250	-0.495	-0.664
STK40	0.389	0.950	-0.201	0.463	-0.444	0.232	0.265	-0.305	0.113	0.012	-0.167	-0.228	0.391	0.155	0.483	0.518	0.690	0.139	-0.326	0.534	0.195
PAK3	-0.595	-2.720	1.112	1.202	-0.792	3.306	-0.511	0.077	0.484	-2.642	1.955	-1.416	0.467	-0.863	-1.120	2.470	-0.929	-1.077	-0.791	0.016	-1.055
CCNE1	0.042	0.287	0.111	0.043	0.736	0.461	-0.305	-0.303	0.324	1.360	0.784	-0.446	0.275	0.545	-0.164	0.033	0.191	-0.403	0.032	-0.318	0.368
RPS6KA4	-0.514	-0.017	-0.006	0.366	-0.503	-0.380	0.072	-0.266	-0.774	-0.511	-0.781	-0.437	-0.021	0.113	0.971	-0.011	0.029	0.160	0.569	0.157	-0.028
TGFBR1	0.368	-0.408	-0.547	-2.055	-0.293	0.576	-0.511	-1.000	-0.249	0.079	-0.080	-0.225	0.744	2.639	0.861	0.573	-1.504	0.038	-0.963	-0.134	0.643
SRC	-0.359	1.818	-0.277	-0.803	0.602	-1.329	-0.181	-0.915	0.035	0.247	-0.109	-0.356	0.688	0.077	0.765	0.336	-0.363	-0.554	0.342	0.502	-0.362
CHEK2	0.842	0.336	-0.178	-0.692	-0.197	-0.362	0.196	1.612	0.344	0.368	0.632	0.035	-0.585	0.184	-0.526	-0.019	0.517	0.425	-0.481	-0.147	-0.007
IKBKE	-1.239	1.383	-0.137	1.213	-1.540	-1.096	-0.340	-0.058	-1.479	-1.507	0.022	-0.528	-0.792	-0.533	0.414	0.858	0.168	-0.376	-0.490	-2.229	-0.841
KDR	-1.932	1.698	0.061	0.227	0.090	-0.935	-0.855	0.212	-0.047	-0.963	-0.783	1.015	0.507	-0.572	0.545	1.107	-1.799	0.343	-0.731	-0.197	-0.407
AXL	-0.645	-1.171	0.259	-1.962	-0.123	-1.219	-0.419	-0.862	-0.649	-2.039	-0.996	-0.398	-1.537	-0.529	1.546	0.351	-1.410	-0.367	0.475	-0.519	0.521
FGFR2	1.467	2.434	-0.797	2.308	0.608	0.403	0.706	-0.854	0.791	0.962	2.093	-0.068	0.635	0.606	-0.052	1.210	-1.289	-0.146	-0.015	-0.236	-0.119
PIM1	-1.152	-2.069	-0.805	-1.121	0.296	-2.159	-0.436	-0.741	-0.820	-2.268	-1.400	0.375	0.220	-1.597	-0.966	0.669	-0.934	-0.233	0.034	-0.944	-0.519
FLT3	-0.247	-3.778	-1.126	-1.069	-1.240	-3.176	-0.837	0.275	-0.244	-0.431	-0.699	1.470	-1.057	-1.947	-0.665	-0.152	0.282	-1.457	0.535	0.073	0.004
GSK3B	0.088	0.251	-0.010	-0.188	0.014	0.161	0.263	-0.500	0.517	0.474	0.293	0.297	0.262	0.339	-0.280	-0.236	0.500	-0.058	0.383	-0.213	-0.095
SOX9	0.961	-0.353	0.490	1.093	0.130	1.259	0.257	-0.993	-1.408	2.664	-0.024	0.449	0.607	1.769	-0.351	-0.081	1.496	-0.271	1.262	-0.250	0.007
CSF1R	-0.690	-1.305	-0.119	-1.426	-0.791	-0.791	-0.763	-0.162	-0.136	-1.814	-0.793	0.111	-1.529	-0.682	1.591	0.673	-2.403	-0.480	0.559	0.249	1.211
ROS1	-0.489	0.977	-0.365	-0.152	-0.756	2.164	-0.144	-0.766	0.365	0.130	-2.595	3.284	4.078	-0.325	-0.331	-3.421	-0.230	0.622	-1.123	-3.452	0.108
CDK4	0.339	0.838	-0.331	-1.293	0.417	-0.356	0.243	0.328	-0.570	0.396	0.193	-1.011	-0.029	0.391	-0.184	0.279	0.147	0.286	0.240	0.305	0.067
ERCC3	-0.087	0.548	-0.047	0.950	0.033	0.027	0.178	0.293	0.214	0.299	0.366	-0.130	0.081	0.275	0.166	0.427	0.098	0.278	0.238	-0.255	-0.012
ALK	-0.712	0.147	1.028	0.910	-0.479	0.593	-0.732	0.482	-0.601	-0.553	0.336	0.103	0.749	-0.775	1.071	-0.216	0.546	-0.299	-1.218	1.653	0.474
SYK	-0.879	-2.336	-0.271	-2.190	-0.351	-1.649	-0.279	0.317	-0.136	-0.184	-0.282	0.142	-0.774	-1.654	0.082	0.056	-1.537	-0.010	0.427	-0.186	0.125
MET	0.407	-4.249	0.601	-1.250	1.012	-0.556	0.045	-1.597	-0.080	-5.088	0.435	0.888	1.862	-2.845	-1.746	-0.277	-0.025	-1.693	-0.245	0.048	0.785
FIP1L1	0.840	-0.162	0.367	0.512	-0.177	0.438	-0.168	0.073	0.724	0.428	0.336	0.280	0.084	0.031	-0.763	-0.603	-0.319	0.221	-0.068	-0.043	0.018
FGFR4	1.083	1.569	0.758	3.835	0.061	4.984	0.097	0.557	-0.052	-0.691	1.671	-0.998	0.481	5.424	0.817	0.495	0.768	0.016	0.578	1.601	-0.182
DDR2	-1.299	-1.436	-0.231	-1.530	0.302	-2.011	-1.220	-1.160	0.764	-3.102	-0.969	1.781	-0.415	-0.647	1.079	0.690	-1.336	-0.141	-2.379	-0.320	0.672
STK11	-0.196	1.877	-0.035	-0.332	-0.075	-0.473	0.130	-0.586	-0.124	0.182	0.073	0.013	-0.090	-0.079	0.242	0.335	0.002	0.356	0.108	-0.520	0.002
PDK1	0.457	0.615	-0.301	0.353	-0.658	-0.352	-0.531	1.184	-0.767	0.676	0.266	-0.211	0.277	0.841	-0.493	-0.305	0.039	-0.252	-1.593	0.440	-0.073
AURKA	0.832	0.420	-0.219	-1.134	-0.310	1.032	-0.851	0.413	0.420	1.767	0.652	-0.282	-0.415	0.738	-0.841	-0.235	0.436	-1.165	-0.862	-0.128	-0.660
NTRK2	0.116	-0.683	2.843	1.963	0.989	2.532	0.022	0.716	0.726	-1.667	2.966	0.660	-0.830	1.284	1.971	2.181	1.587	0.393	-1.802	1.232	1.648
CDKN2B	-2.244	-0.430	-0.096	-0.738	-1.105	-0.817	1.182	-0.415	-0.124	-0.226	-0.332	-0.271	0.141	-0.626	0.804	1.758	-0.211	0.317	2.540	-0.087	0.409
CDK12	0.005	0.710	-0.175	0.286	-0.499	2.560	1.817	0.001	0.055	0.346	-0.081	-0.276	-0.024	0.159	0.213	-0.645	3.308	-0.090	-0.154	-0.016	-0.199
RET	-0.852	1.831	-1.280	-0.430	1.564	3.238	0.936	0.684	-0.199	3.450	-0.032	-0.827	-0.032	3.892	0.525	1.931	1.639	-0.136	-1.151	-0.700	2.319
FGFR1	-0.180	-0.271	-1.008	-1.428	0.017	-2.201	-0.729	-0.808	-0.169	-2.859	-0.501	0.659	-0.810	0.546	0.320	-0.156	-0.782	-0.751	-0.370	0.484	-0.210
AKT2	0.289	1.556	-0.268	0.914	0.539	0.048	0.335	-0.195	0.068	0.482	-0.043	-0.430	0.508	-0.428	-0.478	0.850	0.073	0.504	0.477	0.043	-0.053

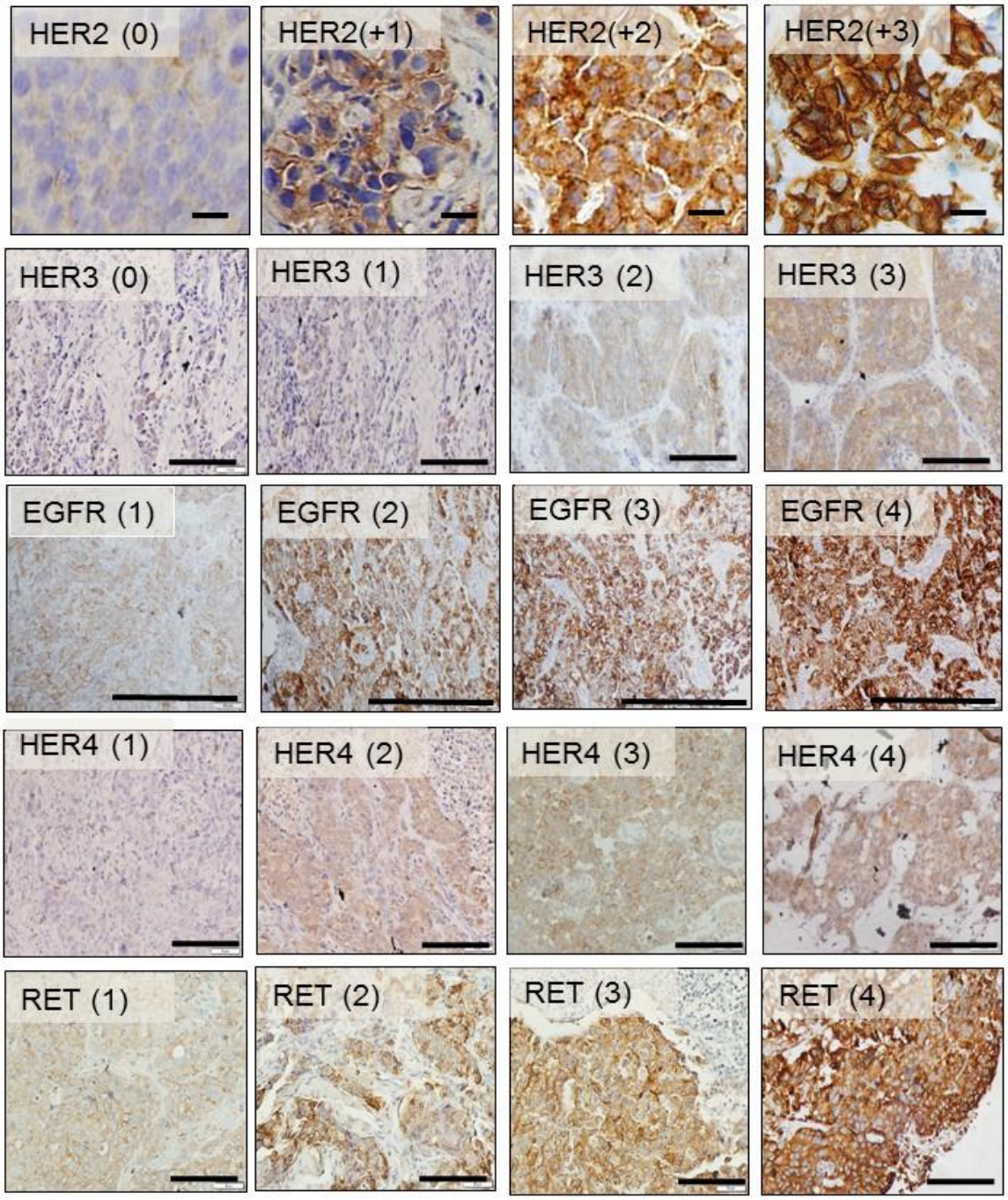

Figure 8.1: Representative images of total HER and total RET IHC staining in human breast cancer brain metastases.

HER2 IHC scoring was based on a 0-3 scale with tumours scoring 0, 1+, 2+ and 3+ being interpreted as negative, weak, equivocal and strong, respectively. The adopted scoring system for assessing RET and HER family IHC staining was based on a 0-4 scale with tumours scoring 0, 1+, 2+, 3+ and 4+ being interpreted as negative, weak, moderate, strong and very strong, respectively. Images shown were captured at 10x, 20x and 40x magnifications; scale bars correspond to 100μm, 50μm and 20μm, respectively.

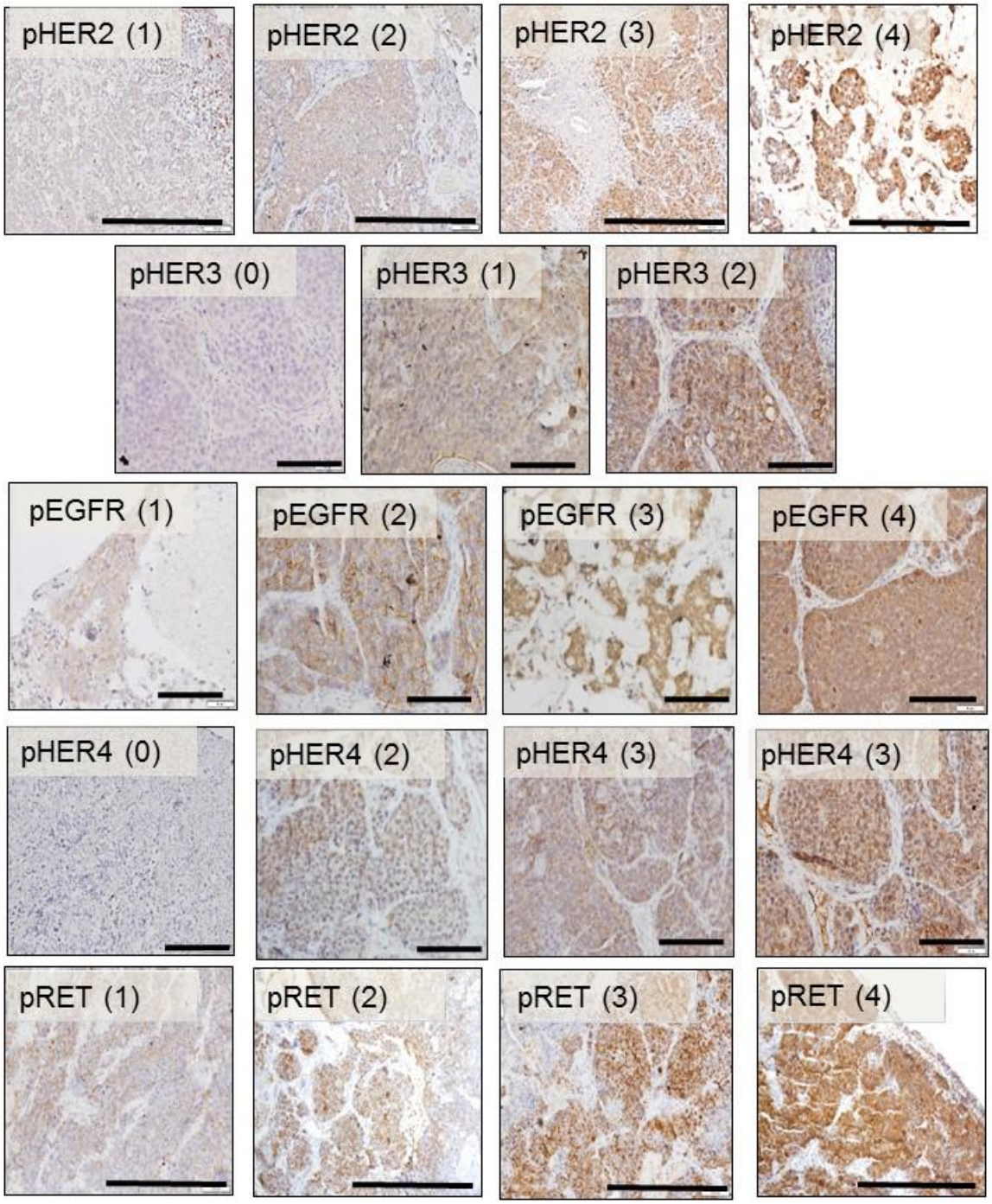

Figure 8.2: Representative images of phospho -HER and phospho- RET IHC staining in human breast cancer brain metastases.

The adopted scoring system for assessing phospho-RET and phospho-HER family IHC staining was based on a 0-4 scale with tumours scoring 0, 1+, 2+, 3+ and 4+ being interpreted as negative, weak, moderate, strong and very strong, respectively. Images shown were captured at 10x or 20x magnifications; scale bars correspond to 100μm and 50μm, respectively.

9. Appendix II

Publications

Publications obtained during the course of this research

- Varešlija D, Priedigkeit N, Fagan A, **Purcell SP**, Cosgrove N, O'Halloran PJ, Ward E, Cocchiglia S, Hartmaier R, Castro CA, Zhu L, Tseng GC, Lucas PC, Puhalla SL, Brufsky AM, Hamilton RL, Mathew A, Leone JP, Basudan A, Hudson L, Dwyer R, Das S, O'Connor DP, Buckley PG, Farrell M, Hill ADK, Oesterreich S, Lee AV, Young LS. Transcriptome Characterisation of Matched Primary Breast and Brain Metastatic Tumours to Detect Novel Actionable Targets. J Natl Cancer Inst. 2018 Jun 28. doi: 10.1093/jnci/djy110.
- Ward E, Varešlija D, Charmsaz S, Fagan A, Browne AL ,Cosgrove N, Cocchiglia S, **Purcell SP**, Hudson L, Das S, O'Connor D, O'Halloran PJ, Sims A, Hill AD, Young LS. Epigenome-wide SRC-1 mediated gene silencing represses cellular differentiation in advanced breast cancer. Clin Cancer Res. 2018 Mar 22. pii: clincanres.2615.2017. doi: 10.1158/1078-0432.CCR-17-2615
- Browne AL, Varešlija D, Charmsaz S, Fagan A, Browne AL ,Cosgrove N, Cocchiglia S, **Purcell SP**, Ward E, Fiona Bane FT, Hudson L, Hill AD, Carroll JS, Redmond AM, Young LS. Network analysis of SRC-1 reveals a novel transcription factor hub which regulates endocrine resistant breast cancer. Oncogene (2018) doi:10.1038/s41388-017-0042-x
- Varešlija D, McBryan J, Fagan A , Redmond AM, Hao Y , Sims A, Turnbull A, Dixon JM, O Gaora P , Hudson L**, Purcell SP**, Hill AD, Young LS. Adaptation to AI Therapy in Breast Cancer Can Induce Dynamic Alterations in ER Activity Resulting in Estrogen-Independent Metastatic Tumours. Clin Cancer Res. 2016 Jun 1;22(11):2765-77. doi: 10.1158/1078-0432.CCR-15-1583.

National Communications (Oral and Poster)

Purcell SP, Varešlija D, Priedigkeit N O'Halloran PJ , Farrell M, Hill AD, Oesterreich S, Lee AV, Young LS. Thesis in 3: Identifying new drug targets for breast cancer brain metastasis. Oral presententation at RCSI Research Day 2018; 2018 March 7th; Royal College of Surgeons, Dublin.

Purcell SP, Varešlija D, Priedigkeit N O'Halloran PJ , Farrell M, Hill AD, Oesterreich S, Lee AV, Young LS. Identifying new drug targets for breast cancer brain metastasis. Poster presentation at Irish Association For Cancer Research 54th Annual Meeting 2018; 2018 Feb 21-23; Crowne Plaza Hotel, Santry, Dublin

Purcell SP, Varešlija D, Priedigkeit N O'Halloran PJ , Farrell M, Hill AD, Oesterreich S, Lee AV, Young LS. Thesis in 3: Identifying new drug targets for breast cancer brain metastasis. Poster presentation at Beamont Hospital 2017 Translational Research Awards; 2017 Oct 17; Beaumont Hospital, Dublin.